IL
NUOVO CIMENTO
ORGANO DELLA SOCIETÀ ITALIANA DI FISICA
SOTTO GLI AUSPICI DEL CONSIGLIO NAZIONALE DELLE RICERCHE

VOL. I, N. 3 *Serie decima* 1° Marzo 1955

La viscosità di volume (III).

A. CARRELLI e F. CENNAMO
Istituto di Fisica dell'Università - Napoli

(ricevuto il 30 Novembre 1954)

Riassunto. — In questa nota viene illustrato un metodo seguito per la determinazione del rapporto η'/η e si riportano i risultati relativi all'acqua per la frequenza: $\nu = 1{,}8$ MHz.

In due precedenti note [1] abbiamo riferito relativamente a misure sul secondo coefficiente di viscosità dei liquidi ottenute seguendo, per lo meno nelle sue linee essenziali, un metodo suggerito dal LIEBERMANN [2]. In questo metodo, il cilindro contenente il liquido nel quale vengono prodotti gli ultrasuoni è chiuso da un disco mobile di potere riflettente R. Per effetto degli ultrasuoni si generano su questo disco due forze: una dovuta alla pressione di radiazione ed una dovuta al moto d'insieme del liquido; la seconda per effetto d'inerzia si produce con un certo ritardo rispetto alla prima, ed è quindi discernibile da questa.

Il nostro metodo, riportato nelle note citate, si differenzia da quello del LIEBERMANN solo in quello che concerne il sistema usato per la misura di queste forze. Dalla prima di queste si risaliva alla misura di I (intensità ultra-

---

(1) A. CARRELLI e F. CENNAMO: *Nuovo Cimento*, **11**, 429 (1954); **12**, 1 (1954).
(2) L. N. LIEBERMANN: *Phys. Rev.*, **73**, 537 (1948); **75**, 1915 (1949).

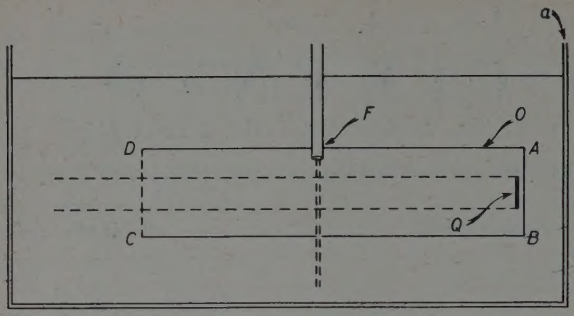

Fig. 1.

sonora) e dalla seconda alla misura di v, e conosciuti i valori di I e di v si poteva determinare il valore di η'/η, quindi del secondo coefficiente di viscosità in base alla formula di Eckart ([3]).

Il metodo non è però esente da critiche, sia per il fatto che il tubo non è perfettamente chiuso all'estremo, come è richiesto dalla teoria, (e ciò per permettere una sufficiente mobilità del disco) e sia per il fatto che questo stesso disco non può avere potere riflettente nullo nè trascurabile in quanto la misura di I vien fatta proprio attraverso la misura della pressione di radiazione che è funzione lineare di R.

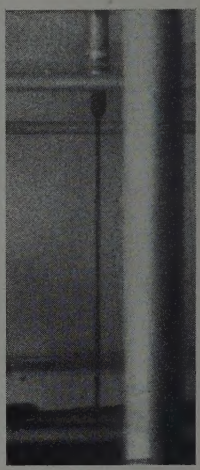

Fig. 2.

Il verificarsi di queste due condizioni è invece essenziale in quanto proprio su tali premesse si basa la teoria la quale porta alla seguente formula, che dà le velocità v assunte dal fluido appunto in funzione fra l'altro di I e di η'/η:

$$v = G\frac{r^2\omega^2}{\varrho c^4} I\left(2 + \frac{\eta'}{\eta}\right), \tag{1}$$

(essendo: $G = \frac{1}{2}\left((r^2/r_0^2) - 1\right) - \log r/r_0$, dove r = raggio del tubo; r_0 = raggio del fascio ultrasonoro); da tale formula, noti tutti gli elementi, si può ricavare il valore di η'/η.

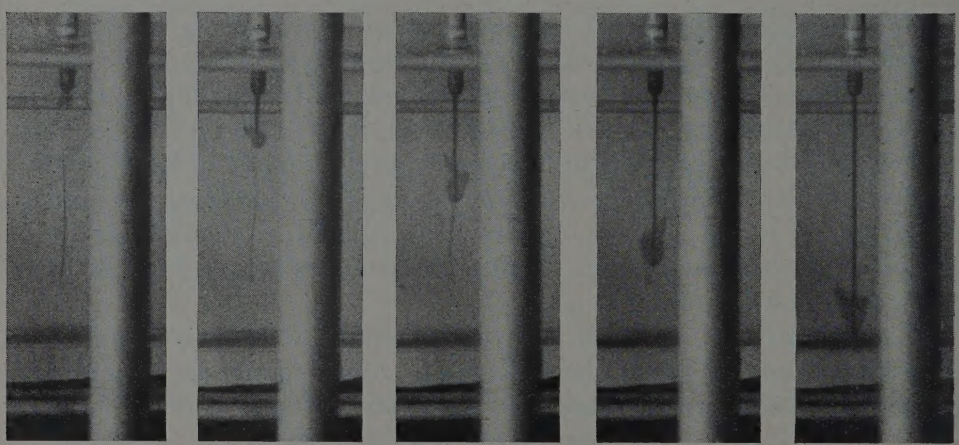

a) b) c) d) e)

Fig. 3.

([3]) C. Eckart: *Phys. Rev.*, **73**, 68 (1948).

Data l'importanza dell'argomento e tenuto conto anche del fatto che nei lavori precedenti abbiamo ritrovato, almeno per quanto riguarda i valori relativi di η' per il benzene e per il tetracloruro di carbonio, dei risultati che concordano con quelli del LIEBERMANN, abbiamo in queste ricerche voluto riprendere il problema, cercando di metterci, quanto più possibile, nelle condizioni previste dalla teoria.

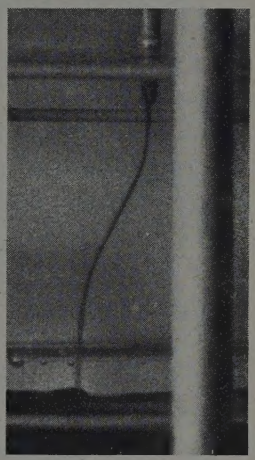

Fig. 4.

Il dispositivo sperimentale ora usato è schematizzato in fig. 1: nella vaschetta a, a pareti di vetro, contenente acqua, è disposto un cilindro O di plexiglas, orientabile in tutte le direzioni a mezzo di viti micrometriche, sul cui fondo AB è fissato il quarzo Q. Il cilindro O, riempito di acqua ed immerso, come si è detto in acqua, é limitato all'estremo DC da una sottilissima lamina di cellofane ben tesa e di potere riflettente praticamente nullo: $R=1{,}86\cdot10^{-3}$ ($\nu = 1{,}8$ MHz).

La parete del cilindro O presenta lungo la generatrice CB una stretta fenditura ed in F è attraversata da un tubicino capillare attraverso il quale si fa fluire dell'acqua colorata con permanganato proveniente da una boccia di Mariotte. In assenza di ultrasuoni

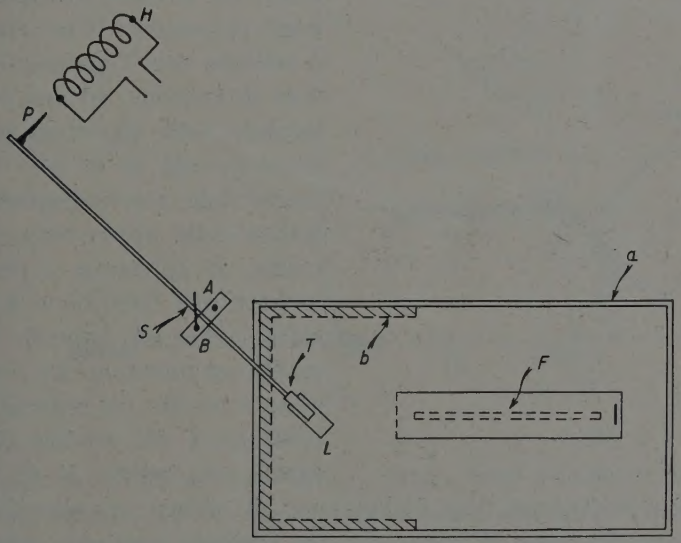

Fig. 5.

un filetto fluido rettilineo di velocità costante attraversa così il cilindro secondo un diametro (fig. 2).

È possibile, mediante una serie d'istantanee, effettuate ad intervalli di

tempo noti, procedere alla misura della velocità V_c di caduta del filetto nell'acqua (fig. 3, *a-b-c-d-e*).

Producendo gli ultrasuoni nel liquido, a causa del moto di insieme che questo acquista, il filetto fluido assume una diversa configurazione (fig. 4) dalla quale si può, conosciuta la V_c, ricavare il valore della velocità v acquistata dal liquido.

La misura della intensità I del fascio sonoro viene effettuata contemporaneamente alla misura di v. Nella vaschetta a (fig. 5), all'uscita del fascio ultrasonoro dal tubo, è disposta una laminetta L di Al, dello spessore di $5 \cdot 10^{-3}$ cm, fissata su di un tamburo T anche di Al, solidale con un pendolo di torsione a sospensione bifilare (nella figura i punti A e B rappresentano le tracce dei fili di sospensione).

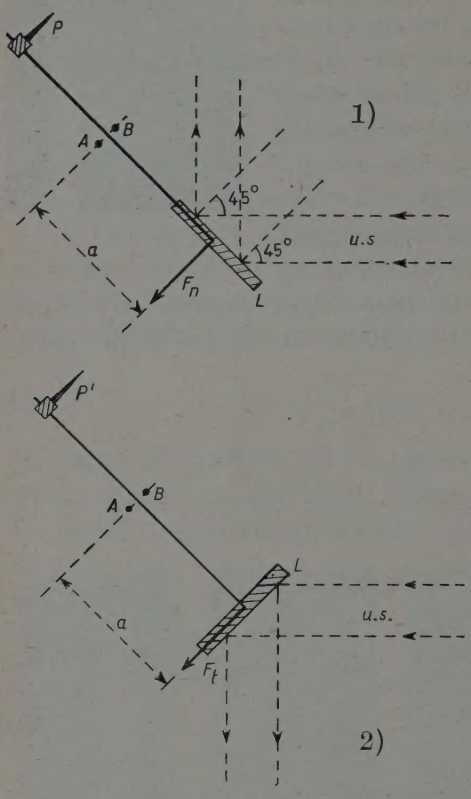

Fig. 6.

La lamina L può assumere, per mezzo di una rotazione di 90°, le due posizioni 1) e 2) (fig. 6) rispetto al fascio di ultrasuoni e le pareti laterali della vaschetta a (fig. 5) sono rivestite di materiale assorbente in modo da evitare riflessioni dannose degli ultrasuoni. Uno specchietto S è solidale con l'equipaggio del pendolo di torsione, ed una rotazione del pendolo viene registrata su carta sensibile avvolta su di un cilindro per mezzo dello stesso dispositivo già descritto nella prima nota. Per un momento M applicato al pendolo si registrerà una deviazione d tale che risulta: $M = kd$, essendo k una costante strumentale. La costante k è stata misurata nel seguente modo: all'estremo C del pendolo (di ottone) è fissata una punta P di ferro dolce (fig. 5) e ad una distanza fissa dall'estremo di questa un solenoide privo di nucleo di ferro nel quale si fa passare una corrente continua nota. Con una taratura preliminare è stata misurata, per mezzo di una bilancia di precisione, la forza attrattiva che si desta sulla punta P al variare della corrente i che circola nel solenoide. Applicando quindi sul pendolo un momento noto, misurata la deviazione, si conosce k; si è ottenuto: $k = 2{,}0$ (dine·cm/mm). La taratura viene però ripetuta ad ogni registrazione.

Proceduto alla taratura del sistema, si pone il pendolo nella posizione 1) registrando la deviazione che si produce per effetto degli ultrasuoni; in fig. 7 è riportata una di queste registrazioni: la curva *a* dà la misura della deviazione ottenuta applicando al sistema il momento noto. Contemporaneamente alla

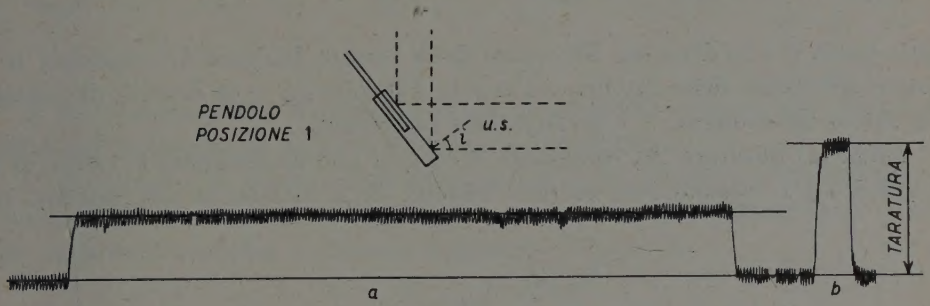

Fig. 7.

registrazione *a*, ad intervalli di tempo costanti si fotografa il filetto fluido. È interessante osservare che, contrariamente a quanto si verifica nelle registrazioni riportate a pag. 433 della prima nota, nelle attuali condizioni la devia-

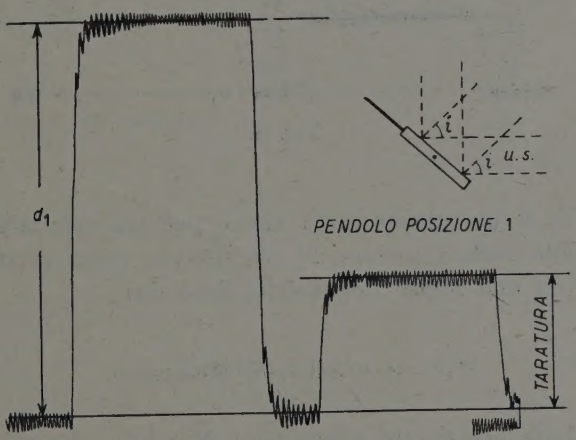

Fig. 8.

zione accusata dal pendolo è per tutta la durata degli ultrasuoni, perfettamente costante; sul pendolo agisce solo la forza dovuta alla pressione di radiazione, essendo, nelle attuali condizioni sperimentali, il moto d'insieme del liquido bloccato dalla finestra di cellofane.

R. Lucas [4] ha dimostrato che con la lamina nella posizione 1), per effetto

---

[4] R. Lucas: *Suppl. Nuovo Cimento*, 7, 236 (1950).

degli ultrasuoni compare sul pendolo un momento M_1 generato da una forza normale del valore:

$$M_1 = w \cdot a \cdot S(1 + R) \cos^2 i , \tag{2}$$

nella quale a è la distanza del centro della lamina dall'asse di rotazione, R il potere riflettente della lamina, i l'angolo d'incidenza, w la densità di energia del fascio ultrasonoro, S è la superficie interessata.

Dalla (2) misurato M, conosciuti R ed i, si può determinare il valore di w e quindi di I essendo $I = wc$ (c = velocità degli ultrasuoni nel liquido). La

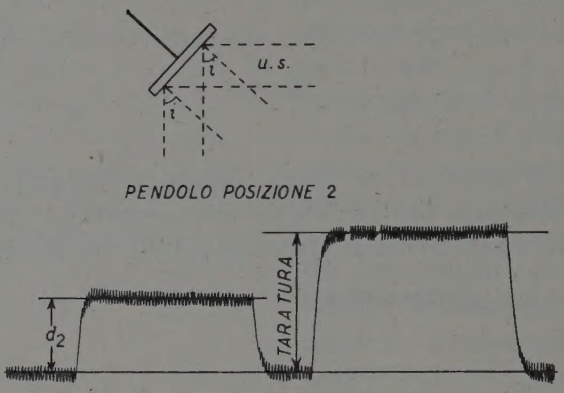

Fig. 9.

determinazione di R può essere fatta anche per via sperimentale ed infatti, ponendo il pendolo nella posizione 2) sul sistema compare un momento M_2 generato invece da una forza tangenziale, dato da:

$$M_2 = w \cdot a \cdot S(1 + R) \sin i \cos i . \tag{3}$$

Dalla (2) e dalla (3), tenuto conto che: $M = kd$ e che nel nostro caso è: $i = 45°$, si ottiene:

$$R = \frac{M_1 - M_2}{M_1 + M_2} = \frac{d_1 - d_2}{d_1 + d_2} .$$

Nella fig. 8 si riporta una registrazione ottenuta col pendolo nella posizione 1 e nella fig. 9 invece una registrazione ottenuta col pendolo nella posizione 2.

I risultati ottenuti con l'acqua, per $\nu = 1{,}8$ MHz e con $G = 0{,}553$ sono riportati nella seguente tabella:

v_c cm/s	w erg/cm^3	I erg/cm^2·s	R	v cm/s	$\frac{\eta'}{\eta}$
0,14	0,25	3,74	0,69	$5\ 10^{-2}$	2,42

È da osservare che il risultato ottenuto concorda abbastanza bene con quello del LIEBERMANN ($\eta'/\eta = 2{,}30$ per $\omega = 5$ MHz).

Ci proponiamo di procedere ad ulteriori misure del rapporto η'/η per l'acqua e per altri liquidi, con questo metodo di misura molto più preciso e più vicino alle condizioni teoriche, a diverse frequenze.

SUMMARY (*)

This paper relates on a method for the determination of the ratio η'/η and results are gives for water at the frequency $\nu = 1{,}8$ MHz.

(*) *Traduzione a cura della Redazione.*

IL NUOVO CIMENTO Vol. I, N. 3 1° Marzo 1955

Phenomenological Study of the New Particles. Λ-Particles and Λ-Nuclei.

R. Gatto

Istituto di Fisica dell'Università - Roma
Istituto Nazionale di Fisica Nucleare - Sezione di Roma

(ricevuto il 29 Dicembre 1954)

Summary. — Some questions on the new unstable particles are discussed, with the deliberate avoidance of any very specific assumption. The slowness of the decay rates imposes, by semi-qualitative arguments, relevant restrictions. We try to develop fully such a viewpoint, and conclusions are drawn about production processes, about processes in which the excited hyperon takes part, and about processes which occur after the capture of a heavy meson or a hyperon by a nucleus. The important question is here to know what other independent assumptions must be added to that of the long mean lives to get a consistent scheme. The Λ^0-nuclei are moreover analyzed from a more phenomenological standpoint. The implications of this analysis on the high spin model of the Λ^0 are discussed. The arguments, of course, are not strictly quantitative; however their possible failure would be in any case an interesting conclusion. The possible composite nature of the new particles is briefly discussed in connection with the role of weak interactions and with the possible validity of charge independence at production. Charge independence at decay is not expected to hold and this question is discussed in the case of the θ^0-meson.

Introduction.

In the last few years a considerable amount of data has been collected on the new unstable particles. Of some of them it has been possible to measure accurately the mass, the charge, the mean life, and to establish the precise decay scheme. Of others the existence is not definitely ascertained, or in some

cases the decay scheme is poorly understood. Some precise information is already available concerning other experimental aspects, such as production, capture and interaction with nuclei. Perhaps some time will be necessary before we can have secure information on the parities and on the spins (this problem is somewhat simpler in the case of the τ-meson), and on the possible isotopic spins.

Although the experimental data are still incomplete, some typical traits of the phenomenology of the new particles have already appeared in a very definite form. The copious production, which seems to be in contrast with the long mean lives, constitutes perhaps the most suggestive aspect of this phenomenology. Closely connected are other aspects, rather singular *per se*, such as the too frequent occurrence of double production, the evidence of a relatively stable bond of some hyperons with nucleons, cascade disintegrations, and other aspects which will be discussed in the following. At present the possibility of a clear theoretical systematization of these phenomena seems rather distant. However we think that the occurrence of such a singular phenomenology already offers an opportunity for profitable discussion.

1. – A General Discussion.

1·1. *A semi-phenomenological approach.* – We would like to begin by giving a semi-phenomenological approach to these problems, which has been so far more or less explicitly adopted in all the theoretical discussions [1]. In the absence of an accepted theoretical background for the subject, it offers, at least, a definite language for enunciating the main problems. Essentially, this approach uses the general properties of the S matrix and certain regularity hypotheses which will be specified as they occur. The general properties of the S matrix express some general theorems of undisputed validity, such as the conservation of the normalization of the wave function in time (unitarity of the S matrix), the reciprocity theorem (symmetry of the S matrix), and the well-known mechanical conservation theorems (invariance of the S matrix under Lorentz transformation). The regularity hypotheses have to do with, for example, the behaviour of the matrix elements for different values of the orbital angular momenta, or they are more or less plausible order of magnitude considerations. For example, it will be supposed in some cases that the matrix element for a reaction, which can be thought of as the result of other reactions considered as inter-

---

[1] A. PAIS: *Phys. Rev.*, **86**, 663 (1952); *Physica*, **19**, 869 (1953); M. GELL-MANN: *Phys. Rev.*, **92**, 833 (1953).

mediate steps, is large if the matrix elements for the intermediate steps are large. Such a reasoning would be generally, but not necessarily, correct if perturbation theory were applicable. Similarly, it will be supposed in some cases that the matrix element for $a = \bar{b} + c + d$ is large if the matrix element for $a + b = c + d$ is large, $\bar{b}$ denoting the charge conjugate of b. Hypotheses of this kind are not necessarily verified as are the general properties of the S matrix. We shall not attempt here to give any justification of them. The only point we want to note is that in the discussion of the data on the new particles one finds an extremely sharp distinction between fast processes and very slow processes. [For example, the measured cross-section for hyperon production in pion-nucleon collisions is an appreciable fraction of the total cross-section. A recent experiment with the cosmotron has given a cross-section of the order of 1 mb for the production processes $\pi^- + p \to Y + K$ at 1.5 GeV (2). At the same energy the cross-section for the elastic π^--p processes is believed to be of the order of one fourth of the total interaction cross-section (3). For this last cross-section a recent attenuation experiment has given a value of about 34 mb at 1.5 GeV (4). Therefore one expects a cross-section of the order of 8 mb for the elastic π^--p processes at 1.5 GeV. At this energy the ratio between the statistical weight of the final state consisting of an hyperon and K-particle and the statistical weight of the final state consisting of a pion and a nucleon is about one half, ignoring spin and isotopic spin multiplicities. If the matrix elements for the two processes were equal, one would therefore expect a cross-section of the order of 4 mb for the first process, in rough agreement with the proposed value of 1 mb (5). On the other hand, the mean life of the produced hyperon is a factor of the order of 10^{10}-10^{13} longer than the expected mean life for a strongly interacting particle]. Therefore the regularity hypotheses mentioned above do not need to be valid with great accuracy in order to draw presumably correct conclusions.

1·2. *Production processes.* – All the possible decay processes, if not forbidden, are slow processes. This follows directly from the fact that the new particles have long mean lives. It is easy then to recognize, assuming the regularity hypotheses, that any process leading to single production (such as: nucleon + + nucleon → nucleon + hyperon, nucleon + nucleon → nucleon + nucleon + heavy meson, pion + nucleon → pion + hyperon, pion + nucleon → heavy meson + nucleon) must be slow. If, in fact, a process leading to the single production of

---

(2) W. B. FOWLER, R. P. SHUTT, A. M. THORNDIKE and W. L. WHITTEMORE: *Phys. Rev.*, **93**, 861 (1954).

(3) W. D. WALKER and J. CRUSSARD: *Bull. Am. Phys. Soc.*, **29**, 7 (1954).

(4) R. L. COOL, L. MADANSKI and O. PICCIONI: *Phys. Rev.*, **93**, 637 (1954).

(5) Taken from: C. CASTAGNOLI and R. GATTO (unpublished report).

a new particle were a fast process, there would be at least one fast decay process for the new particle, in contrast with the long mean life. On similar arguments one cannot exclude that some of the double production processes (such as: nucleon + nucleon → hyperon + hyperon, nucleon + nucleon → heavy meson + hyperon + nucleon, pion + nucleon → heavy meson + hyperon, pion + nucleon → heavy meson + heavy meson + nucleon) are fast. The evidence of a copious production requires that some of these processes be fast. There exists considerable evidence ([6]) that the double production process pion + nucleon → heavy meson + hyperon is extremely favoured with respect to the single production process pion + nucleon → pion + hyperon, which up to now has not been directly observed.

The conclusion that single production processes must be slow thus follows from the assumed regularity hypotheses. If experiment were to give evidence of copious single production, this would mean that some of the assumed regularity hypotheses are not valid. Such a conclusion would be, *per se*, very important.

1·3. *The hyperon* Y* *and remarks concerning its production.* – The mere distinction between slow and fast processes, and the character of the assumed regularity hypotheses, would seem to indicate a simple odd-even rule. It is known, for instance, that in the first model proposed by PAIS ([1]) such a rule was obtained by the introduction of a suitable isotopic parity. Actually it does not seem that an odd-even rule can explain all the known facts. Among the slow decay processes one has been observed which deserves some interest in this respect. It is the decay of a heavy hyperon, which we will call Y*, into a lighter hyperon Y with the emission of a pion ([7]). The mean life is again of the order of 10^{-10} s. An odd-even rule would still be sufficient to discourage the process Y → nucleon + pion, but then one of the processes Y* → Y + pion, or Y* → nucleon + pion, would be fast.

It is of interest at this point to study the possible consequences of the fact that the decay processes of the Y* are slow processes. Of course, these conclusions, as well as the preceding ones, will also be subject to the limitations implicit in assuming regularity hypotheses which are not necessarily valid. It still follows that single production processes must be slow, while, observed cop-

---

([6]) See reference ([1]); and R. W. THOMSPON, J. R. BURWELL, R. W. HUGGEF and C. J. KARKMARK: *Phys. Rev.*, **95**, 1576 (1954).

([7]) R. ARMENTEROS, K. H. BARKER, C. C. BUTLER, A. CACHON and C. M. YORK: *Phil. Mag.*, **43**, 597 (1952); C. M. YORK, R. B. LEIGHTON and E. K. BJORNERUD: *Phys. Rev.*, **90**, 167 (1953); C. D. ANDERSON, E. W. COWAN, R. B. LEIGHTON, V. A. J. VAN LINT: *Phys. Rev.*, **92**, 1089 (1953); E. W. COWAN: *Phys. Rev.*, **94**, 161 (1954); W. B. FRETTER and W. FRIESEN: *Bull. Am. Phys. Soc.*, **29**, 9 (1954).

ious production is presumably, due to some fast double production processes. Further limitations however appear. For example, the two production processes, nucleon + nucleon $\rightarrow$ Y* + Y, and nucleon + nucleon $\rightarrow$ Y + Y, can not both be fast. The point to be noted is that these processes, if supposed to be fast, would not by themselves directly contradict the long mean lives. The possibility *that they are simultaneously fast* can, instead, be contrasted with the fact that the process Y* $\rightarrow$ Y + pion is a slow process.

1·4. *Interaction with nucleons.* – Conclusions can also be drawn for the cases of capture by nuclei. For example, the mean life of the τ^- is presumably long enough to allow capture in a Bohr orbit by an emulsion nucleus. Interaction with nucleons will then occur by processes of the kind:

$$\text{(I)} \quad \tau^- + \text{nucleon} \rightarrow \text{nucleon} + \tau \text{ (or } \theta, \ldots),$$

$$\text{(II)} \quad \begin{cases} \tau^- + \text{nucleon} \rightarrow \text{hyperon} + \text{pion } (+ \text{ pion}) \\ \tau^- + \text{nucleon} + \text{nucleon} \rightarrow \text{hyperon} + \text{nucleon } (+ \text{ pion } (+ \text{ pion})), \end{cases}$$

These processes may well be fast, while processes of the kind

$$\tau^- + \text{nucleon} \rightarrow \text{nucleon} + \text{pion } (+ \text{ pion } (+ \text{ pion})),$$

$$\tau^- + \text{nucleon} + \text{nucleon} \rightarrow \text{nucleon} + \text{nucleon } (+ \text{pion } (+ \text{pion } (+ \text{pion})))$$

should be slow, as they would lead to a fast decay of the τ^-. The processes (II) would lead to a rapid disintegration of the capturing nucleus. The first of these two processes has been sometimes postulated ([8]). It is perhaps the main process in the case of capture by an hydrogen nucleus. However for heavier nuclei the second also should play a role. In this connection a study of the stars produced would be very useful.

Now let us consider the capture of a negative hyperon. We first examine the nuclear interactions of the suggested Y^-, having a same mass as the established Y^+. The process

$$Y^- + \text{nucleon(s)} \rightarrow \Lambda^0 + \text{nucleon(s)}$$

is energetically possible, and may well be fast. It would lead to a rapid disintegration of the capturing nucleus. In the case of a Y^{*-} captured by a

([8]) M. GOLDHABER: *Phys. Rev.*, **92**, 1279 (1953); H. DE STAEBLER: *Phys. Rev.*, **95**, 1110 (1954).

nucleus, it must first be noted that the analogous process

$$Y^{*-} + \text{nucleon(s)} \to Y + \text{nucleon(s)} \ (+ \text{pion})$$

must be a slow one, in order to avoid rapid decay of the Y* into a Y. However the process

$$Y^{*-} + \text{nucleon(s)} \to \Lambda^0 + \Lambda^0 \ (+ \text{nucleons})$$

is energetically permitted, and it cannot be excluded that it is fast by our regularity hypotheses only. [This process may thus lead to a rapid disintegration of the capturing nucleus. This is perhaps the right place to make the following remark. Suppose the process nucleon + nucleon $\to \Lambda^0 + \Lambda^0$ were found to be fast. It would follow, by our regularity hypotheses, that the process $Y^* +$ nucleon $\to \Lambda^0 + \Lambda^0$ is slow to avoid fast decay of the Y* into a nucleon and a pion. The argument can be reversed. If $Y^* +$ nucleon $\to \Lambda^0 + \Lambda^0$ were proved to be fast, for instance through an analysis of the capture process, then nucleon + nucleon $\to \Lambda^0 + \Lambda^0$ can not be fast. This is an example of the many interesting conclusions which may be inferred if one adds some other *independent* assumption to that of long mean lives and then uses the regularity hypotheses. We believe that a first point of attack for future theory may be to discuss the possible independent assumptions which can be added, in a consistent way, to the requirement of long mean lives, and the consequences which would follow using the regularity hypotheses. For instance, which of the allowed production processes are in fact fast? Of course, the final answer will come from experiment]. Coming back to our discussion, we see that, in any case of capture of negative hyperons by nuclei, a rapid disintegration cannot be excluded by our regularity hypotheses. The opposite conclusion can be drawn in the case of a Λ^0 bound to a nucleus. Such a situation is realized by the unstable fragments found recently in nuclear emulsion. Detailed discussion will be given in a next section.

1·5. – We have shown, in these sections, how the consistent use of the regularity hypotheses leads to a number of very important predictions about production and interaction with nucleons. Similar reasoning may be applied to any case of interest. All predictions seem in remarkable agreement with experiment so far. No attempts have been made to justify the regularity hypotheses. We consider that this semi-phenomenological approach may turn out to be of great help in the discussion of the experimental data.

The deductive line of reasoning is to start from the observed slowness of the decay rates and then to conclude that other processes must be slow in order to account for it. Of course, we do not know if this procedure will be sufficient to make slow all processes which future experiments will reveal

as slow. It may happen that further experiments will reveal that some of the processes, which are not necessarily slow by our argument, are in fact slow processes. Such a situation, for example, is suspected to occur for the pair production process nucleon + nucleon → hyperon + hyperon. It would mean that our starting point is still insufficient and should accordingly be enlarged.

2. – Λ-nuclei.

2·1. *The unstable heavy fragments.* – Many examples have been found of heavy fragments which are emitted from cosmic ray stars, come to rest in the emulsion, and then disintegrate after a mean life of the order of 10^{-12} s or longer. The first example was found by DANYSZ and PNIEWSKI ([9]); other examples have been reported later by different groups ([10]). The relatively large number of examples found definitely excludes the possibility of change coincidences. The first point to be noted is that any explanation of the phenomenon in terms of the purely nuclear motion of the nucleons in the fragment is excluded by the very long lifetime: the lifetime of a highly excited nuclear state is much shorter than 10^{-12} s. The possibility that the fragment may be a mesonic ion, which successively disintegrates after the meson is absorbed, has been considered. A direct refutation of this interpretation rests on the measured energy release of the fragment, which in some cases is definitely above 140 MeV.

A very convincing explanation which has been advanced for this phenomenon is to consider these fragments as bound systems (such as a nucleus) consisting of ordinary nucleons and one Λ^0. Such a bound system consisting of nucleons and a Λ-particle will be denoted as a Λ-nucleus. A Λ^0-nucleus can be considered as an ordinary nucleus in which a Λ^0 has been substituted

([9]) M. DANYSZ and J. PNIEWSKI: *Phil. Mag.*, **44**, 348 (1953).

([10]) D. A. TIDMAN, G. DAVIES, A. J. HERTZ and R. M. TENNENT: *Phil. Mag.*, **44**, 350 (1953); G. CRUSSARD and D. MORELLET: *Compt. Rend.*, **236**, 64 (1953); G. LOVERA, L. BARBANTI-SILVA, C. BONACINI, C. DE PIETRI, R. PERILLI-FEDELI and A. ROVERI: *Nuovo Cimento*, **10**, 986 (1953); P. S. FREIER, G. W. ANDERSON and J. E. NAUGLE: *Phys. Rev.*, **94**, 677 (1954); R. D. HILL, E. O. SALANT, M. WIGDOFF, L. S. OSBORNE, A. PEVSNER and D. M. RITSON, J. CRUSSARD and W. D. WALKER: *Bull. Am. Phys. Soc.*, **29**, 60A (1954); A. BONETTI, R. LEVI-SETTI, M. PANETTI, L. SCARSI and G. TOMASINI: *Nuovo Cimento*, **11**, 330 (1954); **11**, 210 (1954); P. CIOK, M. DANYSZ and J. GIERULA: *Nuovo Cimento*, **11**, 436 (1954); W. F. FRY and G. R. WHITE: *Nuovo Cimento*, **11**, 551 (1954); P. H. BARRETT: *Phys. Rev.*, **94**, 1328 (1954); J. E. NAUGLE, P. S. FREIER and E. P. NEY: *Phys. Rev.*, **96**, 829 (1954); W. F. FRY and M. S. SWAMI: *Phys. Rev.*, **96**, 809 (1954); F. FRY, J. SCHNEPS and M. S. SWAMI: *Bull. Am. Phys. Soc.*, **29**, W4 (1954); M. BALDO, G. BELLIBONI, M. CECCARELLI, M. GRILLI, B. SECHI, B. VITALE and G. T. ZORN (preprint) Rome group (o be published).

for a neutron. The processes which may occur between the Λ^0 and the nucleons in the Λ^0-nucleus may be of the type

$$\text{(I)} \quad \Lambda^0 + \text{nucleon} \rightarrow \Lambda^0 + \text{nucleon}$$

or of the type

$$\text{(II)} \quad \Lambda^0 + \text{nucleon} \rightarrow \text{nucleon} + \text{nucleon} + \text{pion}$$

$$\text{(II}') \quad \Lambda^0 + \text{nucleon} \rightarrow \text{nucleon} + \text{nucleon} .$$

This follows from simple energy considerations and from heavy particle conservation. The discussion in the preceding section suggests that (I) can well be a fast process, while (II) and (II′) ought to be slow since they would lead to a rapid decay of the Λ^0. There are thus two important conclusions to be drawn from this analysis: (i) there exists a presumably fast elastic process, (I), which can give rise to a strong binding of the Λ^0 with nucleons; (ii) the Λ^0-nucleus can disintegrate by way of inelastic reactions of the type (II) (meson decay) or of the type (II′) (non-mesonic decay), which are the only ones energetically permitted: they are presumably slow, since if they were fast they would lead to a fast decay of the Λ^0. As one sees, these deductions are in accord with the existence of Λ^0-nuclei (that is, there exists a strong binding between the Λ^0 and the nucleons) having a long lifetime on the order of 10^{-12} to 10^{-10} s (that is, only slow processes may produce the disintegration).

Of the two decay schemes permitted, the non-mesonic would be favoured with respect to the mesonic as the mass number of the Λ^0-nucleus increases ([11]). In the case of non-mesonic decay, the charged secondaries should be either low energy protons with one very energetic proton among them (if the Λ^0 interacts with a proton) or all low energy protons. The experimental evidence confirms the existence of both decay schemes, mesonic decay for light Λ^0-nuclei, and non-mesonic decay for the heavier Λ^0-nuclei. Conclusive evidence in favour of this interpretation of the fragments as Λ^0-nuclei is to be found in the consistency of the Q-values observed; excluding exceptional cases, the Q value is unique and of the order of the Q value of the free Λ^0-decay (including the mass of the meson in the case of non-mesonic decay).

2·2. *A purely phenomenological analysis.* – The behaviour of the Λ^0 in the Λ-nucleus can be studied in more detail. The lifetime of the Λ^0-nucleus is of the order of 10^{-12} to 10^{-10} s. A very large number of collisions between the Λ^0 and the nucleons occur during this time interval. An accurate estimate of this number is not necessary. The mean free path between two successive

([11]) W. Cheston and H. Primakoff: *Phys. Rev.*, **92**, 1537 (1953).

collisions can certainly not be greater than the dimension of the Λ^0-nucleus. (The dimensions of a Λ^0-nucleus may be greater than an ordinary nucleus, but the difference will not be such as to alter the validity of the following arguments). Thus the time between two successive collisions will be of the order of 10^{-23} to 10^{-21} s. As one sees the mean life of the Λ^0-nucleus is longer by a factor of about 10^9 to 10^{13}. Thus there will be a very large number of collisions, of the order of 10^9 to 10^{13}, between the Λ^0 and the nucleons before the fragment disintegrates. On the one hand, we are led to suppose a strong elastic interaction between the Λ^0 and the nucleons. The intensity of the interaction is presumably weaker than in the nucleon-nucleon case, but the difference will not be such as to alter the order of magnitude. (In some cases it has been possible to measure the binding energy of the Λ^0 in the fragment from the energy-momentum balance. The binding energies thus measured are of the order of one MeV; in any case less than the binding energy of a neutron, but not very different in magnitude). On the other hand, to explain the long life of the Λ^0-nucleus, we must suppose that the inelastic interaction between the Λ^0 and the nucleons, which leads to the decay of the Λ^0 into an ordinary nucleon, is much smaller than the elastic interaction. In other terms, the Λ^0 will be elastically scattered by a nucleon with a cross-section not much less than geometric, and will only very rarely disintegrate as a result of a collision with a nucleon. The ratio of these two cross-sections will be on the order of 10^9 to 10^{13}.

Some consequences of the above remarks can be derived using the reciprocity theorem. We have been led to the conclusion that the cross-section for the process $\Lambda^0 + \text{nucleon} \to \text{nucleon} + \text{nucleon}$ must be very small. From the reciprocity theorem we get a relation between the total unpolarized cross-sections for the two processes $\text{nucleon} + \text{nucleon} \to \Lambda^0 + \text{nucleon}$ and $\Lambda^0 + \text{nucleon} \to \text{nucleon} + \text{nucleon}$

$$\sigma(\mathrm{NN} \to \Lambda^0\mathrm{N}) = (2S+1)[1+(m/M)]^{-1}[\varepsilon/(\varepsilon+Q)]\,\sigma(\Lambda^0\mathrm{N} \to \mathrm{NN})\,.$$

Here S is the spin of the Λ^0, m the mass of the nucleon, M the mass of the Λ^0, ε is the total kinetic energy of $\Lambda^0 + \mathrm{N}$ in the centre of mass system, Q the energy liberated in the reaction $\Lambda^0 + \mathrm{N} \to \mathrm{N} + \mathrm{N}$, of the order of 178 MeV; $\varepsilon + Q$ is the total kinetic energy of $\mathrm{N} + \mathrm{N}$ in the centre of mass system. Thus the cross-section for the process $\text{nucleon} + \text{nucleon} \to \Lambda^0 + \text{nucleon}$ must be very small, at least for energies not much above threshold. It must be noted that if an appreciable abundance of singly produced Λ^0 in nucleon-nucleon collisions should be observed for not too high energies, the interpretation of the fragments as Λ^0-nuclei will have to be reexamined. This does not seem to be the case at present. The artificial production of hyperons in meson-nucleon collisions is by now definitely ascertained and is known to occur with a large

cross-section (on the order of 1 mb). Instead, in the case of nucleon-nucleon collisions the experimental evidence suggests that not only are single production processes of the type nucleon + nucleon → hyperon + nucleon very infrequent, but also that pair production processes of the type nucleon + nucleon → → hyperon + hyperon are very rare. Presumably the production scheme in nucleon-nucleon collisions is of the type nucleon + nucleon → nucleon + hyperon + heavy meson.

Concluding, we wish to recall the important inference which has been drawn in this section from the existence of unstable Λ^0-nuclei, having a relatively long lifetime. The process Λ^0 + nucleon → nucleon + nucleon must be a slow process, at least for the relative energies which may be reached in the purely nuclear motion, in order to account for the long lifetime of the Λ^0-nucleus. The reciprocity theorem tells us that the inverse process must also be slow. Differently from the conclusions of the preceding sections, this conclusion does not use any of the regularity hypotheses. Rather, it rests on the simplified description we have used of the Λ^0-nucleus. Of course, the same conclusions would follow from the regularity hypotheses and from the long life of the free Λ^0. Our further object will be to look for the implications on possible models of the Λ^0.

3. – The High Spin Model of Λ^0.

3·1. – As we have seen, further evidence for supposing a strong interaction between Λ^0's and nucleons, besides the frequent production, is the strong binding of the Λ^0 in the Λ^0-nucleus, which, although smaller, is still of the same order of nuclear binding. The coupling of the Λ^0 with the meson field should not be much weaker than the coupling of the nucleons with the meson field. A first guess as to the order of magnitude of the lifetime of the Λ^0 having a strong interaction with the meson field would be $(\hbar/pc)(\hbar c/g^2)$, p denoting the relative momentum of the two final particles and g the coupling constant; thus, a lifetime of about 10^{-23} s. This value is smaller than that observed by a factor of 10^9 to 10^{13}. One sees that the order of magnitude of this factor is about the same as that deduced above for the ratio between the elastic scattering of the Λ^0 in the Λ^0-nucleus and the inelastic scattering, which leads to the disintegration of the fragment. This evaluation of the lifetime could be mistaken even if the hypothesis of a strong interaction with mesons were essentially right. There is an observation worth noting by SACHS [12] on this point. If hyperons are to be regarded as excited nucleons, a complex structure should be assumed as result of their strong interaction with the meson field.

---

[12] R. G. SACHS: *Phys. Rev.*, **84**, 305 (1951).

States containing up to a large number of pions should occur, and this diminishes the probability of occurrence of the particular state which leads to disintegration. The point of view adopted by other authors (PAIS, GELL-MANN) is to consider the long lifetimes as indicative of one or more weak selection rules. These would slow down the decay processes and would weaken single production. Conclusions from such theories are in general of a more specific character than those reached through our semi-phenomenological approach.

We would like to discuss here an alternative point of view, which has been suggested from early times to account for the long lifetimes of the new particles. It assumes that the new particles have large spins. The transition probabilities would then be strongly influenced in some cases by the appearance of large orbital angular momenta. This mechanism could explain the long lifetimes, and moreover it would lead to the predominance of double production over single production for production processes at low energy. At high energy, where short wavelengths and thus high orbital angular momenta occur, the mechanism would be less efficient and thus single production, for instance, would be no longer discouraged.

3·2. *Decay of* Λ^0. – Consider the decay of a Λ^0 at rest

$$\Lambda^0 \to \mathrm{p} + \pi^- .$$

We assign to the Λ^0 a spin S and a well defined parity P with respect to the proton. The parity is defined as follows. The final state will in general consist of a superposition of states of well defined relative orbital angular momentum between the final particles. In this superposition there can enter either only even orbital angular momenta or only odd orbital angular momenta. For a given spin S there can be only a single relative orbital angular momentum between the two particles. Further, the intrinsic parity of the pion is negative. If the relative orbital angular momentum is odd the parity P will be even, and viceversa. Table I shows for each value of the spins S and for each parity P the unique value $\boldsymbol{l}$ of the relative orbital angular momentum between the proton and the negative pion permitted by angular momentum and total parity conservation.

We use a non-relativistic approximation, presumably justified at these energies. The great simplification of the non-relativistic approximation consists in writing the wave function as the product of a space part and a spin part, which would not be correct in the relativistic case. Let S be the spin of the Λ^0 and m_s its component. This completely characterizes the initial state. To individuate the final state it is sufficient to assign the direction, with the unit vector $\boldsymbol{n}$, of the momentum of one of the two emerging particles (the

momentum of the other particle must be equal and opposite and its absolute value is fixed), and to assign the component m_s of the proton spin ($s = \frac{1}{2}$).

TABLE I.

S	P	l
$\frac{1}{2}$	$+1$	1
	-1	0
$\frac{3}{2}$	$+1$	1
	-1	2
$\frac{5}{2}$	$+1$	3
	-1	2
$\frac{7}{2}$	$+1$	3
	-1	4
$\frac{9}{2}$	$+1$	5
	-1	4
$\frac{11}{2}$	$+1$	5
	-1	6
$\frac{13}{2}$	$+1$	7
	-1	6

The decay will be described by the element $\langle f|T|i\rangle$ of the general transition matrix. To take advantage of the rotational and reflection invariance of T we transform to the representation where the total angular momentum J and its component m_J are diagonal, together of course with energy,

$$\langle f| = \langle \boldsymbol{n} s m_s| = \sum_{l m_l J m_J} \langle \boldsymbol{n} s m_s | l s m_l m_s\rangle \langle l s m_l m_s | l s J m_J\rangle \langle l s J m_J|$$

where l is the relative orbital angular momentum between the final proton and pion, and m_l its component. Making use of the rotational invariance of T, the transition matrix element becomes

$$\langle f|T|i\rangle = \langle \boldsymbol{n} s m_s|T|S m_S\rangle = \sum_{l m_l} \langle l s m_l m_s | l s S m_S\rangle Y_l^{m_l}(\boldsymbol{n}) T(l) \,,$$

where $T(l) = \langle l s S m_S|T|S m_S\rangle$ is the matrix element from the initial state to the final state where particles have a relative orbital angular momentum l. The addition coefficient $\langle l s m_l m_s | l s S m_S\rangle$ is different from zero for only two values of l, $l = S - \frac{1}{2}$ and $l = S + \frac{1}{2}$, and for only one value of m_l, $m_l = m_S - m_s$. Further $T(l)$ will be different from zero only for that particular value of l, $\boldsymbol{l}$, among the two preceding ones, which permits conservation of total parity ($\boldsymbol{l}$

given in Table I) ([13]). Using the well-known properties of addition coefficients, the mean lifetime τ for the decay of the free Λ^0 into a proton and a pion is found to be

$$\frac{1}{\tau} = \sum_{l=S-\frac{1}{2}}^{S+\frac{1}{2}} |T(l)|^2 = |T(\boldsymbol{l})|^2 .$$

In the absence of a theory for the dependence of $T(\boldsymbol{l})$ on $\boldsymbol{l}$, we can only give the usual order of magnitude estimations. We suppose that some average of the final wave function in the region where the interaction takes place gives the principal dependence on $\boldsymbol{l}$ of the matrix element $T(\boldsymbol{l})$. A regular behaviour of the matrix element is in the spirit of a theory which tries to explain the whole story of the new particles in terms of large spins only. We assume that the interaction region extends to some radius r_0, and that r_0 is

---

([13]) As a consequence the angular distribution follows directly from geometrical considerations only. Using the well-known Racah technique we get, after summing over final polarizations

$$f_{m_S}(\cos\theta) = \sum_{m_{l/2}} |\langle \boldsymbol{n}\tfrac{1}{2}m_{\frac{1}{2}}|T|Sm_S\rangle|^2 =$$

$$= \mathcal{C} \sum_L \langle \boldsymbol{ll}00|\boldsymbol{ll}L0\rangle\langle SLm_S0|SLSm_S\rangle W(S\boldsymbol{l}S\boldsymbol{l}\tfrac{1}{2}L) Y_{L0}(\cos\theta)$$

where $\mathcal{C}$ is a normalization constant and $W(S\boldsymbol{l}S\boldsymbol{l}\frac{1}{2}L)$ is a Racah coefficient (given by $\alpha(-)^l(2\boldsymbol{l}+L+2)^{\frac{1}{2}}(2\boldsymbol{l}-L+1)^{\frac{1}{2}}$ for $\boldsymbol{l}=S-\frac{1}{2}$, and by $\beta(-)^{L+1}(2\boldsymbol{l}+L+1)^{\frac{1}{2}}(2\boldsymbol{l}-L)^{\frac{1}{2}}$ for $\boldsymbol{l}=S+\frac{1}{2}$, α and β being constants independent of L). The addition coefficient $\langle \boldsymbol{ll}00|\boldsymbol{ll}L0|$ limits the summation to even values of L (conservation of parity) from 0 to $2\boldsymbol{l}$. However, when $\boldsymbol{l}=S+\frac{1}{2}$, the triangular condition for the other addition coefficient can not be satisfied for $L=2\boldsymbol{l}$, and so the summation is in any case interrupted at $L=2S-1$, irrespective of the parity of the Λ^0. Thus, for the particular case $S=\frac{1}{2}$, one always gets an isotropic distribution (independent of the polarization). We can give a more general proof of this statement, which is only based on elementary concepts. Consider the two-body decay of a spin $\frac{1}{2}$ particle in its rest system. We immagine a statistical ensemble of such decays, assuming that the decaying particle has « spin up ». We call N_+ the number of events with the relative momentum of the final particles in a fixed direction $\boldsymbol{n}$. Obviously N_+ may only depend on μ_+, the cosine of the angle formed by $\boldsymbol{n}$ with the direction of the spin of the decaying particle. Moreover the final state has a well defined parity, therefore the module square of the coefficient which gives the probability of decay into $\boldsymbol{n}$, must be an even function of μ_+. Now consider the same statistical ensemble but assume this time that the decaying particle has « spin down », and call N_- the number of events with the relative momentum of the final particles in the fixed direction $\boldsymbol{n}$. Since the spin direction has been reversed the cosine of the angle formed by $\boldsymbol{n}$ with the direction of the spin of the decaying particle is now $\mu_- = -\mu_+$. But N_- will be the same function of μ_- as N^+ was of μ_+. Such function being even, it follows that $N_- = N_+$. Now imagine the statistical ensemble formed by the superposition of the two. The total number of events going into $\boldsymbol{n}$ will be independent of $\boldsymbol{n}$. This number is given by $N_+ + N_- = 2N_+$. Therefore it follows that N_+ (N_-) does not depend on $\boldsymbol{n}$.

sufficiently smaller than $\lambda\!\!\!^{-} = \hbar/p$, so that keeping only the first term of the expansion of $j_l(kr)$ near the origin does not change the order of magnitude. The dependence on r_0 is, of course, very sensitive. Taking for r^0 the Compton, wavelength of the Λ_0 it is estimated that with spin values from 5/2 to 9/2 the matrix element is sufficiently diminished to explain the mean life. However it would seem more justifiable to choose an r_0 of about 1/3 of the Compton wave length of the meson. In this case it is estimated that a spin value from 7/2 to 11/2 may explain the mean life.

3·3. *Non-mesonic decay of* Λ^0*-nucleus.* – We now wish to study the reaction $\Lambda^0 +$ nucleon $\rightarrow$ nucleon + nucleon, which presumably is that leading to the non-mesonic decay of the Λ^0-nucleus. To be definite we consider the collision, in the centre of mass system, of the Λ^0 with a proton. The two final nucleons will be a neutron and a proton. We use a non-relativistic approximation. The spin s of the initial channel may assume the two values $S - \frac{1}{2}$ and $S + \frac{1}{2}$. The spin s' of the final channel will be 0 or 1. In the centre of mass system, the initial state is completely defined if the total kinetic energy ε of the initial particles, a unit vector $\boldsymbol{n}$, for example in the direction of the colliding Λ^0, the spin s and its component m_s are given. The kinetic energy ε' of the final state is given simply by $\varepsilon + Q$, where Q is about 178 MeV. The final state is thus completely defined if the unit vector $\boldsymbol{n}'$, for example in the direction of the escaping neutron, the spin s' of the final channel and its component $m_{s'}$ are given. The process will be described by the element $\langle f|T_{\mathrm{I}}|i\rangle$ of the general transition matrix. For convenience suppose T_{I} to be defined so that $\varrho_{\mathrm{I}}(f)\,|\langle f|T_{\mathrm{I}}|i\rangle|^2$ gives the cross-section, $\varrho_{\mathrm{I}}(f)$ being the density of the final states per unit energy and per unit solid angle. In order to use the invariance of T_{I} for space rotation and reflection, we transform to the representation where the total angular momentum and its component are diagonal

$$|i\rangle = |\boldsymbol{n}sm_s\rangle = \sum_{Jm_J lm_l} |lsJm_J\rangle\langle lsJm_J|lsm_lm_s\rangle\langle lsm_lm_s|\boldsymbol{n}sm_s\rangle$$

$$\langle f| = \langle \boldsymbol{n}'s'm_{s'}| = \sum_{J'm_{J'}l'm_{l'}} \langle \boldsymbol{n}'s'm_{s'}|l's'm_{s'}m_{s'}\rangle\,\langle l's'm_{l'}m_{l'}|l's'J'm_{J'}\rangle\,\langle l's'J'm_{J'}|\,.$$

In these expressions l is the relative orbital angular momentum between the Λ^0 and the initial proton, m_l its component, J is the total angular momentum of the system, and m_J the component. For the final state l', $m_{l'}$, J', and $m_{J'}$ have a similar meaning. For simplicity we take the z-axis along $\boldsymbol{n}$. Making use of the rotational invariance of T_{I}, the transition matrix element may be written

$$\langle f|T_{\mathrm{I}}|i\rangle = \langle \boldsymbol{n}'s'm_{s'}|T_{\mathrm{I}}|\boldsymbol{n}sm_s\rangle =$$
$$= (4\pi)^{\frac{1}{2}} \sum_{Jm_J ll'm_{l'}} (2l+1)^{\frac{1}{2}}\langle lsom_s|lsJm_J\rangle\,\langle l's'm_{l'}m_{s'}|l's'Jm_J\rangle Y_{l'}^{m_{l'}}(\boldsymbol{n}')T_{\mathrm{I}}(J\,|\,l's';\,ls)$$

The total cross section for unpolarized particles is given by

$$\sigma(\Lambda^0 p \to pn) = \varrho_I(f) \frac{1}{2(2S+1)} \sum_{sm_s} \sum_{s'm_{s'}} \int d\boldsymbol{n}' \langle \boldsymbol{n} s m_s | T_I | \boldsymbol{n}' s' m_{s'} \rangle |^2 .$$

The initial states are $2(2S+1) = [2(S+\frac{1}{2})+1] + [2(S-\frac{1}{2})+1]$. Using the properties of the addition coefficient we get

$$\sigma(\Lambda^0 p \to pn) = \varrho_I(f) \frac{1}{2(2S+1)} \sum_{J=0}^{\infty} (2J+1) \sum_{ss'} \sum_{l=|J-s|}^{J+s} \sum_{l'=|J-s'|}^{J+s'} | T(J | l's'; ls) |^2 .$$

It will be noted that the invariance of T_I for spatial reflections has not yet been used; only those matrix elements of T_I are different from zero which conserve the total parity. A completely analogous formula, of course, may be written for the elastic scattering, $\Lambda^0 +$ proton $\to \Lambda^0 +$ proton. In this case the spin s' of the final channel takes the two values $S - \frac{1}{2}$ and $S + \frac{1}{2}$ as for the initial channel. We thus can write

$$\sigma(\Lambda^0 p \to \Lambda^0 p) = \varrho_{II}(f) \frac{1}{2(2S+1)} \sum_{J=0}^{\infty} (2J+1) \sum_{s,s'} \sum_{l=|J-s|}^{J+s} \sum_{l'=|J-s'|}^{J+s'} | T_{II}(J | l's'; ls) |^2 .$$

The density of the final states $\varrho_{II}(f)$ is proportional to the product of the momentum of one of the two final particles in the centre of mass system and the reduced mass of the channel

$$\varrho_I(f) \sim (\alpha p^2 + mQ)^{\frac{1}{2}}$$

$$\varrho_{II}(f) \sim \alpha^{-1} p$$

where $\alpha = \frac{1}{2}(1 + m/M) \cong 0.92$. The kinetic energy of the original system $\Lambda^0 +$ p in the centre of mass system is given by $\varepsilon = (p^2/2m) + (p^2/2M) = \alpha(p^2/m)$.

For simplicity we assume gaussian distributions for the nucleon momenta and for the momenta of the Λ^0 in the Λ^0-nucleus. It is reasonable to suppose that the two gaussians correspond to the same value of the mean kinetic energy, of the order of 20 MeV. In the centre of mass system the two colliding particles have equal and opposite momenta, $\boldsymbol{p}$. The distribution of $\boldsymbol{p}$ will also clearly be gaussian and will correspond to the same value of the mean kinetic energy (of the two colliding particles in the centre of mass system). The states with low orbital angular momenta, $l = 0, 1, 2$ give the most important contributions to the cross-section. It is difficult to estimate exactly this effect. Besides the hypothesis of a regular behaviour of the matrix elements, it is also necessary to make some hypothesis on the range of the inter-

action. It is a consistent viewpoint in the high spin model to assume that no particular restriction exists apart from the possible inhibitions due to the high angular momenta. The copious production would require a strong coupling of the Λ^0 with pions. This coupling would produce an interaction of the Λ^0 with the nucleons having a range presumably of the order of magnitude of the Compton wave length of the meson. In this case one can estimate that from 20 to 50 % of the collisions may already occur with $l = 1$, and from 1 to 10 % with $l = 2$. In the inelastic reaction, which is strongly exothermic, the momentum of the outgoing particles, in the centre of mass system is much higher than that of the initially colliding particles. It is estimated that orbital angular momenta of $l' = 0, 1, 2, 3$ and even 4 may well occur without presumably introducing very significant reduction in the matrix element.

To be definite let us consider the case of a spin $S = 11/2$ for the Λ^0, the largest of the values considered before. Of course, for a smaller value the arguments which follow would a fortiori hold. The cross-section, with the presumably more important matrix elements in evidence, can be written as

$$\sigma(\Lambda^0 p \to pn) =$$
$$= \tfrac{1}{24}\, \varrho_I(f)[9\,|\,T_I(4\,|\,31;15)\,|^2 + 7\,|\,T_I(3\,|\,21;\,25)\,|^2 + 11\,|\,T_I(5\,|\,41;\,05)\,|^2 + \ldots]$$

or

$$\sigma(\Lambda^0 p \to pn) = \tfrac{1}{24}\, \varrho_I(f)[11\,|\,T_I(5\,|\,41;\,16)\,|^2 +$$
$$+ 9\,|\,T_I(4\,|\,40\,|\,15)\,|^2 + 9\,|\,T_I(4\,|\,31;\,26)\,|^2 + 7\,|\,T_I(3\,|\,30;\,25)^2 + \ldots]$$

according to the parity of the Λ^0 respect to the proton. Similarly, for the scattering, the cross-section can be written in every case as

$$\sigma(\Lambda^0 p \to \Lambda^0 p) = \tfrac{1}{24}\, \varrho_{II}(f)[3\,|\,T_{II}(1\,|\,01;\,01)\,|^2 + |\,T_{II}(0\,|\,00\,|\,00)\,|^2 + \ldots]\,.$$

Of course, in addition to the matrix elements shown explicitly, and which are presumably large, there may be other matrix elements giving contributions of the same order. As is seen, in the case of the scattering, large orbital angular momenta are not necessarily required, and the reaction may very well occur for small momenta of the colliding particles in the center of mass system. In the inelastic case only the collisions with sufficiently high momenta of the colliding particles in the centre of mass system contribute in an appreciable way. Limited to these collisions, however, the matrix elements of T_I should not differ greatly from those of T_{II}, since, for the high spin model, no other mechanism apart from high angular momenta should play a relevant role. As regards statistical weights, for the energies of interest here, $\varrho_I(f)$ is always greater than $\varrho_{II}(f)$. On the basis of the preceding estimate, one must conclude that

it is not possible to explain the very large reduction of the inelastic process with respect to the elastic (a factor on the order of 10^9 to 10^{13}), assuming the same mechanism of the large spin used to explain the mean life. In order to obtain the required reduction, still larger spins are necessary than those required to explain the long mean life of the free Λ^0. A reliable estimate of these values is very difficult and delicate and will not be attempted here. As is seen, there are essentially two facts which constitute the main difference with respect to the case of the free Λ^0 decay. Firstly, the energy release of the exothermic reaction $\Lambda^0 + \text{nucleon} \to \text{nucleon} + \text{nucleon}$ is sufficient to permit relatively high orbital angular momenta for the final states. Secondly, differently from the case of the decay of the free Λ^0, which has zero momentum in the rest system, the Λ^0 of the above reaction is bound to the fragment. An approximate way of describing this situation is to assign a convenient distribution to the momentum of the Λ^0 in the Λ^0-nucleus. Obviously the hypotheses about the matrix elements, and the approximate description of the dynamics of the Λ^0 in the Λ^0-nucleus are both very far from having a secure basis. It must be noted that, unfortunately, there exists no theory which allows a more physically significant discussion.

4. – Problem of Charges.

4·1. The confirmed existence of the new particles brings us back to the more fundamental problem of a theory of elementary particles. It appears that a discussion on this point is not at all academic, as at first sight it would seem, but that it is closely bound to some important experimental aspects. One asks if the new particles, or at least some of them, are to be regarded as states of the meson-nucleon field, rather than as new elementary particles. The problem has sense from two different viewpoints. From a purely theoretical viewpoint, a criterion must be found for classifying the existing particles, so as to distinguish those which are truly elementary. However such a criterion could not be based, for example, on the order of magnitude of the mean life, or on other similarly imprecise distinctions. It seems that, in a future theory, to a truly elementary particle should correspond a well defined invariance of the formalism. It should guarantee, among other things the absolute stability of the true elementary particle. As an example, the absolute stability of the electron necessarily follows from the conservation of electric charge, assuming that no charged particles exist with mass smaller than the electron. Presumably, also in the future formalism electric charge conservation will still be expressed by that particular invariance known as gauge invariance of the first kind. The absolute stability of nuclear matter leads one to expect a conservation principle for heavy part-

icles. The way that such an invariance property ought to be expressed is still unknown. But it will in any case constitute a very stringent limitation.

From a more limited viewpoint, the meaning of the above question can be rephrased in the following way. Is pion-nucleon interaction capable of explaining the existence of new particles and thus of providing a description of them? The objection that particles other than pions or nucleons are often emitted in the decay of these particles (there certainly exist charged heavy mesons giving a μ-meson among decay products) is not a difficulty. In fact, the pion-nucleon field (possibly also including photons) can only approximatively be supposed to be an isolated system. And the lifetime of $\pi^{\pm} \to \mu^{\pm} + \nu$ is not much longer than that of $K \to \mu + ?$. [The K_{μ} observed at Paris ([14]) is assumed to decay into a μ plus a neutrino. The decay of the charged pion is usually explained by postulating a direct coupling of the three fields. For a pseudoscalar meson it is convenient to assume vector coupling or pseudovector coupling, according to the relative parity of the two final fermions, so as to reproduce, using the same coupling constant, the small ratio ($\sim 10^{-3}$ to 10^{-4}) of the decay into $e+\nu$ to the decay into $\mu + \nu$. If we assume that K_{μ} also has spin zero, and postulate for it the same interaction with the same coupling constant, then it is easy to obtain, using well-known formulae, a mean lifetime for $K_{\mu} \to \mu + \nu$ in satisfactory agreement with experiment ([15])]. A more serious objection seems to be that concerning long lifetimes. The remarks of SACHS, already mentioned, are important in regard to this point.

4·2. *Charge independence at the decay.* – At present it seems difficult to suggest experiments which would decide whether new particles are composite. However, some simple conclusions can be deduced from this hypothesis. Pion-nucleon interaction is by now accepted as charge independent. Particles composed of pions and nucleons, if bosons, should have integral isotopic spin, and if fermions half-integral isotopic spin. Charge independence should also be valid. In fast processes such as production processes, perturbations which would destroy charge independence should be negligible. In slow processes, such as decay processes, this may not necessarily be true. Of course, one cannot speak of charge independence if some decay products are other than pions and nucleons. However, even for decays into pions and nucleons the validity of charge independence would still be questionable. The usually

---

([14]) B. GREGORY, A. LAGARRIGUE, L. LEPRINCE-RINGUET, F. MULLER et C. H. PEYROU: *Nuovo Cimento*, **11**, 292 (1954).

([15]) Some authors have used only statistical weight arguments for this comparison. However, it must be noted that the value which one obtains for the above ratio of the two π-meson decay modes by comparing only the statistical weights is in error by a factor of the order of $0.5 \cdot 10^5$ with respect to the exact result.

neglected charge dependent interactions can be quite important in these cases. Such a question should be resolved experimentally. DALITZ ([16]) has noted that a necessary implication of charge independence is that the ratio of the frequency of $\tau^+ \to \pi^+ + \pi^- + \pi^+$ to the frequency of $\tau^+ \to \pi^+ + \pi^0 + \pi^0$ lies between $\frac{1}{4}$ and 1. This follows from assigning an isotopic spin of 1 to the τ-meson and assuming charge independence at the decay. Up to now, although the comparison of so few cases cannot be trusted, this inequality seems to be satisfied. But it must be noted that it is merely a necessary and not a sufficient condition for validity of charge independence. Even if the above condition is definitely satisfied it is still incorrect to conclude that charge independence holds for τ-meson decay. It could be useful to have at hand some more decisive criterion. [For example, consider the decay of the θ^0. The observed decay mode is $\theta^0 \to \pi^+ + \pi^-$. Let P be the parity of the θ^0 and S the spin. The relation $P = (-)^S$ must be satisfied to agree with the observed decay mode. If the θ^0 is to be described by a suitable field, the above relation means that such a field can never be a pseudo-field. To avoid frequent confusion, intrinsic parity is here defined so that pseudoscalar has parity -1 and pseudovector $+1$. Of course, to define (relative) parity of a particle it is not required that the particle should have its own field (see also the preceding discussion of the Λ^0). Parity in such cases is directly defined by looking at the final states. Now, it has been pointed out that the mass of the τ^+ is coincident within experimental errors with the mass of the θ^0 (493.3 ± 0.4 MeV for τ^+ and 493 ± 5 MeV for θ^0). They could be considered as different charge states of the same particle with isotopic spin 1. Of course, this could not be the case for a spin $S = 0$, for the θ^0 would have parity $+1$, and the τ^+ parity -1. It could occur for higher spins. However, as shown by MICHEL ([17]), isotopic spin would not be a good quantum number in that case. The other case is that the θ^0 has isotopic spin zero and is not the zero charge state of the τ. It is still possible to say something. In this case, if the spin of the θ^0 is odd then isotopic spin is certainly not a good quantum number. Indeed for odd spin $\theta^0 \to \pi^0 + \pi^0$ is clearly forbidden. But if charge independence is to hold, then the observed $\theta^0 \to \pi^+ + \pi^-$ would also be forbidden ([18]). The argument could be refined so as to include cases of even spin with particular assignment of charge conjugation and charge parity quantum numbers. It is hoped that the spin of the θ^0 may be measured using angular correlations of the kind noted at Brookhaven.]

([16]) R. H. DALITZ: *Proc. Phys. Soc.*, **66**, 710 (1953).

([17]) L. MICHEL: 2° *Thèse* (to be published).

([18]) Note that a similar argument does not hold for isotopic spin 1, due to the fact that $\langle 1100 | 1110 \rangle = 0$.

4·3. *Charge independence at production.* – Coming back to production processes, we note that charge independence does not necessarily imply that particles are produced with the same abundance in all charge states. Rather it gives relations between cross-sections of processes which differ only in the charges of the particles. This question has already been discussed [19]. In some cases interesting remarks may be made. It is known, for example, that a larger number of Λ^0's is found than of charged Λ's. It may be difficult to reconcile this fact with charge independence, or at least with some assignments of isotopic spin. The isotopic spin of the Λ, regarded as a composite particle, might be $\frac{1}{2}$ or $\frac{3}{2}$, excluding higher values which would require a still larger charge multiplicity. For the case of isotopic spin $\frac{3}{2}$ it can be shown that in nucleon-nucleus collisions the total number of doubly and negatively charged Λ-particles produced must equal the total number of positivelycharg ed and neutral ones. Such a relation holds either for direct production in nucleon-nucleon collision, or for secondary production via pions, which, before excaping from the nucleus, collide against other nucleons. Essentially, no other hypothesis is needed other than charge independence. It is reasonable to assume that some fraction of the Λ-particles found in Wilson chambers are produced in nucleon-nucleus collisions. Firstly, direct evidence exists of Λ-particles produced in nucleon-nucleon collision [20]. Secondly, at higher energies even the secondary collisions in the same nucleus of the pions produced will contribute [21]. Therefore it seems that, if charge independence holds at production, a value of $\frac{3}{2}$ for the isotopic spin of the Λ-particle must be excluded. Of course, the simple statement that doubly charged Λ-particles have as yet not been found does not constitute an equivalent proof, since the objection could always be raised that these particles may well exist but very rarely be produced. Our argument is just to avoid this objection. Similar arguments may be derived in analogous cases, however we believe that only artificial production will give a definite answer to these questions.

In this section our object was essentially to point out how, at least in the discussion of these topics of isotopic spin and of charge independence, the original question as to the possible composite nature of these particles may possibly have a direct connection with experiment.

5. – Final Remarks.

In our critical discussion of some important questions concerning the new unstable particles, our effort has been to mantain as far as possible a phenome-

---

[19] R. Gatto: *Nuovo Cimento*, **11**, 445 (1954); *Nuovo Cimento*, **12**, 160 (1954).

[20] M. M. Block and E. M. Harth, W. B. Fowler, R. P. Shutt, A. M. Thorndike and W. L. Whittemore: *Bull. Am. Phys. Soc.*, **7**, W10 (1954).

[21] C. F. Powell: *Suppl. Nuovo Cimento*, **11**, 165 (1954).

nological viewpoint. However, it is a particular feature of the phenomenology of the new particles to bring forth each time problems of more theoretical nature. The conservation law of heavy particles has clearly a direct connection with experiment. The problem of establishing whether the new particles, or at least some of them, are to be regarded as composite particles, rather than as new elementary particles, is in many respects closely bound to experimental results.

The important fact brought to light by recent experiments is the preponderance of double production. Up to the present, no direct evidence of single production exists. This circumstance suggests reasoning of a qualitative character, which can serve for a preliminary systematization of the present incomplete results. Assuming some regularity hypotheses for the matrix elements, conclusions may be drawn concerning production and interaction with nucleons. All these conclusions are in remarkable agreement with experiments so far. In this sense new particles are not completely strange. However, does the only requirement of the long mean lives imply all other aspects? This is perhaps the best line of attack for future theory.

In the present work we have spoken for the most part about Λ^0-particles and Λ^0-nuclei. Perhaps the most important conclusion is that the large spin which could explain the long mean life of the free Λ^0 is not sufficient by itself to account for the long lifetime of the Λ^0-nucleus. For simplicity we have pictured the relatively stable binding of the Λ^0 in the Λ^0-nucleus as the result of a succession of elastic processes, $\Lambda^0 + \text{nucleon} \rightarrow \Lambda^0 + \text{nucleon}$. It is estimated that a very large number, of the order of 10^9 to 10^{13} of such processes occur, before the Λ^0-nucleus disintegrates. Only after such a large number of elastic processes does an inelastic process occur, with subsequent disintegration of the Λ^0-nucleus. If one considers, in particular, the inelastic process $\Lambda^0 + \text{nucleon} \rightarrow \text{nucleon} + \text{nucleon}$, which corresponds to the non-mesonic decay of the Λ^0-nucleus, it is very difficult to conceive how it could be so strongly forbidden by the large spin only. A very large spin would be required, a value larger than that required to explain the long lifetime of the free Λ^0-particle. It is noted, firstly, that the energy release of the inelastic process is sufficiently high to permit large orbital angular momenta for final state, and, secondly, that the initial momenta of the colliding particles may take on high values due to the tail of the momenta distribution in the Λ^0-nucleus.

Other topics, such as the possible composite nature of the new particles, the role of weak interactions, questions on isotopic spin assignements and on the possible validity of charge independence at production and at decay, have been examined and particular conclusions have been drawn.

We wish to repeat explicitly that many of the arguments here considered have, of necessity, an approximate and qualitative character. It may very

well be that some of them will not be valid. Nevertheless, it is felt that the preceding discussion may contribute to the understanding of these important problems. We hope to continue in the near future the discussion of these problems and of others not examined here.

Acknowledgments.

It is my pleasure to thank Prof. E. AMALDI and Prof. B. FERRETTI for stimulating discussions. Thanks are also due to Prof. B. TOUSCHEK for some discussion on the subject.

RIASSUNTO

Vengono discusse alcune questioni sulle nuove particelle instabili. Ci si aspetta, sulla base di argomenti qualitativi, che il fatto delle lunghe vite medie debba portare delle notevoli restrizioni circa gli altri processi. Possono così ricavarsi informazioni sui possibili processi di produzione e di interazione con i nucleoni. Se si cerca di sviluppare a fondo un tale punto di vista, sorge l'importante questione di sapere quali altri assunti indipendenti debbono venire aggiunti a quello delle lunghe vite medie per ottenere uno schema più completo e consistente. I nuclei Λ^0 vengono discussi in maggiore dettaglio e soprattutto in connessione col modello a spin elevato del Λ^0. Gli argomenti usati naturalmente non possono essere rigorosi e potrebbero anche risultare sbagliati; anche questa però sarebbe una indicazione importante. Infine vengono discussi l'eventuale ruolo delle interazioni deboli e la eventuale validità della charge-independence alla produzione. Ci si aspetterebbe che la charge independence non valga al decadimento e questo problema viene esaminato per il caso del mesone θ^0.

IL NUOVO CIMENTO Vol. I, N. 3 1° Marzo 1955

Models of Hyperons.

H. Enatsu (*) and C. Ihara

Department of Physics, Kyoto University - Kyoto, Japan

(ricevuto il 15 Gennaio 1955)

Summary. -- Methods of mixed fields are extended to the case of hyperons. In order to take into account a new particle (Y-particle) which decays into a Λ-particle and a π-meson, a set of the so-called strong interactions between hyperons and mesons is assumed. Then the Λ-particle self-energy is calculated to the second-order terms through the use of the method of the present field theory. Some relations in which the masses of these hyperons and mesons are included are derived from the cancellation of its divergence. It is shown that their masses estimated in terms of the relations are as follows: $Y \sim 2600\ m_e$, $\Lambda \sim 2200\ m_e$, and the masses of scalar mesons which decay into two π-mesons are $800\ m_e$ — $1500\ m_e$. The model presented here gives results being in qualitative agreement with experiment.

The present paper should be considered as a continuation of preceding papers [1]. Our main aim is to consider more fully the model of nucleon family and mass relations between various heavy particles.

One of us has recently discussed the model of unstable heavy particles and in particular the mass relations of them from the viewpoint of the so-called mixed theory. Our model can give results which seem to be in qualitatively good agreement with experimental facts, at least to the second-order terms in the coupling constants. Recently, however, evidence has been presented which indicates that there may be a heavy particle which decays according

---

(*) Now at Institute for Theoretical Physics, Copenhagen, Denmark.

(1) H. Enatsu: *Prog. Theor. Phys.*, **11**, 125 (1954); **12**, 363 (1954); H. Enatsu, H. Hasegawa and P. Y. Pac: *Phys. Rev.*, **95**, 263 (1954). Hereafter these papers will be referred to as A, B, and C.

to the scheme [2]

$$Y^- \to \Lambda^0 + \pi^-, \qquad \Lambda^0 \to N^+ + \pi^-, \tag{1}$$

where $Y^- \sim 2600\ m_e$ and $\Lambda^0 \sim 2200\ m_e$.

In the foregoing considerations we have not taken into account such a cascade particle. Therefore, it is our next task to investigate a possible model in terms of which the existence of the new particle would be explained. In the following a reasonable model will be discussed, which is simple in its fundamental assumption and which appears to give a much better understanding of the properties of hyperons.

We begin by a brief discussion of the principle of mixed fields. It has been suggested [3] that the divergent parts of self-energies must be cancelled by considering various fields, and moreover it has been expected that the exact compensation has to be achieved in such cases as higher order corrections of self-energies, divergent self-charges and so forth. However, the question now arises: What is the fundamental reason for such a procedure? In connection with this point, in the papers A and B we have suggested a possible interpretation of the principle of mixed theory. At present it is most convenient to explain our idea in the language of the eigenvalue problem of mass. Suppose that we are dealing with a nucleon interacting with an electromagnetic field and π-mesons, being of pseudoscalar type with pseudoscalar or pseudovector coupling (PS(Ps) or PS(Pv) for short), and we confine ourselves to the second-order expression of the nucleon self-energy in space-time. Then we have positive logarithmic divergences for the nucleon self-energy caused by the fields considered above. For such positive divergences, according to our general theory described in A and B, there would be no discrete mass spectrum of the nucleon family. Therefore it is important here to use the method of mixed fields to quantize the mass. That is to say, one more field has to be assumed for that purpose. For example, consider a scalar meson interacting with the nucleon. It gives us a negative logarithmic divergence of the nucleon self-energy. If the coupling between the scalar meson and nucleon is strong enough so that the contribution due to the scalar meson to the nucleon self-

(2) R. Armenteros, K. H. Barker, C. C. Butler, A. Cachon and C. M. York: *Phil. Mag.*, **43**, 597 (1952); C. D. Anderson, E. W. Cowan, R. B. Leighton and V. A. J. van Lint: *Phys. Rev.*, **92**, 1089 (1953); E. W. Cowan: *Phys. Rev.*, **94**, 161 (1954); *Report of the cosmic ray Conference, Bagnéres-de-Bigorre*, 1953; M. W. Friedlander: *Phil. Mag.*, **45**, 418 (1954): A. Bonetti, R. Levi-Setti, M. Panetti and G. Tomasini: *Nuovo Cimento*, **10**, 345, 1736 (1953); C. M. York, R. B. Leighton and E. K. Bjornerud: *Phys. Rev.*, **90**, 167 (1953); H. W. Johnston and C. O'Ceallaigh: *Phil. Mag.*, **45**, 424 (1954).

(3) A. Pais: *Phys. Rev.*, **68**, 227 (1948); *Verh. Kon. Ac. Wetenschappen Amsterdam*, **19**, 1 (1947); S. Sakata and O. Hara: *Prog. Theor. Phys.*, **2**, 30, 145 (1947).

energy overcomes that due to the electromagnetic field and π-mesons, one may expect that the quantization of the nucleon mass will be possible. Therefore the mass values of interacting particles most likely to be found by the method of compensation may indicate the critical ones which are just sufficient in magnitude for the mass quantization. Unfortunately for practical calculations the space-time representation of self-energies is inconvenient. The reason is that the order of the singularity of the nucleon self-energy is logarithmic for all direct and derivative couplings, so that we get only one relation derived from the compensation, while we have many masses and coupling constants at our disposal. On the other hand, if we employ a momentum space representation of self-energies, which is essentially expressed in three-dimensional notation, we have the advantage of getting more conditions for the determination of masses. For example, in the case of derivative couplings, we have quadratic divergences as well as logarithmic ones. It then follows that more conditions may be imposed on the masses and coupling constants involved. In this way, taking account of the applicability of the mixed theory, we may attempt to look for a set of interactions in terms of which we understand what can be learned from the experiments. Thus we think it of interest to investigate the mixed theory from the practical point of view.

Now the essentials of the present consideration are as follows: the method used in B will be applied to the case of the hyperons. For this purpose, we further assume some interactions between the hyperons and mesons. However, such an introduction of couplings into our original scheme does not lead to any modification in the conclusion stated so far in B and C. The results obtained seem to indicate that the lowest order calculation gives us qualitatively acceptable masses of hyperons.

We now proceed to discuss a new possible model. We may summarize our fundamental ideas in the following postulates concerning the form of interactions.

(I). The set of the so-called strong couplings can be written as

(2) $g\,(\mathrm{N\,N\,\pi})$ PS(Pv),

(3) $G\,(\mathrm{N\,\Lambda\,\theta})$ S(v),

(4) $g\,(\Lambda\,\Lambda\,\pi)$ PS(Pv),

(5) $G\,(\Lambda\,\mathrm{Y}\,\theta_1)$ S(v),

(6) $g\,(\mathrm{Y\,Y}\,\pi)$ PS(Pv),

. . . . ,

where the mass relations are

$$m(\mathrm{N}) < m(\Lambda) < m(\Upsilon) < \dots ,$$

$$\text{i.e.} \quad m < m_1 < m_2 \quad \dots ,$$

and

$$m(\pi) < m(\theta) \sim m(\theta_1) \sim \dots ,$$

$$\text{i.e.} \quad \varkappa' \quad < \mu' \quad \sim \mu_1' \quad \sim \dots .$$

In this expression for the interactions, we subdivide the strong couplings (2)-(6) into two groups. One is a π-meson group and, the other is a scalar meson group. That it is possible to use the same coupling constant for each of the groups is not justified on an *a priori* basis. In general, there is no need to do so, but it is an interesting trial to invoke the principle of symmetry so as to avoid too enormous numbers of coupling constants to be dealt with. If necessary, we may introduce more new interactions between mesons and hyperons according to the principle which is apparently suggested by the scheme mentioned above. That is, if there were heavier fermions than the Y-particle, the coupling scheme (2)-(6) would be extended downwards. The new interactions to be devised should be in harmony with them. Generally, careless introduction of strong coupling gives rise to the rapid decay of the hyperons in short lifetimes compared to those learned by experience. Our new interactions to be assumed are therefore such that the nucleon is stable and the rapid decay of the hyperons cannot be deduced.

It should be noted that in our scheme there is an asymmetry in respect to the masses of scalar mesons; we have assumed two kinds of them. There seems to be some experimental indication ([2,4]) of the existence of various heavy mesons which are presumed to decay into two π-mesons and apparently have different mass values. We consider it of importance, so that we postulate tentatively two scalar mesons corresponding to such experimental facts. The number of scalar mesons would be increased from two to three, four and so on, if necessary. In the evaluation of the self-energies, we shall always use the neutral form of interactions. This expression is not expected to be valid for the actual situation since the heavy particles seem to have their own isotopic spins. In order to better understand the charge property of them, we must study in more detail the isotopic spins. However, since the charge dependence of particles is unimportant for the mass relation ([1]) but *may* be

([4]) « A discussion on V-particles and heavy mesons », *Proc. Roy. Soc.*, A 221, 278 (1954). Also see other papers cited there.

significant for the decay and production scheme, as many authors have suggested ([5]), we shall not touch upon this point in this paper.

(II). It may be sufficient to assume that the following set of weak interactions is responsible for the decays of the heavy unstable particles,

$$(7) \qquad f\,(\mathrm{N}\,\mathrm{N}\,\theta) \qquad \mathrm{S(s)}\,,$$

$$(8) \qquad f_1\,(\Lambda\,\Lambda\,\theta) \qquad \mathrm{S(s)}\,,$$

$$(9) \qquad f_2\,(\mathrm{N}\,\mathrm{N}\,\theta_1) \qquad \mathrm{S(s)}\,,$$

$$(10) \qquad f_3\,(\Lambda\,\Lambda\,\theta_1) \qquad \mathrm{S(s)}\,,$$

$$(11) \qquad f_4\,(\mathrm{Y}\,\mathrm{Y}\,\theta_1) \qquad \mathrm{S(s)}\,,$$

$$\ldots\ldots \qquad \ldots,$$

It may be expected to introduce some other weak interactions. However, as was discussed in C, these weak interactions would not give rise to appreciable contribution to the mass relation of the particles involved.

Having assumed the set of interactions, we can next easily determine the mass values of the Y and θ_1-particles by making use of the results obtained in B. The essence of the investigation carried out in B and C is its prediction of the masses of Λ and θ particles, which are derived from the cancellation of the *nucleon self-energy*. Now to estimate the Y and θ_1-masses, we merely need to consider the case of the *Λ-particle self-energies* caused by the interactions (3), (4) and (5). However, the analysis described in B shows that it is impossible to determine uniquely the method of evaluation for the self-energy even within the framework of the present field theory. We therefore shall adopt two different ways of calculation mentioned in B. It is rather gratifying to see that, whichever we may choose, a considerable amount of information about the order of magnitude of the Y and θ_1 masses can be obtained on the basis of such methods of computation.

a) *First case.* – The divergent self-energies of the Λ-particle due to the interactions (3), (4) and (5) can be expressed in the forms

$$(12) \qquad \delta M_1(3) = M_1 \left(\frac{G^2}{4\pi\hbar c}\right)\left(\frac{M_1}{\mu}\right)^2\left[\frac{1}{2\pi}\left(\frac{M}{M_1}-1\right)Q + \frac{1}{4\pi}\left(1-\frac{M}{M_1}\right)\cdot\right.$$

$$\left.\cdot\left\{3\left(\frac{M}{M_1}\right)^2-\left(\frac{M}{M_1}\right)-\frac{2}{3}+\left(\frac{\mu}{M_1}\right)^2\right\}L\right],$$

([5]) A. PAIS: *Phys. Rev.*, **86**, 663 (1952); *Prog. Theor. Phys.*, **10**, 457 (1953); M. GELL-MANN: *Phys. Rev.*, **92**, 833 (1953); K. NISHIJIMA: *Prog. Theor. Phys.*, **9**, 414 (1953); T. NAKANO and K. NISHIJIMA: *Prog. Theor. Phys.*, **10**, 581 (1953); T. NAKANO and R. UTIYAMA: *Prog. Theor. Phys.*, **11**, 411 (1954).

$$\delta M_1(4) = M_1\left(\frac{g^2}{4\pi\hbar c}\right)\left(\frac{M_1}{\varkappa}\right)^2\left[-\frac{1}{\pi}Q + \frac{1}{4\pi}\left\{\frac{20}{3} + 2\left(\frac{\varkappa}{M_1}\right)^2\right\}L\right], \tag{13}$$

and

$$\delta M_1(5) = M_1\left(\frac{G^2}{4\pi\hbar c}\right)\left(\frac{M_1}{\mu_1}\right)^2\left[\frac{1}{2\pi}\left(\frac{M_2}{M_1}-1\right)Q + \frac{1}{4\pi}\left(1-\frac{M_2}{M_1}\right)\cdot\right.$$
$$\left.\cdot\left\{3\left(\frac{M_2}{M_1}\right)^2 - \left(\frac{M_2}{M_1}\right) - \frac{2}{3} + \left(\frac{\mu_1}{M_1}\right)^2\right\}L\right], \tag{14}$$

where $M = mc/\hbar$, $\varkappa = \varkappa' c/\hbar$ etc., and Q and L represent the *quadratic* and *logarithmic* parts of the divergences. These results can be obtained in terms of the expressions (79) and (85) of B by taking into account the necessary change of the masses of the particles being considered. Furthermore, in the equation (86) of B it is shown that for the case of the nucleon self-energy there exists the following relation between the coupling constants of (2) and (3),

$$\frac{G^2}{\mu^2} = \frac{2}{((M_1/M)-1)}\frac{g^2}{\varkappa^2} \quad (*). \tag{15}$$

If we work out the condition for the elimination of quadratically diverging parts of (12), (13) and (14) with the help of (15), we get

$$\frac{1}{\mu^2}\left(\frac{M}{M_1}-1\right) - \frac{1}{\mu^2}\left(\frac{M_1}{M}-1\right) + \frac{1}{\mu_1^2}\left(\frac{M_2}{M^1}-1\right) = 0\,. \tag{16}$$

It is convenient to make the substitutions

$$\frac{\mu_1}{\mu} = \lambda\,, \qquad \frac{M_2}{M} = a\,, \qquad \frac{M_1}{M} = b\,, \tag{17}$$

in terms of which (16) becomes

$$a = \lambda^2(b^2-1) + b\,. \tag{18}$$

Now the logarithmic parts of (12), (13) and (14) are cancelled by means of the relation

$$\left(\frac{1}{\mu}\right)^2\left(1-\frac{M}{M_1}\right)\left\{3\left(\frac{M}{M_1}\right)^2 - \frac{M}{M_1} - \frac{2}{3} + \left(\frac{\mu}{M_1}\right)^2\right\} + \left(\frac{1}{\varkappa}\right)^2\left(\frac{M_1^2}{M}-1\right)\left(\frac{\varkappa}{\mu}\right)^2\left\{\frac{10}{3} + \left(\frac{\varkappa}{M_1}\right)^2\right\} +$$
$$+\left(\frac{1}{\mu_1}\right)^2\left(1-\frac{M_2}{M_1}\right)\left\{3\left(\frac{M_2}{M_1}\right)^2 - \frac{M_2}{M_1} - \frac{2}{3} + \left(\frac{\mu_1}{M_1}\right)^2\right\} = 0\,. \tag{19}$$

(*) This is misprinted in B.

Substitutions of (17) into (19) gives us

$$\lambda^2\left(1-\frac{1}{b}\right)\left\{3\left(\frac{1}{b}\right)^2-\frac{1}{b}-\frac{2}{3}+\left(\frac{\mu}{M_1}\right)^2+\frac{10}{3}b+\left(\frac{\varkappa}{M_1}\right)^2 b\right\}- \tag{20}$$
$$-\left(\frac{a}{b}-1\right)\left\{3\left(\frac{a}{b}\right)^2-\frac{a}{b}-\frac{2}{3}+\lambda^2\left(\frac{\mu}{M_1}\right)^2\right\}=0\,.$$

From (18) we get

$$\frac{a}{b}=\lambda^2\left(b-\frac{1}{b}\right)+1\,. \tag{21}$$

The equation (20) can be simplified through the use of the relation (21). Thus after some evaluations, one finds

$$3\left(b-\frac{1}{b}\right)^3\lambda^4+\left(b-\frac{1}{b}\right)\left\{5\left(b-\frac{1}{b}\right)+\left(\frac{\mu}{M_1}\right)^2\right\}\lambda^2- \tag{22}$$
$$-\left(1-\frac{1}{b}\right)\left[3\left(\frac{1}{b}\right)^2-\frac{1}{b}-2+\left(\frac{\mu}{M_1}\right)^2+\left\{2+\left(\frac{\varkappa}{M_1}\right)^2\right\}b\right]=0\,.$$

We are now in a position to find the mass values of the Y and 0_1 particles. As an example we consider the following set of numerical values, which is shown in the Table II of B (in units of m_e) and which have been derived from the compensation of the divergent *nucleon* self-energy,

$$m=1836\,,\quad m_1=2280\,,\quad \varkappa'=276\quad\text{and}\quad \mu'=1460\,, \tag{23}$$

so that

$$b=1.242\,,\qquad 1/b=0.805\,. \tag{24}$$

It is easy to solve the equation (22) with the result, being physically significant,

$$\lambda^2=0.329\,,\qquad \text{i.e.}\quad \lambda=0.574\,. \tag{25}$$

Then one finds

$$m_2=2609\,,\qquad \mu_1'=838\,, \tag{26}$$

with the help of (17) and (18). In Table I some numerical values obtained in similar ways are listed.

TABLE I. – *Masses of* Λ*-particle,* θ*-meson,* Y*-particle and* θ_1*-meson in units of* m_e. ($m(N)=1836$, $m(\pi)=276$, $Y\to\Lambda+\pi$, $\Lambda\to N+\pi$, $\theta\to\pi+\pi$, $\theta_1\to\pi+\pi$).

$m(\Lambda)$	2280	2380	2420
$m(\theta)$	1460	970	610
$m(Y)$	2609	2703	2739
$m(\theta_1)$	838	494	296

b) *Second case.* – In a manner quite analogous to that presented for the first case, various corresponding expressions can be derived from the formulas (98), (99) and (100) of B. The relation for the coupling constants is then

$$\frac{G^2}{\mu^2} = \frac{3}{[2(M_1/M)-1]}\frac{g^2}{\varkappa^2}. \tag{15*}$$

We find the condition for the quadratic parts of divergences,

$$\frac{a}{b} = \lambda^2\left(b-\frac{1}{b}\right)+\frac{1}{2}. \tag{21*}$$

Finally the convergence relation for the logarithmic parts is

$$\begin{aligned}(22^*)\quad & 20\left(b-\frac{1}{b}\right)^3\lambda^6+5\left(b-\frac{1}{b}\right)\left\{\left(b-\frac{1}{b}\right)+8\left(\frac{\mu}{M_1}\right)^2\right\}\lambda^4+\\ & +\left[20\left(\frac{1}{b}\right)^3-25\left(\frac{1}{b}\right)^2+\left\{10+40\left(\frac{\mu}{M_1}\right)^2\right\}\frac{1}{b}+\frac{71}{3}-50\left(\frac{\mu}{M_1}\right)^2+25\left(\frac{\varkappa}{M_1}\right)^2-\right.\\ & \left.-b\left\{\frac{94}{3}+50\left(\frac{\varkappa}{M_1}\right)^2\right\}\right]\lambda^2+\frac{37}{4}=0.\end{aligned}$$

One can find the solution of (22*) for λ, corresponding to the mass values of the Λ and 0-particles given in the Table III of B. The results are collected in Table II.

TABLE II. – *Masses of* Λ*-particle,* 0*-meson,* Y*-particle and* θ_1*-meson in units of* m_e. ($m(N) = 1836$, $m(\pi) = 276$, $Y \to \Lambda+\pi$, $\Lambda \to N+\pi$, $\theta \to \pi+\pi$, $\theta_1 \to \pi+\pi$).

$m(\Lambda)$	2200	2250	2300
$m(\theta)$	1050	990	900
$m(Y)$	2580	2701	2820
$m(\theta_1)$	1430	1295	1137

Now we may draw the following preliminary conclusion from the estimates summarized in the Tables I and II. The results obtained here are in essential agreement with the order of magnitude of the observed masses [2,4]. It is interesting to see that, if we assume the masses of the Λ and Y-particles to be about 2200 m_e and 2600 m_e respectively, the masses of the scalar mesons are found to be 800 m_e – 1500 m_e which are within the range of the observed mass value for heavy mesons.

We have restricted ourselves throughout this paper to the neutral form of interactions. As mentioned already, it is likely that we have to assign various

isotopic spins to these hyperons and heavy mesons. We feel that it is necessary to analyze this problem in more detail, and our model will still not be free from some revision in this point. It is hoped that further experimental evidence may lead to a discrimination among several possibilities concerning isotopic spins. However, one must note that some assignment of isotopic spins would not provide serious effects to the mass relations (22) and (22*) since it means merely the multiplication of coupling constants by some numerical factors. Therefore the mass estimates do not depend strongly upon the charge properties of the particles. We conclude that the values in the Tables I and II are applicable to the cases of charged particles.

Now we remark here the fact that the Y-particle may at least decay through the interactions (4), (5) and (10) into a π-meson and a Λ-particle. Considering the symmetrical character of the interactions (2)-(6), we may infer that *the lifetime of the* Y*-particles would be of the same order of magnitude as that obtained in the case of the* Λ*-particle in* C. *The same situation holds for the* θ_1*-meson as for the* θ*-meson in* C.

Finally we have to emphasize the crudity of our theory; higher order corrections and the introduction of isotopic spins probably affect the result mentioned above. Therefore the conclusion is not to be taken too seriously. We believe that the main feature of our theory is in the fact that the principle of mixed fields yields enough information about the masses of elementary particles to merit such a detailed approach, and it provides incidentally the mass values which appear to be compatible with experimental ones.

We are indebted to Professor H. YUKAWA for several interesting discussions.

RIASSUNTO (*)

Si estendono al caso degli iperoni i metodi dei campi misti. Per tener conto di una nuova particella (particella Y) che decade in una particella Λ e un mesone π, si assume una serie di interazioni cosiddette forti tra iperoni e mesoni. Poi per mezzo della presente teoria di campo si calcola fino ai termini del secondo ordine l'energia propria (self-energy) della particella Λ. Dall'annullamento della sua divergenza si derivano alcune relazioni riguardanti le masse degli iperoni e dei mesoni. Si dimostra che le loro masse espresse in termini di queste relazioni sono le seguenti: $Y \sim 2\,600\ m_e$, $\Lambda \sim 2\,200\ m_e$, e le masse dei mesoni scalari che decadono in due mesoni π sono $800\ m_e - 1\,500\ m_e$. Il modello qui presentato dà risultati in accordo qualitativo con l'esperienza.

(*) *Traduzione a cura della Redazione.*

IL NUOVO CIMENTO Vol. I, N. 3 1° Marzo 1955

Measurements of Ultrasonic Absorption in Rubber.

I. Gabrielli and G. Iernetti

Istituto di Fisica dell'Università - Trieste

(ricevuto il 17 Gennaio 1955)

Summary. — Absorption measurements of ultrasonic longitudinal waves in vulcanized natural rubber with and without carbon loading (50/100 carbon to rubber) are presented within the temperature and frequency ranges from 4 °C to 70 °C and from 0.4 MHz to 4 MHz. Experimental data were obtained by measuring, with a torsion balance, ultrasonic attenuation due to rubber samples immersed in water. Diagrams of absorption versus temperature for carbon loaded natural rubber show the usual behaviour of vulcanized rubbers. Corresponding diagrams for unloaded natural rubber show minima which indicate discrimination between two different relaxation effects. An unusual example of absorption decreased by carbon loading has been detected.

1. – Introduction.

Measurements of velocity and attenuation of ultrasonic waves in high polymers allow the determination of their mechanical properties and give informations about polymer chains and their motions. Furthermore, owing to the prominent role played by relaxation mechanisms in this case, a useful aid can be found for studying the various and important discrepancies occurring between experimental data and theoretical calculations for the attenuation of non-polymeric liquids and solids.

Velocity and attenuation measurements in vulcanized rubbers and rubber-like materials have been carried out by various methods ([1-5,9]).

Methods based on impedance changes are available for liquid high polymers, which give directly viscoelastic moduli ([6-8]). Optical methods are also available ([9]) (*).

For liquid high polymers and for high polymer liquid solutions it is possible to measure bulk and shear moduli both elastic B_1, μ_1 and viscous B_2, μ_2 (see § 4); relaxation effects appear not to be overlapped, i.e. relaxation times due to well defined relaxation mechanisms are present. This is not the case for solid high polymers such as rubbers. At high frequencies (MHz region), where the elastic Poisson coefficient is no more equal to 0.5, four viscous-elastic moduli are necessary for the description of the viscoeleastic behaviour of rubber-like materials. The only attempt to get velocity and attenuation measurements for both longitudinal and transversal waves has been made by A. W. NOLLE and P. W. SIECK ([4]), but, owing to the high absorption of transversal waves at 5 and 10 MHz, only quantitative indications about the four moduli separately have been achieved. Therefore, the only reliable data for rubber are those concerning velocity and attenuation for longitudinal waves and the corresponding values of the « effective moduli » $B_1+4\mu_1/3$ and $B_2+4\mu_2/3$. Only under simplifying assumptions it is possible to separate the effective moduli into their compressional and shear constituents and to evaluate other viscoelastic moduli as, for instance, the Young modulus (elastic and viscous) ([3]). From these values and from those available for lower frequencies it appears that the relaxation mechanisms are intermixed, requiring, therefore, the calculation of the strength of a relaxation spectrum, under the assumption of a continuous distribution of relaxation times ([3]).

It can be pointed out that this calculation from velocity data can be in some cases less significant than the corresponding calculation from absorption data. In fact, considering non-polymeric liquids, many examples can be found of an absorption deviating from the square law dependence on frequency and a corresponding velocity constant with frequency in all the explorable range.

([1]) P. HATFIELD: *Brit. Journ. Appl. Phys.*, **1**, 252 (1950).

([2]) A. W. NOLLE and S. C. MOWRY: *Journ. Acoust. Soc. Am.*, **20**, 432 (1948).

([3]) D. G. IVEY, B. A. MROWKA and E. GUTH: *Journ. Appl. Phys.*, **20**, 486 (1949).

([4]) A. W. NOLLE and P. W. SIEK: *Journ. Appl. Phys.*, **23**, 888 (1952).

([5]) H. J. MCSKIMIN: *Journ. Acoust. Soc. Am.*, **22**, 413 (1950); **23**, 429 (1951).

([6]) W. P. MASON, W. O. BAKER, J. H. MCSKIMIN and J. H. HEISS: *Phys. Rev.*, *a*) **73**, 1074 (1948); *b*) **75**, 936 (1949).

([7]) W. P. MASON and H. J. MCSKIMIN: *Bell. Syst. Tech. Journ.*, **31**, 122 (1952).

([8]) W. O. BAKER and J. H. HEISS: *Bell. Syst. Tech. Journ.*, **31**, 306 (1952).

([9]) G. W. WILLARD: *Journ. Acoust. Soc. Am.*, **23**, 83 (1951).

(*) An extensive bibliography about methods is to be found in a recent paper by W. O. BAKER and J. H. HEISS ([8]).

This deviation is generally attributed to the existence of a relaxation mechanism, tough the velocity behaviour would not imply any relaxation.

Bearing in mind this fact, we have carried out attenuation measurements in vulcanized natural rubber (unloaded and carbon loaded) in the frequency and temperature ranges of 0.4 MHz to 4 MHz and 4 °C to 70 °C respectively.

The rubber used was of the following composition (*) (+): Smoked sheet (parts by weight): 100, ZnO: 5, S: 2, Captax: 1.5, Paraffin oil: 5; the loaded rubber has in addition: Carbon black SRF: 50; Curing: 50 min at 120 °C.

2. – Experimental Method.

Longitudinal compressional waves, generated in a horizontal direction by a quartz crystal Q in the kerosene of vessel A (Fig. 1) are sent through a window W, of thin aluminium foil, in vessel B containing water, in which the reflector r of a torsion balance is immersed, to measure the ultrasonic radiation pressure. A sample S is inserted between the window and the reflector. Measurements are made, at constant quartz driving voltage, of the radiation pressure produced by the ultrasonic beam with and without interposed sample. The reflector has a 90° dihedral shape and is made of double thin aluminium foil, separated by an air layer. The ultrasonic beam reflected laterally, falls on the absorbing walls a of vessel B. The radiation pressure on such a reflector is equal to that on a completely absorbing plane ([11]). The reflector is rigidly attached to a vertical arm of a torsion balance (×), projected for a large range of ultrasonic intensities.

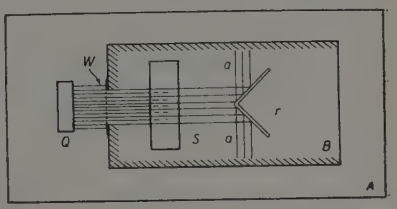

Fig. 1. – Schematic diagram of apparatus for measuring bulk wave attenuation in rubbers by mechanical method.

This method was chosen, because the lowest values of attenuation to be measured were well within the range measurable with a mechanical method, and fell, on the contrary, at the lowest limit of the interval covered by a pulse method ([12]).

(*) We thank the S. p. A. « Pirelli », Milano, for the kind supply of the samples.

(+) Nearly the same composition has been already used for low frequency measurements ([10]).

([10]) A. W. Nolle: *Journ. Polym. Science*, **5**, 1 (1950).

([11]) F. E. Borgnis: *Journ. Acoust. Soc. Am.*, **24**, 468 (1952).

(×) To be described in an article to appear in *Acustica*.

([12]) J. J. Markham, R. T. Beyer and R. B. Lindsay: *Rev. Mod. Phys.*, **23**, 353 (1951).

The following frequencies were used: 0.4, 0.7, 1, 2, 3, 4 MHz for temperatures of 4 °C, 18 °C, 45 °C, 70 °C. Values of the absorption coefficient from 0.4 db/cm to 40 db/cm were obtained.

Samples having a thickness of about 32 mm, 24 mm, 8 mm were used, experimental values being obtained with all the three samples, when possible. For instance with absorption above 10 db/cm only the sample of minimum thickness was used.

The absorption coefficient of water for above mentioned frequencies is negligible compared with that of rubber.

Stationary waves are reduced in the liquid paths by a small angle of inclination of the quartz crystal with respect to the sample.

A stationary wave effect was present in the rubber sample when its attenuation was less than about 3 db/cm. Attenuation values resulted to be dependent on the sample thickness. In order to minimize this error, for each measurement the frequency was increased and decreased by some percent. For the same purpose either rotation of the sample could be used ([13]) or frequency modulated waves ([14]).

Measurements were found affected by different errors, depending on the heating of the sample and on the slope of the attenuation-temperature curve (compare Figs. 4*a*, 4*b*). To reduce the heating effect, in the range where the attenuation changes very rapidly with the temperature, values were obtained with a ballistic method.

It was necessary to keep the samples in water at least one day (HATFIELD ([1])) and to degas the water of vessel *B*; furthermore the surface of the samples had to be carefully cleaned in order to achieve a perfect wetting and to prevent the formation of an air layer during the ultrasonic irradiation, especially at low frequencies, where the cavitation threshold is lower. According to H. KELLER's measurements ([15]), cavitation in water starts for ~ 0.45 W/cm² at 0.4 MHz and for ~ 1.5 W/cm² at 4 MHz.

The intensities used varied from $1.6 \cdot 10^{-2}$ W/cm² to 1.6 W/cm² so that the relative vibration amplitude in the rubber varied from $3 \cdot 10^{-6}$ to $3\ 10^{-5}$.

The highest intensities were used only for the maximum attenuation, so that the measurements were generally made under the cavitation threshold.

To verify if the values of attenuation obtained with different intensities are comparable, measurements of the absorption coefficient with varying ultrasonic intensities incident on the samples (relative variation 1 to 100) have been performed at constant temperature and frequency. Within experimental errors no absorption dependence on the intensity has been detected in the considered range.

([13]) R. D. FAY and O. V. FORTIER: *Journ. Acoust. Soc. Am.*, **23**, 339 (1951).
([14]) H. S. SACK and R. W. ALDRICH: *Phys. Rev.*, **75**, 1285 (1949).
([15]) H. KELLER: *Der Ultraschall in der Medizin* (Zürich, 1949) pag. 77.

3. – Experimental Results.

The curve of Fig. 2, taken from the paper of IVEY *et al.* [3], represents for natural rubber, the attenuation L in db/cm versus temperature in centigrades at constant frequency (10 MHz).

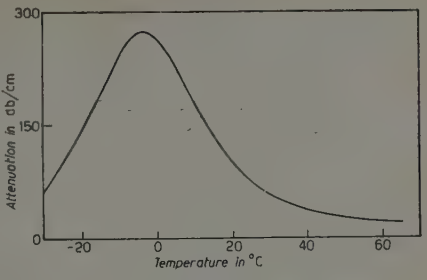

Fig. 2. – Bulk wave-attenuation vs. temperature at 10 MHz for natural rubber (from IVEY *et al.* [3]).

Its characteristic bell shape has a maximum which increases and shifts towards higher temperatures as the frequency is increased; this can be explained by relaxation (see ALFREY [16]: frequency-temperature equivalence). We shall refer to this maximum as M_2.

The temperature, at which attenuation is at its maximum, varies for different rubbers [2,3]; as can be seen in Fig. 2, this temperature is, for natural rubber, about -10 °C at 10 MHz.

Our diagrams are to be put in relation with the decreasing part of the bell curve, on account of our temperature range (4 °C to 70 °C).

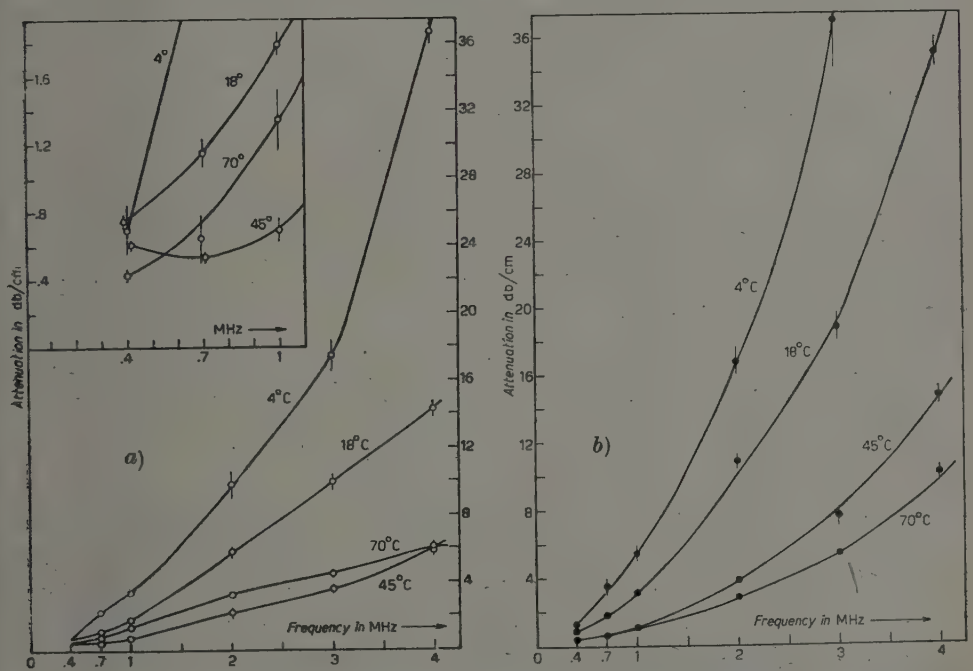

Fig. 3. – *a*) Bulk waves attenuation vs. frequency for unloaded natural rubber; *b*) Bulk waves attenuation vs. frequency for carbon loaded natural rubber (50 parts by weight carbon on 100 parts rubber).

---

[16] T. ALFREY: *Mechanical Behaviour of High Polymers* (New York, 1948).

Figs. 3*a* and 3*b* show the variation of the absorption with frequency, at four different temperatures, for unloaded and loaded rubber, respectively.

The attenuation of loaded rubber shows a nearly parabolic increase with frequency.

While for the loaded rubber the attenuation always increases with increasing frequency and decreasing temperature, the unloaded rubber presents at 70 °C an attenuation higher than that at 45 °C for frequencies from 0.7 MHz to 4 MHz. This inversion of the temperature coefficient, for unloaded rubber, corresponds to the minima of the curves of absorption plotted against temperature in the Figs. 4*a* and 4*b*.

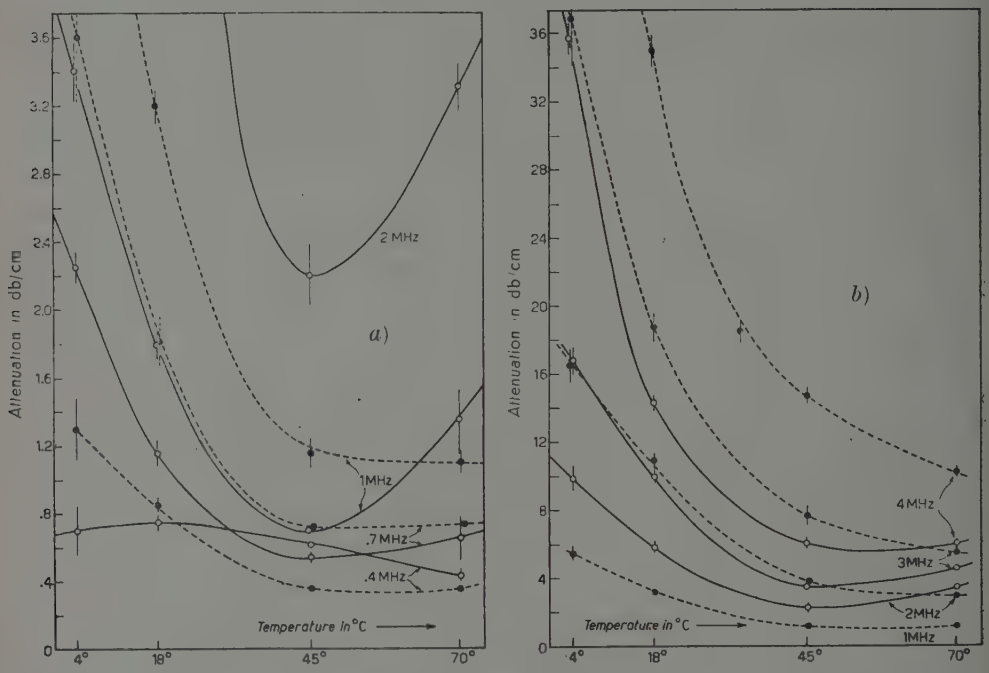

Fig. 4*a*, *b*. – Bulk wave-attenuation vs. temperature for unloaded (——) and loaded (------) natural rubber.

The relative depth of these minima diminishes for the highest and lowest frequencies. It may be said that the minimum lies between two maxima, one being the main maximum M_2. The other maximum, which is to be found at a higher temperature, will be called maximum M_3. It falls within our temperature range only for the frequency of 0.4 MHz.

There is in the literature another example of a maximum (M_1) distinct from the main maximum M_2. It was found by A. W. NOLLE and S. MOWRY [2] in butyl at 10 MHz at a temperature below that of the maximum M_2, i.e. at about — 45 °C.

This unusual separation of maxima indicates a discrimination between different relaxation mechanisms.

If they are referred to the same temperature and τ_i indicates a mean relaxation time related with the maximum M_i, it must be concluded that $\tau_3 > \tau_2 > \tau_1$, so that the relaxation mechanisms involved are mainly related to configurational, quasi-configurational and crystalline elasticity, respectively.

The attenuation for carbon loaded rubber presents no minima, as it appears from the dashed-line curves in Figs. 4*a* and 4*b*. The relaxation mechanisms concerning the maximum M_3 are not discriminated from those of the maximum M_2.

Carbon loading diminishes the relaxation mechanism related with the maximum M_3, which will be called P_3, whereas it exalts the relaxation mechanism P_2, related with M_2.

In fact, Figs. 4*a* and 4*b* show that while at low temperatures, within the range governed by the relaxation mechanism P_2, the values of absorption are increased in a rather regular manner by carbon, the reverse occurs above a given temperature, in the range governed by relaxation mechanism P_3.

This decrease of attenuation with carbon loading at high temperature, in a particular frequency range, (compare also Fig. 5), is the first example of a reverse effect of the carbon loading on absorption.

Our experimental values agree, by extrapolation with IVEY's measurements at 10 MHz ([3]) for unloaded natural rubber, and with Hatfield's data for carbon loaded natural rubber, for frequencies from 50 kHz to 350 kHz at room temperature ([1]).

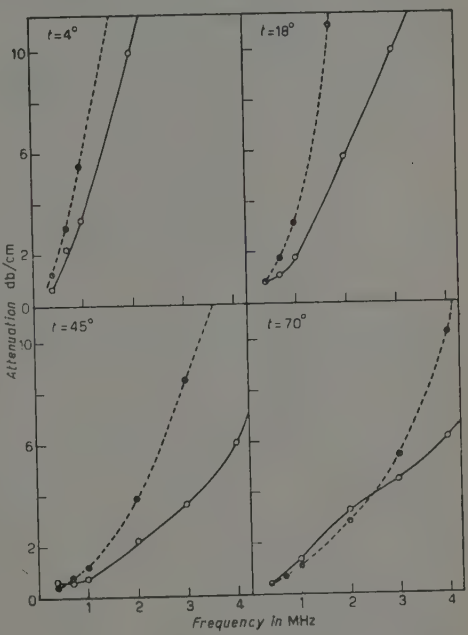

Fig. 5. – Bulk wave-attenuation vs. frequency for unloaded (——) and loaded (- - - -) natural rubber.

4. – Discussion of Experimental Results.

It is well known that, in order to give a mathematical treatment to the fact that in elastomers stress and strain are not in phase, the mechanical behaviour of viscoelastic substances is described by the formulae of perfect elasticity, by substitution of the elastic moduli with complex ones.

For longitudinal waves a bulk modulus B_1+iB_2 and a shear modulus $\mu_1+i\mu_2$ are to be considered, because the propagation of such waves implies bulk, as well as shear strains. In fact, velocity v and absorption α appear to be related with the real (elastic) part of an « effective modulus » $B_1+4\mu_1/3$ and with its imaginary (viscous) part $B_2+4\mu_2/3$ as follows:

$$B_1+\frac{4}{3}\mu_1=\frac{\varrho v^2[1-(\alpha^2v^2/\omega^2)]}{[1+(\alpha^2v^2/\omega^2)]^2}, \tag{1}$$

$$B_2+\frac{4}{3}\mu_2=\frac{2\varrho\alpha v^3}{\omega^2[1+(\alpha^2v^2/\omega^2)]^2}, \tag{2}$$

where α is the absorption coefficient in neper/cm, $\omega=2\pi f$ is the angular frequency and ϱ is the density.

From these formulae the following expressions are obtained for v and α, considering that a^2v^2/ω^2 is negligible with respect to unity:

$$v=\left(\frac{B_1+\frac{4}{3}\mu_1}{\varrho}\right)^{\frac{1}{2}}, \tag{3}$$

$$\alpha=\frac{2\pi^2f^2(B_2+\frac{4}{3}\mu_2)}{\varrho v^3}, \tag{4}$$

or, using Lamé's constants, as it is customary with liquid polymers:

$$v=\left(\frac{\lambda_1+2\mu_1}{\varrho}\right)^{\frac{1}{2}}, \tag{3'}$$

$$\alpha=\frac{2\pi^2f^2(\lambda_2+2\mu_2)}{\varrho v^3}. \tag{4'}$$

Normally, for elastomers, the absorption coefficient is given in db/cm (L):

$$L\ (\text{db/cm})=8.686\ \alpha\ (\text{neper/cm}).$$

Formula (4) may be applied if we take into account the experimental values of velocity given by IVEY *et al.* [3] for natural unloaded rubber.

From these values [3] (Fig. 8, pag. 489), it appears that, in the considered frequency and temperature ranges, the velocity of longitudinal waves for natural unloaded rubber is constant at a given temperature or eventually slowly increasing (not more than 10 percent) with frequency.

For loaded rubber the curves of Fig. 3*b*, concerning temperatures of 45 °C and 70 °C, have, within experimental errors, the shape of exact parabolas.

It follows that equation (4) gives a constant value of the viscous effective modulus in this range. Loaded rubber shows a relaxation effect only for the lower temperatures.

For unloaded rubber, comparison of the curves of Fig. 3*a* with parabolas, shows a distorsion at low temperatures but also a more remarkable bell-shaped deformation at the two higher temperatures. On the other hand, it has to be noted that the square law dependence ensues to tend to Ive's data for 10 MHz ([3]), so that relaxation effects do not appear at higher frequencies.

When attenuation (or velocity) is plotted against temperature, taking the frequency as a parameter, a much more comprehensive look on relaxation mechanism may be acquired, because relaxation times depend exponentially on temperature, while, by variation of the frequency of the elastic waves, relaxation times are linearly explored. In fact the curves of Figs. 4*a* and 4*b* give evidence, for unloaded rubber, of a discrimination between relaxation mechanisms P_2 and P_3, which could not be observed in the curves of Fig. 3*a*.

The main maximum of attenuation with respect to temperature, which we have called M_2, is attributable to μ_2, assuming Stokes' hypothesis $B_2 = 0$ (as is generally done, see ref. ([2,3,9])).

The investigations of A. W. Nolle and P. W. Sieck ([4]), in the range of temperature lower than the temperature corresponding to maximum M_2, with the aim of finding out the values of B_2/μ_2, did not give discriminative results for the limits of validity of Stokes' hypothesis in this temperature range.

The existence of maximum M_3, at temperatures higher than that corresponding to maximum M_2, could be explained by the following considerations, based on the comparison of the absorption data for loaded and unloaded rubber, which will lead to a value of B_2 not negligible with respect to μ_2 for natural rubber at high temperatures.

We will now consider the influence of carbon loading on the two viscoelastic deformations, involved in longitudinal waves, i.e. on shear and volume compression separately.

In Fig. 6 are represented simple shear- and volume compression-deformations, schematizing an elementary cubic volume of carbon loaded rubber as a small sphere (some tenth of a micron in diameter) surrounded by rubber. Thus, to simplify, flocculation is neglected, which however is already present at 50/100 carbon to rubber ([18]).

The shear elastic modulus of rubber μ_1, which is an increasing function of frequency, is in our frequency range still much lower than the corresponding modulus of carbon (see paper on carbon reinforcement at low frequencies ([17-19])).

([17]) J. Rehner Jr.: *Journ. Appl. Phys.*, **14**, 638 (1943).
([18]) E. Guth: *Journ. Appl. Phys.*, **16**, 20 (1945).
([19]) D. Parkinson: *Trans. Inst. Rubber Industry*, **21**, 7 (1945).

Motions of rubber relative to carbon at the boundary are to be considered, this implies energy dissipation and determines an increase of μ_2 due to carbon loading. Evidence of this is given for example by Parkinson's measurements concerning the increase of energy losses with increasing specific carbon area at constant loading ([19]). The increase of μ_2 can be found in the absorption values at low temperatures of the diagrams of Figs. 4*a*, 4*b* and 5. See also references ([10,17-20]).

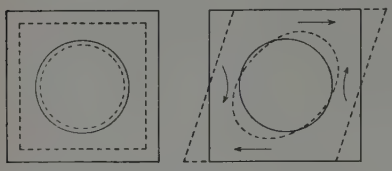

Fig. 6. – Schema of simple shear and all-sided compression deformations for loaded rubber (carbon sphere in a volume element of rubber).

The volume compression deformation does not involve relative motions at the rubber-carbon interfaces, even disregarding the fact that, actually, the elastic (bulk) moduli of the two substances are less different than in the shear case ([17]). The non occurence of this energy dissipation in the boundary layers, involves that the loading is a mere partial substitution of rubber with carbon, possessing a modulus B_2 lower than that of rubber. In fact, the latter has, at a given frequency, for any kind of elastic waves, an attenuation of several orders of magnitude higher than that of any non porous solid. Therefore, it seems consistent to suppose that B_2 is decreased by the addition of carbon.

Furthermore, another reason exists which leads to a value of B_2 for carbon loaded rubber less than that for pure rubber. W. P. MASON and co-workers ([6]) (compare also ref. ([7,8])) have investigated the variation of the compressional viscosity of a given liquid high polymer (for instance polyisobutylene, base of butyl rubber), with the variation of the average molecular weight. They found that the compressional viscosity $\lambda_2' = \lambda_2/\omega$, which is negligible for the shorter chains, becomes a considerable fraction of shear viscosity for the longer chains. If this result is extrapolated to vulcanized rubber (considering that the temperature is about 70 °C), taking into account that carbon loading shortens the apparent chain segment between cross-links (at equivalent vulcanization degree) ([8]), B_2 for unloaded rubber should be higher than that for loaded rubber.

It must be concluded that the effect of carbon loading on the two terms of the viscous effective modulus is opposite: μ_2 is increased, while B_2 is decreased.

With reference to the curves of Figs. 4*a* and 4*b*, it may be said that the increase of attenuation, at high temperatures, for unloaded rubber, which does not occur for the loaded one, would be attributable to the term B_2 of the viscous effective modulus. Taking, for example, the curve at 1 MHz, it appears that.

([20]) S. OBERTO and G. PALANDRI: *The Rubber Age*, **63**, 725 (1948).

under this assumption, at 70 °C, B_2 is equal or even higher than μ_2 for natural unloaded rubber.

5. – Conclusions.

The observation of the different behaviour of loaded and unloaded rubber has been made possible by the good sensitivity of the method in the considered range of attenuation.

To obtain values of the ratio B_2/μ_2, it would be interesting to carry out measurements also with pure shear waves ([4]) or with other methods ([5]), in the same frequency and temperature ranges.

We emphasize the fact that measurements at very high frequencies and at low temperatures must be treated with care, because when mere crystalline (or glassy) elasticity is involved, it becomes ambiguous to state whether a relaxation is involved or the attenuation of the sample is that of a normal microcrystalline or vitrous solid (see measurements of absorption till 200 MHz made by R. A. RAPUANO ([21])). It follows that, as for viscoelastic behaviour at high frequency, measurements are more significant if carried out below a certain frequency, which depends on the temperature and on the peculiar viscoelastic material.

6. — Acknowledgements.

We wish to express our gratitude to Prof. A. GIACOMINI, who suggested the subject of the present research. The useful advice of Dr. S. OBERTO is also gratefully acknowledged.

([21]) R. A. RAPUANO: *Phys. Rev.*, **72**, 78 (1947).

RIASSUNTO

Si riportano misure di assorbimento delle onde ultrasonore longitudinali in gomma naturale vulcanizzata, senza carica e con 50 parti di nero fumo per 100 di gomma, per frequenze tra 0,4 MHz e 4 MHz e temperature tra 4 °C e 70 °C. I coefficienti di assorbimento sono stati ottenuti misurando, mediante una bilancia di torsione, l'attenuazione che subisce un fascio di ultrasuoni propagantesi in acqua, nell'attraversare i campioni di gomma. L'assorbimento, in funzione della temperatura, presenta, per la gomma con carica, il comportamento già noto per le gomme sia naturali che sintetiche. Quello relativo alla gomma naturale senza carica presenta un minimo, che indica una separazione tra due diversi effetti di rilassamento. Si è trovato un esempio di diminuzione del coefficiente di assorbimento con la carica.

A Note Concerning the Quantization of Spinor Fields.

Y. Takahashi (*)

Division of Physics, National Research Council - Ottawa, Canada

(ricevuto il 17 Gennaio 1955)

Summary. — Jauch's paper with the same title is re-examined by use of the usual quantization formalisms. Schwinger's action principle can give the commutation relations suggested by Jauch, if we choose appropriate canonical independent variables, different from the variational independent variables. Quantization in the interaction representation is also discussed. The interaction between Jauch's field and the electromagnetic field is considered.

1. – Introduction and Summary.

We have the method of Jordan-Pauli-Fierz (1) for the manifestly covariant quantization of a force free field, which is quite useful in clarifying the relation between the transformation properties of field quantities and the quantization procedure and, further, gives a theoretical derivation of the empirical law of the connection between spin and statistics. Nevertheless, their method has two faults (2).

The first point is that there is no general rule to define directly the function $R_{\alpha\beta}(\partial)\Delta(x-x')$ which appears in the commutation relations of the field quantities Q_α

$$[Q_\alpha(x), Q_\beta(x')]_\pm = iR_{\alpha\beta}(\partial)\,\Delta(x-x')\,, \tag{1.1}$$

(*) National Research Laboratories Postdoctorat Fellow.

(1) P. Jordan and W. Pauli: *Zeits. f. Phys.*, **47**, 15 (1928); M. Fierz: *Helv. Phys. Acta*, **12**, 3 (1939); M. Fierz and W. Pauli: *Proc. Roy. Soc.*, A **173**, 211 (1939); W. Pauli: *Solvey Berichte* (1939); *Rev. Mod. Phys.*, **13**, 203 (1941).

(2) This fact is stressed by Professor Yukawa in his book, *Introduction to the Theory of Elementary Particles* (in Japanese, 1948), first edition, p. 193.

this, therefore, has to be obtained by way of four steps, i.e., first, to construct the Lagrangian for each case, second, to define the canonical variables, third, to apply the three-dimensional procedure of Heisenberg-Pauli [3] to it and fourth, to make it manifestly covariant by use of the method given by WENTZEL [4] for boson fields and extended by UMEZAWA [5] to fermion fields.

The second point is the difficulty in the treatment of the interaction of fields.

In connection with the first point, we gave a simple rule by which the force free field with any spin can be quantized without canonical formalism [6]. Suppose the equation of motion obtained directly from a Lagrangian is

$$\Lambda_{\alpha\beta}(\partial)Q_\beta(x) = 0\,, \tag{1.2}$$

i.e., (1.2) can be reduced to the equation of harmonic oscillators

$$(\Box - \varkappa^2)Q_\alpha(x) = 0$$

and several subsidiary conditions, then $R_{\alpha\beta}(\partial)$ is determined by an identity

$$\Lambda_{\alpha\beta}(\partial)R_{\beta\gamma}(\partial) = (\Box - \varkappa^2)\delta_{\alpha\gamma}\,. \tag{1.3}$$

We shall term this the method of quantization by the Green's function of a si nple harmonic oscillator.

In connection with the second point, we developed a general theory of interaction representation based on the identity (1.3) for a system with any kinds of interaction. Thus the above two points which are mentioned to Professor YUKAWA have been solved from a unified view point.

On the other hand, we have, as a unified theory of quantized fields, a formalism of Schwinger based on the variational principle of an action integral [7]. It seems in his formalism that the quantum feature of a system can be uniquely determined by the variational principle when its classical Lagrangian is given.

At this stage, JAUCH proposes [8] rather strange covariant commutation relations for the spin $\frac{1}{2}$ field which coincides with the usual electron-positron field and the MAJORANA field [9] as extreme cases and cannot follow, he asserts, from Schwinger's action principle.

---

[3] W. HEISENBERG and W. PAULI: *Zeits. f. Phys.*, **56**, 1 (1929); **59**, 168 (1930).
[4] G. WENTZEL: *Einführung in die Quantentheorie der Wellenfelder* (1943).
[5] H. UMEZAWA: *Theory of Elementary Particles* (in Japanese, 1953).
[6] Y. TAKAHASHI and U. UMEZAWA: *Prog. Theor. Phys.*, **9**, 14, 501 (1953).
[7] J. SCHWINGER: *Phys. Rev.*, **82**, 914 (1951).
[8] J. M. JAUCH: *Helv. Phys. Acta*, **27**, 89 (1954).
[9] E. MAJORANA: *Nuovo Cimento*, **14**, 171 (1937); W. H. FURRY: *Phys. Rev.*, **54**, 56 (1938).

He gives the commutation relations

$$\text{(1.4)} \qquad \begin{cases} \{\psi_\alpha(x), \bar{\psi}_\beta(x')\} = \dfrac{1}{i} S_{\alpha\beta}(x - x') , \\ \{\psi_\alpha(x), \hat{\psi}_\beta(x')\} = \dfrac{1}{i} \varrho S_{\alpha\beta}(x - x') , \end{cases} \qquad 0 \leqslant \varrho \leqslant 1 ,$$

instead of the usual commutation relations of the electron-positron field

$$\text{(1.5) } [10] \qquad \begin{cases} \{\psi_\alpha(x), \bar{\psi}_\beta(x')\} = \dfrac{1}{i} S_{\alpha\beta}(x - x') , \\ \{\psi_\alpha(x), \hat{\psi}_\beta(x')\} = 0 . \end{cases}$$

In this note the relation will be examined between the arbitrariness of (1.4) and the pre-existing quantization rules, i.e., the usual canonical formalism, Schwinger's action principle formalism, the method of the Green's function of the simple harmonic oscillator and the interaction representation formalism [11].

According to our discussion below, the usual quantization rule has still the following two degrees of freedom corresponding to the steps mentioned above:

i) The construction of the Lagrangian, i.e., we can adopt a Lagrangian for the field with spin $\frac{1}{2}$

$$\text{(1.6)} \qquad L = -\bar{\psi}(\gamma\partial + \varkappa)\psi - \lambda\{\bar{\psi}(\gamma\partial + \varkappa)\psi^* + \hat{\psi}(\gamma\partial + \varkappa)\psi\} .$$

instead of the usual one

$$\text{(1.7)} \qquad L = -\bar{\psi}(\gamma\partial + \varkappa)\psi ,$$

---

[10] We introduce a representation which is slightly different from that in JAUCH's paper. That is,

$$\gamma_\mu\gamma_\nu + \gamma_\nu\gamma_\mu = 2\,\delta_{\mu\nu}$$

and all the matrix elements of γ_i ($i=1, 2, 3$) and γ_4 are real and purely imaginary, respectively. $+$, T and * stand for Hermitian conjugation, transposition and complex conjugation, respectively. Also, $\bar{\psi} \equiv \psi^+\gamma_4$ and $\hat{\psi} \equiv \psi^T\gamma_4$.

[11] Besides, we have the quantization rule which is given by PEIERLS (*Proc. Roy. Soc.*, A 214, 143 (1952)). Some erroneous points are found in his proof and are quite essential in our present discussion. A quantity of the Heisenberg representation and one of the interaction representation cannot generally be combined with each other by a unitary transformation, as in equation (3.5) in his paper. This is the very reason why $Q_\alpha(x, \sigma)$ has to be introduced in addition to the quantities in the Heisenberg and interaction representation. As will be shown in section 2 (iii) in our paper, the field quantity in the Heisenberg representation is Jauch's field and the quantity in the interaction representation is the electron-positron field which satisfies a different commutation relation from Jauch's. This is a typical example contradicting his equation (3.5). The neutral vector field interacting with a spin 1/2 field is also such a case.

both of which are Lorentz invariant and Hermitian and yield the same equations of motion if $\lambda \neq \frac{1}{2}$.

As soon as we are going to quantize (1.6), we have to define canonical variables, thus we should state either

ii) The definition of the canonical independent variables of this system (when using the canonical formalism or Schwinger's action principle), or

ii′) The definition of the interaction part of the Lagrangian (when using the interaction representation formalism).

In § 2, it is shown that the arbitrariness mentioned by JAUCH comes from these two degrees of freedom.

It must be noted that the Green's function of the simple harmonic oscillator which is not based on the canonical formalism immediately gives (1.4) from (1.6) independent of ii) or ii′) and that Schwinger's action principle or the usual canonical formalism is applicable only for $|2\lambda| < 1$, although the interaction representation formalism can always be useful except for $|2\lambda| = 1$. In the last paragraph, the interaction between Jauch's and the electromagnetic fields is discussed.

2. – Derivation of Jauch's Commutation Relation by the Usual Quantization Formalism.

For the variation of the Lagrangian (1.6) which is invariant relativistically and under Hermitian conjugation, we have, bearing in mind the fact that $\delta\bar{\psi}$ and $\delta\hat{\psi}$ anticommute with ψ, $\bar{\psi}$, etc.,

$$\delta_{\psi} L = -\delta\bar{\psi}\{(\gamma\partial + \varkappa)\psi + \lambda(\gamma\partial + \varkappa)\psi^* + \lambda\varkappa\psi^*\} + \frac{\partial\delta\bar{\psi}}{\partial x_\mu}\lambda\gamma_\mu\psi^* \tag{2.1}$$

and

$$\delta_{\hat{\psi}} L = -\delta\hat{\psi}\{\varkappa\psi^* + \lambda(\gamma\partial + \varkappa)\psi + \lambda\varkappa\psi\} + \frac{\partial\delta\hat{\psi}}{\delta x_\mu}\{\gamma_\mu\psi^* - \lambda\gamma_\mu\psi\} . \tag{2.1′}$$

Thus the Euler equations of motion are

$$-(\gamma\partial + \varkappa)\psi - 2\lambda(\gamma\partial + \varkappa)\psi^* = 0 , \tag{2.2}$$

$$-(\gamma\partial + \varkappa)\psi^* - 2\lambda(\gamma\partial + \varkappa)\psi = 0 . \tag{2.2′}$$

Therefore we obtain

$$(\gamma\partial + \varkappa)\psi = 0 , \tag{2.3}$$

$$(\gamma\partial + \varkappa)\psi^* = 0 , \tag{2.3′}$$

which coincide with the Dirac wave equation, except in the case

$$\begin{vmatrix} 1 & 2\lambda \\ 2\lambda & 1 \end{vmatrix} = (1 - 4\lambda^2) = 0 \quad (12). \tag{2.4}$$

Now in order to quantize this field, we shall use the following four methods:

i) *Quantization by the canonical formalism.* – In this formalism we regard, as is customary, the variational independent variable as the canonical independent variable. Therefore the canonical momentum of ψ is, from (2.1′),

$$\pi_\alpha(x) = -i\lambda\psi_\alpha(x) + i\psi^*_\alpha(x) . \tag{2.5}$$

The commutation relations at $t = t'$ are

$$\begin{cases} 0 = \{\psi_\alpha(x), \psi_\beta(x')\} , \\ i\,\delta_{\alpha\beta}\,\delta(x - x') = \{\psi_\alpha(x), \pi_\beta(x')\} = i\{\psi_\alpha(x), \psi^*_\beta(x')\} , \\ 0 = \{\pi_\alpha(x), \pi_\beta(x')\} = \lambda\{\psi_\alpha(x), \psi^*_\beta(x')\} + \lambda\{\psi^*_\alpha(x), \psi_\beta(x')\} , \end{cases} \tag{2.6}$$

the three equations of (2.6) are consistent with each other only when $\lambda = 0$ and this field becomes the usual electron-positron field. Thus, we can conclude that the canonical formalism in which ψ itself is the canonical independent variable is impossible so long as $\lambda \neq 0$. This is the same situation as occurs with the KONOPINSKI and UHLENBECK field (6).

We have three methods to avoid this difficulty. The first one is to use a method independent of the canonical formalism. The second one is to quantize by the interaction representation formalism which is based on the field quantities satisfying the equation of motion with $\lambda = 0$. The third one is the quantization by the canonical formalism in which the canonical independent variables are different from ψ and $\bar{\psi}$ themselves and the λ-term is eliminated.

We shall discuss (1.6) by these three methods in the following:

ii) *Quantization by the Green's function of the simple harmonic oscillator, which is independent of canonical formalism* (5). – In this case the equation of motion obtained directly from the Lagrangian is

$$-(\gamma\partial + \varkappa)\{\psi(x) + 2\lambda\psi^*(x)\} = 0 .$$

(12) When $\lambda = \pm 1/2$, (2.3) amd (2.3′) are not independent of each other. This means that $\delta\bar{\psi}$ and $\delta\hat{\psi}$ cannot be independent from the beginning.

Therefore, we obtain, by use of the identity (1.3) and (1.5),

$$\{\psi_\alpha(x) + 2\lambda\psi_\alpha^*(x),\ \bar{\psi}_\beta(x') + 2\lambda\hat{\psi}_\beta(x')\} = \frac{1}{i} S_{\alpha\beta}(x - x'), \tag{2.7}$$

$$\{\psi_\alpha(x) + 2\lambda\psi_\alpha^*(x),\ \hat{\psi}_\beta(x') + 2\lambda\bar{\psi}_\beta(x')\} = 0\,. \tag{2.7'}$$

From (2.7), (2.7′) and their complex conjugate equations, we get

$$\{\psi_\alpha(x),\ \bar{\psi}_\beta(x')\} = \frac{1}{i}\frac{(1+4\lambda^2)}{(1-4\lambda^2)^2} S_{\alpha\beta}(x - x')\,, \tag{2.8}$$

$$\{\psi_\alpha(x),\ \hat{\psi}_\beta(x')\} = \frac{1}{i}\frac{4\lambda}{(1-4\lambda^2)^2} S_{\alpha\beta}(x - x')\,, \tag{2.8'}$$

except for

$$(1 - 4\lambda^2) = 0\,. \tag{2.9}$$

If we put ψ_α in place of

$$\frac{1-4\lambda^2}{\sqrt{1+4\lambda^2}}\,\psi_\alpha(x)\,,$$

then (2.8) and (2.8′) are

$$\{\psi_\alpha(x),\ \bar{\psi}_\beta(x')\} = \frac{1}{i} S_{\alpha\beta}(x - x')\,, \tag{2.10}$$

$$\{\psi_\alpha(x),\ \hat{\psi}_\beta(x')\} = \frac{1}{i}\frac{4\lambda}{1+4\lambda^2} S(x_{\alpha\beta} - x')\,. \tag{2.10'}$$

From the condition (2.9), we have

$$0 < (1 \pm 2\lambda)^2 = 1 + 4\lambda^2 \pm 4\lambda$$

therefore

$$\left|\frac{4\lambda}{1+4\lambda^2} \equiv \varrho\right| < 1\,. \tag{2.11}$$

The field with $\lambda = \pm\,\frac{1}{2}$ must be quantized by the original method of Majorana, i.e., the Lagrangian is

$$L \cong -\tfrac{1}{2}(\psi \pm \hat{\psi})(\gamma\partial + \varkappa)(\psi \pm \psi^*)\,,$$

where $\cong$ means equality apart from a divergence term and $+$ and $-$ correspond to $\lambda = \frac{1}{2}$ and $\lambda = -\frac{1}{2}$, respectively.

According to MAJORANA ([7])

$$\{\psi_\alpha(x), \hat{\bar{\psi}}_\beta(x')\} = \pm \frac{1}{i} S_{\alpha\beta}(x - x') . \tag{2.12}$$

Expressing in a unified way (2.10), (2.10′) and (2.12), we have

$$\{\psi_\alpha(x), \bar{\psi}_\beta(x')\} = \frac{1}{i} S_{\alpha\beta}(x - x') , \tag{2.13}$$

$$\{\psi_\alpha(x), \hat{\bar{\psi}}_\beta(x')\} = \frac{1}{i} \varrho S_{\alpha\beta}(x - x') , \qquad |\varrho| \leqslant 1 , \tag{2.13′}$$

which is the commutation relation given by JAUCH.

iii) *Quantization by the interaction representation* ([6]). – We first regard the λ-term as an interaction. We have to begin with the equation of motion

$$-(\gamma\partial + \varkappa)\psi - 2\lambda(\gamma\partial + \varkappa)\psi^* = 0 , \tag{2.2}$$

$$-(\gamma\partial + \varkappa)\psi^* - 2\lambda(\gamma\partial + \varkappa)\psi = 0 . \tag{2.2′}$$

From (2.2), we have

$$\psi(x) = \psi^0(x) - 2\lambda \int_{-\infty}^{\infty} (\gamma\partial + \varkappa) S_c(x - x') \psi^*(x') \, \mathrm{d}x' , \tag{2.14}$$

where

$$\begin{cases} (\gamma\partial + \varkappa)\psi^0(x) = 0 , \\ (\gamma\partial + \varkappa) S_c(x - x') = \delta(x - x') , \\ \{\psi^0_\alpha(x), \bar{\psi}^0_\beta(x')\} = \dfrac{1}{i} S_{\alpha\beta}(x - x') , \\ \{\psi^0_\alpha(x), \hat{\bar{\psi}}^0_\beta(x')\} = 0 . \end{cases} \tag{2.15}$$

We define from (2.14) the quantity

$$\psi(x, \sigma) = \psi^0(x) - 2\lambda \int_{-\infty}^{\sigma} (\gamma\partial + \varkappa) S(x - x') \psi^*(x') \, \mathrm{d}x' = \psi^0(x) , \tag{2.16}$$

which satisfies the free equation of motion. Then, if we express $\psi(x)$ by means of $\psi(x, \sigma)$, we obtain

$$\psi(x) = \psi^0(x) - 2\lambda\psi^*(x) = \psi(x, \sigma) - 2\lambda\psi^*(x, \sigma) + \ldots = \tag{2.17}$$

$$= \frac{1}{1 - 4\lambda^2} \{\psi(x, \sigma) - 2\lambda\psi^*(x, \sigma)\}$$

and

$$\psi^*(x) = \frac{1}{1-4\lambda^2}\{\psi^*(x,\sigma) - 2\lambda\psi(x,\sigma)\} \tag{2.17'}$$

except for $1-4\lambda^2 = 0$.

There exists a unitary transformation combining $\psi_\alpha(x,\sigma)$ and $\psi^0_\alpha(x)$, because of

$$\{\psi_\alpha(x,\sigma), \bar{\psi}_\beta(x',\sigma)\} = \frac{1}{i} S_{\alpha\beta}(x-x'), \tag{2.18}$$

$$\{\psi_\alpha(x,\sigma), \hat{\psi}_\beta(x,\sigma)\} = 0. \tag{2.18'}$$

By use of (2.18), (2.18'), we get from (2.17) and (2.17')

$$\{\psi_\alpha(x), \bar{\psi}_\beta(x')\} = \frac{1}{(1-4\lambda^2)^2}\{\psi_\alpha(x,\sigma) - 2\lambda\psi^*_\alpha(x,\sigma), \bar{\psi}_\beta(x',\sigma) - 2\lambda\hat{\psi}_\beta(x',\sigma)\} =$$

$$= \frac{1+4\lambda^2}{(1-4^2)^2}\frac{1}{i} S_{\alpha\beta}(x-x'),$$

$$\{\psi_\alpha(x), \hat{\psi}_\beta(x')\} = \frac{1}{i}\frac{-4\lambda}{(1-4\lambda^2)^2} S_{\alpha\beta}(x-x').$$

If we replace

$$\frac{1-4\lambda^2}{\sqrt{1+4\lambda^2}}\psi_\alpha \tag{2.19}$$

by ψ_α, then

$$\{\psi_\alpha(x), \bar{\psi}_\beta(x')\} = \frac{1}{i} S_{\alpha\beta}(x-x'), \tag{2.20}$$

$$\{\psi_\alpha(x), \hat{\psi}_\beta(x')\} = \frac{1}{i}\varrho S_{\alpha\beta}(x-x'), \tag{2'20'}$$

where

$$\left|\varrho \equiv \frac{-4\lambda}{1+4\lambda^2}\right| < 1.$$

Quantizing according to MAJORANA when $\varrho = 1$, we have

$$\{\psi_\alpha(x), \bar{\psi}_\beta(x')\} = \frac{1}{i} S_{\alpha\beta}(x-x'), \tag{2.21}$$

$$\{\psi_\alpha(x), \hat{\psi}_\beta(x')\} = \frac{1}{i}\varrho S_{\alpha\beta}(x-x'), \qquad |\varrho| \leqslant 1. \tag{2.21'}$$

Incidentally, we define the energy-momentum tensor of this system. From the equation

$$[\psi(x,\sigma),\ H(x'/\sigma)] = 0\,,$$

$$[\psi^*(x,\sigma),\ H(x'/\sigma)] = 0\,,$$

we have

$$H(x/\sigma) = 0$$

and

$$T_{\mu\nu}(x) = U^{-1}(\sigma)\,T^0_{\mu\nu}(x)\,U(\sigma)\,|_{x/\sigma} = U^{-1}(\sigma)\bar{\psi}^0(x)\gamma_\mu\,\frac{\partial\psi^0(x)}{\partial x_\nu}\,U(\sigma) \cong$$

$$\cong \frac{1+4\lambda^2}{(1-4\lambda^2)^2}\,(\bar{\psi}+2\lambda\hat{\bar{\psi}})\gamma_\mu\,\frac{\partial}{\partial x_\nu}\,(\psi+2\lambda\psi^*) \quad [13].$$

It can be easily proved by considering (2.21) and (2.21′) that the equation

$$i\,\frac{\partial\psi(x)}{\partial x_\mu} = [\psi(x),\,P_\mu(\sigma)] \qquad P_\mu(\sigma) = \int T_{\mu\nu}(x)\,\mathrm{d}\sigma_\nu\,,$$

agrees with the equation of motion

$$(\gamma\partial + \varkappa)\,\psi(x) = 0\,.$$

iv) *Quantization by Schwinger's action principle* [7]. – So long as ψ itself is the canonical independent variable, the formalism for $\lambda \neq 0$ cannot be self-consistent, as in the case (i).

We are going to eliminate the λ-term by the transformation

$$\left\{\begin{aligned} \psi &\equiv a\varphi + b\varphi^*\,,\\ \psi^* &\equiv a\varphi^* + b\varphi\,. \end{aligned}\right. \tag{2.22}$$

From (1.6)

$$L \cong -\lambda_a\bar{\varphi}(\gamma\partial+\varkappa)\varphi - \lambda_b\left(-\frac{\partial\hat{\bar{\varphi}}}{\partial x_\mu}\,\gamma_\mu + \varkappa\hat{\bar{\varphi}}\right)\varphi^* - \tag{2.23}$$

$$-\lambda_c\bar{\varphi}(\gamma\partial+\varkappa)\varphi^* - \lambda_c\hat{\bar{\varphi}}(\gamma\partial+\varkappa)\varphi\,,$$

where

$$\left\{\begin{aligned} \lambda_a &= a^2 + 2\lambda ab\,,\\ \lambda_b &= b^2 + 2\lambda ab\,,\\ \lambda_c &= ab + \lambda(a^2+b^2)\,. \end{aligned}\right. \tag{2.24}$$

[13] $\cong$ means the equality upon the replacement (2.19).

Euler's equations of motion are

$$-(\lambda_a+\lambda_b)(\gamma\partial+\varkappa)\varphi(x)-2\lambda_c(\gamma\partial+\varkappa)\varphi^*(x)=0\,, \tag{2.25}$$

$$-(\lambda_a+\lambda_b)(\gamma\partial+\varkappa)\varphi^*(x)-2\lambda_c(\gamma\partial+\varkappa)\varphi(x)=0\,. \tag{2.2'}$$

If and only if

$$|2\lambda|\leqslant 1\,, \tag{2.26}$$

we can eliminate the term λ_c, i.e.,

$$\lambda_c=0\,. \tag{2.27}$$

In this case, we can evaluate the infinitesimal generating operator of $\delta\varphi_\alpha$ and the commutation relations [14],

$$\begin{cases} \{\varphi_\alpha(x),\,\bar{\varphi}_\beta(x')\}=\dfrac{1}{i}\,\dfrac{1}{\lambda_a+\lambda_b}\,S_{\alpha\beta}(x-x') \\ \{\varphi_\alpha(x),\,\hat{\varphi}_\beta(x')\}=0\,. \end{cases} \tag{2.28}$$

If we go back to the original field ψ by means of (2.22) and normalize appropriately, then we get

$$\{\psi_\alpha(x),\,\bar{\psi}_\beta(x')\}=\frac{1}{i}\,S_{\alpha\beta}(x-x')\,,$$

$$\{\psi_\alpha(x),\,\hat{\psi}_\beta(x')\}=\frac{1}{i}\,\varrho S_{\alpha\beta}(x-x')\,,$$

$$\left|\varrho\equiv\frac{2ab}{a^2+b^2}\right|<1\,.$$

In the case of $\varrho\geqslant 1$, we have to use Majorana's original formalism.

3. – The Interaction Between Jauch's and the Electromagnetic Fields.

We shall consider in this section the interaction between Jauch's and the electromagnetic fields. It is stated by JAUCH that this interaction cannot be possible because the commutation relation (1.4) is not invariant under the phase transformation. However, since we get a transformation by which

---

[14] Schwinger's action principle gives only the commutation relation at $t=t'$. See reference [5].

Dirac's and Jauch's fields can be connected with each other, it is not impossible to make an interaction between Jauch's and the electromagnetic fields.

We put, for the sake of simplicity,

$$\Psi(x) = \begin{pmatrix} \psi(x) \\ \psi^*(x) \end{pmatrix}, \tag{3.1}$$

then, the usual Lagrangian for the Dirac field interacting with the electromagnetic field can be written as follows:

$$L = -\frac{1}{2}\bar{\Psi}(x)\left(\gamma_\mu \frac{\partial}{\partial x_\mu} + \varkappa\right)\Psi(x) - i\frac{1}{2}e\bar{\Psi}(x)\gamma_\mu\tau_3\Psi(x)A_\mu(x) - \frac{1}{2}\frac{\partial A_\mu}{\partial x_\nu}\frac{\partial A_\mu}{\partial x_\nu}, \tag{3.2}$$

where

$$\tau_3 = \begin{pmatrix} 1 & 0 \\ 0 & -1 \end{pmatrix}. \tag{3.3}$$

This Lagrangian is invariant under the usual gauge transformation

$$\begin{cases} A_\mu(x) \to A_\mu(x) - \dfrac{\partial \Lambda(x)}{\partial x_\mu}, \\ \Psi(x) \to G[\Lambda(x)]\Psi(x), \\ \qquad G[\Lambda(x)] = \begin{pmatrix} \exp[ie\Lambda(x)] & 0 \\ 0 & \exp[-ie\Lambda(x)] \end{pmatrix}. \end{cases} \tag{3.4}$$

We will now define a transformation, in view of (2.22) [15],

$$A \equiv \frac{1}{\sqrt{a^2 - b^2}}\begin{pmatrix} a & b \\ b & a \end{pmatrix}, \tag{3.5}$$

where both a and b are real numbers and $|a| > |b|$. By using A, we can get another field

$$\Phi(x) \equiv A\Psi(x), \tag{3.6}$$

which corresponds to Jauch's field. The Lagrangian (3.2) can be rewritten in terms of (3.6) as

$$L = -\frac{1}{2}\bar{\Phi}(x)\xi\left(\gamma_\mu \frac{\partial}{\partial x_\mu} + \varkappa\right)\Phi(x) - i\frac{1}{2}e\bar{\Phi}(x)\gamma_\mu\tau_3\Phi(x)A_\mu(x) - \frac{1}{2}\frac{\partial A_\mu}{\partial x_\nu}\frac{\partial A_\mu}{\partial x_\nu}, \tag{3.7}$$

[15] a and b in this section are not always same as those in the section 2.

where we used relations

$$\xi \equiv (A^{-1})^* A^{-1} = \frac{1}{a^2 - b^2} \begin{pmatrix} a^2 + b^2 & -2ab \\ -2ab & a^2 + b^2 \end{pmatrix}, \tag{3.8}$$

$$(A^{-1})^* \tau_3 A^{-1} = \begin{pmatrix} 1 & 0 \\ 0 & -1 \end{pmatrix} = \tau_3 . \tag{3.9}$$

Corresponding to the transformation (3.4), (3.6) is transformed as

$$\Phi(x) \to AGA^{-1}\Phi(x) \equiv \bar{G}\Phi , \tag{3.10}$$

$$\bar{G} = AGA^{-1} = \frac{1}{a^2 - b^2} \begin{pmatrix} a & b \\ b & a \end{pmatrix} \begin{pmatrix} \exp[ie\Lambda] & 0 \\ 0 & \exp[-ie\Lambda] \end{pmatrix} \begin{pmatrix} a & -b \\ -b & a \end{pmatrix} = \tag{3.11}$$

$$= \begin{pmatrix} \cos e\Lambda + i\,\dfrac{a^2 + b^2}{a^2 - b^2} \sin e\Lambda & -\dfrac{2iab}{a^2 - b^2} \sin e\Lambda \\ +\dfrac{2iab}{a^2 - b^2} \sin e\Lambda & \cos e\Lambda - i\,\dfrac{a^2 + b^2}{a^2 - b^2} \sin e\Lambda \end{pmatrix} .$$

Therefore, the Lagrangian (3.7) is invariant with respect to the transformation

$$\begin{cases} A_\mu(x) \to A_\mu(x) - \dfrac{\partial \Lambda(x)}{\partial x_\mu} \\ \Phi(x) \to \bar{G}\Phi(x) \end{cases} \tag{3.12}$$

which is a generalization of the diagonal gauge transformation for the Dirac field.

Thus, we conclude that, contrary to the opinion of Jauch himself, Jauch's field can interact with the electromagnetic field when the gauge transformation is generalized in a non-diagonal way.

Note added in proof.

The physical meaning of the transformation A can be seen as follows: Let us put

$$\Psi \equiv \begin{pmatrix} \psi \\ \psi^* \end{pmatrix}, \qquad \Psi_\gamma \equiv \begin{pmatrix} \psi_1 \\ \psi_2 \end{pmatrix},$$

where ψ_1 and ψ_2 are real fields introduced by MAJORANA. Ψ and Ψ_γ may be connected with each other by

$$\Psi_\gamma = B\Psi , \qquad B = \frac{1}{\sqrt{2}} \begin{pmatrix} 1 & 1 \\ i & -i \end{pmatrix}.$$

Therefore, the gauge transformation G' of Ψ_γ is defined by

$$\Psi'_\gamma = G'\Psi_\gamma\,, \qquad G' = BGB^{-1} = \begin{pmatrix} \cos e\Lambda & \sin e\Lambda \\ -\sin e\Lambda & \cos e\Lambda \end{pmatrix}.$$

This simply means that the gauge transformation is a rotation of angle $e\Lambda$ in (ψ_1, ψ_2)-space.

$$A_\gamma = \begin{pmatrix} \sqrt{\dfrac{a+b}{a-b}} & 0 \\ 0 & \sqrt{\dfrac{a-b}{a+b}} \end{pmatrix},$$

i.e.,

$$\overline{\Psi}_\gamma = A_\gamma \Psi_\gamma\,.$$

Gauge transformation is, therefore,

$$\Psi'_\gamma = \overline{G}_\gamma \Psi_\gamma\,, \qquad \overline{G}_\gamma = \begin{pmatrix} \cos e\Lambda & \dfrac{a+b}{a-e}\sin\Lambda \\ -\dfrac{a-b}{a+b}\sin e\Lambda & \cos e\Lambda \end{pmatrix},$$

which is no longer a rotation in this space, in other words, our transformation A makes ψ_1 long and ψ_2 short or vice versa.

Thanks are due to Dr. Y. Katayama for suggesting the point.

Acknowledgements.

The author would like to thank Dr. D. Feldman for his discussion at an early stage of this work and Dr. Ta-You Wu for his kind hospitality at the National Research Council, Ottawa.

RIASSUNTO (*)

Per mezzo del normale formalismo di quantizzazione si riesamina il lavoro di Jauch con lo stesso titolo. Il principio di azione di Schwinger può dare le relazioni di commutazione proposte da Jauch se si scelgono variabili canoniche indipendenti adeguate, differenti dalle variabili indipendenti variazionali. Si discute anche la quantizzazione nella rappresentazione d'interazione. Si esamina l'interazione fra il campo di Jauch e il campo elettromagnetico.

(*) *Traduzione a cura della Redazione.*

IL NUOVO CIMENTO Vol. I, N. 3 1° Marzo 1955

On the Theory of Circularly Symmetric TM Waves in Infinite Irisloaded Guides.

C. C. Grosjean (*)

Interuniversitair Instituut voor Kernwetenschappen
Centrum van de Rijksuniversiteit - Gent, Belgio

(ricevuto il 18 Gennaio 1955)

Summary. — The exact theory of the propagation of circularly symmetric TM waves in infinite irisloaded guides with perfectly conducting walls is worked out and discussed in detail, starting with two arbitrary functions in the description of the E_z component at the corrugation mouths and making use of the well-known Floquet theorem. The final equations form an infinite linear system which can be transformed in several interesting ways leading to new formulae, but has not yet been solved explicitly.

1. – Introduction.

In the past years, several papers (1) have been published concerning the propagation of circularly symmetric TM waves in periodically irisloaded wave guides. However, in preparation for future work and because of the fact that we have modified and completed some aspects of the theory, we found it interesting to reexamine the entire problem in the present paper.

Indeed, although our method is still one of matching electric and magnetic fields, it differs from the earlier calculations in the sense, that from the beginning, we introduce two arbitrary functions to describe E_z along the cylindrical surface $r=a$, taking into account some general theorems. All the field com-

(*) Address: Natuurk. Laboratorium, Universiteit Gent, Rozier, 6, Gent, Belgium.

(1) Cfr., e.g.: W. Walkinshaw: *Proc. Phys. Soc. London*, **61**, 246 (1948); *Journ. App. Phys.*, **20**, 634 (1949); W. Walkinshaw and J. S. Bell: *Report G/R* 675 (1951), *Report T/R* 864 (1952), A.E.R.E. (Harwell).

ponents can then be expressed as series containing the coefficients of certain Fourier expansions of $E_z(a, z)$. At this point, all the boundary conditions are satisfied and although the component $E_z(r, z)$ is given by two completely different Fourier series in both regions $(0 \leqslant r \leqslant a)$ and $(a \leqslant r \leqslant b)$, it is *automatically* continuous at the corrugation mouths, no matter how the functions representing $E_z(a, z)$ are in reality. Since it can be proved that making the magnetic component continuous at the corrugation mouths is sufficient to make all the field components analytical in each point inside the guide, this continuity condition alone leads to the desired final equations, forming an infinite system which is formally different from the one obtained in other papers. Although we did not yet succeed in solving the system explicitly, we were able to transform it in two interesting new systems, offering new possibilities for a further solution of the problem. This has not been the case with the infinite system resulting from older calculations, since it gave rise to an infinite determinant which does not lend itself to further changes or simplifications. It should also be noted that our method and final results enable us to draw general conclusions about the dependence of $E_z(a, z)$ on the propagation constant β_0. This is particularly important for choosing suitable trial functions for $E_z(a, z)$ to obtain useful approximate frequency equations.

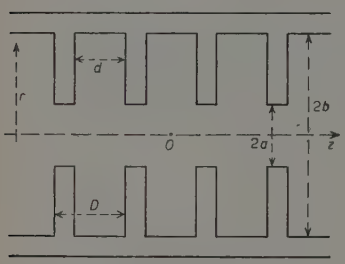

Fig. 1.

2. – Theoretical Development.

Let us consider an infinite wave guide with axial symmetry, whose cross-section is shown on Fig. 1. For the design of a linear electron accelerator, one is particularly interested in the circularly symmetric solutions of the electromagnetic field equations, containing an axial and a radial electric field component and a circular magnetic component. In this case, the complete solution corresponding to a guide wavelength λ_g can be written as follows in the region $(0 \leqslant r \leqslant a)$:

$$(1) \qquad \mathcal{E}_z(r, z, t) = E_z(r, z)e^{i\omega t}; \quad \mathcal{E}_r(r, z, t) = E_r(r, z)e^{i\omega t}; \quad \mathcal{H}_\theta(r, z, t) = H_\theta(r, z)e^{i\omega t},$$

$$(2) \qquad E_z = \sum_{m=-\infty}^{\infty} A_m J_0(\chi_m r) \exp[-i\beta_m z],$$

$$(3) \qquad E_r = i \sum_{m=-\infty}^{\infty} A_m \frac{\beta_m}{\chi_m} J_1(\chi_m r) \exp[-i\beta_m z],$$

$$(4) \qquad Z_0 H_\theta = i \sum_{m=-\infty}^{\infty} A_m \frac{k}{\chi_m} J_1(\chi_m r) \exp[-i\beta_m z].$$

in which: $k = 2\pi/\lambda_0$, λ_0 being the free space wavelength, $\beta_0 = 2\pi/\lambda_g$, $\beta_m = \beta_0 + (2\pi m/D)$ $(m = 0, \pm 1, \ldots)$ (due to Floquet's theorem), $\chi_m = \sqrt{k^2 - \beta_m^2}$, $Z_0 =$ intrinsic impedance of free space.

The coefficients A_m can be expressed in terms of the field component E_z along $r = a$, which is an unknown function of z, so far. However, writing a general expression for $E_z(a, z)$, one should take into account

1) Floquet's theorem;

2) a theorem proved by WALKINSHAW and BELL [2] concerning the symmetry properties of E_z.

Knowing that $E_z(a, z)$ should vanish on the metal walls inside the irises, we have in the n-th corrugation

$$(5) \qquad E_z(a, z) = \begin{cases} 0 & \left(-\frac{D}{2} \leqslant x_n < -\frac{d}{2}\right) \\ \left[g_1\left(\frac{2x_n}{d}\right) + ig_2\left(\frac{2x_n}{d}\right)\right] \exp\left[-i\beta_0 nD\right] & \left(-\frac{d}{2} \leqslant x_n \leqslant \frac{d}{2}\right) \\ 0 & \left(\frac{d}{2} < x_n \leqslant \frac{D}{2}\right) \end{cases}$$

$$(x_n \equiv z - nD), \ (n = 0, \pm 1, \ldots);$$

in which $g_1(x)$ and $g_2(x)$ are two real functions existing in the interval $(-1 \leqslant x \leqslant 1)$, being respectively symmetrical and antisymmetrical with respect to $x = 0$ and possibly depending on certain constants appearing in the problem. Identifying (2) for $r = a$ with (5), we can write

$$\sum_{m=-\infty}^{\infty} A_m J_0(\chi_m a) \exp\left[-2\pi i m \frac{z}{D}\right] = \begin{cases} 0 & \left(-\frac{D}{2}, -\frac{d}{2}\right) \\ (g_1 + ig_2) \exp\left[i\beta_0 x_n\right] & \left(-\frac{d}{2}, \frac{d}{2}\right) \\ 0 & \left(\frac{d}{2}, \frac{D}{2}\right) \end{cases}$$

in which both sides are really periodic functions of z. Hence:

$$(6) \qquad A_m = \frac{1}{DJ_0(\chi_m a)} \int_{-d/2}^{d/2} \left[g_1\left(\frac{2z}{d}\right) + ig_2\left(\frac{2z}{d}\right)\right] \exp\left[i\beta_m z\right] dz =$$

$$= \frac{d}{DJ_0(\chi_m a)} \left[G_1\left(\frac{\beta_m d}{2}\right) - G_2\left(\frac{\beta_m d}{2}\right)\right]$$

---

[2] W. WALKINSHAW and J. S. BELL: *Report T/R* 864, A.E.R.E. (Harwell) (1952).

with

$$G_1(x) \equiv \int_0^1 g_1(z) \cos xz \, dz , \qquad G_2(x) \equiv \int_0^1 g_2(z) \sin xz \, dz . \tag{7}$$

This completes the solution in the region $(0 \leqslant r \leqslant a)$. Let us now consider the field components inside each corrugation $(-d/2 \leqslant x_n \leqslant d/2, \ a \leqslant r \leqslant b)$. In these regions, $E_z(r, z)$ must be a linear combination of terms of the type

$$\left[AJ_0(\sqrt{k^2 - \gamma^2} \cdot r) + BY_0(\sqrt{k^2 - \gamma^2} \cdot r) \right] \begin{matrix} \sin \\ \cos \end{matrix} \gamma x_n \tag{8}$$

in which it is supposed that $k > |\gamma|$. Otherwise the Bessel function of the second kind must be suitably replaced. Due to the fact that the component E_r must vanish on the side walls of the corrugations, its Fourier expansion should only contain the following types of eigenfunctions:

$$\sin \frac{2p\pi x_n}{d} \quad (p = 1, 2, \ldots) \quad \text{and} \quad \cos \frac{(2q+1)\pi x_n}{d} \quad (q = 0, 1, \ldots) . \tag{9}$$

Using the Maxwell relations between the various field components, it can be seen that the expansion of $E_z(r, z)$ must be constructed with the terms

$$\cos \frac{2p\pi x_n}{d} \quad \text{and} \quad \sin \frac{(2q+1)\pi x_n}{d} \qquad (p, q = 0, 1, \ldots) , \tag{10}$$

forming an orthogonal set. This enables us to represent the arbitrary functions g_1 and g_2 as follows:

$$g_1\left(\frac{2x_n}{d}\right) + ig_2\left(\frac{2x_n}{d}\right) = G_1(0) + 2 \sum_{p=1}^{\infty} G_1(p\pi) \cos \frac{2p\pi x_n}{d} + \\ + 2i \sum_{q=0}^{\infty} G_2\left[\left(q + \frac{1}{2}\right)\pi\right] \sin \frac{(2q+1)\pi x_n}{d} . \tag{11}$$

The last boundary condition is

$$E_z(b, x_n) = 0 \qquad \left(-\frac{d}{2} \leqslant x_n \leqslant \frac{d}{2}\right) . \tag{12}$$

Since the eigenvalues represented by γ in (8) are well defined according to (10), the only way to make an expression like (8) vanish for $r = b$ consists in choosing A and B resp. proportional to $Y_0(\sqrt{k^2 - \gamma^2} \cdot b)$ and $-J_0(\sqrt{k^2 - \gamma^2} \cdot b)$. The resulting function is needed for real as well as for imaginary values of

$\sqrt{k^2-\gamma^2}$. Therefore, let us define at once:

$$F_0(\xi; r, b) \equiv J_0(\xi r)\left[\frac{\partial J_\nu(\xi b)}{\partial \nu}\right]_{\nu=0} - J_0(\xi b)\left[\frac{\partial J_\nu(\xi r)}{\partial \nu}\right]_{\nu=0}. \tag{13}$$

This function becomes

1) for ξ real:

$$F_0(\xi; r, b) = \frac{\pi}{2}\left[J_0(|\xi| r) Y_0(|\xi| b) - Y_0(|\xi| r) J_0(|\xi| b)\right];$$

2) for $\xi = 0$:

$$F_0(0; r, b) = \log b - \log r,$$

3) for ξ imaginary:

$$F_0(\xi; r, b) = -\left[I_0(|\xi| r) K_0(|\xi| b) - K_0(|\xi| r) I_0(|\xi| b)\right].$$

In this way, the function F_0 shows no discontinuity when ξ passes from real to imaginary values over $\xi = 0$. The second function which we shall need can be defined as

$$F_1(\xi; r, b) \equiv -\frac{1}{k}\frac{\partial F_0}{\partial r}, \tag{14}$$

so that

$$F_1(\xi; r, b) = \frac{\pi}{2}\frac{|\xi|}{k}\left[J_1(|\xi| r) Y_0(|\xi| b) - Y_1(|\xi| r) J_0(|\xi| b)\right] \qquad (\xi: \text{real})$$

$$= \frac{1}{kr} \qquad (\xi = 0)$$

$$= \frac{|\xi|}{k}\left[I_1(|\xi| r) K_0(|\xi| b) + K_1(|\xi| r) I_0(|\xi| b)\right] \qquad (\xi: \text{imag.})$$

which is also continuous. Furthermore, F_0 and F_1 satisfy the equation

$$F_0(\xi; r, b) = \frac{k}{\xi^2 r}\frac{\partial r F_1}{\partial r}. \tag{15}$$

Making use of F_0, the exact expansion of $E_z(r, x_n)$ satisfying (12) and coinciding at $r = a$ with (5) in the interval $(-d/2, d/2)$ is

$$E_z = \exp\left[-in\beta_0 D\right]\left[\frac{F_0(k; r, b)}{F_0(k; a, b)} G_1(0) + 2\sum_{p=1}^{\infty}\frac{F_0(\xi_p; r, b)}{F_0(\xi_p; a, b)} G_1(p\pi)\cos\frac{2p\pi x_n}{d} + \right. \tag{16}$$

$$\left. + 2i\sum_{q=0}^{\infty}\frac{F_0(\zeta_q; r, b)}{F_0(\zeta_q; a, b)} G_2\left[\left(q+\frac{1}{2}\right)\pi\right]\sin\frac{(2q+1)\pi x_n}{d}\right]$$

in which

$$\xi_p = \sqrt{k^2 - \frac{4p^2\pi^2}{d^2}}; \qquad \zeta_q = \sqrt{k^2 - \frac{(2q+1)^2\pi^2}{d^2}}. \tag{17}$$

The remaining field components can be found by the use of Maxwell's equations:

$$E_r = 2k \exp[-in\beta_0 D]\left[\sum_{p=1}^{\infty} \frac{2p\pi}{d} \frac{F_1(\xi_p; r, b)}{\xi_p^2 F_0(\xi_p; a, b)} G_1(p\pi) \sin\frac{2p\pi x_n}{d} - \right.$$
$$\left. - i\sum_{q=0}^{\infty} \frac{(2q+1)\pi}{d} \frac{F_1(\zeta_q; r, b)}{\zeta_q^2 F_0(\zeta_q; a, b)} G_2\left[\left(q+\frac{1}{2}\right)\pi\right] \cos\frac{(2q+1)\pi x_n}{d}\right], \tag{18}$$

$$Z_0 H_\theta =$$
$$= i \exp[-in\beta_0 D]\left\{\frac{F_1(k; r, b)}{F_0(k; a, b)} G_1(0) + 2\sum_{p=1}^{\infty} \frac{k^2 F_1(\xi_p; r, b)}{\xi_p^2 F_0(\xi_p; a, b)} G_1(p\pi) \cos\frac{2p\pi x_n}{d} + \right.$$
$$\left. - 2i\sum_{q=0}^{\infty} \frac{k^2 F_1(\zeta_q; r, b)}{\zeta_q^2 F_0(\zeta_q; a, b)} G_2\left[\left(q+\frac{1}{2}\right)\pi\right] \sin\frac{(2q+1)\pi x_n}{d}\right\}. \tag{19}$$

This completes the solution in the corrugations. The problem is reduced to the calculation of λ_g, $g_1(x)$ and $g_2(x)$ as functions of the guide dimensions and the free space wavelength λ_0. The equations permitting the further solution of the problem have to be obtained from continuity conditions for the fields along $r = a$. Using the four Maxwell relations between E_z, E_r and H_θ, and taking into account that the obtained formulae for E_z namely (16) and (2) match along $r = a$ in each corrugation mouth, it can be easily proved that by matching both expressions (19) and (4) for H_θ in the same regions, the three field components and their first partial derivatives with respect to r and z will match at the mentioned boundary. This is sufficient for the electromagnetic fields to be described by functions which are analytical in all points inside the wave guide. Identifying (19) with (4) along $r = a$ in each corrugation mouth, we get

$$D\sum_{m=-\infty}^{\infty} \frac{k}{\chi_m} \frac{J_1(\chi_m a)}{J_0(\chi_m a)}\left|G_1\left(\frac{\beta_m d}{2}\right) - G_2\left(\frac{\beta_m d}{2}\right)\right| \exp[-i\beta_m x_n] =$$
$$= \frac{F_1(k; a, b)}{F_0(k; a, b)} G_1(0) + 2\sum_{p=1}^{\infty} \frac{k^2 F_1(\xi_p; a, b)}{\xi_p^2 F_0(\xi_p; a, b)} G_1(p\pi) \cos\frac{2p\pi x_n}{d} +$$
$$+ 2i\sum_{q=}^{\infty} \frac{k^2 F_1(\zeta_q; a, b)}{\zeta_q^2 F_0(\zeta_q; a, b)} G_2\left[\left(q+\frac{1}{2}\right)\pi\right] \sin\frac{(2q+1)\pi x_n}{d}, \qquad \left(-\frac{d}{2} \leqslant x_n \leqslant \frac{d}{2}\right)$$
$$(n = 0, \pm 1, \ldots). \tag{20}$$

Making use of the orthogonality properties of the sine and the cosine functions

on the right hand side, this equation can be shown to be equivalent to the following infinite set:

$$(21)\quad \begin{cases} \dfrac{k^2}{\xi_p^2}\dfrac{F_1(\xi_p;\,a,\,b)}{F_0(\xi_p;\,a,\,b)}\,G_1(p\pi) = (-1)^p\dfrac{d}{D}\displaystyle\sum_{m=-\infty}^{\infty}\dfrac{k}{\chi_m}\dfrac{J_1(\chi_m a)}{J_0(\chi_m a)}\cdot \\ \qquad\qquad \cdot\left[G_1\left(\dfrac{\beta_m d}{2}\right) - G_2\left(\dfrac{\beta_m d}{2}\right)\right]\dfrac{(\beta_m d/2)\sin(\beta_m d/2)}{(\beta_m d/2)^2 - p^2\pi^2}\,, \qquad (p = 0,\,1,\,\ldots) \\ \dfrac{k^2}{\zeta_q^2}\dfrac{F_1(\zeta_q;\,a,\,b)}{F_0(\zeta_q;\,a,\,b)}\,G_2\left[\left(q+\dfrac{1}{2}\right)\pi\right] = (-1)^q\dfrac{d}{D}\displaystyle\sum_{m=-\infty}^{\infty}\dfrac{k}{\chi_m}\dfrac{J_1(\chi_m a)}{J_0(\chi_m a)}\cdot \\ \qquad\qquad \cdot\left[G_1\left(\dfrac{\beta_m d}{2}\right) - G_2\left(\dfrac{\beta_m d}{2}\right)\right]\dfrac{(\beta_m d/2)\cos(\beta_m d/2)}{(\beta_m d/2)^2 - (q+\frac{1}{2})^2\pi^2}\,, \qquad (q = 0,\,1,\,\ldots). \end{cases}$$

This infinite system can be transformed in two interesting ways:

A) Knowing that (16) and (2) represent the same function along $r = a$ in each corrugation mouth, one can write:

$$(22)\quad \frac{d}{D}\sum_{m=-\infty}^{\infty}\left[G_1\left(\frac{\beta_m d}{2}\right) - G_2\left(\frac{\beta_m d}{2}\right)\right]\exp\left[-i\beta_m x_n\right] =$$

$$= G_1(0) + 2\sum_{p=1}^{\infty} G_1(p\pi)\cos\frac{2p\pi x_n}{d} + 2i\sum_{q=0}^{\infty} G_2\left[\left(q+\frac{1}{2}\right)\pi\right]\sin\frac{(2q+1)\pi x_n}{d} \qquad \left(-\frac{d}{2},\,\frac{d}{2}\right)$$

which is equivalent to

$$(23)\quad \begin{cases} G_1(p\pi) = (-1)^p\dfrac{d}{D}\displaystyle\sum_{m=-\infty}^{\infty}\left[G_1\left(\dfrac{\beta_m d}{2}\right) - G_2\left(\dfrac{\beta_m d}{2}\right)\right]\dfrac{(\beta_m d/2)\sin(\beta_m d/2)}{(\beta_m d/2)^2 - p^2\pi^2} \qquad (p = 0,\,1,\,\ldots) \\ G_2\left[\left(q+\dfrac{1}{2}\right)\pi\right] = (-1)^q\dfrac{d}{D}\displaystyle\sum_{m=-\infty}^{\infty}\left[G_1\left(\dfrac{\beta_m d}{2}\right) - G_2\left(\dfrac{\beta_m d}{2}\right)\right]\dfrac{(\beta_m d/2)\cos(\beta_m d/2)}{(\beta_m d/2)^2 - (q+\frac{1}{2})^2\pi^2} \\ \qquad\qquad (q = 0,\,1,\,\ldots). \end{cases}$$

Using these equations to replace $G_1(p\pi)$ and $G_2[(q+\frac{1}{2})\pi]$ in (21), one gets:

$$(24)\quad \begin{cases} \displaystyle\sum_{m=-\infty}^{\infty}\left[G_1\left(\frac{\beta_m d}{2}\right) - G_2\left(\frac{\beta_m d}{2}\right)\right]\left[\frac{k^2}{\xi_p^2}\frac{F_1(\xi_p;\,a,\,b)}{F_0(\xi_p;\,a,\,b)} - \frac{k}{\chi_m}\frac{J_1(\chi_m a)}{J_0(\chi_m a)}\right]\cdot\frac{(\beta_m d/2)\sin(\beta_m d/2)}{(\beta_m d/2)^2 - p^2\pi^2} = 0\,, \\ \displaystyle\sum_{m=-\infty}^{\infty}\left[G_1\left(\frac{\beta_m d}{2}\right) - G_2\left(\frac{\beta_m d}{2}\right)\right]\left[\frac{k^2}{\zeta_q^2}\frac{F_1(\zeta_q;\,a,\,b)}{F_0(\zeta_q;\,a,\,b)} - \frac{k}{\chi_m}\frac{J_1(\chi_m a)}{J_0(\chi_m a)}\right]\cdot \\ \qquad\qquad \cdot\frac{(\beta_m d/2)\cos(\beta_m d/2)}{(\beta_m d/2)^2 - (q+\frac{1}{2})^2\pi^2} = 0\,, \qquad (p, q = 0,\,1,\,\ldots). \end{cases}$$

This is a set of linear and homogeneous equations for the unknown quantities $[G_1(\beta_m d/2) - G_2(\beta_m d/2)]$ $(m = 0,\,\pm 1,\,\ldots)$. Their coefficients form an infinite determinant which must be zero leading to the exact frequency equation of the problem. The equations (24) seem to differ from those obtained in a

similar way by WALKINSHAW [3], who has to integrate over the interval $(-D/2 \leqslant x_n \leqslant D/2)$ in a transition similar to the one from (22) to (23). In our calculations, this would lead to the more complicated equations

$$
(25)\quad \begin{cases}
\displaystyle\sum_{m=-\infty}^{\infty}\left[G_1\left(\frac{\beta_m d}{2}\right)-G_2\left(\frac{\beta_m d}{2}\right)\right]\left\{(-1)^p\,\frac{k^2}{2\xi_p^2}\,\frac{F_1(\xi_p;\,a,\,b)}{F_0(\xi_p;\,a,\,b)}\left[\frac{\sin\,(\beta_m+(2p\pi/d))D/2}{(\beta_m d/2)+p\pi}+\right.\right. \\
\qquad\left.\left.+\,\frac{\sin\,(\beta_m-(2p\pi/d))D/2}{(\beta_m d/2)-p\pi}\right]-\frac{k}{\chi_m}\,\frac{J_1(\chi_m a)}{J_0(\chi_m a)}\,\frac{(\beta_m d/2)\sin\,(\beta_m d/2)}{(\beta_m d/2)^2-p^2\pi^2}\right\}=0 \\
\qquad\qquad\qquad\qquad\qquad\qquad\qquad\qquad\qquad\qquad\qquad\qquad (p=0,\,1,\,\ldots) \\
\displaystyle\sum_{m=-\infty}^{\infty}\left[G_1\left(\frac{\beta_m d}{2}\right)-G_2\left(\frac{\beta_m d}{2}\right)\right]\left\{(-1)^q\,\frac{k^2}{2\zeta_q^2}\,\frac{F_1(\zeta_q;\,a,\,b)}{F_0(\zeta_q;\,a,\,b)}\cdot\right. \\
\qquad\cdot\left[\frac{\sin\,(\beta_m+(2q+1)\pi/d)D/2}{(\beta_m d/2)+(q+\frac{1}{2})\pi}-\frac{\sin\,(\beta_m-(2q+1)\pi/d)D/2}{(\beta_m d/2)-(q+\frac{1}{2})\pi}\right]- \\
\qquad\left.-\,\frac{k}{\chi_m}\,\frac{J_1(\chi_m a)}{J_0(\chi_m a)}\,\frac{(\beta_m d/2)\cos\,(\beta_m d/2)}{(\beta_m d/2)^2-(q+\frac{1}{2})^2\pi^2}\right\}=0 \qquad (q=0,\,1,\,\ldots)\,.
\end{cases}
$$

These equations are only formally different from (24), since the infinite series resulting from the difference between both system (25) and (24) turn out to be identically zero. This can be proved for any set of functions $G_1(x)$ and $G_2(x)$ provided they can be represented by integrals as those used in the definitions (7).

B) The equations (21) can be transformed using a method similar to the one presented in a previous paper [4]. This is worked out in detail in a separate article, leading to the following result:

$$
(26)\quad \begin{cases}
\dfrac{(-1)^{p-1}J_0(\xi_p b)G_1(p\pi)}{2\xi_p^2 a^2 J_0(\xi_p a)F_0(\xi_p;\,a,\,b)}=\displaystyle\sum_{n=1}^{\infty}\frac{1}{\varkappa_n^2+(4p^2\pi^2a^2/d^2)}\cdot \\
\cdot\left[\cosh\frac{\varkappa_n D}{a}\left(1-\frac{d}{2D}\right)-\cos\beta_0 D\cosh\frac{\varkappa_n d}{2a}\right]G_1\left(\frac{i\varkappa_n d}{2a}\right)-i\sin\beta_0 D\sinh\frac{\varkappa_n d}{2a}\,G_2\left(\frac{i\varkappa_n d}{2a}\right) \\
\qquad\qquad\qquad\qquad\qquad\qquad\cosh\frac{\varkappa_n D}{a}-\cos\beta_0 D \\
\qquad\qquad\qquad\qquad\qquad\qquad\qquad\qquad\qquad\qquad (p=0,\,1,\,\ldots) \\
\dfrac{(-1)^{q-1}J_0(\zeta_q b)G_2[(q+\frac{1}{2})\pi]}{2\zeta_q^2 a^2 J_0(\zeta_q a)F_0(\zeta_q;\,a,\,b)}=\displaystyle\sum_{n=1}^{\infty}\frac{1}{\varkappa_n^2+((2q+1)^2\pi^2a^2/d^2)}\cdot \\
\sin\beta_0 D\cosh\frac{\varkappa_n d}{2a}\,G_1\left(\frac{i\varkappa_n d}{2a}\right)-i\left[\sin\mathrm{h}\,\frac{\varkappa_n D}{a}\left(1-\frac{d}{2D}\right)+\cos\beta_0 D\sinh\frac{\varkappa_n d}{2a}\right]G_2\left(\frac{i\varkappa_n d}{2a}\right) \\
\qquad\qquad\qquad\qquad\qquad\qquad\cosh\frac{\varkappa_n D}{a}-\cos\beta_0 D \\
\qquad\qquad\qquad\qquad\qquad\qquad\qquad\qquad\qquad\qquad (q=0,\,1,\,\ldots)
\end{cases}
$$

[3] Loc. cit. (*Journ. Appl. Phys.*).

[4] C. C. GROSJEAN: *Nuovo Cimento*, **1**, 174 (1955).

in which $\varkappa_n \equiv \sqrt{\alpha_n^2 - k^2 a^2}$, α_n being the n-th positive root of $J_0(x)$.

The problem is reduced to the solution of the infinite set of equations given by (21) or the equivalent forms (24) and (26). This means that for given dimensions of the wave guide, one should be able to calculate the exact relationship between k and β_0, and find the corresponding field configurations $g_1(x)$ and $g_2(x)$, from which all the fields can be obtained. Using some qualitative results obtained elsewhere [5], it can be foreseen that the solution of the general frequency equation mentioned in (*A*) must give rise to an infinite number of pass bands in each (β_0, k) diagram corresponding to a particular cut off frequency of the unloaded guide. However, in the general case, the infinite systems mentioned before are still too complicated to permit a direct confirmation of this statement.

3. – Remarks.

Examining the equations (26), we see that the phase angle $\beta_0 D$ appears entirely separated from the other variables in the coefficients of the unknown quantities

$$G_1(p\pi)\,, \qquad G_2\left[\left(q+\frac{1}{2}\right)\pi\right], \qquad G_1\left(\frac{i\varkappa_n d}{2a}\right) \quad \text{and} \quad G_2\left(\frac{i\varkappa_n d}{2a}\right).$$

This enables us to draw a general conclusion about the dependence of $g_1(x)$ and $g_2(x)$ on β_0. Indeed, first of all, we wish to point out that the systems (21), (24) and (26) hold equally well for positive as for negative values of β_0, since we did not specify its sign. For, when we wrote

$$\beta_0 = \frac{2\pi}{\lambda_g}\,, \tag{27}$$

in which the guide wavelength is usually regarded as a positive quantity, we had particularly in mind the absolute value of the parameters. Therefore, strictly speaking, (27) is only valid for waves traveling in the positive z-direction, whereas for those traveling in the negative z-direction, one should write

$$\beta_0 = -\frac{2\pi}{\lambda_g}\,.$$

Now, let us suppose that we solved the problem explicitly and that we found the functions $g_1(x)$ and $g_2(x)$ corresponding to the curve $k(\beta_0)$ in each particular pass band. Then, if we calculated G_1 and G_2 from (7) and if we introduced them in both sides of one equation chosen among those of the

(5) J. C. SLATER: *Microwave Electronics* (New York, 1951), Chapter VIII.

system (26), e.g. the one with $p = 0$, we would again obtain the frequency equation describing the (β_0, k) curve. Suppose that all the quantities $G_1(i\varkappa_n d/2a)$ or all the quantities $G_2(i\varkappa_n d/2a)$ are not equal to zero at the same time. Then, if g_1 and g_2 were both independent of β_0, the frequency equation would contain both terms $\cos \beta_0 D$ and $\sin \beta_0 D$, leading to a periodic curve $k(\beta_0)$ which would not be even. However, it is well-known from relatively simple arguments that $k(\beta_0)$ should always be an even periodic function. Therefore, apart from some exceptional cases which are a priori not excluded, we may conclude that at least one of the functions $g_1(x)$ or $g_2(x)$ must be depending on β_0, and that it must be a periodic function with period $2\pi/D$.

This is also confirmed by the following considerations. Using two successive transformations which do not change the physical situation ([6]), namely changing from a wave function to its conjugate and reversing the time t, propagation of waves in the negative z-direction can be obtained from the description in the positive z-direction and vice versa. This transforms $E_z(a, z)$ (given by (5)) at the corrugation mouths into

$$\left[g_1\left(\frac{2x_n}{d}\right) - ig_2\left(\frac{2x_n}{d}\right)\right] \exp[i\beta_0 nD]\,. \tag{28}$$

This can also be obtained by simple reversion of the z-axis. On the other hand, after having made the suitable choice for the time origin, so as to get the desired phase angle, the waves with the same amplitudes traveling in the opposite direction can also be derived from

$$\left[g_1^*\left(\frac{2x_n}{d}\right) + ig_2^*\left(\frac{2x_n}{d}\right)\right] \exp[i\beta_0 nD]\,, \tag{29}$$

which is included in the general representation (5). Therefore, (28) and (29) should only differ by a proportionality factor, whose absolute value must be equal to unity and which must be real due to the identification of functions with the same parity with respect to x_n. Hence the factor can only be equal to ± 1, so that

$$g_1^*\left(\frac{2x_n}{d}\right) = \pm\, g_1\left(\frac{2x_n}{d}\right), \qquad g_2^*\left(\frac{2x_n}{d}\right) = \mp\, g_2\left(\frac{2x_n}{d}\right),$$

or, in fact,

$$g_1(x, -\beta_0) = \pm\, g_1(x, \beta_0)\,, \qquad g_2(x, -\beta_0) = \mp\, g_2(x, \beta_0)\,. \tag{30}$$

This shows that in both cases at least one of the functions changes its sign and is therefore depending on β_0, if it is not identically zero. This would then correspond to one of the exceptional cases in which either all the terms $G_1(i\varkappa_n d/2a)$ or all the terms $G_2(i\varkappa_n d/2a)$ would vanish at once. At the same time, we see that one of the functions must be symmetric in β_0, while the

([6]) See ref. ([5]), p. 171.

other must be antisymmetric. However, considering a particular pass band in a certain (β_0, k) diagram, it cannot directly be decided from these calculations whether the upper or the lower signs in (30) will be the correct ones in this band.

Another final remark concerns the theorem proved by WALKINSHAW and BELL, which we took into account writing (5). If we had not introduced it from the beginning, we would have been obliged to start with an arbitrary complex function in $(-d/2, d/2)$, e.g.:

$$(31)\qquad E_z(a,z)=\begin{cases}0 & \left(-\frac{D}{2}\leqslant x_n<-\frac{d}{2}\right)\\ \psi\left(\frac{2x_n}{d}\right)\exp[-i\beta_0 nD] & \left(-\frac{d}{2}\leqslant x_n\leqslant\frac{d}{2}\right)\\ 0 & \left(\frac{d}{2}<x_n\leqslant\frac{D}{2}\right),\end{cases}$$

$\psi(x)$ being defined in $(-1\leqslant x\leqslant 1)$ and having no definite parity. Eq. (6) would have been

$$(32)\qquad A_m=\frac{d}{2DJ_0(\chi_m a)}\int_{-1}^{1}\psi(z)\exp\left[\frac{i\beta_m dz}{2}\right]\mathrm{d}z=\frac{d}{DJ_0(\chi_m a)}\left[\Psi_1\left(\frac{\beta_m d}{2}\right)+i\Psi_2\left(\frac{\beta_m d}{2}\right)\right],$$

in which

$$(33)\qquad \Psi_1(x)\equiv\int_0^1\frac{\psi(z)+\psi(-z)}{2}\cos xz\,\mathrm{d}z,\quad \Psi_2(x)\equiv\int_0^1\frac{\psi(z)-\psi(-z)}{2}\sin xz\,\mathrm{d}z,$$

and it would have been possible to develop the theory just as before. The final equations would have been written as follows:

$$(34)\qquad \begin{cases}\dfrac{k^2}{\xi_p^2}\dfrac{F_1(\xi_p;a,b)}{F_0(\xi_p;a,b)}\Psi_1(p\pi)=(-1)^p\dfrac{d}{D}\displaystyle\sum_{m=-\infty}^{\infty}\frac{k}{\chi_m}\frac{J_1(\chi_m a)}{J_0(\chi_m a)}\left[\Psi_1\left(\frac{\beta_m d}{2}\right)+i\Psi_2\left(\frac{\beta_m d}{2}\right)\right]\cdot\\ \qquad\cdot\dfrac{(\beta_m d/2)\sin(\beta_m d/2)}{(\beta_m d/2)^2-p^2\pi^2}\qquad(p=0,1,\ldots)\\ \dfrac{k^2}{\zeta_q^2}\dfrac{F_1(\zeta_q;a,b)}{F_0(\zeta_q;a,b)}\Psi_2\left[\left(q+\frac{1}{2}\right)\pi\right]=(-1)^q\dfrac{d}{D}\displaystyle\sum_{m=-\infty}^{\infty}\frac{k}{\chi_m}\frac{J_1(\chi_m a)}{J_0(\chi_m a)}\cdot\\ \qquad\cdot\left[i\Psi_1\left(\frac{\beta_m d}{2}\right)-\Psi_2\left(\frac{\beta_m d}{2}\right)\right]\cdot\dfrac{(\beta_m d/2)\cos(\beta_m d/2)}{(\beta_m d/2)^2-(q+\frac{1}{2})^2\pi^2}\qquad(q=0,1,\ldots).\end{cases}$$

Both sides of these equations are complex, but this is only caused by the quantities

$$\Psi_1(p\pi),\quad \Psi_2\left[\left(q+\frac{1}{2}\right)\pi\right]\quad\text{and}\quad \Psi_1\left(\frac{\beta_m d}{2}\right)+i\Psi_2\left(\frac{\beta_m d}{2}\right)$$

being complex, since the propagation constant β_0 is real in the pass bands From the definition of $\psi(x)$ and from (33), we know that $\Psi_1(x)$ and $\Psi_2(x)$ must be complex so that we may write:

$$\Psi_1(x) = A_1(x) + iB_1(x), \qquad \Psi_2(x) = A_2(x) + iB_2(x)$$

in which A_1, B_1, and A_2 and B_2 are real functions, the first two being representable by a cosine integral analogous to Ψ_1 and the last two being representable by a sine integral analogous to Ψ_2. Introducing this into the system (34) we get after separation of the real and imaginary parts: two systems of equations exactly of the type (21), one in which $A_1(x)$ and $B_2(x)$ replace $G_1(x)$ and $G_2(x)$, and the other in which $B_1(x)$ and $-A_2(x)$ replace these functions. Since the uniqueness of the solution for $G_1(x)$ and $G_2(x)$ can be proved for each pass band using the equivalent homogeneous systems (24) or (25), we can conclude that the set B_1, $-A_2$ can only differ from A_1, B_2 by a real constant:

$$B_1(x) = CA_1(x),$$
$$-A_2(x) = CB_2(x),$$

so that

$$\Psi_1(x) = (1 + iC)A_1(x),$$
$$\Psi_2(x) = i(1 + iC)B_2(x).$$

Both sets correspond to the same wave configurations shifted over 90°, the one with respect to the other. Therefore, the problem is solved with the same generality if the constant $(1+iC)$ is omitted so that $\Psi_1(x)$ is a real function whereas $\Psi_2(x)$ is imaginary. Considering (33), this is equivalent to saying that the symmetric part of $\psi(x)$ is real whereas the antisymmetric part is imaginary. It is evident that the preceding calculations and discussion constitute another proof of the theorem studied by WALKINSHAW and BELL.

It is a pleasure to thank the Institut Interuniversitaire des Sciences Nucléaires and Prof. Dr. J. L. VERHAEGHE for his interest in this research.

RIASSUNTO (*)

Partendo, nella descrizione della componente E_z all'ingresso delle ondulazioni, da due funzioni arbitrarie e servendosi del ben noto teorema di Floquet, si elabora e si discute dettagliatamente la teoria esatta della propagazione delle onde TM in guide d'onda infinite con diaframmi ad iride e pareti perfettamente conduttrici. Le equazioni finali formano un sistema lineare infinito che può esser trasformato in vari modi interessanti che conducono a nuove formule, ma che non è stato ancora esplicitamente risolto.

(*) *Traduzione a cura della Redazione.*

IL NUOVO CIMENTO Vol. I, N. 3 1° Marzo 1955

Mathematical Transformation of a System of Equations Appearing in the Theory of TM Wave Propagation in Corrugated Guides.

C. C. GROSJEAN

Interuniversitair Instituut voor Kernwetenschappen
Centrum van de Rijksuniversiteit - Gent, Belgio

(ricevuto il 18 Gennaio 1955)

Summary. — Generalizing a method used in a previous article, an infinite system of equations appearing in a problem of wave propagation through periodically irisloaded guides, has been exactly transformed into a new system of equations which may be of interest for the further solution of the problem.

1. – Introduction.

In the preceding article (1), in which the theory of circularly symmetric TM waves propagating through a periodically irisloaded guide with axial symmetry was reexamined and completed, it was shown that certain continuity conditions for the field components lead to the following infinite system of equations:

$$(1)\quad \begin{cases} \dfrac{k^2 F_1(\xi_p; a, b)}{\xi_p^2 F_0(\xi_p; a, b)} G_1(p\pi) = (-1)^p \dfrac{d}{D} \displaystyle\sum_{m=-\infty}^{\infty} \dfrac{k}{\chi_m} \dfrac{J_1(\chi_m a)}{J_0(\chi_m a)} \left[G_1\left(\dfrac{\beta_m d}{2}\right) - G_2\left(\dfrac{\beta_m d}{2}\right) \right] \cdot \\ \qquad \cdot \dfrac{(\beta_m d/2) \sin(\beta_m d/2)}{(\beta_m d/2)^2 - p^2\pi^2}, \qquad (p = 0, 1, \ldots), \\ \dfrac{k^2 F_1(\zeta_q; a, b)}{\zeta_q^2 F_0(\zeta_q; a, b)} G_2\left[\left(q + \dfrac{1}{2}\right)\pi\right] = (-1)^q \dfrac{d}{D} \displaystyle\sum_{m=-\infty}^{\infty} \dfrac{k}{\chi_m} \dfrac{J_1(\chi_m a)}{J_0(\chi_m a)} \left[G_1\left(\dfrac{\beta_m d}{2}\right) - G_2\left(\dfrac{\beta_m d}{2}\right) \right] \cdot \\ \qquad \cdot \dfrac{(\beta_m d/2) \cos(\beta_m d/2)}{(\beta_m d/2)^2 - (q + \frac{1}{2})^2\pi^2}, \qquad (q = 0, 1, \ldots), \end{cases}$$

(1) C. C. GROSJEAN: *Nuovo Cimento*, **1**, 427 (1955).

in which

d, D, a, b are guide dimensions,

$$k = \frac{2\pi}{\lambda_0}, \qquad \beta_0 = \frac{2\pi}{\lambda_g}, \qquad \beta_m = \beta_0 + \frac{2\pi m}{D},$$

$$\chi_m = \sqrt{k^2 - \beta_m^2}, \qquad \xi_p = \sqrt{k^2 - \frac{4p^2\pi^2}{d^2}}, \qquad \zeta_q = \sqrt{k^2 - \frac{(2q+1)^2\pi^2}{d^2}},$$

$$G_1(x) = \int_0^1 g_1(z) \cos xz \, dz, \qquad G_2(x) = \int_0^1 g_2(z) \sin xz \, dz,$$

$$F_0(\xi; r, b) = J_0(\xi r) \left[\frac{\partial J_\nu(\xi b)}{\partial \nu}\right]_{\nu=0} - J_0(\xi b) \left[\frac{\partial J_\nu(\xi r)}{\partial \nu}\right]_{\nu=0},$$

$$F_1(\xi; r, b) = -\frac{1}{k} \frac{\partial F_0}{\partial r}.$$

In an earlier paper (2) on the same general subject, we have presented a transformation method applicable to a frequency equation which was in fact identical to the first mentioned equation of (1) where we put $p = 0$. It is our purpose to show that this method can also be used to transform all the equations of the more complicated system (1) into entirely new equations, which may be of interest for the further solution of the considered problem.

2. – Theoretical Development.

Replacing the factor

$$\frac{J_1(\chi_m a)}{\chi_m a J_0(\chi_m a)},$$

by its series representation obtained in the second paragraph of the last mentioned paper, and making use of the integrals

$$(2) \qquad \int_0^1 \cos \frac{\beta_m d}{2} x \cos p\pi x \, dx = (-1)^p \frac{(\beta_m d/2) \sin (\beta_m d/2)}{(\beta_m d/2)^2 - p^2\pi^2},$$

$$(3) \qquad \int_0^1 \sin \frac{\beta_m d}{2} x \sin \left(q + \frac{1}{2}\right) \pi x \, dx = (-1)^{q-1} \frac{(\beta_m d/2) \cos (\beta_m d/2)}{(\beta_m d/2)^2 - (q + \frac{1}{2})^2 \pi^2},$$

(2) C. C. GROSJEAN: *Nuovo Cimento*, **1**, 174 (1955).

the system (1) can easily be written in the following form:

$$\frac{k^2}{\xi_p^2}\,\frac{F_1(\xi_p;\,a,\,b)}{F_0(\xi_p;\,a,\,b)}\,G_1(p\pi) = \frac{2kad}{D}\sum_{n=1}^{\infty}\int_0^1 s_1^{(n)}(x)\cos p\pi x\,\mathrm{d}x - \tag{4}$$

$$-\frac{2kad}{D}\sum_{n=1}^{\infty}\int_0^1 s_2^{(n)}(x)\cos p\pi x\,\mathrm{d}x\,,$$

$$\frac{k^2}{\zeta_q^2}\,\frac{F_1(\zeta_q;\,a,\,b)}{F_0(\zeta_q;\,a,\,b)}\,G_2\left[\left(q+\frac{1}{2}\right)\pi\right] = -\frac{2kad}{D}\sum_{n=1}^{\infty}\int_0^1 s_3^{(n)}(x)\sin\left(q+\frac{1}{2}\right)\pi x\,\mathrm{d}x + \tag{5}$$

$$+\frac{2kad}{D}\sum_{n=1}^{\infty}\int_0^1 s_4^{(n)}(x)\sin\left(q+\frac{1}{2}\right)\pi x\,\mathrm{d}x\,,$$

in which we introduced the following symbols:

$$s_{1,2}^{(n)}(x) = \sum_{m=-\infty}^{\infty}\frac{1}{\varkappa_n^2+\beta_m^2a^2}\,G_{1,2}\left(\frac{\beta_m d}{2}\right)\cos\frac{\beta_m d}{2}\,x\,, \tag{6}$$

$$s_{3,4}^{(n)}(x) = \sum_{m=-\infty}^{\infty}\frac{1}{\varkappa_n^2+\beta_m^2a^2}\,G_{1,2}\left(\frac{\beta_m d}{2}\right)\sin\frac{\beta_m d}{2}\,x\,, \tag{7}$$

$$(0 \leqslant x \leqslant 1)\,,$$

with $\varkappa_n \equiv \sqrt{\alpha_n^2 - k^2a^2}$, α_n being the n-th positive zero of $J_0(x)$. (We have replaced the previously used symbol K_n by $\varkappa_n$ in order to avoid confusion with the imaginary Bessel function of the second kind $K_n(x)$).

Both types of series appearing in (6) have been calculated in our preceding article, without specifying $G_1(x)$, $G_2(x)$ and K. Using the obtained results, we may write:

$$s_1^{(n)}(x) = \frac{D}{2a\varkappa_n(\cosh(\varkappa_n D/a) - \cos\beta_0 D)}\left[\sinh\frac{\varkappa_n D}{a}\left(1-\frac{dx}{2D}\right)\int_0^x g_1(z)\cosh\frac{\varkappa_n d}{2a}\,z\mathrm{d}z + \right. \tag{8}$$

$$+\cosh\frac{\varkappa_n d}{2a}\,x\int_x^1 g_1(z)\sinh\frac{\varkappa_n D}{a}\left(1-\frac{dz}{2D}\right)\mathrm{d}z +$$

$$+\cos\beta_0 D\sinh\frac{\varkappa_n d}{2a}\,x\int_0^x g_1(z)\cosh\frac{\varkappa_n d}{2a}\,z\mathrm{d}z +$$

$$\left.+\cos\beta_0 D\cosh\frac{\varkappa_n d}{2a}\,x\int_x^1 g_1(z)\sinh\frac{\varkappa_n d}{2a}\,z\,\mathrm{d}z\right],$$

$$s_2^{(n)}(x) = \frac{D\sin\beta_0 D\cosh(\varkappa_n d/2a)x\,G_2(i\varkappa_n d/2a)}{2ia\varkappa_n(\cosh(\varkappa_n D/a) - \cos\beta_0 D)}\,. \tag{9}$$

The series $s_3^{(n)}(x)$ and $s_4^{(n)}(x)$ can be summed in a very similar way leading to the results:

$$s_3^{(n)}(x) = \frac{D \sin \beta_0 D \sinh (\varkappa_n d/2a) x\, G_1(i\varkappa_n d/2a)}{2a\varkappa_n(\cosh (\varkappa_n D/a) - \cos \beta_0 D)}, \tag{10}$$

$$\begin{aligned} s_4^{(n)}(x) = {} & \frac{D}{2a\varkappa_n(\cosh (\varkappa_n D/a) - \cos \beta_0 D)} \left[\cosh \frac{\varkappa_n D}{a}\left(1 - \frac{dx}{2D}\right)\int_0^x g_2(z) \sinh \frac{\varkappa_n d}{2a} z\, \mathrm{d} \right. \\ & + \sinh \frac{\varkappa_n d}{2a}\, x \int_x^1 g_2(z) \cosh \frac{\varkappa_n D}{a}\left(1 - \frac{dz}{2D}\right) \mathrm{d}z - \\ & - \cos \beta_0 D \cosh \frac{\varkappa_n d}{2a}\, x \int_0^x g_2(z) \sinh \frac{\varkappa_n d}{2a} z\, \mathrm{d}z - \\ & \left. - \cos \beta_0 D \sinh \frac{\varkappa_n d}{2a}\, x \int_x^1 g_2(z) \cosh \frac{\varkappa_n d}{2a} z\, \mathrm{d}z \right]. \end{aligned} \tag{11}$$

Let us now calculate the terms on the right hand sides of eqs. (4) and (5) starting with $s_2^{(n)}(x)$ and $s_3^{(n)}(x)$ which do not give rise to complicated integrations:

$$\begin{aligned} \frac{2kad}{D} \sum_{n=1}^{\infty} \int_0^1 s_2^{(n)}(x) \cos p\pi x\, \mathrm{d}x = {} & \frac{kd \sin \beta_0 D}{i} \sum_{n=1}^{\infty} \varkappa_n \frac{G_2(i\varkappa_n d/2a)}{(\cosh (\varkappa_n D/a) - \cos \beta_0 D)} \cdot \\ & \cdot \int_0^1 \cosh \frac{\varkappa_n d}{2a}\, x \cos p\pi x\, \mathrm{d}x = \\ = {} & (-1)^{p-1} 2ika \sin \beta_0 D \sum_{n=1}^{\infty} \frac{\sinh (\varkappa_n d/2a)\, G_2(i\varkappa_n d/2a)}{[\varkappa_n^2 + (4p^2\pi^2a^2/d^2)](\cosh (\varkappa_n D/a) - \cos \beta_0 D)}; \end{aligned} \tag{12}$$

$$\begin{aligned} \frac{2kad}{D} \sum_{n=1}^{\infty} \int_0^1 s_3^{(n)}(x) \sin\left(q + \frac{1}{2}\right)\pi x\, \mathrm{d}x = {} & kd \sin \beta_0 D \sum_{n=1}^{\infty} \frac{G_1(i\varkappa_n d/2a)}{\varkappa_n(\cosh (\varkappa_n D/a) - \cos \beta_0 D)} \cdot \\ & \cdot \int_0^1 \sinh \frac{\varkappa_n d}{2a}\, x \sin\left(q + \frac{1}{2}\right)\pi x\, \mathrm{d}x = \\ = {} & (-1)^q 2ka \sin \beta_0 D \sum_{n=1}^{\infty} \frac{\cosh (\varkappa_n d/2a) G_1(i\varkappa_n d/2a)}{[\varkappa_n^2 + ((2q+1)^2\pi^2a^2/d^2)](\cosh (\varkappa_n D/a) - \cos \beta_0 D)}. \end{aligned} \tag{13}$$

The calculation of the remaining terms is more involved. We get for the first expression:

$$(14)\qquad \frac{2kad}{D}\sum_{n=1}^{\infty}\int_0^1 s_1^{(n)}(x)\cos p\pi x\,\mathrm{d}x = kd\sum_{n=1}^{\infty}\frac{1}{\varkappa_n(\cosh(\varkappa_n D/a)-\cos\beta_0 D)}\cdot$$

$$\cdot\Big[\int_0^1 \sinh\frac{\varkappa_n D}{a}\left(1-\frac{dx}{2D}\right)\cos p\pi x\,\mathrm{d}x\int_0^x g_1(z)\cosh\frac{\varkappa_n d}{2a}z\,\mathrm{d}z +$$

$$+\int_0^1\cosh\frac{\varkappa_n d}{2a}x\cos p\pi x\,\mathrm{d}x\int_x^1 g_1(z)\sinh\frac{\varkappa_n D}{a}\left(1-\frac{dz}{2D}\right)\mathrm{d}z +$$

$$+\cos\beta_0 D\int_0^1\sinh\frac{\varkappa_n d}{2a}x\cos p\pi x\,\mathrm{d}x\int_0^x g_1(z)\cosh\frac{\varkappa_n d}{2a}z\,\mathrm{d}z +$$

$$+\cos\beta_0 D\int_0^1\cosh\frac{\varkappa_n d}{2a}x\cos p\pi x\,\mathrm{d}x\int_x^1 g_1(z)\sinh\frac{\varkappa_n d}{2a}z\,\mathrm{d}z\Big].$$

The first two double integrals can be transformed into

$$(15)\qquad \sinh\frac{\varkappa_n D}{a}\int_0^1\cosh\frac{\varkappa_n d}{2a}x\cos p\pi x\,\mathrm{d}x\int_0^1 g_1(z)\cosh\frac{\varkappa_n d}{2a}z\,\mathrm{d}z -$$

$$-\cosh\frac{\varkappa_n D}{a}\int_0^1 g_1(z)\cosh\frac{\varkappa_n d}{2a}z\,\mathrm{d}z\int_z^1\sinh\frac{\varkappa_n d}{2a}x\cos p\pi x\,\mathrm{d}x -$$

$$-\cosh\frac{\varkappa_n D}{a}\int_0^1 g_1(z)\sinh\frac{\varkappa_n d}{2a}z\,\mathrm{d}z\int_0^z\cosh\frac{\varkappa_n d}{2a}x\cos p\pi x\,\mathrm{d}x,$$

and making use of the integrals

$$(16)\qquad \int_0^z\cosh\frac{\varkappa_n d}{2a}x\cos p\pi x\,\mathrm{d}x = \frac{1}{(\varkappa_n d/2a)^2+p^2\pi^2}\left[\frac{\varkappa_n d}{2a}\sinh\frac{\varkappa_n d}{2a}z\cos p\pi z + \right.$$

$$\left. + p\pi\cosh\frac{\varkappa_n d}{2a}z\sin p\pi z\right],$$

$$(17)\qquad \int_z^1\sinh\frac{\varkappa_n d}{2a}x\cos p\pi x\,\mathrm{d}x = \frac{1}{(\varkappa_n d/2a)^2+p^2\pi^2}\left[(-1)^p\frac{\varkappa_n d}{2a}\cosh\frac{\varkappa_n d}{2a} - \right.$$

$$\left. -\frac{\varkappa_n d}{2a}\cosh\frac{\varkappa_n d}{2a}z\cos p\pi z - p\pi\sinh\frac{\varkappa_n d}{2a}z\sin p\pi z\right],$$

we find that two of the terms cancel each other and that the four remaining terms can finally be reduced to:

$$(18)\qquad \frac{\varkappa_n d/2a}{(\varkappa_n d/2a)^2 + p^2\pi^2}\left[\cosh\frac{\varkappa_n D}{a}\,G_1(p\pi) + \right.$$

$$\left. + (-1)^{p-1}\cosh\frac{\varkappa_n D}{a}\left(1-\frac{d}{2D}\right)G_1\left(\frac{i\varkappa_n d}{2a}\right)\right].$$

In the same way, we obtain for the last two double integrals:

$$(19)\qquad \frac{(\varkappa_n d/2a)\cos\beta_0 D}{(\varkappa_n d/2a)^2 + p^2\pi^2}\left[(-1)^p\cosh\frac{\varkappa_n d}{2a}\,G_1\left(\frac{i\varkappa_n d}{2a}\right) - G_1(p\pi)\right].$$

and finally we get

$$(20)\qquad \frac{2kad}{D}\sum_{n=1}^{\infty}\int_0^1 s_1^{(n)}(x)\cos p\pi x\,\mathrm{d}x = 2ka\sum_{n=1}^{\infty}\frac{1}{\varkappa_n^2 + (4p^2\pi^2a^2/d^2)}\left[G_1(p\pi) + \right.$$

$$\left. + (-1)^{p-1}\,\frac{\cosh(\varkappa_n D/a)(1-(d/2D)) - \cos\beta_0 D\cosh(\varkappa_n d/2a)}{\cosh(\varkappa_n D/a) - \cos\beta_0 D}\,G_1\left(\frac{i\varkappa_n d}{2a}\right)\right].$$

The terms containing $G_1(p\pi)$ can be exactly summed, applying the formula

$$(21)\qquad \frac{J_1(x)}{2xJ_0(x)} = \sum_{n=1}^{\infty}\frac{1}{\alpha_n^2 - x^2}.$$

We find

$$(22)\qquad \sum_{n=1}^{\infty}\frac{1}{\varkappa_n^2 + (4p^2\pi^2a^2/d^2)} = \sum_{n=1}^{\infty}\frac{1}{\alpha_n^2 - (k^2 - (4p^2\pi^2/d^2))a^2} =$$

$$= \sum_{n=1}^{\infty}\frac{1}{\alpha_n^2 - \xi_p^2 a^2} = \frac{J_1(\xi_p a)}{2\xi_p a J_0(\xi_p a)},$$

and (20) becomes

$$(23)\qquad \frac{2kad}{D}\sum_{n=1}^{\infty}\int_0^1 s_1^{(n)}(x)\cos p\pi x\,\mathrm{d}x = \frac{k}{\xi_p}\frac{J_1(\xi_p a)}{J_0(\xi_p a)}\,G_1(p\pi) + 2ka(-1)^{p-1}\cdot$$

$$\cdot\sum_{n=1}^{\infty}\frac{1}{\varkappa_n^2 + (4p^2\pi^2a^2/d^2)}\,\frac{\cosh(\varkappa_n D/a)(1-(d/2D)) - \cos\beta_0 D\cosh(\varkappa_n d/2a)}{\cosh(\varkappa_n D/a) - \cos\beta_0 D}\,G_1\left(\frac{i\varkappa_n d}{2a}\right).$$

Using the same transformation method, the series containing $s_4^{(n)}(x)$

becomes

$$(24)\qquad \frac{2kad}{D}\sum_{n=1}^{\infty}\int_0^1 s_4^{(n)}(x)\sin\left(q+\frac{1}{2}\right)\pi x\,\mathrm{d}x = \frac{k}{\zeta_q}\,\frac{J_1(\zeta_q a)}{J_0(\zeta_q a)}\,G_2\left[\left(q+\frac{1}{2}\right)\pi\right] +$$

$$+ 2ika(-1)^q\sum_{n=1}^{\infty}\frac{1}{\varkappa_n^2+((2q+1)^2\pi^2a^2/d^2)}\cdot$$

$$\cdot\frac{\sinh(\varkappa_n D/a)(1-(d/2D))+\cos\beta_0 D\sinh(\varkappa_n d/2a)}{\cosh(\varkappa_n D/a)-\cos\beta_0 D}\,G_2\left(\frac{i\varkappa_n d}{2a}\right).$$

Finally, the right hand sides of (12), (13), (23) and (24) have to be introduced into (4) and (5), and the last operation consists in putting together the terms containing $G_1(p\pi)$ and $G_2[(q+\frac{1}{2})\pi]$. This requires the calculation of the expression

$$(25)\qquad \frac{k^2}{\xi^2}\,\frac{F_1(\xi;a,b)}{F_0(\xi;a,b)} - \frac{k}{\xi}\,\frac{J_1(\xi a)}{J_0(\xi a)},$$

which can be simplified for all real and imaginary values of ξ. Using the definitions of F_0 and F_1, explicitly given in the preceding article, we may write

— for ξ real and $\neq 0$:

$$(26)\qquad \frac{k^2}{|\xi|^2}\,\frac{F_1(\xi;a,b)}{F_0(\xi;a,b)} - \frac{k}{|\xi|}\,\frac{J_1(|\xi|a)}{J_0(|\xi|a)} =$$

$$= \frac{\pi k J_0(|\xi|b)[J_1(|\xi|a)\,Y_0(|\xi|a) - J_0(|\xi|a)\,Y_1(|\xi|a)]}{2|\xi|J_0(|\xi|a)F_0(\xi;a,b)};$$

— for ξ imaginary and $\neq 0$:

$$(27)\qquad -\frac{k^2}{|\xi|^2}\,\frac{F_1(\xi;a,b)}{F_0(\xi;a,b)} - \frac{k}{|\xi|}\,\frac{I_1(|\xi|a)}{I_0(|\xi|a)} =$$

$$= -\frac{kI_0(|\xi|b)[I_0(|\xi|a)K_1(|\xi|a)+I_1(|\xi|a)K_0(|\xi|a)]}{|\xi|I_0(|\xi|a)F_0(\xi;a,b)}.$$

In the theory of Bessel functions, it is shown that

$$(28)\quad J_0(z)Y_1(z)-J_1(z)Y_0(z)=-\frac{2}{\pi z},\qquad I_0(z)K_1(z)+I_1(z)K_0(z)=\frac{1}{z},\qquad (z>0),$$

so that (26) and (27) become respectively:

$$\frac{kJ_0(|\xi|b)}{|\xi|^2 aJ_0(|\xi|a)F_0(\xi;\,a,\,b)} = \frac{kJ_0(\xi b)}{\xi^2 aJ_0(\xi a)F_0(\xi;\,a,\,b)}\,, \tag{29}$$

$$-\frac{kI_0(|\xi|b)}{|\xi|^2 aI_0(|\xi|a)F_0(\xi;\,a,\,b)} = \frac{kJ_0(\xi b)}{\xi^2 aJ_0(\xi a)F_0(\xi;\,a,\,b)}\,. \tag{30}$$

For $\xi \to 0$, the expression (25) diverges as $1/\xi^2$, as it can be seen from the common result of (29) and (30).

Making use of all the obtained formulae, our final result namely an infinite system of equations which is completely equivalent to (1), can be written as follows:

$$\left\{\begin{aligned}
&\frac{(-1)^{p-1}J_0(\xi_p b)\,G_1(p\pi)}{2\xi_p^2 a^2 J_0(\xi_p a)F_0(\xi_p;\,a,\,b)} = \sum_{n=1}^{\infty}\frac{1}{\varkappa_n^2 + (4p^2\pi^2a^2/d^2)}\cdot\\
&\cdot\frac{\left[\cosh\frac{\varkappa_n D}{a}\left(1-\frac{d}{2D}\right) - \cos\beta_0 D\cosh\frac{\varkappa_n d}{2a}\right]G_1\left(\frac{i\varkappa_n d}{2a}\right) - i\sin\beta_0 D\sinh\frac{\varkappa_n d}{2a}\,G_2\left(\frac{i\varkappa}{2}\right.}{\cosh\frac{\varkappa_n D}{a} - \cos\beta_0 D}\\
&\qquad (p = 0, 1, \ldots)\,,\\
&\frac{(-1)^{q-1}J_0(\zeta_q b)\,G_2[(q+\tfrac{1}{2})\pi]}{2\zeta_q^2 a^2 J_0(\zeta_q a)F_0(\zeta_q;\,a,\,b)} = \sum_{n=1}^{\infty}\frac{1}{\varkappa_n^2 + ((2q+1)^2\pi^2a^2/d^2)}\cdot\\
&\cdot\frac{\sin\beta_0 D\cosh\frac{\varkappa_n d}{2a}\,G_1\left(\frac{i\varkappa_n d}{2a}\right) - i\left[\sinh\frac{\varkappa_n D}{a}\left(1-\frac{d}{2D}\right) + \cos\beta_0 D\sinh\frac{\varkappa_n d}{2a}\right]G_2\left(\frac{i\varkappa}{2}\right.}{\cosh\frac{\varkappa_n D}{a} - \cos\beta_0 D}\\
&\qquad (q = 0, 1, \ldots)\,.
\end{aligned}\right. \tag{31}$$

RIASSUNTO (*)

Generalizzando un metodo impiegato in un precedente lavoro, un sistema infinito di equazioni che compare in un problema di propagazione d'onde lungo guide d'onda periodicamente diaframmate ad iride è stato trasformato esattamente in un nuovo sistema di equazioni che possono essere di interesse per l'ulteriore trattazione del problema.

(*) *Traduzione a cura della Redazione.*

IL NUOVO CIMENTO Vol. I, N. 3 1° Marzo 1955

On the (β_0, k) Diagrams for Circularly Symmetric TM. Waves in Infinite Irisloaded Waveguides.

V. J. VANHUYSE

Interuniversitair Instituut voor Kernwetenschappen
Centrum van de Rijksuniversiteit - Gent, Belgio

(ricevuto il 18 Gennaio 1955)

Summary. — Due to some simplifications in the final equations of the theory of circularly symmetric T.M.-waves in infinite irisloaded waveguides, arising in the case of guides with infinitely thin irises, the results can be brought directly in connection with the pass bands in the different (β_0, k) diagrams (frequency vs. propagation constant).

In a preceding article C. C. GROSJEAN (1) considers the problem of wave propagation in an irisloaded guide, whose cross-section is shown on Fig. 1. This problem results in the solution of an infinite set of equations. GROSJEAN transforms this system into two other infinite sets which are equivalent to the first.

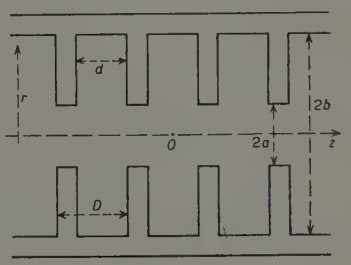

Fig. 1.

It is known that, for given guide dimensions, the solution of this general frequency equations must give rise to an infinite number of pass bands in each diagram (frequency vs. propagation constant) corresponding to a particular cut off frequency of the unloaded guide (2).

As each of the mentioned infinite sets of equations is very complicated and no one is resolved, this can not be found out of them immediately. However, there is an interesting special case in which the previous statements can be nicely

---

(1) C. C. GROSJEAN: *Nuovo Cimento*, **1**, 427 (1955).
(2) J. C. SLATER: *Microwave Electronics*, (New York 1951), Chapter VIII.

illustrated, namely when the iris walls become infinitely thin. Indeed, let us use e.g. the system

$$(1)\quad \begin{cases} \dfrac{k^2}{\xi_p^2}\dfrac{F_1(\xi_p;\,a,\,b)}{F_0(\xi_p;\,a,\,b)}\,G_1(p\pi) = (-1)^p\dfrac{d}{D}\sum\limits_{m=-\infty}^{+\infty}\dfrac{k}{\chi_m}\dfrac{J_1(\chi_m a)}{J_0(\chi_m a)}\cdot \\ \qquad\cdot\left[G_1\left(\dfrac{\beta_m d}{2}\right)-G_2\left(\dfrac{\beta_m d}{2}\right)\right]\dfrac{(\beta_m d/2)\sin(\beta_m d/2)}{(\beta_m d/2)^2-p^2\pi^2} \qquad (p=0,1,\ldots) \\ \dfrac{k^2}{\zeta_q^2}\dfrac{F_1(\zeta_q;\,a,\,b)}{F_0(\zeta_q;\,a,\,b)}\,G_2\left[\left(q+\dfrac{1}{2}\right)\pi\right] = (-1)^q\dfrac{d}{D}\sum\limits_{m=-\infty}^{+\infty}\dfrac{k}{\chi_m}\dfrac{J_1(\chi_m a)}{J_0(\chi_m a)}\cdot \\ \qquad\cdot\left[G_1\left(\dfrac{\beta_m d}{2}\right)-G_2\left(\dfrac{\beta_m d}{2}\right)\right]\dfrac{(\beta_m d/2)\cos(\beta_m d/2)}{(\beta_m d/2)^2-(q+\frac{1}{2})^2\pi^2} \qquad (q=0,1,\ldots), \end{cases}$$

in which

$$k=\frac{2\pi}{\lambda_0}\,,\quad (\lambda_0 = \text{free space wavelenght})$$

$$\beta_0=\frac{2\pi}{\lambda_g}\,,\quad (\lambda_g = \text{guide wavelenght}),\ \beta_m=\beta_0+2\pi m/D\ \ (m=0,\pm1,\ldots),$$

$$\chi_m\equiv(k^2-\beta^2)^{\frac{1}{2}}\,,\qquad \xi_p\equiv\left(k^2-\frac{4p^2\pi^2}{D^2}\right)^{\frac{1}{2}}\,,\qquad \zeta_q\equiv\left[k^2-\frac{(2q+1)^2\pi^2}{D^2}\right]^{\frac{1}{2}}\,,$$

$$F_0(\xi;\,r,\,b)\equiv J_0(\xi r)\left[\frac{\partial J_\nu(\xi b)}{\partial\nu}\right]_{\nu=0}-J_0(\xi b)\left[\frac{\partial J_\nu(\xi r)}{\partial\nu}\right]_{\nu=0}\,,\qquad F_1(\xi;\,r,\,b)\equiv-\frac{1}{k}\frac{\partial F_0}{\partial r}\,,$$

$$G_1(x)\equiv\int_0^1 g_1(z)\cos xz\,\mathrm{d}z\,,\qquad G_2(x)\equiv\int_0^1 g_2(z)\sin xz\,\mathrm{d}z\quad;$$

$g_1(x)$ and $g_2(x)$ are two real functions existing in the interval $(-1\leqslant x\leqslant 1)$, being respectively symmetrical and antisymmetrical with respect to $x=0$. The expression

$$E_z(a,z)=\left\{g_1\left[\frac{2}{d}(z-nD)\right]+ig_2\left[\frac{2}{d}(z-nD)\right]\right\}\exp\left[-i\beta_0 nD\right]$$

represents the electric field component in the z direction along $r=a$ for the n-th cavity.

Putting $d=D$, let us first consider $\beta_0 D=2\pi s$ $(s=0,\pm1,\ldots)$. Using the relation

$$\frac{\alpha\pi\sin\alpha\pi}{\alpha^2\pi^2-\beta^2\pi^2}=\begin{cases}0 & (\alpha\neq\beta)\\ 1 & (\alpha=\beta=0)\\ \dfrac{(-1)^\beta}{2} & (\alpha=\pm\beta\neq0)\,,\end{cases}$$

then the system (1) becomes:

$$(2)\quad \begin{cases} \left[\dfrac{k^2}{\xi_p^2}\dfrac{F_1(\xi_p;\,a,b)}{F_0(\xi_p;\,a,b)} - \dfrac{k}{\xi_p}\dfrac{J_1(\xi_p a)}{J_0(\xi_p a)}\right] G_1(p\pi) = 0 & (p = 0, 1, \ldots) \\ (-1)^q \dfrac{k^2}{\zeta_q^2}\dfrac{F_1(\zeta_q;\,a,b)}{F_0(\zeta_q;\,a,b)}\, G_2\left[\left(q+\dfrac{1}{2}\right)\pi\right] = \\ \qquad = \dfrac{2}{\pi}\sum_{m=1}^{\infty}(-1)^m \dfrac{k}{\xi_m}\dfrac{J_1(\xi_m a)}{J_0(\xi_m a)}\,\dfrac{m\,G_2(m\pi)}{(q+\frac{1}{2})^2 - m^2} & (q = 0, 1, \ldots). \end{cases}$$

Making use of the definition of F_0 and F_1, and applying the well-known relations:

$$\begin{vmatrix} J_0(x) & Y_0(x) \\ \dfrac{\mathrm{d}J_0}{\mathrm{d}x} & \dfrac{\mathrm{d}Y_0}{\mathrm{d}x} \end{vmatrix} = \frac{2}{\pi x}, \qquad \begin{vmatrix} I_0(x) & K_0(x) \\ \dfrac{\mathrm{d}I_0}{\mathrm{d}x} & \dfrac{\mathrm{d}K_0}{\mathrm{d}x} \end{vmatrix} = -\frac{1}{x} \qquad (x > 0),$$

we find that the first equations of (2) are equivalent to

$$(3)\qquad J_0(\xi_p b)\, G_1(p\pi) = 0 \qquad (p = 0, 1, \ldots),$$

whereas the remaining equations cannot directly be simplified. Starting from one of the two other sets of equations we should find the same results. The determinant of (2), in which the first equations are replaced by (3), turns out to be equal to

$$(4)\qquad \left[\prod_{p=0}^{\infty} J_0(\xi_p b)\right] \Delta(A_{q,m})$$

in which

$$A_{q,m} \equiv \frac{(-1)^m m}{(q+\frac{1}{2})^2 - m^2}\left[\frac{k^2}{\zeta_q^2}\frac{F_1(\zeta_q;\,a,b)}{F_0(\zeta_q;\,a,b)} - \frac{k}{\xi_m}\frac{J_1(\xi_m a)}{J_0(\xi_m a)}\right]$$

and Δ represents the infinite determinant of the equations containing G_2. The frequency equation obtained by putting (4) equal to zero, splits into the equations

$$(5)\qquad J_0(\xi_p b) = 0, \qquad (p = 0, 1, \ldots)$$

$$(6)\qquad \Delta(A_{q,m}) = 0.$$

The solutions of (5) are

$$k = \left[\left(\frac{\alpha_n}{b}\right)^2 + \left(\frac{2p\pi}{D}\right)^2\right]^{\frac{1}{2}} \qquad (n = 1, 2, \ldots)\ (p = 0, 1, \ldots),$$

in which α_n are the roots of $J_0(x) = 0$.

For each value of n (corresponding to a cut off frequency $k_0 = \alpha_n/b$ of the unloaded guide), we can represent the points

$$\beta_0 = \frac{2\pi s}{D}\,; \qquad k = \left[\left(\frac{\alpha_n}{b}\right)^2 + \left(\frac{2p\pi}{D}\right)^2\right]^{\frac{1}{2}} \qquad \begin{matrix}(s = 0,\ \pm 1, \ldots)\\ (p = 0,\ 1, \ldots)\end{matrix}$$

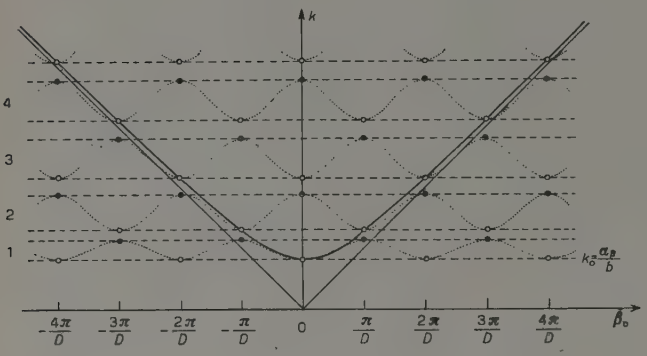

Fig. 2.

in a (β_0, k) diagram, as shown on Fig. 2. They constitute the minima of the periodic curves (k vs. β_0) in the pass bands characterized by an odd number. The more complicated solutions for k resulting from (6), provide the maxima of the periodic curves in the even pass bands. In the general case, all the obtained frequencies will be different from each other. Therefore, a frequency making

$$J_0(\xi_p b) = 0$$

must necessarily be associated with

$$G_1(m\pi) = 0 \qquad (m = 0, 1, \ldots,\ p-1,\ p+1, \ldots)$$
$$G_2(m\pi) = 0 \qquad (m = 0, 1, \ldots)\,.$$

This corresponds directly to

$$g_1(x) = C\cos p\pi x\,, \qquad g_2(x) = 0\,,$$

so that

$$E_z(a, z) = C\cos\frac{2p\pi x_n}{D} \qquad \left(-\frac{D}{2} \leqslant x_n \leqslant \frac{D}{2}\right).$$

In both regions $(0 \leqslant r \leqslant a)$ and $(a \leqslant r \leqslant b)$, the field components are described by the same functions. For E_z, we find

$$E_z = C\,\frac{J_0(\alpha_n r/b)}{J_0(\alpha_n a/b)}\cos\frac{2p\pi z}{D}\,.$$

This shows that for the odd pass bands, the solutions represent standing waves with the same field configurations as the travelling waves with the same frequencies in the unloaded guide. It can also be seen on Fig. 2, that only

the points situated on the branch of the hyperbola

$$k = \left[\left(\frac{\alpha_n}{b}\right)^2 - \beta^2\right]^{\frac{1}{2}},$$

valid for the unloaded guide, represent really existing waves with a non-zero amplitude. The other points correspond to Fourier components whose amplitudes, existing when d is different from D, are just vanishing together with the thickness of the iris walls. For a frequency satisfying (6), one obtains in general

$$G_1(m\pi) = 0 \qquad (m = 0, 1, \ldots)$$

$$G_2(m\pi) \neq 0 \qquad (m = 1, 2, \ldots)$$

so that the fields for the 0 modes in the even pass bands will have an infinite number of Fourier components. For instance, in the region $(0 \leqslant r \leqslant a)$, we can write for E_z:

$$E_z = 2i \sum_{m=1}^{\infty} G_2(m\pi) \frac{J_0(\xi_m r)}{J_0(\xi_m a)} \sin \frac{2\pi m z}{D},$$

only containing antisymmetric functions with respect to z.

Let us now consider the π modes. Putting $\beta_0 D = (2s+1)\pi$ $(s = 0, \pm 1, \ldots)$ in the set (1), again one half of the equations will only contain G_1, but this time they will form the complicated set. The other half, constituting the simple equations, will only depend on G_2. Indeed, using the relation

$$\frac{(\alpha + \frac{1}{2})\pi \cos(\alpha + \frac{1}{2})\pi}{(\alpha + \frac{1}{2})^2\pi^2 - (\beta + \frac{1}{2})^2\pi^2} = \begin{cases} 0 & (\alpha \neq \beta) \\ \dfrac{(-1)^\beta}{2} & (\alpha = \beta), \end{cases}$$

the equations resulting from (1) are now:

$$\begin{cases} (-1)^p \dfrac{k^2}{\xi_p^2} \dfrac{F_1(\xi_p; a, b)}{F_0(\xi_p; a, b)} G_1(p\pi) = \dfrac{2}{\pi} \displaystyle\sum_{m=0}^{\infty} (-1)^m \frac{k}{\zeta_m} \frac{J_1(\zeta_m a)}{J_0(\zeta_m a)} G_1\left[\left(m + \frac{1}{2}\right)\pi\right] \cdot \\ \qquad \cdot \dfrac{m + \frac{1}{2}}{(m + \frac{1}{2})^2 - p^2} \qquad (p = 0, 1, 2, \ldots) \\ J_0(\zeta_q b) G_2[(q + \frac{1}{2})\pi] = 0 \qquad (q = 0, 1, 2, \ldots). \end{cases}$$

The simple solutions

$$k = \left[\left(\frac{\alpha_n}{b}\right)^2 + \frac{(2q+1)^2\pi^2}{D^2}\right]^{\frac{1}{2}} \qquad (n = 1, 2, \ldots)(q = 0, 1, \ldots)$$

provide the minima of the periodic curves in the even pass bands of each (β_0, k) diagram, whereas the complicated solutions correspond to the maxima of the curves in the odd pass bands. The electromagnetic fields associated with these frequencies are again represented by standing waves. In the even pass bands, the waves are described by only one Fourier component and $E_z(r, z)$ is antisymmetric with respect to z. In the odd bands, however, the solutions are generally given by infinite Fourier series and $E_z(r, z)$ contains only even functions of the coordinate z.

For all other modes, the sets of equations remain so complicated that they do not enable us to make a further discussion. This is also the case for all the modes (including 0 and π modes), when the iris walls have a finite thickness $(d \neq D)$. It can only be stated qualitatively, that this more general case can be regarded as a perturbation on the previous case $(d = D)$ and that therefore the general picture of the band structures obtained in the (β_0, k) diagrams remains valid.

It is a great pleasure to thank the Belgian Institute for Nuclear Sciences and Prof. Dr. J. L. VERHAEGHE for his constant interest in our work.

RIASSUNTO (*)

In seguito ad alcune semplificazioni nelle equazioni finali della teoria delle onde TM a simmetria circolare, propagantisi in guide d'onda infinite con diaframmi ad iride che si hanno nel caso di guide con diaframmi infinitamente sottili, i risultati possono mettersi direttamente in relazione con i passa banda nei vari diagrammi (β_0, k) (frequenza, costante di propagazione).

(*) *Traduzione a cura della Redazione.*

Sullo spettro dei raggi gamma di bassa energia, nella radiazione cosmica.

M. Ageno, G. Cortellessa e R. Querzoli

Istituto Superiore di Sanità, Laboratorio di Fisica - Roma

(ricevuto il 21 Gennaio 1955)

Riassunto. — Con uno spettrometro a scintillazione a un canale, munito di un cristallo di ioduro di sodio, si studia lo spettro energetico della componente ultra-molle della radiazione cosmica, all'aperto (al livello del mare) e sotto circa 100 g cm^{-2}. Si trova che tale componente è sostanzialmente costituita da fotoni secondari per la maggior parte di energia compresa tra 50 e 200 keV. La banda ha un massimo molto marcato attorno a 80 keV all'aperto e a 90 keV sotto 100 g cm^{-2}. L'intensità incidente all'aperto viene valutata grossolanamente a 100 quanti al minuto, per centimetro quadrato e steradiante attorno alla verticale. Ciò corrisponde, nell'ipotesi (vera in prima approssimazione) che la radiazione incidente sia isotropa, a un flusso di energia pari all'1% circa dell'energia totale incidente sulla superficie del suolo per effetto della radiazione cosmica. Mediante misure di assorbimento in piombo, si conferma la natura fotonica della componente ultra-molle, mettendo in evidenza la discontinuità dell'assorbimento ai due lati del limite K di questo elemento.

1. – Introduzione.

È noto da parecchi anni che nella radiazione cosmica a livello del mare è presente un numero assai elevato di elettroni e fotoni di bassissima energia, che vengono generalmente interpretati come il prodotto finale di degradazione energetica della componente elettromagnetica nell'aria.

Questa radiazione pochissimo penetrante è stata tuttavia fino ad oggi ben poco studiata per due ragioni. In primo luogo, essa non è per la maggior parte in grado di azionare i normali apparati di rivelazione, in quanto di energia inferiore al « taglio » introdotto dalle pareti dei contatori. In secondo luogo, i metodi che hanno permesso di sviluppare completamente la teoria degli sciami moltiplicativi alle alte energie, cadono completamente in difetto a queste energie così basse, di modo che neppure col calcolo si è potuto finora esatta-

mente prevedere la struttura della componente elettromagnetica al di sotto di qualche MeV.

Ciò che se ne sa fino ad oggi si può pertanto riassumere in poche parole. M. SCHÖNBERG [1] fece per il primo osservare, nel 1938, come esistano notevoli divergenze tra le misure dell'intensità della radiazione cosmica eseguite a grande altezza mediante contatori in coincidenza e quelle eseguite con camere di ionizzazione. Le divergenze si possono spiegare ammettendo l'esistenza di una componente assai molle, capace in parte di attraversare l'unica parete di una camera di ionizzazione, ma non le numerose pareti di un gruppo di contatori in coincidenza.

L'esistenza effettiva di questa radiazione ultra-molle fu poi messa sperimentalmente in evidenza da G. BERNARDINI e B. FERRETTI [2,3] al livello del mare, con un sistema di contatori in coincidenza in cui le particelle per essere rivelate dovevano essere capaci di attraversare almeno 3 mm di alluminio. Studiando l'assorbimento di questa radiazione in pochi millimetri di piombo o di ottone e la generazione di secondari elettronici negli stessi schermi, BERNARDINI e FERRETTI giunsero alle seguenti conclusioni:

a) esiste una assai intensa componente ultra-molle della radiazione cosmica, costituita da elettroni e fotoni. Il 10% della radiazione totale viene infatti assorbito da 2 mm di Pb e il 20% da 4 mm di Pb, mentre 8 mm di Pb assorbono praticamente come 4 mm;

b) l'energia media da attribuire alla frazione della radiazione totale che viene assorbita da 4 mm di Pb sembra essere di 5-10 MeV;

c) il numero di fotoni presente nella radiazione ultra-molle sembra essere approssimativamente uguale a 10 volte il numero degli elettroni.

Vanno forse messe in relazione con l'esistenza di questa componente ultra-molle anche alcune osservazioni di altri Autori. P. AUGER e collaboratori [4] dimostrarono l'esistenza di piccoli sciami atmosferici locali capaci di produrre coincidenze tra contatori non schermati e posti tutti nel raggio di una cinquantina di centimetri. J. BARNÓTHY e M. FORRÓ [5,6] ad una profondità equivalente a 1000 m di acqua e successivamente M. MIESOWICZ, L. JURKIEWICZ e J. M. MASSALSKI [7] a profondità equivalente a 600 e 540 m di acqua, trova-

---

(1) M. SCHÖNBERG: *Ric. Scient.*, **9** (2), 459 (1938).
(2) G. BERNARDINI e B. FERRETTI: *Ric. Scient.*, **10** (1), 39 (1939).
(3) G. BERNARDINI e B. FERRETTI: *Nuovo Cimento*, **7**, 173 (1939).
(4) P. AUGER: *Huitième Conseil de l'Institut International de Physique Solvay*, 1948.
(5) J. BARNÓTHY e M. FORRÓ: *Phys. Rev.*, **74**, 1300 (1948).
(6) J. BARNÓTHY e M. FORRÓ: *Phys. Rev.*, **55**, 870 (1939).
(7) M. MIESOWICZ, L. JURKIEWICZ e J. M. MASSALSKI: *Phys. Rev.*, **77**, 380 (1950).

rono anch'essi coincidenze doppie tra contatori, attribuibili a una radiazione assai molle. I primi due Autori con un telescopio di contatori in coincidenza trovarono un eccesso di coincidenze doppie tra i contatori estremi, sulle coincidenze triple, eccesso che attribuiscono a una radiazione scarsamente ionizzante forse secondaria dei mesoni μ. MIESOWICZ, JURKIEWICZ e MASSALSKI confermano in parte l'eccesso di coincidenze doppie trovate da BARNÓTHY e FORRÓ, dimostrano che queste coincidenze doppie in eccesso sono dovute a raggi γ con coefficiente di assorbimento in piombo di circa 1,4 cm^{-1} e suggeriscono, senza per altro dimostrarlo, che si tratti di raggi γ dovuti a radioattività locale e di energia dell'ordine di 1 MeV.

Allo scopo di portare un contributo allo studio di questo campo ancora pressochè inesplorato, ci siamo proposti di studiare la composizione spettrale dei raggi γ di bassissima energia presenti nella radiazione cosmica. Abbiamo fatto uso a questo scopo di uno spettrometro a scintillazione a un canale, munito di un cristallo di ioduro di sodio, il cui schema e le cui prove di taratura sono state già descritte da noi in altro lavoro ([8]). Il cristallo dello spettrometro era in queste misure di forma cilindrica, di 5 cm di altezza e 4,5 cm di diametro, schermato da 0,7 mm di alluminio e da un sottile strato diffondente di MgO. Solo per le prime misure orientative abbiamo fatto uso di un cristallo più piccolo, di 1,27 cm di altezza e 1,27 cm di diametro.

Questa tecnica, da non molto entrata nell'uso, presenta al nostro scopo dei vantaggi veramente notevoli e precisamente: l'elevatissimo rendimento (che con un cristallo delle dimensioni del nostro è praticamente 1 fino a 0,5 MeV e non scende poi mai al di sotto di 1/2) e la proporzionalità tra l'energia lasciata dal raggio γ nel cristallo e l'ampiezza dell'impulso di tensione che ne consegue. Per quanto lo scarso potere risolutivo e la difficoltà di risalire dallo spettro degli impulsi di tensione a quello dei raggi γ incidenti, rappresentino degli inconvenienti spesso abbastanza gravi, tuttavia le informazioni che se ne possono trarre sulla componente ultra-molle della radiazione cosmica sono, come vedremo, molto più estese di quelle ottenibili coi soliti contatori di Geiger.

Le misure che seguono sono state eseguite, assieme a molte altre su cui riferiremo in altra occasione, nel periodo Gennaio-Luglio del 1954.

2. – Misure orientative.

Una prima serie di misure, a carattere orientativo, è stata eseguita in laboratorio e cioè sotto una copertura che si può valutare a circa 100 $g \cdot cm^{-2}$, con un cristallo più piccolo (altezza = diametro = 1,27 cm) di quello poi usato

([8]) M. AGENO, G. CORTELLESSA e R. QUERZOLI: *Rend. Ist. Sup. Sanità* (1954), in corso di stampa.

nelle misure finali. Queste misure hanno subito messo in evidenza una forte concentrazione di impulsi nella parte bassa dello spettro e precisamente tra 50 e 200 keV circa, con un massimo molto marcato attorno a 90 keV (fig. 1).

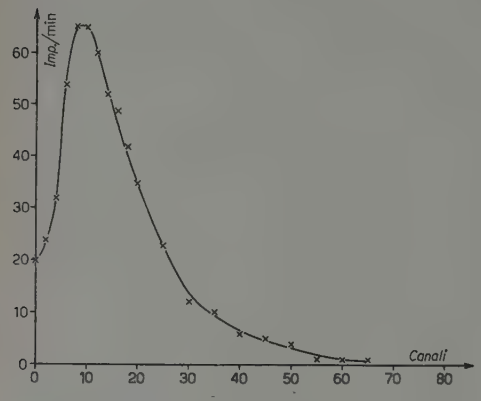

Fig. 1. – Spettro secondari raggi cosmici sotto 100 g cm^{-2} (6,56 keV/can).

Poichè sulla base dei lavori di BERNARDINI e FERRETTI non ci si attendeva un tale resultato, si è ritenuto necessario prendere in esame le tre seguenti possibilità:

a) che l'effetto osservato fosse di carattere strumentale;

b) che si trattasse di un effetto dovuto a radioattività delle pareti o di oggetti circostanti;

c) che fosse un effetto veramente imputabile alla radiazione cosmica.

Per poter escludere la prima di queste alternative, si sono fatte le prove seguenti.

Si è innanzi tutto esaminato lo spettro degli impulsi di fondo del fotomoltiplicatore, in assenza di cristallo. Il numero totale di impulsi registrati con e senza cristallo al variare della soglia è indicato nella tabella I.

TABELLA I.

	Amplificazione	Soglia	Impulsi/min
Con cristallo	17.8 keV/canale	44.5 keV	1 668 ± 29
Senza cristallo . . .	17,8 »	44,5 »	0
» » . . .	2,18 »	5,45 »	6 ± 1
» » . . .	1,64 »	4,1 »	43 ± 3

La fig. 2 mostra la ripartizione spettrale degli impulsi di fondo del fotomoltiplicatore con amplificazione equivalente a 1,64 keV/canale.

Rimesso a posto il cristallo si è fatto quindi uno spettro degli impulsi del contatore a scintillazione nelle stesse condizioni della fig. 1, ma con il cristallo schermato da ogni lato da 2 cm di piombo. Tale spettro è riportato nella fig. 3.

La seconda delle alternative sopra considerate, e cioè quella che l'effetto osservato fosse almeno per la maggior parte imputabile a radioattività delle pareti o di oggetti circostanti, ha richiesto un esame più approfondito. È innanzi tutto da osservare che radiazione di così bassa energia, rivelata al centro di una stanza del laboratorio e cioè sotto una copertura di circa

100 g cm^{-2}, è certamente, almeno in gran parte generata nelle pareti o nel soffitto. Il problema era quindi quello di determinare se si trattasse di secondari di una radiazione proveniente dall'esterno o non piuttosto di radioattività dei materiali circostanti.

Un primo gruppo di prove è consistito essenzialmente nel cambiare la posizione del cristallo nel laboratorio, rispetto alle pareti o al soffitto, e nello scher-

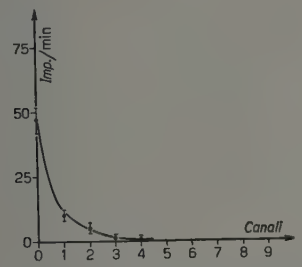

Fig. 2. – Spettro impulsi di fondo del fotomoltiplicatore (1,64 keV/can).

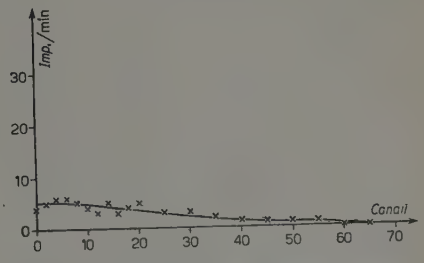

Fig. 3. – Spettro con cristallo schermato da 2 cm Pb (6,56 keV/can).

mare solo parzialmente il cristallo con piombo, allo scopo di vedere se esistesse una direzione preferenziale di provenienza della radiazione in istudio. Si è in tal modo giunti alla conclusione che questa ultima è sensibilmente isotropa, fatto questo in ogni caso spiegabile, se si tratta di raggi γ di molto bassa energia.

Con un altro gruppo di prove si è cercato di stabilire se i raggi γ provenienti da sostanze radioattive contenute nelle pareti (essenzialmente Th, U e K) potessero nelle pareti stesse raggiungere uno spettro di equilibrio simile a quello osservato. A questo scopo in un ambiente prossimo a quello in cui si eseguivano le misure con lo spettrometro è stata posta una sorgente di 400 mC di Radio, schermata da alcuni centimetri di piombo in direzione del cristallo. Tra questo e la sorgente erano interposti due grossi muri maestri dell'edificio. Nella fig. 4 sono posti a confronto i due spettri d'impulsi misurati con e senza la presenza della sorgente di Radio. La differenza tra le due curve, graficata nella fig. 5, dà lo spettro d'impulsi dovuti alla presenza della sorgente. Come si vede, l'andamento di questo spettro è assai diverso da quello osservato senza sorgente, in quanto il massimo è spostato al di sotto della soglia dello spettrometro. Supposto che lo spettro

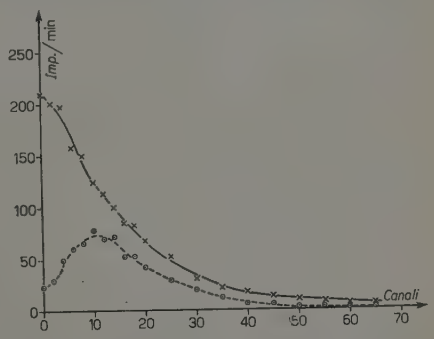

Fig. 4. – Spettro in presenza di una sorgente di Radio, filtrata dalle pareti (6,56 keV/can).

della fig. 1 sia dovuto a raggi γ di parete, sembra che se ne debba concludere che tale spettro non ha ancora raggiunto la sua configurazione di equilibrio. Ciò sembra in accordo col fatto che la posizione del massimo, attorno a 90 keV, coincide bene con la posizione media delle righe X caratteristiche degli elementi più pesanti della famiglia del Torio e dell'Uranio. Resta però allora inesplicabile come tale spettro appaia assai più ricco di raggi γ di energia poco superiore ai 90 keV di quanto non siano gli spettri di raggi X di Torio e Uranio, ottenibili col nostro spettrometro. Basta per convincersene confrontare i due spettri delle fig. 11 e 6 ottenuti (con cristallo di 5 cm) l'uno con cristallo scoperto e l'altro da un preparato di nitrato di uranile tutto schermato, assieme al cristallo, con 2,5 cm di piombo.

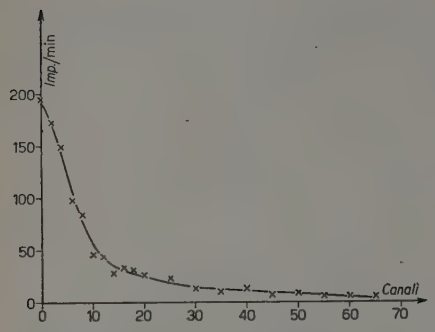

Fig. 5. – Spettro di degradazione di una sorgente di Radio filtrata dalla parete (6,56 keV/can).

Quanto al potassio eventualmente contenuto nelle pareti, sembra che esso non debba neppure essere preso in considerazione, data la debole intensità dei raggi γ che esso emette. D'altra parte 1 kg di KCl posto in prossimità del cristallo dello spettrometro non ha prodotto un sensibile aumento totale degli impulsi di fondo.

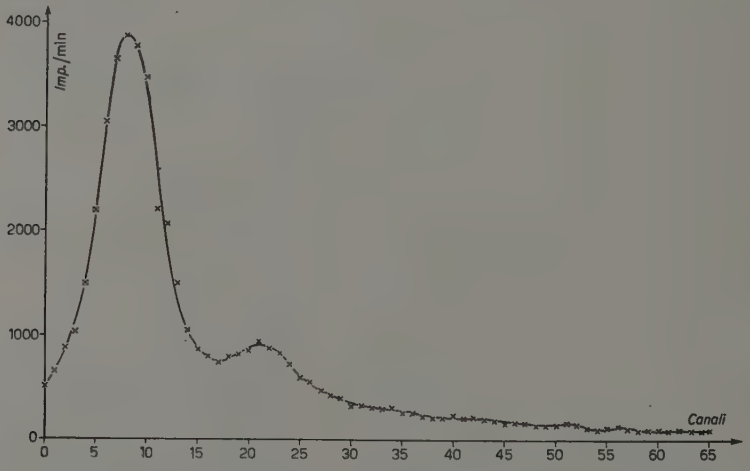

Fig. 6. – Spettro dei raggi X e γ di un preparato di Uranio (7,5 keV/can, $S=4$ can).

Un ultimo gruppo di prove è stato infine eseguito all'esterno del laboratorio su una delle terrazze superiori dell'Istituto. Il contributo delle radiazioni pro-

venienti dai muri dell'edificio avrebbe dovuto qui essere assai minore che all'interno. Le misure orientative hanno invece rivelato una intensità nel massimo solo lievemente inferiore che all'interno, mentre la posizione del massimo era sensibilmente spostata verso le basse energie. La fig. 7 mostra, a titolo di esempio, uno spettro ottenuto col cristallo completamente libero al centro della terrazza e a 4,5 m dal pavimento di essa.

Sulla base di tutte queste misure orientative sembra dunque che si possa concludere quanto segue: la radiazione cosmica genera nella materia un numero assai elevato di secondari di bassa energia, con massimo nell'aria attorno a 80 keV e nel cemento attorno a 90 keV ed estendentesi grosso modo da 50 a 200 keV.

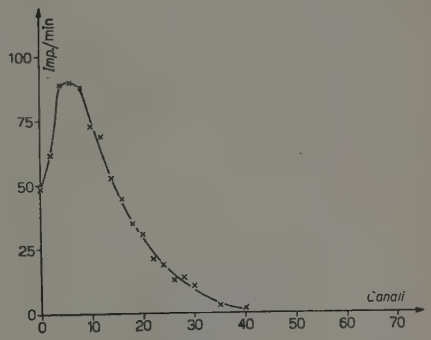

Fig. 7. – Spettro secondari raggi cosmici all'aperto (4,5 m dal suolo) (6,56 keV/can).

3. – Spettro d'impulsi dovuto alla componente ultra-molle.

Giunti, sulla base delle misure orientative descritte nel paragrafo precedente, a questa prima conclusione, ci siamo posti innanzi tutto il problema di determinare con una certa precisione lo spettro degli impulsi generati nel nostro spettrometro dalla componente ultra-molle all'aperto e sotto 100 g cm^{-2}. Tutte le misure che seguono sono state eseguite col cristallo grande dello spettrometro (5 cm di altezza e 4,5 di diametro).

La prima serie di misure è stata eseguita all'aperto, in condizioni geome-

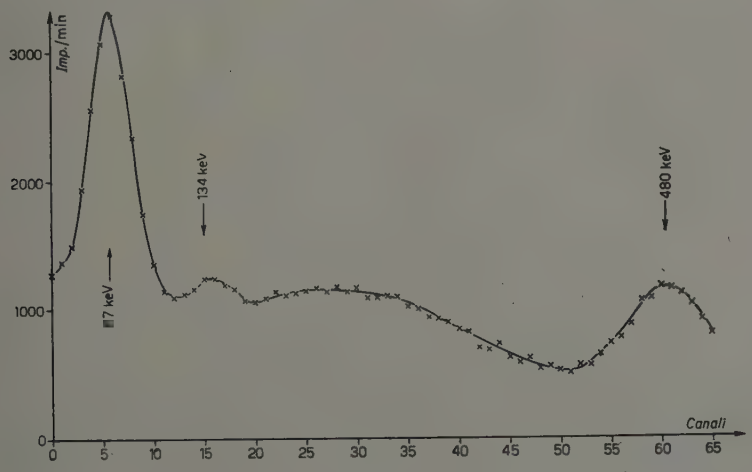

Fig. 8. – Spettro raggi X e γ di ^{187}Re (da W irradiato) (7,5 keV/can).

triche tali, da rendere minimo un eventuale contributo di sostanze radioattive contenute nei materiali dell'edificio. A questo scopo il cristallo è stato messo in un pozzo verticale di piombo, le cui pareti avevano lo spessore di 2,5 cm

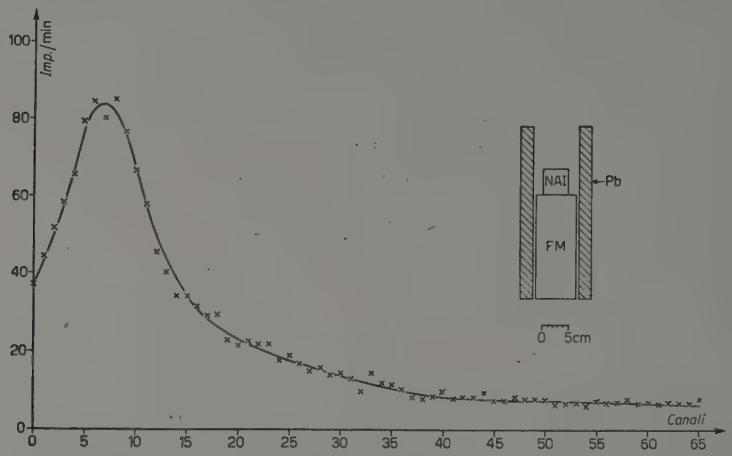

Fig. 9. – Spettro raggi γ cosmici all'aperto, attorno alla verticale (7,5 keV/can).

e un diametro interno di 9 cm. Il centro del cristallo si trovava a 11 cm circa dalla base superiore del pozzo. In queste condizioni, l'angolo solido di provenienza della radiazione ultra-molle registrata dallo spettrometro era 0,53 steradianti, attorno alla verticale. La taratura dello spettrometro è stata fatta

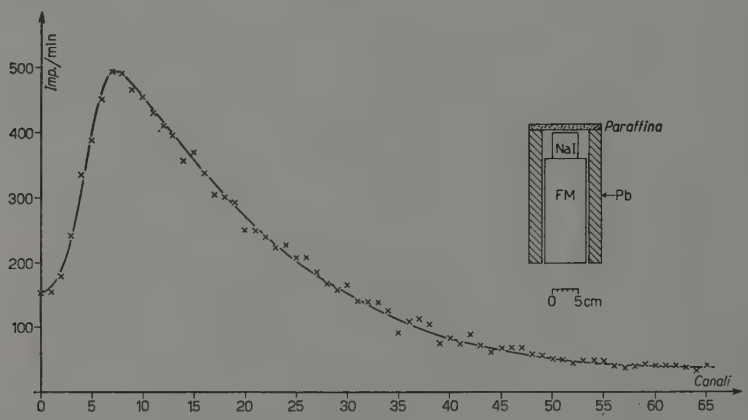

Fig. 10. – Spettro raggi γ cosmici all'aperto, filtrati da 1 cm di paraffina (7,5 keV/can).

mediante i raggi γ e X di conversione di Re^{187} ottenuto mediante bombardamento con neutroni di una lastrina di tungsteno (fig. 8). Nelle condizioni prescelte la costante dello spettrometro era 7,5 keV/canale e la soglia 4 canali. La fig. 9 mostra lo spettro di impulsi dovuto alla componente ultra-molle ottenuto in tal modo.

Non è possibile dire a priori con che precisione tale spettro d'impulsi rappresenti anche lo spettro energetico della radiazione incidente, data la probabilità relativamente elevata che un raggio γ non lasci nel cristallo tutta la sua energia. Abbiamo pertanto voluto vedere innanzi tutto se una frazione sensibile degli impulsi registrati fosse da attribuirsi a elettroni.

Abbiamo fatto a questo scopo una seconda serie di misure, filtrando la radiazione ultra-molle giungente sul cristallo con 1 cm di paraffina. Lo spessore è stato scelto in modo da non attenuare sensibilmente i raggi γ anche di energia molto bassa e da sottrarre invece agli elettroni incidenti non meno di 1,5 MeV (circa). Si era precedentemente verificato che il numero di impulsi al minuto per canale al di sopra di 1,5 MeV era trascurabile in confronto al corrispondente numero, attorno a 100 keV. Lo spettro ottenuto è mostrato nella fig. 10, assieme alle condizioni geometriche in cui è stata eseguita la misura.

Per quanto le intensità assolute delle due curve della fig. 9 e della fig. 10 non siano direttamente confrontabili, data la sostanziale differenza nelle condizioni geometriche, risulta evidente che il massimo sugli 80 keV non è spostato verso le basse energie: esso è quindi sostanzialmente dovuto a raggi γ.

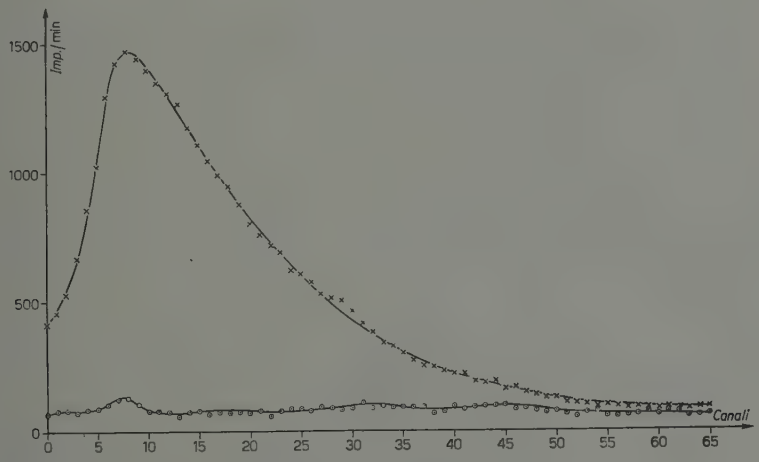

Fig. 11. – Spettro secondari raggi cosmici, sotto 100 g cm^{-2} e fondo con 4 mm di Pb (7,5 keV/can).

Analoghe misure, senza e con 1 cm di paraffina come filtro sono state poi eseguite all'interno del laboratorio, sotto circa 100 g cm^{-2}. I resultati sono mostrati nelle fig. 11 e 12. Qui la misura senza paraffina è stata eseguita prima col cristallo completamente scoperto e poi col cristallo schermato da 4 mm di piombo. Nella misura del fondo, il picchetto a 75 keV sembra doversi attribuire alla radiazione di fluorescenza del piombo ($K\alpha$), emessa a seguito di

ionizzazioni ed effetti fotoelettrici nel livello K provocati dalla radiazione cosmica.

La misura con paraffina è eseguita nelle stesse condizioni geometriche della corrispondente misura eseguita all'esterno (fig. 10). L'intensità sul massimo risulta del 30% circa superiore che all'aperto; ciò non è per altro di per sè molto significativo, dipendendo dalla composizione e struttura dello strato di

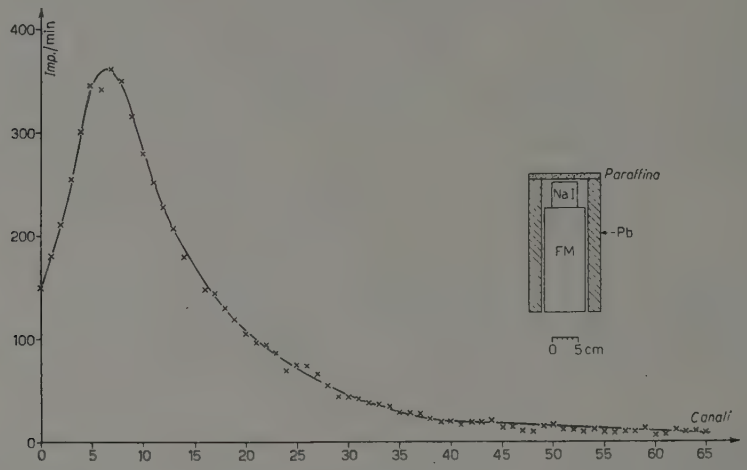

Fig. 12. – Spettro secondari raggi cosmici sotto 100 g cm^{-2} filtrati da 1 cm di paraffina (7,5 keV/can).

materiale in cui si generano i secondari. La presenza dell'assorbitore di paraffina non determina neppure in questo caso uno spostamento del massimo, confermando che la banda di impulsi tra 50 e 200 keV è sostanzialmente da attribuirsi a raggi γ.

La misura eseguita all'esterno attorno alla verticale si presta ad una valutazione grossolana del numero totale di raggi γ nella banda. Essendo in questo campo di energie il rendimento del cristallo assai prossimo ad 1, si può ammettere che ciascun quanto incidente dia luogo ad un impulso, anche se esso non lascia effettivamente tutta la sua energia nel cristallo. Detraendo un fondo (dovuto parte a elettroni e parte a γ di energia molto maggiore) pari all'intensità media tra 40 e 60 canali, si ottiene un flusso di circa 2000 quanti/min·steradiante attorno alla verticale tra 30 e 340 keV, su un'area di quasi 20 cm^2. L'intensità sarebbe quindi attorno alla verticale di circa 100 quanti/min·cm^2·steradiante. Una valutazione dell'intensità, migliore di questa che rappresenta ovviamente soltanto un ordine di grandezza, sarà oggetto di un successivo lavoro.

Accettando per il momento il dato ora stabilito, ed attribuendo ad ogni quanto un'energia pari ad un valore medio attorno ai 100 keV, si ottiene un

flusso di energia di 10 MeV/min·cm²·steradiante. Questo dato è da confrontare con il flusso totale di energia che giunge sulla superficie della Terra da tutte le direzioni e che è approssimativamente di 6000 MeV min·cm² [9]. Ammettendo che la radiazione ultra-molle sia sostanzialmente isotropa, ciò equivale all'1% circa dell'energia totale.

Un problema assai più difficile è quello di risalire dalla distribuzione in ampiezza degli impulsi allo spettro energetico della radiazione incidente. Ciò è dovuto al fatto, ben noto e già citato, che non sempre i quanti incidenti lasciano tutta la loro energia nel cristallo, di modo che in ciascun canale sono presenti sia impulsi dovuti a quanti γ di energia pari a quella del canale sia impulsi dovuti a quanti γ di energia superiore. Le difficoltà dell'analisi dipendono, nel nostro caso, dal fatto che si ha a che fare con uno spettro continuo. È tuttavia presumibile che lo spettro energetico dei γ incidenti non differisca molto dallo spettro osservato, e questo per le ragioni seguenti.

In primo luogo, nel campo di energia che a noi interessa, il cristallo di NaI da 5 cm ha praticamente rendimento 1. La frazione del numero di quanti incidenti assorbita per effetto fotoelettrico è sempre superiore al 50% e, nel caso di interazione Compton, è assai elevata la probabilità del riassorbimento fotoelettrico del quanto diffuso. Ne segue che i quanti gamma incidenti di energia compresa nella banda considerata ($\sim 30 \div 350$ keV) hanno elevata probabilità di lasciare tutta la loro energia nel cristallo e di essere quindi contenuti nel canale corrispondente.

In secondo luogo, i quanti γ incidenti di energia decisamente superiore alla banda possono effettivamente esser contati come appartenenti a canali della banda se dànno luogo nel cristallo ad un effetto Compton sotto un angolo opportuno, seguito da fuga del quanto diffuso. Questi effetti Compton sono però, come è ben noto, almeno in prima approssimazione equiprobabili per tutti i possibili valori dell'energia dell'elettrone di rinculo. Ne segue che questi quanti γ di energia più elevata debbono dar luogo, nella banda energetica che a noi interessa, ad un fondo quasi uniforme (eventualmente un po' più ricco sui canali di più bassa energia). È ciò, d'altra parte, che appunto si osserva, facendo lo spettro del fondo col cristallo schermato da 4 mm di Pb (fig. 12). Questa osservazione giustifica la detrazione, fatta sopra, di un fondo uniforme, per il calcolo approssimativo della intensità.

Per ciò che concerne infine gli elettroni eventualmente presenti, essi sono certamente, come abbiamo visto, assai pochi e la loro distribuzione non può non essere uniforme nella zona che ci interessa, dato che un assorbitore di 1 cm di paraffina non altera sensibilmente l'andamento dello spettro. È quindi da ritenere che la detrazione di un fondo uniforme sia sufficiente ad eliminare,

[9] L. JÁNOSSY: *Cosmic rays* (Oxford, 1948), p. 305.

oltre ai γ di più elevata energia, anche gli elettroni incidenti di energia compresa nella nostra banda.

Riteniamo tuttavia che questo problema, delle correzioni da apportare allo spettro d'ampiezza degli impulsi per tener conto delle interazioni con solo parziale cessione di energia, vada ulteriormente approfondito, il che ci ripromettiamo di fare in un prossimo lavoro. Una riprova che queste correzioni siano piccole è per altro il fatto che l'andamento dello spettro d'impulsi si mantiene sostanzialmente lo stesso, quando al cristallo da 5 cm si sostituisca quello da 1,27 cm, col quale ultimo le interazioni con cessione solo parziale di energia sono evidentemente assai più probabili.

4. – Misure di assorbimento.

Per quanto le misure precedenti fossero già sufficienti per concludere che la intensa banda di secondari tra 50 e 200 keV sia sostanzialmente costituita da raggi γ, abbiamo voluto ottenere del fatto una ulteriore conferma mediante misure di assorbimento. Dato che la radiazione incidente non ha marcate proprietà direzionali, ma è sostanzialmente isotropa, abbiamo ritenuto non opportuna una misura del coefficiente di assorbimento, canale per canale, in una qualsiasi sostanza. Ciò perchè le misure avrebbero richiesto, per tener conto

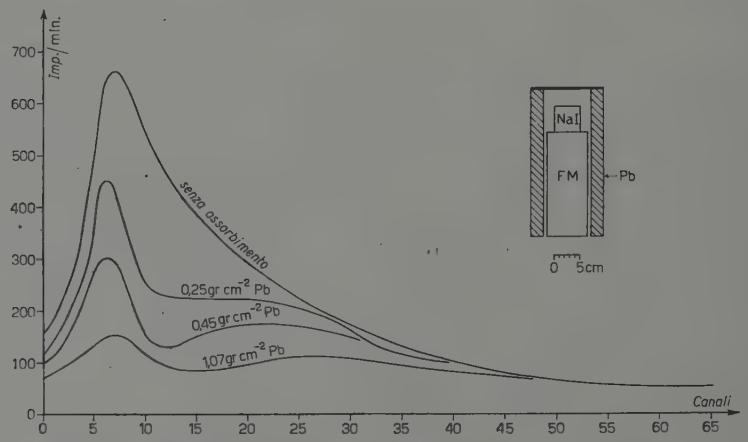

Fig. 13. – Curva di assorbimento in Pb secondari raggi cosmici, sotto 100 g cm^{-2} (7,5 keV/can).

della cattiva geometria, correzioni tali da rendere assai incerto e poco significativo il risultato. È inoltre presumibile che negli assorbitori la radiazione cosmica incidente generi dei secondari (della specie proprio da noi studiata) con un ritmo difficilmente calcolabile a questo punto della nostra ricerca, e di

conseguenza il coefficiente di assorbimento apparente misurato non sarebbe stato in pratica confrontabile coi dati noti in nostro possesso.

Abbiamo però osservato che il limite K di assorbimento del piombo (87,4 keV) cade proprio in prossimità del massimo della nostra banda. Questo fatto ci offriva la possibilità di confermare che la radiazione ultra-molle è sostanzialmente costituita da raggi γ, mettendo in evidenza una netta differenza tra i coefficienti di assorbimento del piombo, a destra e a sinistra del massimo della banda.

Le misure sono state eseguite nelle condizioni geometriche indicate nella fig. 13. Si sono fatti 4 spettri, variando lo spessore di piombo usato come

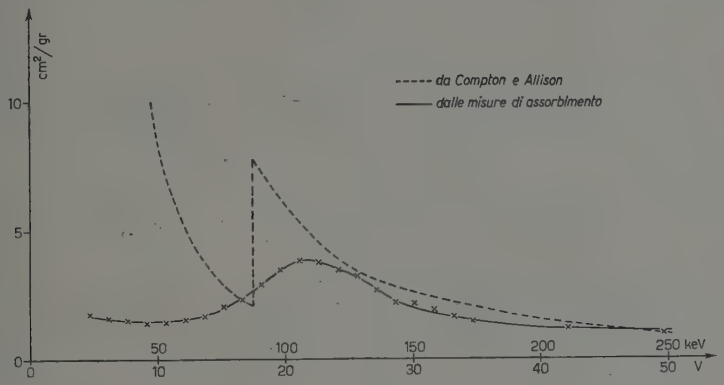

Fig. 14. – Coefficiente di assorbimento massico del Pb.

assorbitore, al di sopra del cristallo. Gli spessori usati sono: 0, 0,25, 0,45 1,07 g cm^{-2}. Nella figura sono riportati gli andamenti dei 4 spettri e non i punti sperimentali, per evitare confusione nella zona di più alta energia, dove le curve vengono praticamente a coincidere. Detratto il fondo con il criterio indicato nel paragrafo precedente, si è determinato canale per canale il coefficiente di assorbimento apparente. Tale valore è riportato (curva a tratto continuo) nella fig. 14, che mostra anche per confronto l'andamento effettivo del coefficiente di assorbimento del piombo in questa zona, secondo i dati di Compton e Allison ([10]). Se si tiene conto del potere risolutivo, assai limitato, di uno spettrometro a scintillazione, si vede che la curva teorica tratteggiata deve dar luogo ad un andamento sperimentale esattamente del tipo di quello da noi ottenuto. La discontinuità al limite K si traduce in un punto di flesso della porzione ascendente della curva. Invece (come del resto si era previsto) i valori assoluti sperimentali risultano molto diversi dal vero, soprattutto nella

([10]) A. H. Compton e S. K. Allison: *X-rays in Theory and Experiment* (New York, 1948), Appendix IX.

zona di bassa energia, attorno ai 50 keV. Ciò è dovuto senza dubbio almeno in parte a generazione di secondari negli assorbitori stessi.

Come controllo del metodo si sono eseguite nelle condizioni geometriche indicate nella fig. 15, delle misure di assorbimento in piombo dei raggi X caratteristici emessi da un preparato di nitrato di uranile, aventi energia assai prossima al massimo della nostra banda di secondari cosmici. Un assorbitore fisso di alluminio eliminava gli elettroni emessi dal preparato. Si sono usati gli stessi spessori di piombo delle misure precedenti. La costante dello spettrometro era in queste misure 4,95 keV/canale e la soglia 2,5 canali.

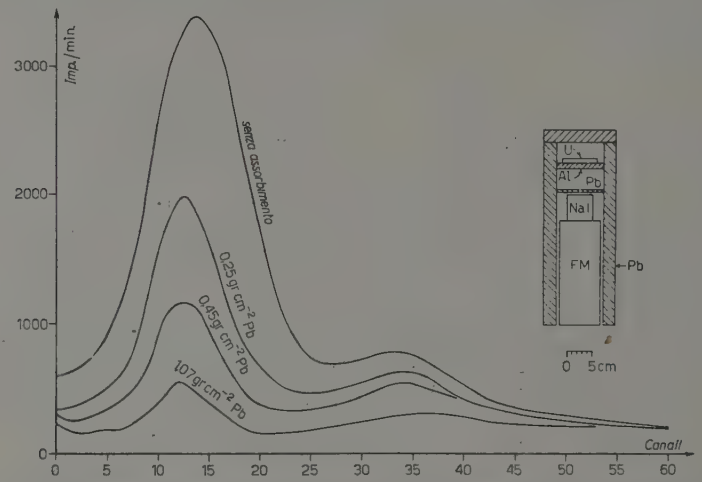

Fig. 15. – Curva di assorbimento in Pb dei raggi X di Uranio (4,95 keV/can, $S = 2.5$ can).

Come risulta dalla fig. 15, ove son riportati i quattro spettri ottenuti, l'andamento del coefficiente di assorbimento apparente per raggi γ di questa energia è proprio quello gia trovato nel caso dei secondari dei raggi cosmici. Ne esce quindi confermata la conclusione che questi ultimi siano sostanzialmente raggi γ, per la maggior parte di energia assai prossima ai 90 keV.

5. – Discussione dei resultati.

Non è possibile istituire un confronto diretto fra le nostre misure e quelle di BERNARDINI e FERRETTI citate nel § 1, data la diversità delle tecniche e delle condizioni sperimentali adottate. È tuttavia da osservare che è possibile stabilire un accordo tra i risultati di questi Autori e i nostri, quando si tenga conto dei fatti seguenti.

In primo luogo, il telescopio di contatori di BERNARDINI e FERRETTI eliminava certamente buona parte della radiazione di più bassa energia. È quindi

naturale che essi trovassero una energia media alquanto maggiore della nostra e un rapporto fotoni-elettroni di circa 10 e quindi sensibilmente inferiore al nostro.

In secondo luogo, è da osservare che essi hanno valutato l'energia media della componente fotonica dal coefficiente di assorbimento in piombo. Ma a ciascun valore di tale coefficiente al di sopra del minimo corrispondono sempre due possibili valori dell'energia dei raggi γ incidenti, uno al di sopra di 3 MeV e l'altro al di sotto. Ad esempio, raggi γ nella banda 5-10 MeV hanno lo stesso coefficiente di assorbimento di raggi γ tra 1,4 e 2 MeV circa. Le loro misure sono quindi compatibili non solo con la loro valutazione dell'energia media ma anche con una energia media attorno a 1,5 MeV, assai più vicina ai nostri risultati.

Non è da escludere che la radiazione γ osservata sotto terra da MIESOWICZ, JURKIEWICZ e MASSALSKI e da questi Autori valutata di energia attorno al MeV, sia una radiazione secondaria, della stessa origine di quella da noi studiata. Anche in questo caso il valore dell'energia media più elevato del nostro si può spiegare con un « taglio » alle basse energie introdotte dal telescopio di contatori.

In un prossimo lavoro daremo conto delle esperienze da noi fatte allo scopo di trarre informazioni sull'origine di questi secondari di bassa energia e delle conclusioni a cui siamo pervenuti a questo riguardo.

SUMMARY

Using a NaI-crystal and a one-channel scintillation spectrometer, we have studied the energy spectrum of the ultra-soft component of the cosmic radiation at sea-level, in the open air and below 100 g cm^{-2} concrete. This component is almost entirely made of secondary photons, mainly between 50 and 200 keV with a prominent peak near 80 keV in the air and 90 keV below concrete. The vertical incident intensity in the air is roughly 100 quanta/min·cm^2·sterad. The ultra-soft component is almost entirely isotropic, so the energy flux is about 1% of the total energy flux due to the cosmic radiation at sea level. The discontinuity of the absorption coefficient at the K critical absorption edge of Pb was put in evidence by means of absorption measurements in this element, confirming the fact that the ultra soft component is made of photons.

Further Evidence for Nuclear Interaction of a Charged Hyperon Arrested in Photographic Emulsion.

R. H. W. Johnston and C. O'Ceallaigh

School of Cosmic Physics, Dublin Institute for Advanced Studies

(ricevuto il 23 Gennaio 1955)

Summary. — A further example is described of the interaction at rest of a particle of protonic mass. The appearance of the interaction is that of a typical σ-star of six branches. The parent particle is ejected from a star of type 23+1 p and comes to rest after a range of 7 mm. Estimates of mass by two independent techniques are in agreement with each other, and are consistent with those of charged hyperons reported by other workers.

1. – Introduction.

Friedlander [1] and Johnston and O'Ceallaigh [2] have reported events which could be interpreted as nuclear disintegrations produced by negative hyperons on being brought to rest in photographic emulsions. The case described by the present authors appeared to be the more clear cut.

A particle of mass intermediate between those of the proton and deuteron was arrested in the emulsion after a range of 7.4 mm. From the point of arrest two particles were emitted, one very steep of range $\sim 2000\ \mu$, the other of range only $4\ \mu$. These tracks were non-coplanar, and momentum could not be conserved in the event without the emission of at least one additional

(1) M. Friedlander: *Phil. Mag.*, **45**, 418 (1954).
(2) R. H. W. Johnston and C. O'Ceallaigh: *Phil. Mag.*, **45**, 424 (1954).

neutral particle. Assuming that the charged particles were both protons, an identification consistent with the appearance of their tracks, the visible energy was ~ 20 MeV. The event was interpreted as being due to the absorption of a negative hyperon. It is aim of the present communication to describe a similar event, a photo-micrograph of which is shown in Plate 1.

2. – Description.

A particle Y is ejected from a star of type 23 + 1p, passes through 4 plates with range 7 mm and ends at P in an interaction which has the appearance of a typical σ-star of 6 branches. Assuming that the emitted particles are all protons, the visible energy is 22 MeV.

The mean gap-length in the neighbourhood of the point of interaction is consistent with that of a particle of protonic mass moving with negligible velocity. It will be assumed therefore, in what follows, that the interacting particle was at rest and of negative charge. The mass was estimated by the techniques of scattering versus range, and mean gap-length versus range.

a) *Scattering range.* – The technique of constant sagitta was used using the tables of FAY *et al.* [3] $\pi = 0.5\ \mu$, $\tau = 0.5\ \mu$ and $\mathrm{p} = 0.5\ \mu$ with the modifications described in another publication [4], the observations $\pi = 0.5\ \mu$ being used to effect elimination of noise. The estimates of mass were

$$\text{Scheme} \quad \tau = 0.5\ \mu, \quad 2\,950^{+530}_{-420}\ \mathrm{m_e},$$

$$\mathrm{p} = 0.5\ \mu, \quad 2\,580^{+530}_{-400}\ \mathrm{m_e}.$$

b) *Mean Gap-Length vs. Range.* – $\bar{G}$ was measured in various plates in the stack following the method described by one of us (5), for protons selected by δ-ray counts, and also for a number of identified π-mesons. For the same plates, values of b_0, the plateau blob-density, were estimated from counts on electrons originating from decays and suitable ρ–e events.

These values of b_0 were used to estimate the corresponding values of G_0, the mean gap-length corresponding to plateau. The results were checked by direct measurement of $\bar{G}_0$ in those plates through which the interacting particle passed. The values of the normalized parameter $\bar{G}^* = \bar{G}_0/\bar{G}$ found from the measured protons and π-mesons, were plotted as a function of residual range on log-log paper. They were fitted by a straight line in the region 0.1 cm $\leqslant$

(3) H. FAY, K. GOTTSTEIN and K. HAIN: *Suppl. Nuovo Cimento*, 11, 234 (1954).
(4) R. H. W. JOHNSTON and C. O'CEALLAIGH: *Phil. Mag.* (in the press).
(5) C. O'CEALLAIGH: *CERN* B.S. 11 (1954).

$\leqslant R_p \leqslant 10$ cm. A line parallel to this, fitted visually to the points $\overline{G}^*$ for the interacting particle, yielded the mass estimate

$$^{p}_{b}m_{Y} = 2\,400 \pm 250 \ \mathrm{m_e}.$$

c) δ-ray count. – The integrated number of δ-rays containing, according to the usual convention, 4 or more grains, observed as a function of residual range of the interacting particle, was compared with those calculated for a τ-meson and a deuteron. The expectation figures for the latter have been calculated from the work of DAINTON and FOWLER (6) and SÖRENSEN (7). They have been normalized to the published figures for protons given by the former workers.

TABLE I.

Range (μ)	Number of δ-rays ⩾4 grains			
	Deuteron	Interacting Particle	Proton	τ-meson
300	0	0	0.06	0.1
500	0	0	0.2	1.5
1 000	0.02	1	2.6	6.1
1 500	2.5	3	6.7	10.6
2 000	6.5	6	11.3	14.7

At first sight, it would appear from these figures that the interacting particle is very probably a deuteron. This identification cannot be maintained however on account of the insufficient kinetic energy at the point of interaction. Also, in the present stack of plates, Sardinia Flights S. 30, 1953, the value of plateau blob-density is very low, $b_0 \sim 14$ blobs/100 μ. Hence, the δ-ray density may be expected to be somewhat lower than that in the more normally developed plates calibrated by DAINTON and FOWLER (8). The results are such, however, as to show that it is unreasonable to suppose that the interacting particle is a τ-meson. Since the mean estimated mass is in satisfactory agreement with mass-values of the charged Y-particles which are consistent with various established modes of decay, we may conclude therefore that it is a hyperon.

(6) P. H. FOWLER and D. DAINTON: *Proc. Roy. Soc.*, A **221**, 414 (1954).

(7) S. O. SÖRENSEN: *Thesis*, Oslo (1951).

(8) M. BALDO, G. BELLIBONI, M. CECCARELLI, B. VITALE: *Supplemento al Nuovo Cimento* **12**, 289 (1954).

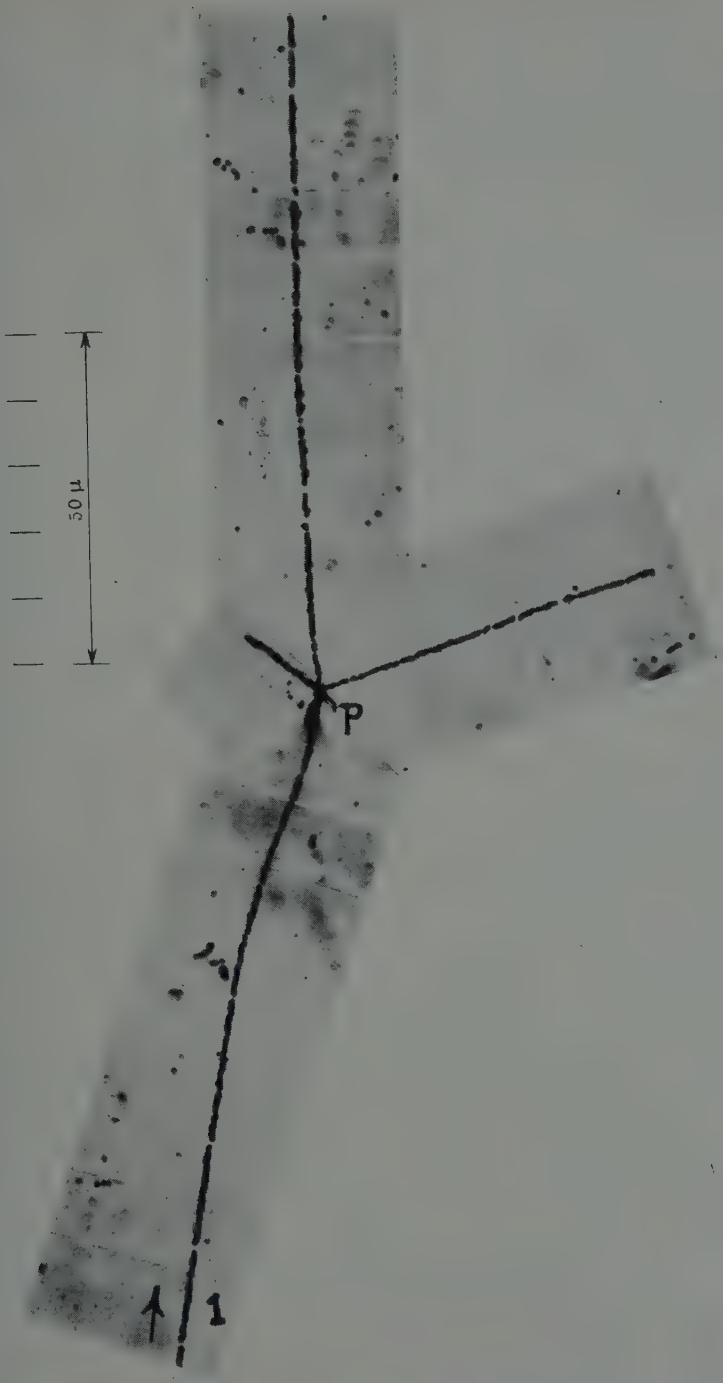

Fig. 1.

3. – Discussion.

To date, 5 examples ([1,2,8]) including the present, have been found which may be interpreted as the production of a small star following the coming to rest in the emulsion of a charged hyperon. Of these, four possess the characteristics of σ-stars as will be seen from Table II in which is summarized the available information.

TABLE II.

	PRIMARY				SECONDARY		
	Origin	Length mm	Mass estimate: Scattering vs range	Mass estimate: Ionization vs range	t=total range o=observed range	Energy (MeV)	Nature
Dublin ([2])	29+1p	7.35	2 170±500	2 300±250	2 000 (t) 4 (t)		proton? proton?
Bristol ([1])	31+3n	4.60	2 680±350	2 200±350	13 200 (o)	100	proton
Padua ([8])	27+2p	9.43	2 000±300		short (t) short (t) 17 000 (t)	 60	proton? proton? proton?
Dublin	23+1p	7.00	2 760±500	2 400±250	430 (t) 343 (t) 52 (t) 15 (t) 5 (t) 4 (t)		proton? proton? proton? proton? ? ?
Bristol	18+4p	0.096			14 (t) 14 900 (t)	 29	proton? π

The visible energy in all these interactions is of the order of 100 MeV and their appearance is that of a small evaporation star. The second Bristol interaction, a full discussion of which is given elsewhere in this issue ([9]) would suggest that the star formation may well be due to the decay of the hyperon within the nucleus. The energy involved in the nuclear disintegration may then be obtained from that released in the decay or perhaps from the nuclear capture of the product π-meson. A more detailed discussion of these points has been given by our Bristol colleagues ([9]).

([9]) M. W. FRIEDLANDER, D. KEEPE and M. G. K. MENON: *Nuovo Cimento*, 1, 482 (1955).

In a routine examination of the primary star in order to detect the production of a K-meson in addition to the interacting hyperon, the branches were traced through the stack. The 20 black tracks all ended uneventfully in the emulsion.

The three grey tracks were examined by blob-counting and scattering. The results for one of them, $g^* = 2.1 \pm 0.04$, $\bar{\alpha}_{100} = 0.07 \pm 0.012$, are consistent with identification as a proton, the probability that it was the track of a π-meson being very small. The other two grey tracks were of very poor geometry. g^* vs. $\bar{\alpha}_{100}$ measurements indicated that one was a π-meson and the other a proton. The track at plateau grain density was identified as being a π-meson, $g^* = 1.04 \pm 0.06$; $\bar{\alpha}_{100} = 0.17 \pm 0.03$.

Acknowledgements.

It is a pleasure to thank Mrs. MAÍRÍN JOHNSTON who found the event and Mr. W. HARBOR of H. H. Wills Physical Laboratory who made the photomicrograph. We also thank Professor C. B. A. MCCUSKER and Dr. M. G. K. MENON who read the manuscript and made helpful suggestions. One of us (R.H.W.J.) is indebted to the Board of the School of Cosmic Physics, Dublin Institute for Advanced Studies for a Scholarship.

RIASSUNTO (*)

Si descrive un ulteriore esempio dell'interazione a riposo di una particella di massa protonica. L'aspetto della interazione è quello di una tipica stella σ a sei rami. La particella originaria è emessa da una stella di tipo 23+1p e si arresta dopo un percorso di 7 mm. Le valutazioni della massa eseguite con due tecniche indipendenti si accordano fra di loro e sono compatibili con quella degli iperoni carichi riferita da altri ricercatori.

(*) *Traduzione a cura della Redazione.*

IL NUOVO CIMENTO Vol. I, N. 3 1° Marzo 1955

Su un metodo per determinare il percorso residuo degli iperoni.

G. Baroni, G. Cortini e A. Manfredini

Istituto di Fisica dell'Università - Roma
Istituto Nazionale di Fisica Nucleare - Sezione di Roma

(ricevuto il 24 Gennaio 1955)

Riassunto. — Si descrive un metodo per misurare il percorso residuo delle particelle che decadono in volo nelle emulsioni fotografiche.

1. – Principio del metodo.

I recenti studi sugli iperoni in lastre fotografiche hanno posto il problema di misurare il percorso residuo (o se si vuole l'energia) di queste particelle nell'istante del decadimento.

Se il percorso residuo X è piuttosto elevato (per esempio 5000 μ) la misura si riconduce agevolmente a misure di ionizzazione. Ma per $X \leqslant 3000\ \mu$ il procedimento diventa sempre più impreciso, perchè la granulazione della traccia va in saturazione. Addirittura, la granulazione difficilmente permette di stabilire se un iperone decada in quiete o con $X \sim 1000\ \mu$. Sorge così il problema di utilizzare le misure di scattering. Precisamente, abbiamo pensato di utilizzare le misure *che si eseguono normalmente sulle tracce a fine percorso, secondo il metodo della sagitta costante* (1).

Questo metodo si basa sulla formula, valida in prima approssimazione (cfr. (1) e più avanti):

$$\langle D_v \rangle = \langle \theta \rangle\, t = f(M, Z) R^{-0.58}\, t^{\frac{5}{8}}, \tag{1}$$

dove $\langle \theta \rangle$ è il valore medio probabile dell'angolo di scattering misurato (in assenza di *noise*) su una cella di lunghezza t, M e Z sono la massa e la carica della particella e R il suo percorso residuo nel punto in cui si fa la misura;

(1) C. C. Dilworth, S. J. Goldsack e L. Hirschberg: *Nuovo Cimento*, **11**, 113 (1954).

$\langle D_v \rangle$ è la corrispondente media delle differenze seconde, dalle quali gli angoli di scattering sono dedotti. Naturalmente, queste *medie* si devono intendere eseguite su una popolazione di tracce prodotte nelle identiche condizioni fisiche.

Ora, il metodo della sagitta costante consiste nel fissare uno « schema », in base al quale la misura i-esima viene esèguita ad un percorso residuo R_i con una cella $t_i = R_{i+1} - R_i$ tale che

$$R_i^{-0.58} t_i^{\frac{8}{3}} = \text{costante} = k .$$

Allora $\langle D_v \rangle$ dipende solo da Z ed M e per $Z = 1$ il suo valore $D_0 = kf(M)$ permette di risalire ad M.

Supponiamo ora che la particella decada in volo con un percorso residuo X, e che, ignorando questa circostanza il suo scattering venga misurato *con lo stesso schema* sopra definito. Il percorso residuo reale corrispondente alla cella i-esima sarà allora $R_i + X$, sicchè in luogo di $\langle D_v \rangle = D_0 = kf(M)$ avremo, come valor medio probabile di D_v:

$$\langle D_{vi}(X) \rangle = D_0 \left(\frac{R_i}{R_i + X} \right)^{0.58} .$$

Se poi le misure sono eseguite con un « noise » ε, il valor medio probabile della misura i-esima, sarà:

$$(2) \qquad D_i(X) = \sqrt{\langle D_{vi} \rangle^2 + \varepsilon^2} = \left[D_0^2 \left(\frac{R_i}{R_i + X} \right)^{1.16} + \varepsilon^2 \right]^{\frac{1}{2}} .$$

Nelle misure a fine percorso il *noise* ε risulta praticamente sempre lo stesso, sicchè possiamo supporre che ε sia una costante nota del sistema microscopio-lastra-osservatore. Allora nella (2) le sole incognite sono D_0 e X. D_0 dipende dalla massa: supposta nota la massa (o perchè il suo valore risulta da altre misure, o perchè si fa un'ipotesi sul tipo di particella in esame) rimane solo l'incognita X. Dato un certo sistema di differenze seconde $\Delta_1, \Delta_2, \ldots$ ottenuto da misure eseguite su una traccia, si tratta di trovare quel valore di X che mediante la (2) fornisce il sistema $D_1, D_2, \ldots$ al quale l'insieme di valori trovati meglio si adatta.

Per eseguire il confronto tra le Δ_i e le D_i abbiamo elaborato due metodi: uno, *di prima approssimazione* ha il pregio di non richiedere che pochi e semplicissimi calcoli, mentre l'altro, che va utilizzato come *metodo di seconda approssimazione*, richiede calcoli un po' più elaborati, ma ha il pregio di utilizzare pienamente l'informazione ricavata dalle misure e di permettere un calcolo corretto dell'errore statistico.

2. – Prima approssimazione.

Si costituiscono dei gruppi di misure

$$\Delta_{mn} = \frac{1}{n-m} \sum_{m+1}^{n} \Delta_i \tag{3}$$

e si confrontano con i corrispondenti valori teorici:

$$D_{mn}(X) = \frac{1}{n-m} \sum_{m+1}^{n} D_i(X) \,. \tag{4}$$

L'espressione (4) dipende da m, da n, da X e dalla massa attraverso D_0. Fissati m ed n e fatta una ipotesi sulla massa si può calcolare facilmente una curva che dà $D_{mn}(X)$ in funzione di X. Abbiamo eseguito questo calcolo raggruppando le misure nel modo seguente: da 1 a 5, da 6 a 10, da 11 a 20 e poi in gruppi di 20 fino alla centesima. Naturalmente, nella scelta dei gruppi c'è una larga arbitrarietà; non è il caso di insistere sui criteri, largamente qualitativi, che ci hanno guidato nella scelta. Per l'iperone di massa 2 300 abbiamo ottenuto le curve della fig. 1. Esse vanno confrontate con un sistema di dati

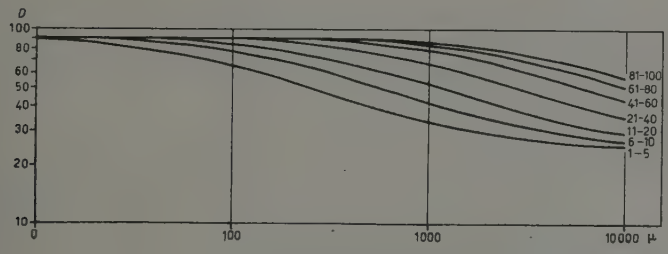

Fig. 1.

sperimentali Δ_{mn} e si deve aggiustare X in modo da ottenere la migliore concordanza. Per eseguire rapidamente il confronto, conviene tracciare assieme alle curve i limiti dell'errore probabile, che sono noti a priori poichè per ogni Δ_{mn} l'errore standard relativo vale $0{,}75/\sqrt{n-m}$. Per evitare la sovrapposizione delle curve abbiamo moltiplicato le ordinate di ogni curva per un certo fattore numerico, diverso da una curva all'altra.

Per esempio, i grafici di fig. 2 forniscono $\frac{1}{2} D_{1,5}$, $D_{6,10}$, $2D_{11,20}$, etc.. Per eseguire il confronto si moltiplicano i Δ_{mn} per gli stessi fattori ($\frac{1}{2}$, 1, 2, ...) e si riportano i valori trovati su una strisciolina di carta, usando le stesse ordinate

di fig. 2. Si trasla la strisciolina parallelamente all'asse X, e si trova la zona di miglior accordo e i suoi limiti.

A tale scopo si può tenere presente che la metà dei punti dovrebbe cadere entro un errore probabile dai rispettivi valori teorici e l'altra metà fuori. Con

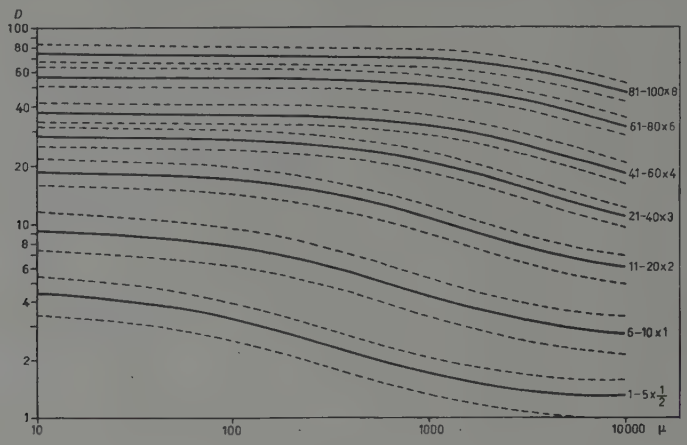

Fig. 2.

maggiore pretesa di precisione, si potrebbe calcolare il χ^2 per diversi valori di X e — fissati dei limiti di fiducia — determinare la corrispondente zona dei possibili valori di X. Ma questi metodi sono resi discutibili dal fatto che la distribuzione della media Δ_{mn} per valori così piccoli di $n - m$ non è ancora una distribuzione normale, anzi se ne scosta notevolmente (2).

3. – Seconda approssimazione.

Le ultime osservazioni mostrano che il metodo descritto può dare soltanto una stima abbastanza grossolana di X.

Tale stima, peraltro, è utile in quanto permette di determinare un valore X_0 di prima approssimazione. Posto

$$X = X_0 + x\,, \tag{5}$$

si può cercare di determinare la correzione x con un metodo più raffinato. Precisamente, abbiamo pensato di utilizzare il metodo dei minimi quadrati, applicandolo all'insieme di tutte le singole misure Δ_i. L'equazione dei minimi

(2) C. O'Ceallaigh e O. Rochat: *Phil. Mag.*, **7**, 1050 (1951).

quadrati è

$$\sum w_i[\Delta_i - D_i(X)]^2 = \text{minimo}\,, \tag{6}$$

in cui w_i rappresenta il peso da attribuire alla misura i-esima. Utilizzando la (5) e ponendo $D_i'(X_0) = (\mathrm{d}D_i/\mathrm{d}X)_{X=X_0}$ la (6) diventa

$$\sum w_i\,[\Delta_i - D_i(X_0) - D_i'(X_0)\cdot x]^2 = \text{minimo}$$

e fornisce, rinunziando a scrivere il comune valore, X_0, dell'argomento:

$$x = \frac{\sum w_i \Delta_i D_i' - \sum w_i D_i D_i'}{\sum w_i D_i'^2}\,. \tag{7}$$

Per trovare i pesi w_i, basta pensare che la distribuzione degli angoli di scattering (e delle differenze seconde) è sempre la stessa (e approssimativamente normale), pur di assumere come unità di misura degli angoli il valor quadratico medio, oppure la media del modulo, che ad esso è proporzionale. Ora $D_i(X)$ è appunto il valore teorico della media del modulo della i-esima differenza seconda. Perciò si deve prendere:

$$w_i = [D_i(X)]^{-2} \sim [D_i(X_0)]^{-2} = D_i^{-2}\,.$$

Con ciò otteniamo la formula risolutiva

$$x = \frac{\sum \Delta_i D_i' D_i^{-2} - \sum D_i' D_i^{-1}}{\sum (D_i' D_i^{-1})^2}\,. \tag{8}$$

I termini delle somme che vi compaiono si calcolano agevolmente, per D_0 e X_0 fissati, utilizzando la (2).

La (8) appare assai complicata e può sembrare che il suo impiego riesca troppo macchinoso. In realtà essa richiede un lavoro notevole ma non eccessivo, in relazione a quello che occorre per misurare lo scattering a fine percorso. Data la particolare importanza che nel momento attuale presentano le tracce iperoniche, sembra che valga la pena di eseguire questa elaborazione, anche — e forse particolarmente — per gli eventi in cui non c'è alcun indizio collaterale che faccia sospettare un decadimento che non sia a fine percorso.

Nell'applicare la (8) conviene scartare le misure per le quali $\Delta_i > 4D_i(X_0)$. In tal modo si rispetta la solita regola di scarto, in base alla quale è calcolata la costante di scattering su cui si fonda la (1). Inoltre occorre applicare ai dati sperimentali delle correzioni (di qualche unità %) per le approssimazioni implicite nella (1), e cioè: *a*) che sia $p = 2E$; *b*) che la costante di scattering sia indipendente da t e da R (cfr. Appendice).

La formula generalmente adottata per calcolare l'errore standard relativo da cui è affetta la misura dell'angolo *medio* di scattering è $0{,}75n^{-\frac{1}{2}}$, dove n è il numero delle misure. Ogni valore Δ_i può essere considerato come una misura di D_i affetta da un errore standard $0{,}75D_i(X) \sim 0{,}75D_i(X_0)$. Con ciò l'errore standard $\sigma(x)$ da cui è affetta la misura di x si ricava dalla (8) mediante la legge di propagazione degli errori:

$$\sigma(x) = 0{,}75 \left[\sum \left(\frac{D_i'}{D_i}\right)^2\right]^{-\frac{1}{2}}. \tag{9}$$

Notiamo che il metodo qui presentato potrebbe essere applicato — in linea di principio — anche alla tecnica delle camere di Wilson ad alta pressione, per misurare il percorso residuo di tracce che siano prossime alla fine del loro percorso. La possibilità pratica di tale applicazione è naturalmente condizionata in quel caso dal numero di celle disponibili.

4. – Controllo sperimentale del metodo e sua applicazione.

Per controllare l'efficienza del metodo abbiamo anzitutto eseguito una serie di misure su un gruppo di protoni aventi un percorso residuo X_v (« vero » cioè misurato direttamente col micrometro oculare) di 1 000 μ. Il calcolo è stato eseguito partendo da diversi valori di X_0 (500, 1 000 e 2 000 μ), scelti in modo da rientrare abbastanza largamente nell'ambito dei risultati ottenuti applicando il metodo di prima approssimazione.

I risultati, per 8 protoni sono raccolti nelle colonne 2, 3 e 4 della tabella I. Le medie (i cui errori sono dedotti dalla dispersione) sono in accordo con il valore « vero » $X_v = 1\,000$ μ. Anche le misure sui singoli protoni risultano soddisfacenti, se si parte da $X_0 = 1000$. Se si parte da diversi valori di X_0 (per poi scegliere, ad esempio, quello che dà il minimo valore di x/X) si trova anche un accordo soddisfacente, salvo forse per il protone n. 8.

La dispersione delle misure conferma la valutazione dell'errore su x, come risulta dalle ultime tre righe della tabella I: σ è l'errore standard (da cui è affetta una singola misura) dedotto dalla (9), σ' quello dedotto dalla dispersione rispetto al valore « vero » di X, σ'' quello dedotto dalla dispersione rispetto al valore medio.

Le altre colonne (dalla 5ª in poi) della tabella I dànno i risultati di misure eseguite per vedere qual'è il minimo percorso residuo che il metodo permette d'apprezzare. L'insieme dei risultati mostra che anche in questo caso la (9) permette di valutare gli errori correttamente, e che in nessun caso delle tracce a fine percorso sarebbero state considerate in volo. In due casi su quattro le tracce per le quali è $X_v = 200$ μ dànno una sicura indicazione di non essere

TABELLA I. *Valori di $X = X_0 + x$, in micron, ottenuti dalle misure di taratura eseguite su protoni. X_v = valore «vero» di X (misurato direttamente con il micrometro oculare).*

X_v	1 000			0		200			
Protone \ X_0	500	1 000	2 000	0	100	0	100	200	500
1	748	896	824	—16	— 87	+ 25	+ 65	+ 12	—337
2	936	1 114	1 183	0	— 29	+108	+225	+281	+229
3	1 029	1 283	1 414	—39	—150	+ 71	+138	+319	+320
4	863	1 088	1 444	+51	+ 59	+ 66	+107	+ 72	—121
5	920	1 271	1 306	—	—	—	—	—	—
6	1 100	1 602	1 960	—	—	—	—	—	—
7	913	1 214	1 438	—	—	—	—	—	—
8	404	760	431	—	—	—	—	—	—
9	—	—	—	+20	+ 6	—	—	—	—
Medie	864	1 154	1 250	+ 3	— 40	+ 68	+134	+171	+ 23
	±85	±138	±233	±22	± 43	± 25	± 49	± 70	±123
σ	240	385	660	49	97	49	97	140	240
σ'	241	286	495	31	84	136	89	135	318
σ''	199	240	437	29	73	30	56	132	266

a fine percorso, mentre per le altre due il risultato è molto dubbio. In questi casi si potrebbe pensare di rimisurare la traccia per sfruttare il breve percorso che nello schema usato non viene utilizzato (i primi 48 μ); ma l'aumento di precisione è trascurabile, e non compensa il lavoro necessario.

In complesso, possiamo dunque dire che i controlli eseguiti confermano la validità del metodo qui presentato, e ne giustificano l'applicazione.

La tabella II raccoglie i risultati delle misure eseguite su 4 tracce iperoniche

TABELLA II. – *Valori di X, in micron, ottenuti da misure eseguite su tracce incognite.*

Particella \ X_0	0	500	1 000	2 000
Y-Ro_2	—	829 ± 252	969 ± 412	929 ± 707
Y-Ro_3	+ 2 ± 50	—	—	—
Y-Ro_4	— 9 ± 50	—	—	—
Y-Ro_9	—43 ± 50	—	—	—
T	—	—	—	2 900 ± 840

(Ro_2 [3]), Ro_3, Ro_4 e Ro_9 [4]) e su una traccia che in un primo tempo era stata interpretata come dovuta ad un iperone negativo (producente stella) a fine percorso.

I risultati relativi all' YRo_2 non lasciano dubbi sul fatto che si tratta di un decadimento in volo, e sul valore approssimativo del percorso residuo.

Quelli relativi agli altri 3 iperoni indicano che con grande probabilità i decadimenti sono avvenuti a fine percorso. Infatti ai loro percorsi residui può essere assegnato un limite largamente superiore di $\sim 105\ \mu$, al quale corrisponde un tempo di rallentamento di solo $0{,}80 \cdot 10^{-11}$ s. Pertanto la probabilità di un decadimento in volo è piccolissima.

Infine, nel caso della traccia T, per la quale il valore di $\langle\theta\rangle$ era compatibile con un tritone, la misura di X era importante per decidere se doveva trattarsi di un tritone « radioattivo » (alla Danysz [5]) o se, viceversa, l'energia cinetica disponibile era compatibile con una normale interazione in volo. Il valore di X indicato nella tabella ha permesso di scegliere la seconda alternativa. Tale conclusione è stata confermata da una misura indipendente, in cui si era adattato direttamente lo schema di misura all'ipotesi che mancassero $2\,500\ \mu$ alla fine percorso. In tal modo è stato ottenuto il valore $X = 2\,520 \pm 890$.

Siamo lieti di esprimere la nostra riconoscenza al Prof. E. Amaldi, per le sue utili critiche e alla Sig.na M. G. Cattaneo per l'esecuzione dei calcoli numerici.

Appendice

Correzioni da apportare alle misure.

L'imperfezione della relazione percorso-energia adottata [1] dà una correzione trascurabile (1%). Restano perciò:

a) *correzione alla relazione* $p\beta \sim 2E$. Se $\gamma = E/2Mc^2$, si trova, fino al secondo ordine in γ, $p\beta = 2E(1-\gamma)$. La correzione si calcola facilmente, per dati X, M ed i (cioè per un dato R_i). Per protoni e iperoni risulta $\gamma < \sim 3\%$;

b) *correzione per la variazione della « costante » di scattering.* Con approssimazioni ragionevoli, questa correzione può essere calcolata prendendo un valore costante di β, cosicchè viene a dipendere *solo* da t, cioè da i. La co-

[3] C. Castagnoli, G. Cortini e C. Franzinetti: *Suppl. Nuovo Cimento*, **12**, 297 (1954).

[4] In preparazione.

[5] M. Danysz e J. Pniewski: *Phil. Mag.*, **44**, 348 (1953).

stante « vera » k può essere uguagliata al valore k_0 assunto da DILWORTH *et al.*, moltiplicato per un fattore $1+\gamma'$, con $\gamma' < 10\%$.

TABELLA III.

Misure da	1	6	11	16	21	41	61	81
Misure a	5	10	15	20	40	60	80	100
$100\,\gamma'$	$-1{,}0$	$+1{,}0$	$+2{,}5$	$+3{,}5$	$+5{,}0$	$+7{,}0$	$+8{,}0$	$+9{,}0$

Per eseguire la correzione conviene procedere così. La prima delle due somme che si trovano al numeratore della (8) viene divisa in somme parziali, comprendenti termini per i quali $\gamma+\gamma'$ non varia apprezzabilmente. Calcolati i corrispondenti valori medi di $\gamma+\gamma'$, ognuna delle dette somme parziali viene moltiplicata per il rispettivo valore di $1-(\gamma+\gamma')$.

La tabella III indica i valori di γ' corrispondenti a gruppi di misure scelti secondo il criterio sopra indicato.

SUMMARY

A method is described for the measurement of the residual range of particles decaying in flight in nuclear emulsions. The scattering is measured following the conventional constant-sagitta scheme and from a suitable least squares treatment of the experimental data the residual range value (eq. (8)) and its standard error (eq. (9)) are obtained.

Hyperon Events in Photographic Emulsions.

M. W. Friedlander, D. Keefe (*) and M. G. K. Menon

H. H. Wills Physical Laboratory, University of Bristol

(ricevuto il 25 Gennaio 1955)

Summary. — Details are given of six hyperon events observed in photographic emulsions. Two of these decay at rest into protons and give Q-values of 115.8 ± 1.0 MeV and 113.5 ± 1.7 MeV for the assumed decay scheme: $Y^+ \to p + \pi^0 + Q$. Three others decay in flight; two give Q-values 115 ± 7 MeV and 103 ± 10.5 MeV for the decay mode: $Y^\pm \to n + \pi^\pm + Q$; the third is in agreement with the cascade type of decay: $Y^- \to \Lambda^0 + \pi^- + Q$ and has a $Q = 59 \pm 11$ MeV. The sixth event has been interpreted as the interaction at rest of a negative hyperon; from the parent star of this hyperon there also emerges a K-meson.

1. – Introduction.

This note describes measurements carried out on six hyperon events observed in this laboratory. The events were found in the following stacks of plates:

$Y\text{-}Br_3$: Flight HA.54: 46 emulsions, each $15 \times 15 \times 0.06$ cm^3.

$Y\text{-}Br_7$: Flight S.35: 40 emulsions, each $15 \times 10 \times 0.06$ cm^3.

$Y\text{-}Br_8$, $Y\text{-}Br_9$, $Y\text{-}Br_{11}$, $Y\text{-}Br_{12}$: Flight A, 80 emulsions, each $20 \times 15 \times 0.06$ cm^3.

Event $Y\text{-}Br_3$ was found in an experiment involving the following out of tracks from stars; all the other events were discovered in the course of systematic scanning.

Two of these, $Y\text{-}Br_7$ and $Y\text{-}Br_{11}$ which are described in § 2 are interpreted as the decay at rest of a charged hyperon into a proton, viz. $Y^+ \to p + ? + Q$. If the neutral particle is a π^0-meson the respective values for Q are 115.8 ± 1.0 MeV

(*) On leave of absence from University College, Dublin.

and 113.5 ± 1.7 MeV. In § **3** are described three examples of the decay in flight of a hyperon into a light meson. Two of these are consistent with the decay scheme: $Y^{\pm} \rightarrow n + \pi^{\pm} + Q$ (~ 110 MeV) the third, (Y-Br_3), gives a measured energy release of 60 ± 11 MeV for this decay scheme, a value significantly lower than 110 MeV. It can be best interpreted in terms of the « cascade decay » process: $Y^{-} \rightarrow \pi^{-} + \Lambda^0 + Q$ (~ 60 MeV); in this case the Q-value is 59 ± 11 MeV. Event Y-Br_{12} described in § **4** appears to be an example of the interaction at rest of a negative hyperon. From the parent star of this hyperon there is also ejected a K-meson which is arrested in the stack and which decays with the emission of a single charged secondary particle.

2. – Decay at Rest: Hyperon → Proton.

Details of the events are given in Table I.

2·1. *The Parent Stars of the Hyperons.* – The hyperon Y-Br_7 was found to originate in the central region of an emulsion strip; there were no associated charged particles other than a slow electron at the point of origin. One other example of a hyperon originating in a nuclear disintegration of type 1+0n, i.e. with the hyperon as the only ejected charged particle, has been observed by the Rome group (Padua Conference Report, 1954); in this case, the hyperon came to rest and decayed into a L-meson. All the tracks emerging from the parent star of Y-Br_{11} with the exception of two steep shower particles were followed; no evidence was found for the presence of any other heavy unstable particle.

2·2. *The Decays.* – The secondary particles in both cases are of protonic mass and have therefore been assumed to be protons. From Table I, it may be seen that the proton ranges in the two events are fairly similar. Until now, there have been nine examples reported in which the ranges of proton secondaries are very nearly equal. This is very strong evidence for a two-body decay of the type:

$$Y^{+} \rightarrow p + [(\pi^0)?] + Q_1 . \tag{1}$$

The nature of the natural particle in scheme (1) is as yet unknown, but it has been generally assumed that it is a π^0-meson and that in fact there exists a hyperon of unique mass which can decay in either of the modes (1) or (2):

$$Y^{+} \rightarrow (n?) + \pi^{+} + Q_2 . \tag{2}$$

This receives strong support from the close agreement in the values of p^*, the momentum in the centre of mass system of the decaying hyperon, for

TABLE I.

Event	PRIMARY PARTICLE				
	Parent Star	Range	Number of emulsions containing track of the primary particle	Time of Flight	Mass: ioniza vs. Rang
Y-Br_7	1 + 0n	3598 μ	4	$7.2 \cdot 10^{-11}$ s	2100 $\pm$ 300
Y-Br_{11}	15 + 3n	2006 μ	2	$4.8 \cdot 10^{-11}$ s	$\sim$ 2000

proton and charged L-meson secondaries. The assumption that the neutral particle in (2) is a neutron would appear to be a reasonable one and enables a close analogy to be drawn between the symmetrical decay modes (1), (2), and that of the neutral hyperon Λ^0. For the moment, we are not considering the other known type of hyperon decay, i.e. the « cascade decay »: $Y^- \rightarrow \Lambda^0 + \pi^- + Q$ (~ 60 MeV).

It is clear that the best estimate of the mass of the hyperon Y^+, which decays in either of the modes (1) or (2) is provided, at the present, by a precise determination of the energy of the proton in scheme (1). This in turn, determines Q_2 of scheme (2) exactly, which is of importance in distinguishing between the various types of hyperons which decay into L-mesons. For this reason, particular care has been taken in the measurement of the ranges of the proton secondaries in the two examples.

Event Y-Br_7 occurred in Stack S.35 in which extensive calibrations of emulsion thicknesses and normalization of the range-energy relation had been carried out previously [1] and so it is possible to define the proton energy within narrow limits; the major contribution to the error in this case, is that due to range straggling. In Y-Br_{11} . which occurred in the less well calibrated stack *A*, the secondary proton had an average dip of only $\sim 5°$ and so its measured range is insensitive to uncertainties in the thicknesses of the emulsions. The range-energy relation employed in this case is the same as that used for S.35 since the conditions of preparation and exposure of the two stacks were very similar. However, in order to take account of any possible systematic error arising as a result of this, wider limits of uncertainty have been assigned to the energy of the proton. In both examples, corrections have been made for effects due to distortion and for traversal of the tissue separating the emulsion strips.

The final Q-values obtained for events Y-Br_7 and Y-Br_{11} are 115.8 $\pm$ 1.0 and

	Secondary particle		
ange	Number of emulsions containing the track of the secondary particle	Energy at Emission	Energy Release, Q, for decay scheme $Y^+ \to p + \pi^0 + Q$ (*)
375 μ	3	$18.77 \pm 0{,}19$ MeV	115.8 ± 1.0 MeV
602 μ	2	18.32 ± 0.32 MeV	113.5 ± 1.7 MeV

(*) $m_p = 938.2$ MeV; $m_{\pi^0} = 134.75$ MeV.

113.5 ± 1.7 MeV respectively. From this the values of the energy release Q_2 for the symmetrical mode of decay (2) is 109 ± 1 MeV.

As has been stated before, the neutral particle involved in decay scheme (1) is as yet unknown. It is, however, possible to determine whether it is a photon or a π^0-meson since the single pair resulting from the former will lie along a line directly opposite the trajectory of the proton, whereas the π^0-meson will decay into two photons in a time of $\sim 10^{-15}$ s and at least one of these photons will convert to give an electron pair which lies within a cone of semivertical angle 36°. For Y-Br_7 the emulsion defined by this cone was scanned for electron pairs up to a distance of 5 mm from the point of decay, but no correctly aligned example was observed. The probability for the conversion of a photon within this distance is $\sim 12\,\%$. A similar scan is being undertaken in the case of Y-Br_{11},

3. – Decays in Flight: Hyperon → Light Meson.

Details of the events are given in Tables II *a*, *b* below.

3·1. *The Parent Stars.* – With the exception of those due to the shower particles, all the tracks from the parent stars of these hyperons were followed. No evidence was found, for the presence of associated heavy unstable particles.

3·2. *The Decays.* – In the deduction of the energies of the secondary particles and for the Q-value calculations it has been assumed that the secondary particles are π-mesons ($m_\pi = 273$ m_e). From observations, on the change in

(1) M. W. Friedlander, D. Keefe, M. G. K. Menon and M. Merlin: *Phil. Mag.*, **45**, 533 (1954).

grain density along the track in event Y-Br_8, and from grain density vs multiple scattering measurements, in event Y-Br_9, it is possible to show that the decay particles in both these events are L-mesons. Direct identification of the secondary particle from Y-Br_3 was not possible since its geometry precluded reliable multiple scattering measurements; the most likely assumption is that it is an L-meson, unless one presumes that the hyperon has a mass greatly exceeding the measured value, (2200 ± 250 m_e).

TABLE II*a*. – *The Primary Particles.*

Event	Parent Star	Length in mm	Number of emulsions containing the track	Mass in m_e	Velocity at decay (β)	Time of flight (*)
Y-Br_3	12+7p	14.6	1	2200 ± 250 ionization vs scattering	0.61 $\pm$ 0.02	$t_1 = 0.54 \cdot 10^{-10}$ s $T_1 = 1.24 \cdot 10^{-10}$ s
Y-Br_8	25+2p	13.86	1	250^{+440}_{-320} change of ionization along the track	0.11 $\pm$ 0.05	$t_2 = 1.80 \cdot 10^{-10}$ s $T_2 = 1.90 \cdot 10^{-10}$ s
Y-Br_9	13+0p	8.79	9	$\gtrsim$ proton change of ionization along the track	0.245 $\pm$0.005	$t_2 = 0.02 \cdot 10^{-10}$ s $T_2 = 0.86 \cdot 10^{-10}$ s

(*) t_1 = Time of flight from creation to decay, less time required for identification (2.0 mm of track).
T_1 = Potential time of observation between creation and exit from stack had no decay occurred, again less time for identification.
t_2 = Time between entry into scanned volume and decay.
T_2 = Potential time between entry into, and arrest within scanned volume.

With the stacks of emulsion at present in use, the great majority of light secondaries from hyperon decays escape, and since no observations on their behaviour at the end of their range are possible, it cannot be decided whether they are π- or μ-mesons. Up to the present there has been only one example reported in which the L-meson has been arrested in an emulsion stack [2]; in this case, the L-meson produced a σ-star at the end of its range and has therefore been identified as a π-meson. Since it is of interest to test whether

[2] A. DEBENEDETTI, C. M. GARELLI, L. TALLONE and M. VIGONE: *Nuovo Cimento*, **12**, 952 (1954).

the secondaries may be interpreted exclusively in terms of π-mesons, it is important to relate the number of interactions produced by such secondaries to the total observed track length. On the track of the secondary of Y-Br_8 there occurs a sharp single deviation of 10°, apparently elastic, at a point corresponding to a π-meson energy of 50 MeV. At these energies, however, a deviation of such a small magnitude could easily arise as a result of Rutherford scattering and cannot be taken as evidence of nuclear interaction.

TABLE II*b*. – *The Secondary Particles.*

Event	Observed length in mm	Number of emulsions containing track	Energy in the laboratory system at emission	Angle between primary and secondary directions	*Q*-value for decay process
Y-Br_3	8.4	10	99 ± 14 MeV from ionization	42.4 ± 2°	$Y \to n + \pi$ 60 ± 11 MeV $Y \to \Lambda^0 + \pi$ 59 ± 11 MeV
Y-Br_8	62.9	70	87.4 ± 3.5 MeV from ionization	112 ± 1°	$Y \to n + \pi$ 115 ± 7 MeV
Y-Br_9	22.9	9	107.9 ± 10 MeV from scattering	54,7 ± 2°	$Y \to n + \pi$ 103 ± 10.5 MeV

The energy at emission of the secondary particle of Y-Br_3 was determined from an ionization estimate based on the frequency of occurrence of gaps of different sizes along the track ([3,4]). Similar measurements were made in several successive emulsions for which comprehensive calibrations had already been carried out and the individual values of ionization obtained in each plate were in complete accord with one another. The velocity of the primary particle was derived by the same method.

The secondary particle of Y-Br_8 traversed 6.29 cm of emulsion before escaping from the stack; grain density measurements on the last 7 mm of its track indicated that it had an energy of 36.9 ± 3,5 MeV at the point of exit from the emulsion and thus the energy of the decay particle is obtained quite precisely. It is difficult to estimate accurately the velocity of the primary hyperon at the point of decay for, though the hyperon was certainly not at rest when it decayed, its ionization was such that, in the stack con-

([3]) C. O'CEALLAIGH: *C.E.R.N.* BS.11 (1954).
([4]) P. H. FOWLER and D. H. PERKINS: *Phil. Mag.* (1955) (in course of publication).

cerned, the grain density in the track provided a very poor measure of velocity. Instead, ionization measurements based on the gap count method mentioned previously were made on the earlier parts of the track and the information was used, by an extrapolation procedure, to provide the best value for the velocity of the hyperon at the point of decay.

The estimation of the energy of the decay particle from Y-Br_9 relies on multiple scattering measurements; the track was sufficiently flat to allow the effect of distortion to be neglected.

Events Y-Br_8 and Y-Br_9 yield Q-values 115 ± 7 MeV and 103 ± 0.5 MeV respectively for the decay mode (2):

$$Y^{\pm} \rightarrow n + \pi^{\pm} + Q_2 \quad \text{(see page 483)}$$

and are consistent with a two body decay scheme with $Q_2 = 109 \pm 1$ MeV.

In the case of Y-Br_3 the observed energy release appears irreconciliable with decay mode (2) with $Q_2 = 109$ MeV. The secondary particle in this event has an energy in the laboratory system of $T_L = 99.0$ MeV and an ionization at emission $g^* = 1.11 \pm 0.03$. In order that this should be consistent with a decay of type (2) with $Q_2 = 109$ MeV these values should have been $T_L \approx 180$ MeV and $g^* \approx 0.98$.

On the other hand there is known to exist yet another hyperon [5] which is generally assumed to decay in the manner [6]

$$Y^- \rightarrow \Lambda^0 + \pi^- + Q \,. \tag{3}$$

The most precise published Q-value to date is the figure 67 ± 12 MeV reported by COWAN. Assuming decay mode (3) the Q-values for Y-Br_3 is 59 ± 11 MeV. The available 1.8 cm within the stack along the predicted line of flight of the Λ^0-particle was examined for evidence of its transformation but none was found.

4. – Associated Production.

Event Y-Br_{12} consists of a star of type 18+4p from which emerge two heavy unstable particles. One of these is a K-meson which is arrested in the stack after travelling 3.5 cm and decays with the emission of a single charged

---

[5] R. ARMENTEROS, K. H. BARKER, C. C. BUTLER and A. CACHON: *Phil. Mag.*, **42**, 1113 (1951).

[6] R. B. LEIGHTON: *Bagnères Conference Report* (1953), p. 97; E. W. COWAN: *Phys. Rev.*, **94**, 161 (1954); W. B. FRETTER: unpublished; L. LEPRINCE-RINGUET: *Varenna Summer School* (1954).

secondary particle. The mass of the K-meson from ionization vs range measurements is 950 ± 80 m_e. No useful measurements could be made on the track of the secondary particle in view of its steepness; it had a value of ionization close to that at plateau.

The other unstable particle, whose direction of emergence made an angle of 108.4° with that of the K-particle, appears to come to rest after a distance of 96 μ. At the end of this track, which seems to be due to a singly charged particle, there is a small star consisting of two prongs: one due to a negative π-meson which comes to rest after 14.90 mm and produces a one-prong star and the other, 14.4 μ long, whose nature is impossible to determine. The angle between the two prongs is 162.5°.

One may seek to interpret the event in one of the three ways: *a*) the nuclear capture of a negative K-meson, *b*) the nuclear capture of a negative hyperon or *c*) the delayed disintegration of a heavy unstable fragment containing a bound Λ^0-particle.

Hypothesis *c*) may be at once ruled out for the following reasons. The evidence of the interconnecting track shows that it is almost certainly due to a particle with $Z = 1$: the possibility of $Z = 2$ cannot be completely disregarded, but the case of $Z = 3$ or higher can be excluded with confidence. One can easily verify from the requirements of conservation of energy, momentum and charge that the disintegration of any nucleus with $Z = 1$ or 2, containing a bound Λ^0, cannot give rise to a configuration of tracks such as that observed.

It is impossible to distinguish between hypothesis *a*) and *b*) by direct observations on the shorth length of track available. In the present case, a comparison has been made with the final 96 μ, of track of protons and of a K-particle stopping in the same emulsion. On the latter, the scattering is more pronounced and the mean number of observable gaps twice as large. From appearance therefore, one would prefer to interpret the track as being that of a hyperon.

There are many examples established of the associated production of a K-meson with a hyperon, whereas the double production of K-mesons has never been proven, though it may perhaps exist. In view of these considerations, for the purpose of this discussion we shall assume that event $Y\text{-}Br_{12}$ is an example of the nuclear absorption of a negative hyperon. A strikingly similar event has been reported previously (7) in which, from a star of type 14+2n, there emerges a particle which is arrested in the emulsion after a range of 308 μ. It had a measured mass of 1000^{+720}_{-400} m_e and at the end of its range produced a three prong star; one of the prongs was due to a π-meson with an energy of 28.1 ± 0.8 MeV.

(7) D. Lal, Yash Pal and B. Peters: *Proc. Ind. Acad., Sc.*, **38**, 398 (1953).

A point of interest in the case of event Y-Br_{12} is the very low energy of emission (~ 4 MeV) of the hyperon. In the diagram which appears in a previous paper ([8]) from this laboratory, is plotted the relation between the energies of emission of a hyperon and K-meson for various values of the included angle, if they are produced in association in a pure π-meson/nucleon collision, i.e. according to the Brookhaven reaction

$$\pi + N \rightarrow Y + K . \tag{4}$$

From an examination of this diagram it is seen that the production of a very low energy hyperon is kinematically forbidden in such a process even for the most favourable choice of the Fermi momentum of the target nucleon in a nucleus. In other words, if the K-meson and hyperon in event Y-Br_{12} were indeed produced in a single act and the hyperon escaped without secondary interaction then the model of a π-meson/nucleon collision is an invalid one. Exactly similar arguments may be adduced in the events Y-Br_7 and Y-Br_{11} if one attempts to explain them in terms of reaction (4) in which the K-meson emerges with neutral charge and so escapes detection. In both these cases the parent disintegrations are produced by neutral primaries, but the reaction (4) might still be expected to occur among the secondary interactions of the created π-mesons within the nucleus. We conclude therefore from these and other similar results, that there appear to be a rather large number of slow hyperons, if they are all to be explained by production in terms of reaction (4), followed by inelastic collisions before escape from the parent nucleus.

Acknowledgements.

We are deeply grateful to Professor C. F. Powell, F.R.S., for the hospitality and facilities of his laboratory. Certain of us wish to thank the following bodies: The National University of Ireland for the award of a Travelling Studentship, and University College, Dublin, for leave of absence and additional financial assistance, (D.K.); The Royal Commission for the Exhibition of 1851, for the award of a Senior Scholarship (M.G.K.M.).

We would also like to thank Dr. D. H. Perkins, who observed event Y-Br_3, for the measurements he made on the event and for useful discussions. The other events were found by Mrs. Anne Boult, (Y-Br_9, Y-Br_{11}), Mrs. D. Keefe (Y-Br_7), Miss Ann Stradling (Y-Br_8) and Miss Marlene Wood (Y-Br_{12}), to whom we are indebted.

([8]) C. Dahanayake, P. E. Francois, Y. Fujimoto, P. Iredale, C. J. Waddington and M. Yasin: *Phil. Mag.*, **45**, 855 (1954).

Appendix

It is becoming of increasing importance to establish experimental points on the range-energy curve in emulsion at considerably higher energies than hitherto investigated; with the exception of a single range measurement for 342.5 MeV protons, previous experimental points have been confined to proton energies less than 40 MeV. If the assumption that there exists a positive hyperon which decays alternatively into a proton and a neutral π-meson (reaction 1) or into a neutron and a positive π-meson (reaction 2), is found to be correct then it is possible to utilise these experimental range-energy measurements for protons of energy < 40 MeV to provide further range-energy points at π-meson energies ~ 100 MeV, corresponding to proton energies ~ 700 MeV. For, by careful measurements of the range of the protons arising in $Y^{\pm}$decay one can determine Q_1 very precisely. Then from (1) and (2) it is clear that

$$Q_2 = Q_1 - (m_{\pi^+} - m_{\pi^0}) - (m_n - m_p) = (Q_1 - 6.3) \text{ MeV}.$$

Knowing now an accurate value for Q_2 one can predict the energy of the π^+-meson arising in decay mode (2), whether in flight or at rest — and if the emulsion volume is large enough to allow the π-mesons to be arrested, corresponding range measurements can be obtained in each case.

RIASSUNTO (*)

Si descrivono in dettaglio sei iperoni osservati in emulsioni fotografiche. Due di di essi decadono a riposo in protoni e danno per Q valori di $115{,}8 \pm 1{,}0$ MeV e $113{,}5 \pm 1{,}7$ MeV per il presunto schema di decadimento $Y^+ \to p + \pi^0 + Q$. Tre altri decadono in volo; due danno per Q valori di 115 ± 7 MeV e $103 \pm 10{,}5$ MeV per lo schema di decadimento $Y^{\pm} \to n + \pi^{\pm} + Q$; il terzo si accorda col tipo di decadimento in cascata: $Y^- \to \Lambda^0 + \pi^- + Q$ e ha un $Q = 59 \pm 11$ MeV. Il sesto evento è stato interpretato come l'interazione a riposo di un iperone negativo; dalla stella da cui origina questo iperone emerge anche un mesone K.

(*) *Traduzione a cura della Redazione.*

Unusual Event Produced by Cosmic Rays.

E. Amaldi, C. Castagnoli, G. Cortini, C. Franzinetti and A. Manfredini

Istituto di Fisica dell'Università - Roma
Istituto Nazionale di Fisica Nucleare - Sezione di Roma

(ricevuto il 18 Febbraio 1955)

Summary. — The authors describe an event consisting of two stars respectively of about 5 and 1-2 GeV energy. The probable value of the number of accidental space coincidences that one expects to observe in the scanned volume, is about $4 \cdot 10^{-4}$. This value, although it does not allow us to exclude an accidental process, justifies the consideration of interpretations in terms of some physical process. Special attention is devoted to the production, capture and annihilation of a negative proton.

1. – Description of the Event.

In the course of an investigation on the capture and decay processes of heavy unstable particles, produced by cosmic rays in stripped emulsions, exposed at high altitude during the Sardinian Expedition 1953 [1], we have observed a peculiar event, a microphotograph of which is given in Fig. 1.

The event consists of two stars A and B connected by a black track p, 89 μ long.

Star A shows 20 black and 3 grey tracks in addition to 3 shower particles. Its energy, evaluated by the usual methods [2,3], is of the order of 5 GeV.

The track connecting the two stars undergoes a deflection of 91° at a

---

[1] *Suppl. Nuovo Cimento*, **12**, 480 (1954), *Rendiconti del Congresso Internazionale di Padova*.

[2] U. Camerini, J. H. Davies, P. H. Fowler, C. Franzinetti, W. O. Lock, H. Muirhead, D. H. Perkins and G. Yekutieli: *Phil. Mag.*, **42**, 124 (1951).

[3] R. H. Brown, U. Camerini, P. H. Fowler, H. Heitler, D. T. King and C. F. Powell: *Phil. Mag.*, **40**, 862 (1949).

distance of 5 μ from the center of star B. It does not show any gap nor δ-rays. The mean angle of scattering, measured with a constant cell (10 μ), is $\bar{\alpha}_{100} = 3°.1 \pm 1.3$.

All these observations make the interpretation of this track in terms of a high energy fragment (1-2 GeV, $Z > 1$, $m > m_p$) very improbable. Such a conclusion is definitely confirmed by the fact that the deflection of a fast fragment through an angle of 90° should be associated with a rather long recoil track, even in the case of a target nucleus as heavy as silver. No recoil is observed in the present case.

One may conclude that this track is due to a low energy particle. If its charge is 1, as it seems very reasonable to assume, its mass can not be very different from that of a proton. An attempt to measure the mean angle of scattering with the constant sagitta method has been done in spite of the shortness of the track: the result, although not very significant, is consistent with the assumption of a protonic mass.

If this assumption is correct, its energy as measured from the range of 89 μ, is 3.4 MeV [4] and its moderation time is $4.8 \cdot 10^{-12}$ s [5]. Unfortunately it is not possible to establish the direction of motion of the particle which produced the track; the only indication is the large angle scattering. If one assumes that the particle is emitted from the star A and moves towards the star B, its energy, at the point where it is scattered through 90°, is 0.45 MeV. Such a scattering process is very probably due to the electrostatic interaction of the particle with a heavy nucleus of the emulsion, the cross-section of which is inversely proportional to the square of the energy. Therefore this circumstance favours, by a factor of the order of 50, the choice of A towards B as direction of motion of the particle.

Star B has been investigated in detail (see Table I). The black tracks b, e, g, come to rest inside the emulsions and therefore the identification of the corresponding particles as well as the determination of their energies, is certain.

The grey tracks a and f have a large angle of dip. Therefore the results of the scattering measurements are not very reliable, while measurements of grain density by comparison with pairs of electrons showing the same angle of dip, allow a satisfactory determination of their velocity. From the fact that their grain density does not vary appreciably along the observed ranges, one can conclude that tracks a and f can not be due to L-mesons. The more probable assumption is that they are due to protons; therefore also the corresponding energies can be established.

---

[4] G. Baroni, C. Castagnoli, G. Cortini, C. Franzinetti and A. Manfredini: BS9, *CERN*, July 1954.

[5] E. Amaldi, G. Baroni, G. Cortini, C. Franzinetti and A. Manfredini: *Suppl. Nuovo Cimento*, **12**, 181 (1954).

TABLE I.

Track	R [1] (μ)		Number of emulsions crossed	I/I_0 (initial)	$p\beta$ (MeV/c)	Identity	E (MeV)	Remarks
a	19950	observed	34	2.19 ± 0.10 [3]	—	proton	174 ± 7	—
b	1000	total	2	black	—	proton	14.3	—
c	25500	observ. [2]	11	1.01 ± 0.03	$\geqslant 200 \pm 40$	π (?)	130 ± 30	
d	33800	observed	34	0.95 ± 0.04	240 ± 44	π (?)	$\geqslant 165 \pm 35$	—
e	840	total	1	black	—	proton	12.6	—
f	21600	observed	34	2.52 ± 0.10 [3]	—	proton	130 ± 7	—
g	15900	total	4	—	—	triton	114	$m = 4610^{+980}_{-800}$ from scatterin measurement $m = 7200 \pm 100$ from gap measurement

[1] Total range is that of the particles which come to rest in the emulsion. Observed range is the visible range of those particles which escape from the stack before stopping.
[2] This track disappears in the emulsion.
[3] These values represent the initial ionization.

Tracks *c* and *d* have a minimum grain density as appears from blob- and grain-counting and gap length measurements. For track *c* the distortion allows scattering measurements only in two of the emulsions which it crosses.

For track *d*, the scattering has been measured by comparison with a fast primary having the same angle of dip. The errors in the values of $p\beta$ given in Table I, represent the statistical errors. The inequality sign is due to the uncertainty introduced by the distortion.

The identification of these two tracks is obviously uncertain; the observed values of $p\beta$ are consistent only with a mass equal to or smaller than that of a π-meson. Furthermore track *c*, after crossing 11 emulsions, disappears, in flight without being associated with the emission of any ionizing particles. This circumstance is an indication in favour of a positron or a negative pion. The mean free path in emulsion for annihilation in flight of a 200 MeV positron is ~ 2.5 m [6] while that for charge exchange in flight of a negative pion is ~ 1.5 m [7].

---

[6] W. HEITLER: *The Quantum Theory of Radiation*, 2nd Edition (Oxford), p. 208.
[7] G. BERNARDINI and F. LEVY: *Phys. Rev.*, **84**, 610 (1951); A. M. THORNDIKE: *Mesons* (New York, 1952), p. 158.

2. – Energy and Momentum Balance.

The value of the visible energy of star B depends, of course, on the assumption made about the identity of the particles c and d; if we assume that they are both electrons one gets

$$E_{\text{vis}} \geqslant 885 \text{ MeV} ; \tag{1}$$

if one assumes that they are both pions

$$E_{\text{vis}} \geqslant 1020 \text{ MeV} . \tag{2}$$

If tracks c and d were due to protons, E_{vis} would be still higher. In the following we will disregard this case because it is very improbable.

The visible energy E_{vis} represents a lower limit for the total energy Q released in star B.

Such a lower limit is to be increased first by taking into account the binding energy of all the emitted nucleons, and second by applying the momentum balance.

In order to make quantitative the first argument, one can assume that besides the 4 protons and the 1 triton actually observed, about 5 neutrons have been emitted, so that the total binding energy absorbed by the separation of the nucleons can be estimated to be around 90-100 MeV.

The second argument is based on the assumption that the star B has been produced by a particle at rest, as is indicated from the arguments given above; then the momenta of all the emitted particles must add to zero. The resultant of the momenta of the observed particles listed in Table I turns out to be 1500 MeV/c. Such a momentum can be balanced by assuming, for instance, that 5 neutrons have been emitted, all nearly in the same direction, each of them having a kinetic energy of 47 MeV.

As a conclusion we can state that a lower limit for the energy release Q of star B can be obtained by adding to the visible energy E_{vis} about 330 MeV:

$$Q > Q_{\min}$$

where

$$Q_{\min} \sim 1200 \div 1350 \text{ MeV} \tag{3}$$

according to the assumption made about the identity of the tracks c and d.

A very rough estimate of the energy release Q of star B can also be made by assuming that 5 neutrons are emitted which take away a kinetic energy equal to that of the observed protons i.e. about 400 MeV which together with

the binding energy and the values (1) and (2) gives

$$Q \gtrsim 1400 \div 1500 \text{ MeV}. \tag{4}$$

A few arguments have been given above in favour of the assumption that this energy Q has been released by the capture of a particle at rest: whatever may be the assumption about the identity of tracks c and d, the released energy is much higher than the total energy produced in the capture of the heavy mesons or hyperons known until now.

3. – Accidental Coincidence.

On the other hand the event of Fig. 1 could also be due to an accidental coincidence in space.

Therefore we have evaluated the probability for such a coincidence taking into account two different possibilities: *a*) the accidental superposition (into a volume v_a) of the ends of two black prongs associated with two different stars; *b*) the accidental superposition (into a volume v_b) of the centre of a star with the end of one black prong associated to another star.

To make the calculation we have classified all the stars present in our emulsion according to their energies E. To simulate an event as that shown in Fig. 1, it is necessary i) that both the accidentally associated stars have an energy $E > 0.5$ GeV (otherwise the event could be interpreted as a K-meson capture), and ii) that the assumed secondary star has an energy $E \lesssim 2$ GeV. Therefore we consider as possible primary stars only those (A-stars) whose visible energy is > 0.5 GeV, and as possible secondary stars, only those (B-stars) whose visible energy E falls into the $0.5 \div 2.0$ GeV interval. The visible energy of stars has been evaluated attributing 870 MeV to each shower track ([2]) (including the primary track for the « p-stars ») and using the well known formula $37N + 4N^2$ ([3]) for the total energy associated with the black and grey tracks. If N_A, n_A are the numbers of A-stars and of their black prongs per cm³ of our emulsion and N_B, n_B have a similar meaning,

$$p_a = v_a n_A n_B \tag{5}$$

$$p_b = v_b(N_A n_B + N_B n_A) \tag{6}$$

are the probabilities (per cm³ of emulsion) of a random coincidence according to the two mentioned schemes *a*) and *b*). To obtain the total probability of *observing* such an event, we must multiply (5) and (6) by the scanned volume V and by scanning factors F_a, F_b (of the order of 1) which give the probability

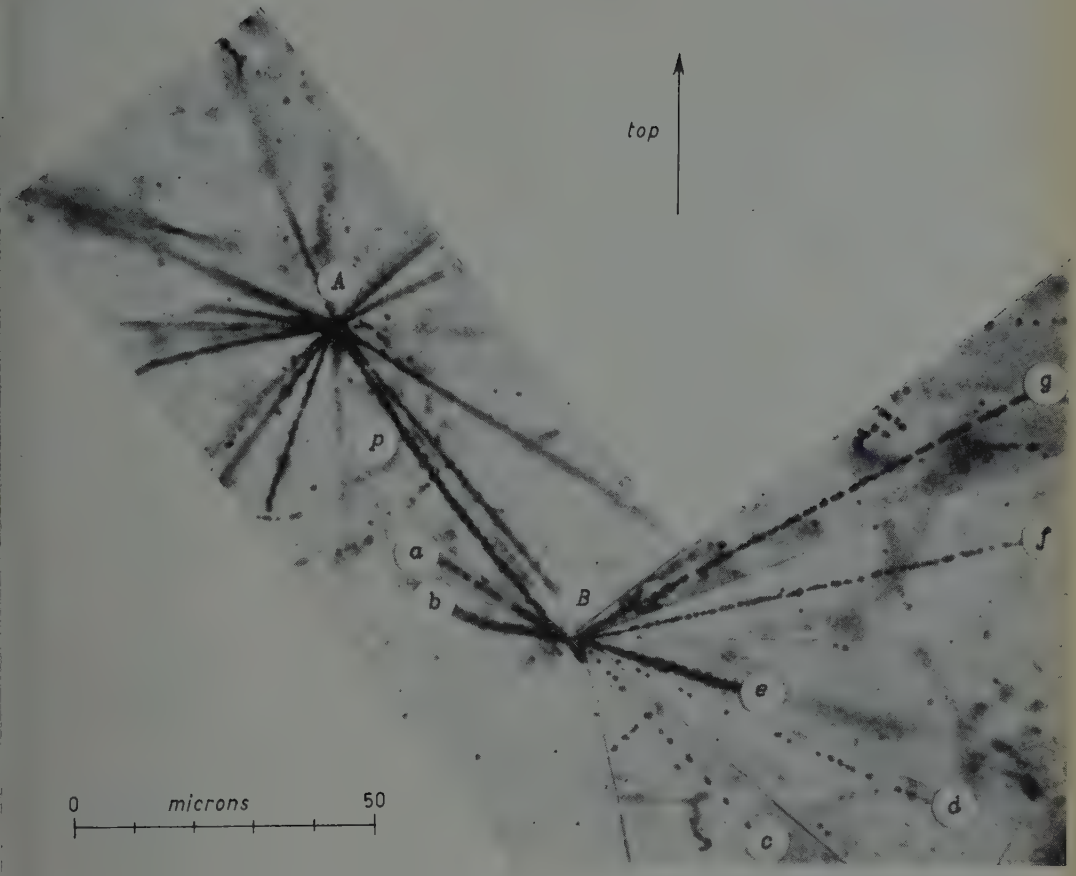

Observed by C. Castagnoli

Fig. 1.

of observing the coincidence if it exists. These factors are largely dependent on the scanning method.

We take $v_a = 2\ \mu^3$, $v_b = 10\ \mu^3$, $V = 58\ \text{cm}^3$, and we deduce N_a, N_b, n_a, n_b from the known frequencies of different types of star in the balloon emulsions ([8]). Our scanning method gives $F_a \sim 0.6$, $F_b \sim 0.7$.

We get

$$p = p_a F_a V + p_b F_b V = (1.26 + 2.54) \cdot 10^{-4}. \tag{7}$$

Formula (7) is correct only for a random distribution of stars in the emulsion. Now, there is some systematic spatial association among the stars due to the high energy neutrons. However, it is easily seen that the effect of this association is fairly small, namely less then 10% of the contribution of the accidental coincidences. Its contribution has already been taken into account in formula (7).

The value (7), although small, is not at all negligible, if one considers that in each of many other laboratories, volumes of emulsion comparable with that investigated by us, have been scanned. On the other hand it is impossible to estimate the corresponding increase of the number of accidental coincidences that we would have to consider, because the various populations of events are not uniform.

In our case the scanning of the volume V (58 cm^3) that led to the observation of the event considered, was done by looking for double stars appearing in the same field of the microscope i.e. at a distance not larger than 300 μ.

4. – Discussion.

The value (7) is sufficiently small to entitle us to look for an interpretation of the observed event in terms of a physical process and not of an accidental coincidence.

We are left to consider the star B as produced by the track p. Then the corresponding particle either has a rest energy of the order of $1.5 \div 2$ GeV, or, being an antiproton, it has been annihilated by a nucleon, releasing $2m_p c^2 = 1876$ MeV.

We do not have any argument in favour of one or the other of these two possibilities apart from the fact that unstable particles of rest energy of the order of $1.5 \div 2$ GeV have never been observed; nor has the antiproton, but this, at least, is expected to exist as a consequence of very general arguments based on symmetry with respect to the sign of the electric charge.

([8]) G. CORTINI, A. MANFREDINI and G. SEGRÈ: *Nuovo Cimento*, **9**, 659 (1951).

On the other hand an event observed in a cloud chamber, which could be interpreted as due to the annihilation of an antiproton with emission of two neutral pions, has been already reported ([9]).

Also other assumptions could be made such as, for instance, the nuclear capture of an antihyperon followed by disintegration and annihilation. Even in this case what we have observed would still be the annihilation of a massive antiparticle. For the sake of simplicity we shall confine ourselves to the assumption that it is an antiproton.

In order to decide which is the most acceptable among the various interpretations suggested above, it would be necessary to know the characteristic of production, capture and annihilation of very particles ($mc^2 \sim 1.5 \div 2$ GeV) and of antiparticles if they exist. Then, we would be in a position to decide whether the observation of such a particle at such a low energy was or not more probable than an accidental overlapping of tracks.

Our speculations in this field are very uncertain, lacking, as we do, any experimental basis. In spite of that we have made some very tentative calculations on the probability of observing an event such as that of Fig. 1, due to the capture and annihilation of an antiproton. This estimate has been made along the following lines:

a) The volume V of emulsions considered contains about 1000 high energy events in which the production of an antiproton was energetically possible.

b) The process of production of antinucleons is in competition with the processes of productions of other particles. Tentatively we may take the corresponding cross-section proportional to the square of the Compton wave lengths: this give a branching ratio of the order of 0.02.

c) The particle p is observed in the laboratory system with a very low energy. Therefore, before emerging from the nucleus, it must have undergone a collision with a high transfer of energy. The probability that after the collision its kinetic energy in the laboratory system is below a given value E, is given for isotropic production with total energy E^* in the centre of mass system, by the expressions

$$\frac{E}{E^* - m_p}.$$

Taking $E^* = 2$ GeV and $E = 7$ MeV (corresponding to a range of 300 μ) and introducing a factor of the order of $\frac{1}{4}$ in order to take into account the fact

([9]) H. S. BRIDGE, H. COURANT, H. DE STAEBLER and B. ROSSI: *Phys. Rev.*, **95**, 1101 (1954).

that the collision does not happen always and that only a fraction of the collisions does not happen always and that only a fraction of the collisions will lead to the escape of the particle, one obtains $\frac{7}{4} \cdot 10^{-3}$.

d) Assuming that at very low energy antiprotons are mainly scattered, as are protons, by the coulomb field, one can calculate the probability of a scattering at 90°.

These considerations can now be used to calculate tentatively the ratio $\mathcal{F}$ of the number of events of the type considered to be expected to be produced by antiprotons, if they exist, and the corresponding number of similar events due to accidental coincidences. One gets $\mathcal{F} \sim 30$ which, although not very large, still favours the interpretation in terms of an antiproton.

Two more points have been considered in detail but not included in the previous estimate.

e) In star B the energy and momentum taken away by n neutrons and the residual nucleus, are respectively $1876 - (1020 + 90) \simeq 770$ MeV and 1500 MeV/c. By considering the corresponding volume of the phase-space one obtains that the probability that with an available energy of 770 MeV, a momentum equal to or larger than $P_0 = 1500$ has been taken away, is, for $n = 5$, $\mathcal{P} \sim 0.2$ i.e. a value sufficiently close to $\mathcal{P} = 0.5$ which defines the more probable value of the disappeared momentum. The situation does not change appreciably by changing n between 3 and 7 while it is still improved by considering the residual nucleus.

f) The observed momentum makes an angle of 75° with the vertical direction upwards. By considering that in only $\sim \frac{1}{5}$ of the stars of energy in the range of 2 GeV, the resulting momentum is oriented in the upwards hemisphere, one could reduce the number of accidental coincidences by roughly a factor ~ 2.

Point *e*) has not been included in the previous estimate because the corresponding probability is not very far from one. The same holds for point *f*) which would, in any case, roughly compensate the effect of *e*).

Finally we notice that the presence of tracks *c* and *d* in star B gives to it the appearence that one must expect for a star produced in the annihilation of a pair of nucleons.

One can conclude that the probability of an accidental coincidence can not be disregarded although it is rather small. If one excludes this possibility the more likely interpretation seems to be that of an annihilation process of a heavy particle.

The many questions raised by the discussion of this event will obviously find their final answer only if other similar events will be observed. We suggest as the most efficient method for looking for this type of phenomenon to select

stars that, from the number of black, grey and shower tracks, appear to have an energy between 0.5 and 2 GeV, and then to search for the possible existence among its black prongs of an incident particle.

We are glad to express our thanks to Prof. B. FERRETTI, Dr. B. TOUSCHEK, Dr. G. MORPURGO and Dr. R. GATTO for various cricitisms, and enlightening discussions.

RIASSUNTO

Si descrive un evento consistente in due stelle di energia rispettivamente di circa 5 e $1 \div 2$ GeV, collegate da un ramo nero lungo 89 μ. Il valore probabile del numero di simili eventi dovuti a coincidenze spaziali casuali che ci si aspetta di osservare nel volume esplorato, è di $4 \cdot 10^{-4}$. Tale valore, pur non potendo escludere che si tratti di un processo casuale, giustifica la ricerca di una interpretazione basata su un processo fisico. Particolare attenzione va rivolta alla produzione, cattura e annichilamento di un protone negativo.

LETTERE ALLA REDAZIONE

(La responsabilità scientifica degli scritti inseriti in questa rubrica è completamente lasciata dalla Direzione del periodico ai singoli autori)

Un modello di sorgente di deutoni a campo magnetico.

G. Perona e A. Persano

Laboratori CISE - Milano

(ricevuto il 13 Gennaio 1955)

La presente comunicazione riferisce sui risultati conclusivi a cui si è pervenuti dopo una serie di ricerche sperimentali eseguite su vari tipi di sorgenti di ioni a pendolamento di elettroni in campo magnetico assiale.

Scopo delle ricerche era la costruzione di una nuova sorgente per l'impianto acceleratore di ioni da 400 keV in funzione nei laboratori del CISE (1).

Poichè l'impianto acceleratore viene usato come generatore di neutroni per impieghi diversi, tra i quali la spettroscopia dei neutroni lenti col metodo del tempo di volo, dovevamo cercare un modello di sorgente che, oltre al normale requisito di avere una forte emissione di ioni con basso consumo di gas, presentasse anche un soddisfacente funzionamento sia continuo che a impulsi.

Ci siamo orientati verso le sorgenti di ioni del tipo a campo magnetico perchè queste hanno una caratteristica corrente-tensione non molto dissimile da quella delle valvole stabilizzatrici, cioè possono essere comandate di corrente senza forti variazioni di tensione. Ciò permette di iniettare per tempi brevi delle correnti elevate pur mantenendo la potenza media a valori abbastanza bassi da non richiedere particolari accorgimenti per il raffreddamento.

Un buon funzionamento a impulsi richiede naturalmente che il tempo di ritardo tra il comando e l'inizio dell'impulso sia breve e, soprattutto, costante, e che il tempo di salita sia molto breve rispetto alla durata dell'impulso stesso in modo che questo risulti non deformato.

Il montaggio sperimentale era di tipo normale. Gli ioni, estratti e accelerati mediante un elettrodo estrattore, venivano raccolti in un pozzetto di Faraday. I valori medi delle correnti erano misurati con strumenti convenzionali, mentre per gli impulsi veniva utilizzato un oscillografo a due tracce. Su di una delle tracce si misurava la caduta di tensione lungo una resistenza in serie con la sorgente (corrente trasversa), e sull'altra la caduta di tensione su un sistema resistenza-capacità, con costante di tempo lunga rispetto alla durata dell'impulso, collegato al pozzetto, mediando sulla durata dell'impulso (corrente di ioni).

L'impulsatore usato generava impulsi squadrati di 600 V con tempo di salita di 0,1 μs e durata di 20 μs. Resistenza interna: circa 200 ohm.

Per analizzare la composizione del fascio di ioni, ossia per determinare le percentuali di ioni mono-, bi-, e triatomici è stato costruito un piccolo spettro-

(1) E. Gatti, G. Perona e A. Persano: *Nuovo Cimento*, **9**, 80 (1953).

metro di massa che può raccogliere contemporaneamente su tre collettori distinti gli ioni H_1^+, H_2^+, H_3^+. In tutto il lavoro di prova è stato usato idrogeno in luogo di deuterio.

Il primo modello studiato è stato quello di KELLER [2], che funziona a catodo freddo e a pendolazione di elettroni in modo simile ad un vacuometro di Penning. Il pendolamento degli elettroni permette di ottenere una intensa ionizzazione del gas e la formazione di un plasma con valori della pressione (dell'ordine di 6 o $7 \cdot 10^{-3}$ mm Hg) per cui il cammino libero medio degli elettroni è molto maggiore delle dimensioni lineari della sorgente.

La sorgente di Keller è stata scartata perchè troppo lenta. Infatti, mantenendo la sorgente debolmente accesa tra un impulso e l'altro, il tempo di ritardo si aggira sui 10 μs mentre il tempo di salita va da 15 a 20 μs a seconda della pressione. Se poi si lascia spengere completamente la sorgente tra un impulso e l'altro, il funzionamento risulta del tutto irregolare.

I modelli studiati successivamente sono tutti derivati da quello di Keller. Sono state apportate modifiche in tre direzioni.

a) È stato montato un catodo caldo allo scopo di aver sempre presente nell'interno della sorgente una nuvola di elettroni, così da ridurre il tempo di formazione della scarica a bagliore. Si sono ottenuti così tempi di ritardo e tempi di salita inferiori a 0,5 μs. Anche la pressione si abbassa a 6 o $7 \cdot 10^{-4}$ mm Hg, riducendo così a circa un decimo il consumo del gas.

Con l'introduzione del catodo caldo la sorgente presenta analogie con quelle studiate da FINKELSTEIN [3].

b) Sono state provate varie geometrie degli elettrodi interni della sorgente, seguendo i risultati ottenuti da KISTEMAKER [4] e da VEENSTRA [5], i quali ritengono importante per lo stabilirsi di un plasma la condizione che l'anodo racchiuda una regione pressochè priva di campo elettrico.

c) È stato sperimentato un tipo di elettrodo estrattore che sporge leggermente verso l'interno della sorgente. Infatti il meccanismo dell'estrazione consiste essenzialmente nel dirigere verso il foro di un elettrodo gli ioni che escono per diffusione dalla superficie del plasma, e questa si dispone in modo che tra plasma ed elettrodo domini un regime di carica spaziale. Perciò quando l'estrattore sporge verso l'interno della sorgente il plasma presenta all'estrattore una superficie concava e quindi il campo elettrico assume una distribuzione focalizzante.

Il risultato di numerose prove è stato il modello schematicamente rappresentato nella fig. 1. Una scatola cilindrica di

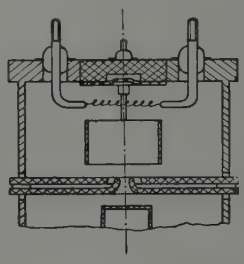

Fig. 1. – Disegno della sorgente di ioni.

rame, ∅ circa 10 cm, porta sulla base superiore quattro passanti kovar, due per il catodo caldo e due per alimentare e sostenere meccanicamente l'anodo, anch'esso cilindrico e di rame. La base inferiore della sorgente e l'elettrodo estrat-

---

[2] R. KELLER: *Helv. Phys. Acta*, **21**, 170 (1948); **22**, 78 (1949).

[3] A. T. FINKELSTEIN: *Rev. Scient. Inst.*, **11**, 94 (1940).

[4] C. J. BAKKER e J. KISTEMAKER: *Helv. Phys. Acta*, **23**, 46 (1950); J. KISTEMAKER e H. L. D. DEKKER: *Physica*, **16**, 209 (1950)

[5] P. C. VEENSTRA e J. M. W. MILAZ: *Physica*, **16**, 528 (1950).

tore sono in ferro dolce. Pure in ferro dolce è la parte centrale della base superiore, che costituisce l'espansione polare dell'elettromagnete che produce il campo

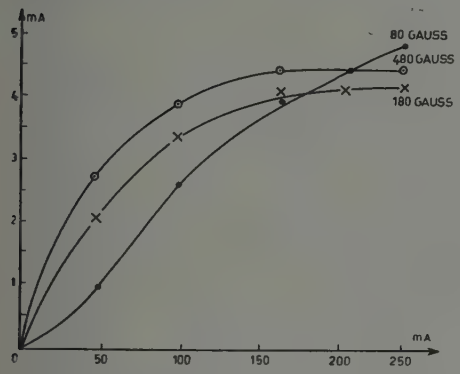

Fig. 2. – Corrente continua di ioni estratta in funzione della corrente anodica, con diversi valori del campo magnetico; $V_e = 3000$ V.

magnetico (assiale) necessario per il funzionamento della sorgente. Nel montaggio in opera della sorgente l'elettromagnete è sostituito da un magnete permanente in Alnico V.

Foro di uscita degli ioni: ∅ 3 mm.

Catodo caldo costituito da cm 12 circa di filo di tungsteno toriato, del diametro di 0,4 mm, alimentato a 12-10 A, avvolto a spirale.

Pressione da 6 a $7 \cdot 10^{-4}$ mm Hg.

La fig. 2 relativa al funzionamento continuo, pone in relazione corrente trasversa e corrente di ioni per tre diversi valori del campo magnetico (80, 180, 480 gauss), e 3 000 V di tensione di estrazione.

La fig. 3, anch'essa relativa al funzionamento continuo, pone in relazione la corrente di ioni e il campo magnetico

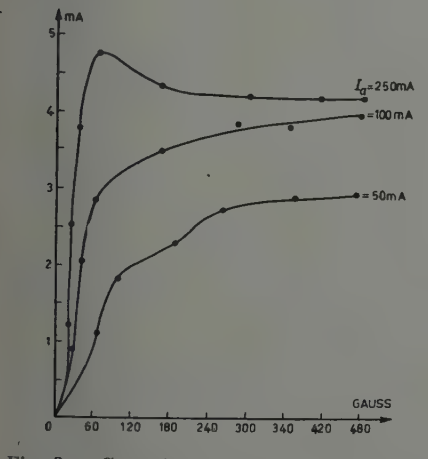

Fig. 3. – Corrente continua di ioni estratta in funzione dell'intensità del campo magnetico e con diversi valori della corrente anodica. Tensione di estrazione: $V_e = 3000$ V.

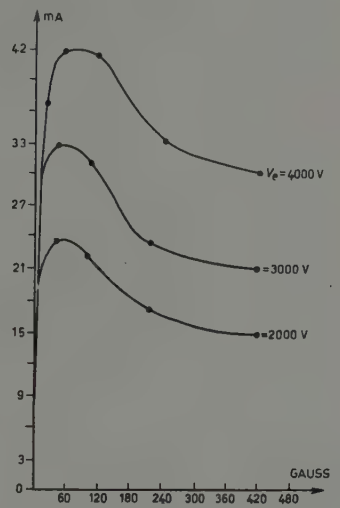

Fig. 4. – Altezza degli impulsi di corrente estratta in funzione della intensità del campo magnetico con diversi valori di tensione di estrazione.

per tre diversi valori della corrente trasversa (50, 100, 250 mA) e 3 000 V di tensione di estrazione.

La fig. 4, relativa al funzionamento a impulsi, pone in relazione la corrente di ioni durante l'impulso e il campo magnetico per tre diversi valori della tensione di estrazione (2 000, 3 000, 4 000 V).

La composizione del fascio di ioni è stata sempre pressochè la stessa per tutti i modelli sperimentati, ed è: circa 10% di ioni H_1^+, circa 40% di ioni H_2^+, circa 50% di ioni H_3^+.

La sorgente è raffreddata ad aria, fatta circolare con un ventilatore.

Sur la mesure du temps de restitution des compteurs de Geiger-Müller pour le seuil de Geiger.

D. Blanc

Laboratoire de Physique Atomique et Moléculaire du Collège de France - Paris

(ricevuto il 25 Gennaio 1955)

Le temps de restitution θ est le temps minimum nécessaire pour que, après le démarrage d'une impulsion, l'impulsion suivante reprenne sa taille normale; il est fonction de la surtension. La méthode oscillographique permet de le mesurer avec une bonne précision, mais, au seuil de Geiger, les impulsions sont de petite taille, et les mesures beaucoup plus difficiles.

Méthode utilisée.

1°) *Compteurs à paroi de verre et graphitage externe.* – Pour une description détaillée de ce type de détecteurs, voir [1]. Nous avons déjà souligné que le seuil de Geiger, pris sous irradiation gamma, augmente avec le taux de comptage [2]: la loi de variation est linéaire jusqu'à une certaine valeur N_R/s du taux de comptage. Au dessus, la courbe prend une allure parabolique (fig. 1): les impulsions ont alors une taille moyenne plus faible que la valeur normale. Si l'on admet que les impulsions se succèdent à cadence régulière, N_R correspond au cas où l'intervalle de temps séparant deux impulsions successives est égal au temps de restitution θ:

$$\theta = \frac{1}{N_R}\,\text{s}\,.$$

Nous avons mesuré θ pour divers remplissages, dans des compteurs en verres « novo » et « UVK-1 »: en effectuant un nombre suffisant de mesures de seuil, nous avons obtenu une précision supérieure à 5%.

2°) *Compteurs à cathode interne du type classique.* – La méthode décrite s'applique aux compteurs classiques, en étudiant la variation du seuil de Geiger obtenue par introduction, entre la cathode et la masse, d'un système résistance-capacité en parallèle, convenablement choisi [3].

Quel que soit le compteur étudié, il est nécessaire que le seuil du circuit de comptage ne dépasse pas quelques cen-

[1] D. Blanc: *Journ. de Phys. et Rad.*, **14**, 260 (1953).

[2] D. Blanc: *C. R. Acad. Sci.*, **239**, 1621 (1954).

[3] D. Blanc: *Journ. de Phys. et Rad.*, **15**, 693 (1954).

tièmes de volt, afin que toutes les impulsions se succédant dans le détecteur soient enregistrées: l'utilisation d'un seuil trop élevé masquerait le phénomène.

sous la pression atmosphérique, la mobilité ionique correspondant au mélange utilisé: k est ici supposée constante quel que soit le champ électrique; en réalité,

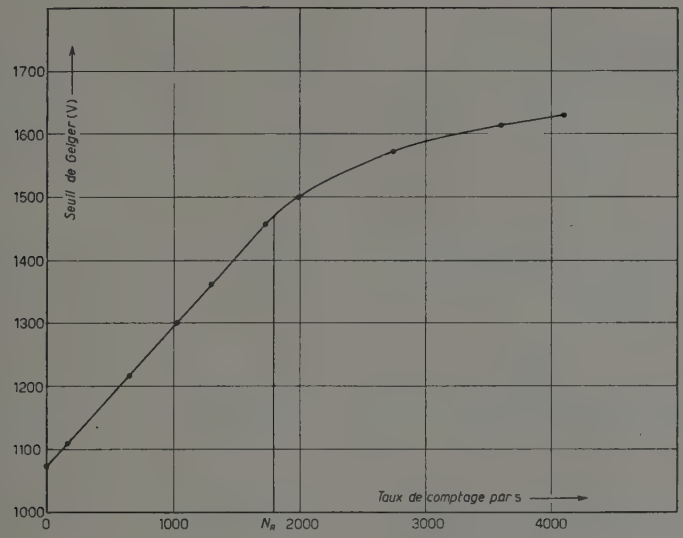

Fig. 1.

Application à la détermination de la mobilité ionique de vapeurs organiques.

1) *Principe du calcul.* – Pour le seuil de Geiger, la gaine ionique formée au voisinage du fil possède une densité assez faible pour que l'on puisse négliger toute diffusion latérale. L'application des formules de Stever [4], van Gemert, Den Hartog et Muller [5] donne:

$$\theta = \frac{(b^2 - a^2)\,\mathrm{Log}_e\,(b/a)\cdot P}{8kV_G^0\cdot P_0},$$

où b est le diamètre interne du cylindre, a le diamètre du fil, P la pression totale à l'intérieur du compteur, P_0 la pression atmosphérique, V_G^0 le seuil de Geiger pour un taux de comptage très faible. k est, cette hypothèse n'est plus valable pour un champ intense, et nous avons constaté que l'accord de l'expérience avec cette formule n'est satisfaisant que pour une valeur de b supérieure à 2 cm environ.

Pour les conditions expérimentales utilisées, la mesure de θ nous a permis de calculer k avec une précision supérieure à 7%.

Soient k_1 la mobilité ionique de la vapeur organique, k_2 la mobilité ionique du gaz rare, P_1 et P_2 leurs pressions partielles respectives. k_1 est calculable par la formule simple:

$$(1) \qquad k = \frac{k_1 k_2}{P_1 k_2 + P_2 k_1}.$$

Cependant, Loeb [6] a constaté que

[4] H. G. Stever: *Phys. Rev.*, **61**, 38 (1954).

[5] A. G. M. van Gemert, H. Den Hartog et F. A. Muller: *Physica*, **9**, 658 (1942).

[6] L. B. Loeb: *The kinetic theory of gases*, 2ème éd. (New-York, 1934).

la formule (1) ne s'applique pas pour certains mélanges, et propose la formule:

$$k = \frac{k_1 k_2}{[P_1 k_2^2 + P_2 k_1^2]^{\frac{1}{2}}}. \qquad (2)$$

2) *Résultats obtenus.* – La fig. 1 correspond à un compteur (verre « novo », graphitage externe) rempli d'éthanol sous la pression de 0,7 cm de mercure et d'argon sous la pression de 17,2 cm de mercure ($a=0{,}01$ cm, $b=2{,}1$ cm, $V_0^0=1075$ V): $N_R=1800$ impulsions par seconde, d'où $\theta=5{,}6\cdot10^{-4}$ s. On en déduit: $k=1{,}16$ cm/s/V/cm. L'argon utilisé étant spectroscopiquement pur, nous prenons $k_2=1{,}31$ cm/s/V/cm [7]. D'où $k_1=0{,}31$ cm/s/V/cm d'après (1), $k_1=0{,}46$ cm/s/V/cm d'après (2), soit la valeur moyenne de 0,38 cm/s/V/cm. L'accord avec la valeur 0,34 cm/s/V/cm donnée par Den Hartog est satisfaisant [8].

Pour le méthylal, $CH_2(O—CH_3)_2$; la mobilité est de 0,25 cm/s/V/cm d'après (1) et 0,39 cm/s/V/cm d'après (2), soit la valeur moyenne $k_1=0{,}32$ cm/s/V/cm.

L'accord des mobilités ainsi calculées avec celles obtenues par la méthode oscillographique, en particulier, démontre que les hypothèses formulées sont valables, et que notre méthode donne bien le temps de restitution intrinsèque du compteur.

En résumé, la méthode décrite permet, avec un dispositif de comptage du type classique, et sans montage électronique spécial, de mesurer, au seuil de Geiger, le temps de restitution d'un compteur, avec une précision d'au moins 5%, dans des conditions où les méthodes habituelles sont difficiles à appliquer.

[7] S. C. Curran et J. D. Craggs: *Counting tubes* (Londres, 1949).

[8] H. Den Hartog: *Compteurs Argon-Alcool* « Thèse Amsterdam » (1948).

IL NUOVO CIMENTO Vol. I, N. 3 1° Marzo 1955

Su dei nuovi orbitali ibridi di tiqo π a simmetria tetraedrica

G. Giacometti

Istituto di Chimica Fisica dell'Università - Padova (*)

(ricevuto il 29 Gennaio 1955)

Il problema della ibridizzazione della parte angolare di orbitali s, p e d a formare orbitali equivalenti con le necessarie caratteristiche direzionali per spiegare legami di tipo σ in composti a simmetria tetraedrica, è stato studiato e risolto molto tempo fa da Pauling [1]. L'analogo problema, della contemporanea ibridizzazione degli altri orbitali semplici restanti, per costruire orbitali equivalenti adatti invece a formare legami di tipo π, sempre nella simmetria tetraedrica, non era ancora stato risolto [2].

Il dimostrare la possibilità, almeno parziale, di tale ibridizzazione porterebbe un notevole contributo alla spiegazione, dal punto di vista della teoria della valenza diretta, della presenza di caratteristiche di doppio legame parziale in composti di coordinazione tetraedrica attorno ad un atomo appartenente ai periodi superiori della tavola degli elementi. È noto, ad esempio, come tali caratteristiche sussistano negli anioni acidi, tipo SO_4^{--}, PO_4^{---}, ClO_4^- [3], come pure in composti tipo $Ni(CO)_4$ [2].

Che sia possibile, e fino a che punto, tale ibridizzazione, si può dimostrare coll'argomento che segue.

Riferiamoci a un tetraedro iscritto in un cubo con le coordinate e i vertici indicati come in fig. 1. Supporremo che il

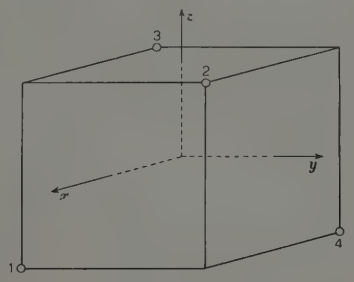

Fig. 1.

nostro ibrido tetraedrico abbia la forma generica indicata in fig. 2. Il piano di antisimmetria conterrà, ad esempio, la direzione $(1\bar{1}\bar{1})$ del cubo (vertice 1 del tetraedro).

Un orbitale dello stesso tipo ma orien-

(*) Lavoro eseguito durante un soggiorno al California Istitute of Technology, Pasadena, California, reso possibile dal conferimento all'Autore di una Borsa di Studio Fulbright.

(1) L. Pauling: *Journ. Am. Chem. Soc.*, 53, 1367 (1931).

(2) L. O. Brockway e P. C. Cross: *Journ. Chem. Phys.*, 3, 828 (1935).

(3) L. Pauling: *The Nature of the Chemical Bond* (Ithaca, N. Y.).

tato invece verso la direzione negativa di z è:

$$\pi_{\bar{z}} = \sqrt{1-a^2}\,p_x - a d_{xy}\,.$$

Ruotando questa funzione di un angolo di 45° intorno a z si ottiene il nuovo orbitale:

$$\pi'_{\bar{z}} = \frac{1}{\sqrt{2}}\left[\sqrt{1-a^2}(p_x + p_y) - \right.$$
$$\left. - a(d_{xz} + d_{yz})\right].$$

Ora, la funzione che si ottiene da una rotazione di $\pi'_{\bar{z}}$ intorno all'asse $x=y$ per un angolo di 54°44′, sarà proprio il

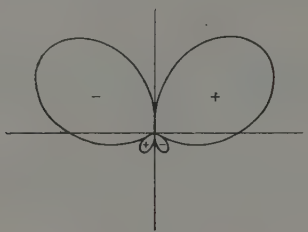

Fig. 2.

nostro orbitale tetraedrico e dovrà risultare espresso in termini delle funzioni p e d.

La matrice di trasformazione per tale operazione è la trasformazione di similitudine $T^{-1}RT$, dove T è una trasformazione di coordinate che porta z a coincidere coll'asse $x=y$, ed R è una rotazione di 54°44′ intorno a z.

Eseguiti i calcoli, l'orbitale che si ottiene è:

$$\tau_1 = \frac{1}{\sqrt{2}}\left[\sqrt{1-a^2}\,(p_x + p_y) - \right.$$
$$\left. - \frac{a}{\sqrt{3}}\,(d_{yz} + d_{xz} + 2d_{x^2-y^2})\right].$$

Quest'orbitale è adatto a formare un legame π con un atomo situato sulla direzione tetraedrica cui appartiene il vertice 1.

Per trovare ora tutte le possibili funzioni di questo tipo, si devono applicare a τ_1 tutte le operazioni di simmetria del gruppo T_d. Si trovano così dodici funzioni, linearmente indipendenti solo a gruppi di tre. Le tre funzioni di ogni gruppo corrispondono a tre vertici differenti del tetraedro di riferimento e possono essere rese mutuamente ortogonali scegliendo: $a = \sqrt{3}/2$:

Esse possono essere rese ortogonali pure alle funzioni tetraedriche di tipo σ, la cui forma generale è (ad esempio per il vertice 1):

$$\sigma_{1\bar{1}} = \frac{1}{2}\,s + \left[(\tfrac{1}{4} - b^2)^{\frac{1}{2}}(p_x - p_y - p_z) + \right.$$
$$\left. + b(d_{yz} - d_{xz} - d_{xy})\right] \qquad (0 \leqslant b \leqslant \tfrac{1}{2}).$$

Basta prendere $b = 1/\sqrt{8}$.

È così dimostrata la possibilità di costruire, partendo da orbitali semplici p e d, degli ibridi di tipo π adatti a contribuire alla formazione di doppi legami in composti a simmetria tetraedrica. Il numero massimo possibile di tali orbitali, linearmente indipendenti, ortogonali fra di loro ed ortogonali agli orbitali tetraedrici σ, è tre; ciò suggerisce che nei composti tetraedrici (per cui il numero di coordinazione è 4) si può avere al massimo 75% di carattere di doppio legame parziale.

Una completa stesura di questo lavoro, comprendente anche casi di altre simmetrie e un tentativo di interpretazione quantitativa delle lunghezze dei legami nei composti interessati, verrà pubblicato tra breve in altro luogo.

IL NUOVO CIMENTO Vol. I, N. 3 1° Marzo 1955

Nucleon-Nucleus Potential at High Energies

E. Clementel

Istituto di Fisica dell'Università - Padova
Istituto Nazionale di Fisica Nucleare - Sezione di Padova

(ricevuto il 1° Febbraio 1955)

The observed polarization of high energy protons elastically scattered by nuclei has been explained in a simple way by Fermi [1] using a potential given by a complex central term, to take into account the absorption properties of nuclear matter, and by a term proportional to the Thomas correction, to give the polarization, i.e. a potential of the kind ($\hbar=1$)

$$V(r) = (1 + i\varepsilon)V_0(r) + V_1(r)\boldsymbol{\sigma}\cdot\boldsymbol{L}\,, \tag{1}$$

where $\boldsymbol{\sigma}/2$ and $\boldsymbol{L}$ are the spin and orbital angular momentum of the proton. In accordance with the well known expression [2] of the realtivistic Thomas effect, the radial dependence of the spin-orbit term $V_1(r)$ has been generally [3] assumed proportional to $(1/r)(\mathrm{d}V_0/\mathrm{d}r)$. It has been shown later by Takeda and Watson [4] that the Serber model of high energy nuclear reactions is able to explain the proton polarization without introducing ad hoc a spin-orbit interaction.

Assuming the impulse approximation valid in the Serber picture, it will be shown briefly in this note that: i) the potential experienced by a nucleon in collision with a nucleus can be split in a central and spin-orbit part; ii) the radial dependence of the spin-orbit term is just of the form given by the Thomas precession.

If $V=\sum_{\alpha} V_\alpha$, where the summation runs over the A nucleons of the nucleus (in a proper analysis distinction should be made between protons and neutrons), is the scattering interaction between the proton and the nucleus, the scattering cross-section depends on the square of the matrix element [5]

$$T_{fi} = (\Phi_f, V\Psi_i^{(+)}) = (\Phi_f, T\Phi_i)\,, \tag{2}$$

---

(1) E. Fermi: *Nuovo Cimento*, **11**, 497 (1954).
(2) W. Heisenberg: *Theorie des Atomkernes* (Göttingen, 1951).
(3) S. Snow, R. Sternheimer and C. Yang: *Phys. Rev.*, **94**, 1073 (1954); W. Heckrotte: *Phys. Rev.*, **94**, 1797 (1954); B. J. Malenka: *Phys. Rev.*, **95**, 522 (1954); R. Sternheimer: *Phys. Rev.*, **95**, 589 (1954); E. Bosco e T. Regge: *Nuovo Cimento*, **12**, 285 (1954).
(4) G. Takeda and K. M. Watson: *Phys. Rev.*, **94**, 1087 (1954).
(5) G. F. Chew and M. L. Goldberger: *Phys. Rev.*, **87**, 778 (1952).

where Φ_i and Φ_f are eigenfunctions of the unperturbed hamiltonian H_0, product of the eigenfunction of the nucleus by a wave function describing the propagation of a plane wave with momentum $\boldsymbol{k}_i$ respectively $\boldsymbol{k}_f$, while T is the so called transition operator defined by $T\Phi_i = V\Psi_i^{(+)}$. $\Psi^{(+)}$ is eigenfunction of the operator $H_0 + V$. Introducing the functions φ and Ψ for the colliding particle and the struck system, we can also write

$$T_{fi} = (\varphi_f, (\Psi_f, T\Psi_i)\varphi_i) \equiv (\varphi_f, T_n, \varphi_i) \,. \tag{3}$$

In the Serber model, where the incoming proton « sees » one nucleon at a time, the nucleon-nucleus scattering can be described in terms of the individual nucleon-nucleon scattering. In the impulse approximation, neglecting the corrections due to the multiple scattering, we can therefore write $T = \sum_\alpha t_\alpha$, where t_α is the transition operator for the α-th nucleon, considered as free. In momentum representation we have [6]

$$t_\alpha = \exp\,[i(\boldsymbol{k}_i - \boldsymbol{k}_f)\boldsymbol{z}_\alpha]\langle f|t|i\rangle \,. \tag{4}$$

The matrix $\langle f|t|i\rangle$ does not depend on the nucleon coordinates $\boldsymbol{z}_\alpha$, but only on the relative momenta of the initial and final states. If with $\boldsymbol{p}_\alpha$ we denote the momentum of the struck nucleon, by using for Ψ a Slater determinant and introducing the Fourier transforms of the individual nucleon functions ψ_α, from (3) and (4) it follows

$$T_n \cong (\Psi_i, \sum_\alpha t_\alpha \Psi_i) = \sum_\alpha \int \psi_\alpha^*(\boldsymbol{k}_i - \boldsymbol{k}_f + \boldsymbol{p}_\alpha)\, \psi_\alpha\,(\boldsymbol{p}_\alpha)\langle f|t|i\rangle \,\mathrm{d}\boldsymbol{p}_\alpha \,. \tag{5}$$

For fast protons ($\boldsymbol{k}_i \gg \boldsymbol{p}_\alpha$), the scattering matrix $\langle f|t|i\rangle$ can be considered [7] as independent from $\boldsymbol{p}_\alpha$, and therefore from (5) we obtain

$$T_n = \int \exp\,[i(\boldsymbol{k}_i - \boldsymbol{k}_f)\boldsymbol{z}]\; \varrho(\boldsymbol{z})\langle f|t|i\rangle \,\mathrm{d}\boldsymbol{z} \,. \tag{6}$$

Use has been made of the relation $\varrho(\boldsymbol{z}) = \sum_\alpha \psi_\alpha^*(\boldsymbol{z})\psi_\alpha(\boldsymbol{z})$. Taking into account only the terms linear in the spin operator of the incoming proton, the general expression for the scattering matrix $\langle f|t|i\rangle$ is the following [8]

$$\langle f|t|i\rangle = A + A'\boldsymbol{\sigma}\cdot\boldsymbol{n} \,, \tag{7}$$

where $\boldsymbol{n} = \boldsymbol{k}_f \wedge \boldsymbol{k}_i$ and the A's are complex constants, functions only of the energy (k_i^2) and $\cos\theta$ (θ is the c.m. scattering angle). For our purposes, it is more convenient to write $A = A(k^2, q)$, with $\boldsymbol{q} = \boldsymbol{k}_f - \boldsymbol{k}_i$. The part of the scattering matrix linear in the spin operator of the target nucleons tends to average to zero in summing over α (this is exactly true only for zero spin nuclei). It is clear now from (3), (6) and (7) that the Fourier transform of T_n gives simply the « potential » V_n describing,

(6) M. LAX: *Rev. Mod. Phys.*, **23**. 287 (1951); K. M. WATSON: *Phys. Rev.*, **89**, 575 (1953).

(7) In the present case: $\langle f|t|i\rangle = \left\langle \frac{2\boldsymbol{k}_f - \boldsymbol{k}_i - \boldsymbol{p}_\alpha}{2} \middle| t \middle| \frac{\boldsymbol{k}_i - \boldsymbol{p}_\alpha}{2} \right\rangle$

(8) L. WOLFENSTEIN and J. ASHKIN: *Phys. Rev.*, **85**, 947 (1952); R. H. DALITZ: *Proc. Phys. Soc.*, **65** A, 175 (1952); D. FELDMAN: *Phys. Rev.*, **92**, 824 (1953).

in our hypotheses, the nucleon-nucleus scattering

$$V_n(\boldsymbol{r}, k_i) = \frac{1}{(2\pi)^{\frac{3}{2}}}\int \exp\,[i(\boldsymbol{r}-\boldsymbol{z})\boldsymbol{q}]\varrho(\boldsymbol{z})\{A(k_i^2, q) + A'(k_i^2, q)\boldsymbol{\sigma}\cdot(\boldsymbol{q}\wedge\boldsymbol{k}_i)\}\,\mathrm{d}\boldsymbol{q}\,\mathrm{d}\boldsymbol{z}\,. \tag{8}$$

Eq. (8) can be written also in the following form

$$V_n(\boldsymbol{r}, k_i) = V_0(\boldsymbol{r}, k_i) + \boldsymbol{\sigma}\cdot\boldsymbol{\nabla}V_1(\boldsymbol{r}, k_i)\wedge\boldsymbol{k}_i\,, \tag{9}$$

where

$$V_0(\boldsymbol{r}, k_i) = \frac{1}{(2\pi)^{\frac{3}{2}}}\int \exp\,[i(\boldsymbol{r}-\boldsymbol{z})\boldsymbol{q}]\varrho(\boldsymbol{z})A(k_i^2, q)\,\mathrm{d}\boldsymbol{q}\,\mathrm{d}\boldsymbol{z}\,. \tag{10}$$

Analogous expression is valid for $V_1(\boldsymbol{r})$ with $B(k_i^2, q) = -iA'(k_i^2, q)$ in place of $A(k_i^2, q)$. Being V_0 and V_1 radial functions, $\boldsymbol{\nabla}V_1(\boldsymbol{r}) = (\boldsymbol{r}/r)(\mathrm{d}V_1/\mathrm{d}r)$, and Eq. (9) reads

$$V_n(r, k_i) = V_0(r, k_i) + \frac{1}{r}\,\frac{\mathrm{d}V_1(r, \boldsymbol{k}_i)}{\mathrm{d}r}\,\boldsymbol{\sigma}\cdot\boldsymbol{L}\,, \tag{11}$$

for $\boldsymbol{r}\wedge\boldsymbol{k}_i = \boldsymbol{L}$. Eq. (11) is the desired expression, which shows clearly the analogy with the Thomas term in the electron case. For low angle scattering, the functions $A(k_i^2, q)$ and $B(k_i^2, q)$, depending on $\cos\theta$, vary slowly with θ, and $B(k_i^2; q)$ can be taken proportional to $A(k_i^2, q)$: only in this hypothesis the spin-orbit term is proportional to the radial derivative of the real part of the central potential. It interesting also to observe that in this formulation both central and spin-orbit part are functions of the energy of the incoming nucleon.

Interaction of π Mesons in Photographic Plates

L. Ferretti and E. Manaresi

Istituto di Fisica dell'Università - Bologna
Istituto Nazionale di Fisica Nucleare - Sezione di Padova

(ricevuto il 1° Febbraio 1955)

In order to extend the knowledge of pions interaction with nuclei towards low energy, we studied the phenomena presented by 17 MeV positive and negative pions in photographic plates. The plates were 600 μ Ilford G.5 radiated by pions from Chicago cyclotron. The mean energy was about 17 MeV, but really there was a very large energetic distribution. The scanning was made « along the track » and we therefore deducted the beam composition, determining, in

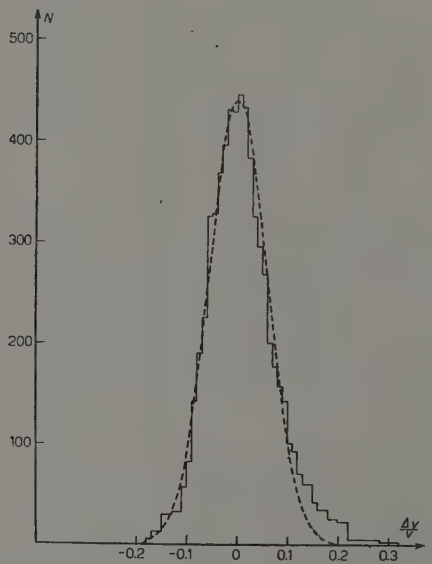

Fig. 1. – Analysis of 66 scattering events for 5-10 MeV π^+.

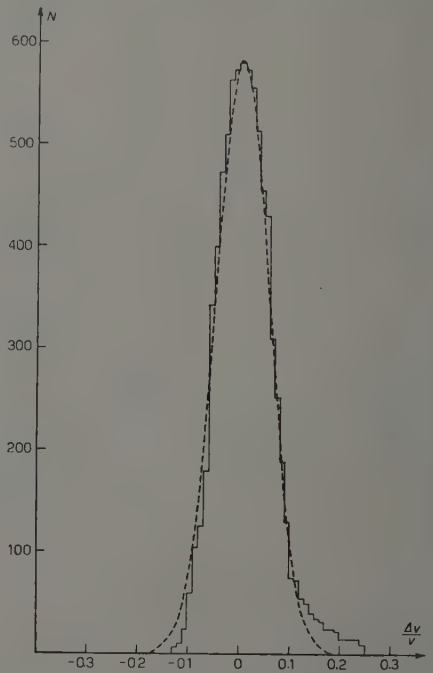

Fig. 2. – Analysis of 79 scattering events for 5-10 MeV π^-.

a certain total length of track, the percentage of range run in relation with each energy. This method allows thus to obviate the non monochromatic beam and to get information about each energetic interval. In the following table I are shown the results of the scanning divided into energetic intervals.

To calculate the mean free path, we considered the fraction of μ particles negligible. In fact the π-mesons going

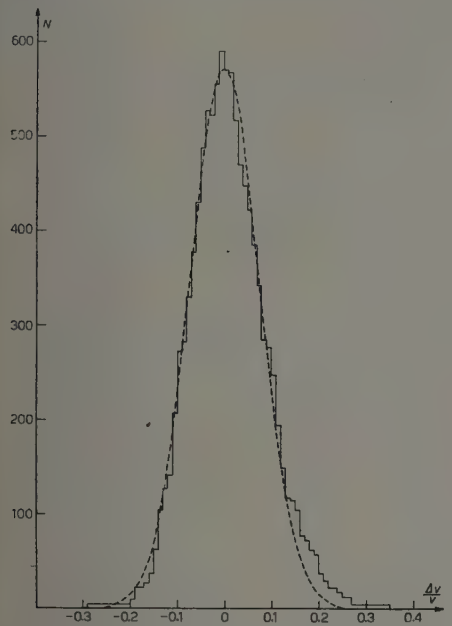

F.g. 3. – Analysis of 109 scattering events for 10-20 MeV π^+.

out from the cyclotron had 67 MeV energy and were then reduced through thick material down to 17 MeV. The μ-particles having the same momentum as 67 MeV pions entered the plates having 43 MeV; therefore they could not be mistaken for π of energy less then 25 MeV, which were selected during the scanning. A confirmation of this lies in the fact that we found stopping muons with ratio less than 1% with reference to stopping pions.

The resulting mean free paths are shown in the following table II.

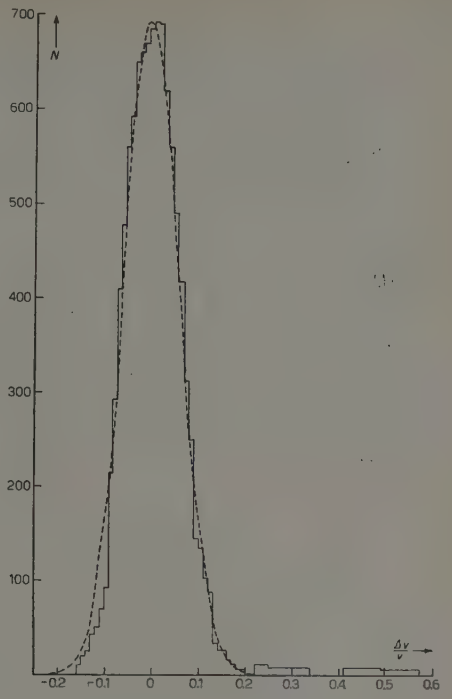

Fig. 4. – Analysis of 104 scattering events for 10-20 MeV π^-.

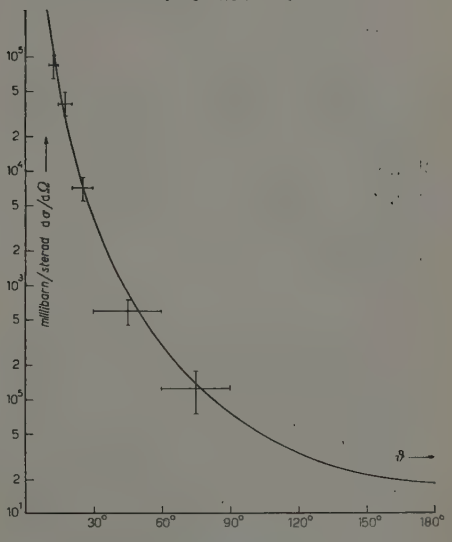

Fig. 5. – Elastic scattering of 5-10 MeV π^+ in p.p. (76 events).

The λ star of π^- has been calculated also in consideration of a supplementary «area scanning»; since both scanning methods agreed perfectly.

TABLE I.

Energy (MeV)	5–10		10–15		15–20		20–25	
	+	−	+	−	+	−	+	−
Length of track (cm) .	328.6	258.7	776,7	491.2	903.4	339.5	524.9	83.5
Stars	0	7	9	12	11	4	5	0
Stops	0	2	0	3	1	0	0	2
Scattering $> 20^{\circ}$ . . .	43	40	74	43	30	13	18	0

TABLE II. – *Mean free paths in G.5* (cm).

Energy (MeV)	5–10		10–20	
	+	−	+	−
Star	∞	35.5 ± 10.7	84.0 ± 18.8	55.8 ± 11.0
Stop	∞	129.3 ± 91.7	1680.1 ± 1680.1	276.9 ± 160.0
Star + stop	∞	27.8 ± 7.7	80.0 ± 17.5	46.5 ± 8.6
Incl. scatt.	130 ± 92	57.5 ± 33.2	550 ± 318	415.0 ± 293.5
Total inel.	130 ± 92	18.8 ± 4.5	69.9 ± 14.3	41.8 ± 7.5
El. scatt. $> 20^{\circ}$	4.0 ± 0.6	4.5 ± 0.8	11.0 ± 1.1	11.4 ± 1.6
El. scatt. $> 30^{\circ}$	11.8 ± 2.5	16.6 ± 4.9	20.8 ± 2.6	28.3 ± 5.6
El. scatt. $> 60^{\circ}$	52.6 ± 21.5	258.7 ± 258.7	60.3 ± 11.6	68.3 ± 19.7
El. scatt. $> 90^{\circ}$	∞	258.7 ± 258.7	98.8 ± 24.0	103.8 ± 36.7

TABLE III.

N. prongs	1	2	3	4	5
% σ Heavy [1]	50	33.3	7.4	7.4	1.9
% π^--stars	43.6 ± 10.6	33.5 ± 9.9	15.4 ± 6.3	2.6 ± 2.6	—

[1] M. G. K. MENON, H. MUIRHEAD and O. PROCHAT: *Phil. Mag.*, **41**, 583 (1950).

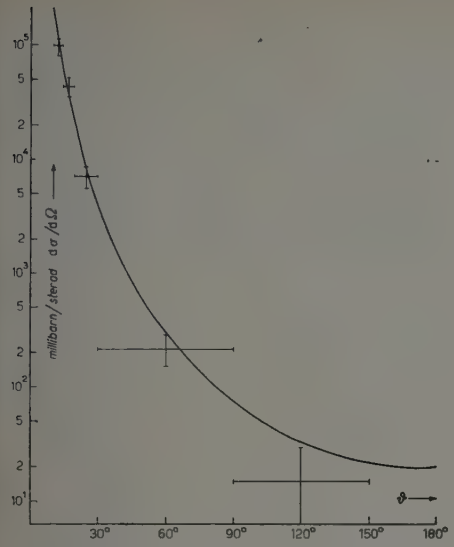

Fig. 6. – Elastic scattering of 5-10 MeV π^- in p.p. (91 events).

It is interesting to remark the effect of Coulomb barrier on the interaction paths for the inelastic processes quite marked both for positive pions and for negative ones. As for the negative pions

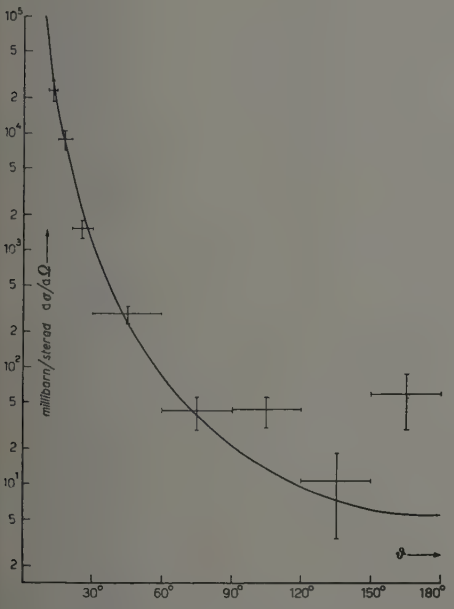

Fig. 7. – Elastic scattering of 10-10 MeV π^+ in p.p. (150 events).

we may add that, in the absorption making stars, the frequence of those versus the number of ionizing prongs quite agrees, at this low energy, with what is found about the capture of pions at rest, in heavy nuclei of photographic emulsion (Table III).

Also the stop percentage quite agrees with the σ_0 one. Since as regards the σ the results are interpretable on the bases of the absorption of the pion by a proton-neutron pair [2], we may deduce that this is substantially true also for the

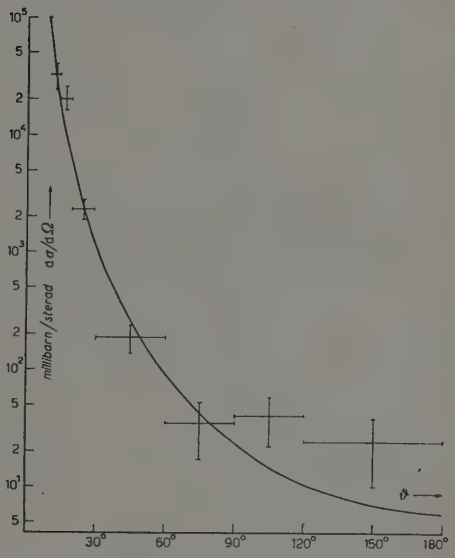

Fig. 8. – Elastic scattering of 10-20 MeV π^- in p.p. (129 events).

capture in flight of negative pions at low energy.

The survey of scatterings has been made by measuring the grain density before and after the angle. In Figs. 1, 2, 3, 4 are shown the distributions $\Delta v/v$. The inelastic scatterings are clearly separated in 10-25 MeV π^- while in 5-10 MeV π^- and in π^+ it is possible to separate only statistically few inelastic scatterings having a small energy loss.

---

[2] V. De Sabbata, E. Manaresi and G. Puppi: *Nuovo Cimento*, **10**, 1704 (1953).

The differential cross-sections for elastic scatterings are shown in Figs. 5, 6, 7, 8. The full line shows the Coulomb scattering calculated for point nuclei. We remark between 10-20 MeV a great contribution by nuclear forces which are substantially liable for cross-sections behind 90°.

We are indebted to Prof. G. PUPPI whose most valuable suggestions and help allowed us to carry out this work and whom we wish to thank heartly. We wish to thank also Dr. J. OREAR who provided us with the plates. Our thanks to Miss C. MARCHI and Mr. F. CIANCABILLA who helped us in scanning.

IL NUOVO CIMENTO Vol. I, N. 3 1° Marzo 1955

A Direct Interchange Mechanism in Liquid Tin and Indium Self Diffusion.

G. Careri and A. Paoletti
Istituto di Fisica dell'Università - Roma

(ricevuto il 12 Febbraio 1955)

After our previous [1] investigation on the liquid indium self-diffusion coefficient, similar experiments were carried out in this laboratory in liquid tin and lead. An appreciable departure was observed from the simple linear dependence in the plot of log D versus $1/T$, where D is the diffusion coefficient and T the Kelvin temperature, linear dependence which was found to hold in our and in other previous experiments on a narrow temperature range. Therefore it was decided to make some measurements again for liquid indium on a wider temperature range, and then it was found that also for indium the straight line is out of the experimental error of the experimental data (see Fig. 1).

At the present time the theory of the liquid state is unable to predict the behaviour of the diffusion coefficient in simple liquids. The well known Eyring picture of the liquid state as a mixture of atoms and vacancies, gives quite an erratic prediction of D, as one can derive from his expression $D=kT/2r\eta$, where r is the atomic radius, η the viscosity coefficient and k the Boltzmann constant.

If one assumes the basic mechanism responsible for diffusion in liquid metals to be the direct interchange between two neighbouring atoms, one can then derive

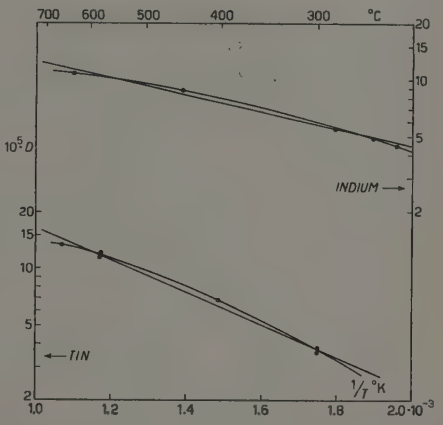

Fig. 1 – The self-diffusion coefficient in liquid tin and indium as a function of the temperature.

an expression for D which fits all our experimental data inside the experimental error (which is never larger than ± 0.03). The expression in question can be obtained from the random walk treatment of the diffusion process, extensively used in solid state physics, when one expresses the mean time of stay of one atom in its site in terms of the

(1) G. Careri, A. Paoletti, F. Salvetti: *Nuovo Cimento*, **11**, 399 (1954).

exchange probability with his neighbours. Then imposing the exchange to take place only when the two atoms move in the right phase, with an energy $\geqslant E$ distributed on the system of the two quantized harmonic oscillators, this exchange probability can be evaluated and yields the expression

$$(1) \qquad D = \frac{A}{(1+\alpha T)^4}\{e^{-\vartheta/T} + (1 - e^{-\vartheta/T}) \cdot (1 - \varepsilon T)\, H/R\theta\}\, e^{-H/RT},$$

where

$A = 4(1/6)^2\, \delta_0^2 \nu_0 e^{\varepsilon H/R}$
$E = H(1 - \varepsilon T)$
$\delta_0 =$ atomic diameter
$\theta = h\nu_0/k =$ Debye temperature
$\alpha =$ linear expansion coefficient of the liquid
$R =$ gas constant.

From two experimental points the quantities A and H were derived and found

	A cm^2 s^{-1}	H cal mole^{-1}
indium	$3.5 \cdot 10^{-4}$	3.140
tin	$10.2 \cdot 10^{-4}$	5.240

With the above values the equation (1) predicts all other data inside the experimental error. Further, if one calculates the quantity ε with a method similar to the one used in the solid state analogous problem, one gets for A a value very close to the one derived from the two experimental points.

The above suggested mechanism of diffusion yields a model of the liquid state in which the molecules are in quasi-crystalline structure, performing oscillations around their equilibrium sites, but sometimes interchanging sites by a ring movement. These rings are not stable, but due to the thermal agitation they break up after half a tour, leading to an interchange of neighbours and this way to a diffusion process. Of course one has a statistical distribution of these rings, the number of rings also increasing with the temperature.

Our work now in progress on liquid lead confirms the above results on tin and indium, results which will be more extensively shown and discussed in a forthcoming paper.

IL NUOVO CIMENTO Vol. I, N. 3 1° Marzo 1955

Virtual Masses of Interacting Fields.

R. Shaw
Trinity College - Cambridge, England

(ricevuto il 12 Febbraio 1955)

Consider a neutral field $\varphi(x)$ with Fourier expansion

$$(1)\qquad \begin{cases} \varphi(x) = \int a(p) \exp[ipx]\, \mathrm{d}^4p\,, \\ a(p) = \dfrac{1}{(2\pi)^4}\int \varphi(x) \exp[-ipx]\, \mathrm{d}^4x\,. \end{cases}$$

We can separate off invariantly the parts of $\varphi(x)$ corresponding to the various « masses » $(-p^2)$. Thus we define $(\theta(p_0) = \frac{1}{2}\{1+p_0/|p_0|\})$ for $m^2 \geqslant 0$,

$$(2)\qquad \begin{cases} \varphi^{(+)}(x; n^2) = \int \theta(p_0)\, a(p) \exp[ipx]\, \delta(p^2 + m^2)\, \mathrm{d}^4p\,, \\ \varphi^{(-)}(x; m^2) = \int \theta(-p_0)\, a(p) \exp[ipx]\, \delta(p^2 + m^2)\, \mathrm{d}^4p\,, \end{cases}$$

and for $m^2 < 0$,

$$\varphi^{(\sim)}(x; m^2) = \int a(p) \exp[ipx]\, \delta(p^2 + m^2)\, \mathrm{d}^4p\,,$$

($p_0 > 0$ or $p_0 < 0$ is not an invariant property of p for $p^2 > 0$). For free fields, only $\varphi(x; \mu^2)$ is non-zero, where μ is the rest mass of the field. We shall be concerned with the more important case of interacting fields with $\varphi(x; m^2)$ non-zero for a continuous range of m^2.

We find

$$\varphi^{(+)}(x; m^2) = \frac{1}{(2\pi)^4}\iint \theta(p_0) \exp[ip(x-y)]\, \delta(p^2 + m^2)\, \varphi(y)\, \mathrm{d}^4p\, \mathrm{d}^4y\,;$$

but

$$\Delta^{(+)}(x-y; m^2) = \frac{-i}{(2\pi)^3}\int \theta(p_0) \exp[ip(x-y)]\, \delta(p^2 + m^2)\, \mathrm{d}^4p\,.$$

Hence

$$(3)\qquad \begin{cases} \varphi^{(+)}(x;\, m^2) = \dfrac{i}{2\pi}\displaystyle\int \Delta^{(+)}(x-y;\, m^2)\,\varphi(y)\,\mathrm{d}^4y\,, \\ \varphi^{(-)}(x;\, m^2) = \dfrac{-i}{2\pi}\displaystyle\int \Delta^{(-)}(x-y;\, m^2)\,\varphi(y)\,\mathrm{d}^4y\,, \\ \varphi^{(\sim)}(x;\, m^2) = \dfrac{1}{2\pi}\displaystyle\int \Delta^{(1)}(x-y;\, m^2)\,\varphi(y)\,\mathrm{d}^4y\,. \end{cases}$$

where $\Delta^{(1)}(x) = i\{\Delta^{(+)}(x) - \Delta^{(-)}(x)\}$. It is easily verified from (3) that

$$(4)\qquad (\Box - m^2)\varphi^{(\cdot)}(x;\, m^2) = 0\,.$$

We now postulate, as usual, the existence of the vacuum state Φ_0, with the property $P_\mu \Phi_0 = 0$, where P_μ is the energy-momentum 4-vector of the system, and assume no state has eigen-value $P_0' > 0$. It follows that

$$\varphi^{(+)}\Phi_0 = \varphi^{(\sim)}\Phi_0 = 0\,, \qquad \text{and} \qquad \Phi_0^*\varphi^{(-)} = \Phi_0^*\varphi^{(\sim)} = 0,$$

and so the only vacuum expectation value we have to calculate is

$$\langle \varphi^{(+)}(x;\, m^2)\,\varphi^{(-)}(x';\, m'^2)\rangle_0\,.$$

Now according to KÄLLÉN [1] and LEHMANN [2] we can express vacuum expectation values of operators quadratic in the interesting fields in terms of the corresponding values for free fields. Thus

$$\langle \varphi(x)\,\varphi(x')\rangle_0 = i\int \varrho(m^2)\,\Delta^{(+)}(x-x';\, m^2)\,\mathrm{d}(m^2), \qquad (\text{with } \varrho \geqslant 0).$$

Hence

$$\langle \varphi^{(+)}(x;\, m^2)\varphi^{(-)}(x';\, m'^2)\rangle_0 =$$

$$= \frac{i}{4\pi^2}\iiint \Delta^{(+)}(x-y;\, m^2)\,\Delta^{(+)}(y-y';\, m''^2)\,\Delta^{(-)}(x'-y';\, m'^2)\,\varrho(m''^2)\,\mathrm{d}^4y\,\mathrm{d}^4y'\,\mathrm{d}(m''^2)\,.$$

Using

$$\int \Delta^{(+)}(x-y;\, m^2)\,\Delta^{(+)}(y-y';\, m''^2)\,\mathrm{d}^4y = -2\pi i\,\delta(m^2-m''^2)\,\Delta^{(+)}(x-x';\, m^2)$$

and

$$\Delta^{(-)}(x-y) = -\Delta^{(+)}(y-x)\,,$$

[1] G. KÄLLÉN: *Helv. Phys. Acta*, **25**, 417 (1952).
[2] H. LEHMANN: *Nuovo Cimento*, **11**, 342 (1954).

we find

$$\langle \varphi^{(+)}(x; m^2)\, \varphi^{(-)}(x; m'^2)\rangle_0 = i\varrho(m^2)\, \delta(m^2 - m'^2)\, \Delta^{(+)}(x - x'; m^2)\,.$$

Putting $\varphi(x; m^2) = \varphi^{(-)}(x; m^2) + \varphi^{(+)}(x; m^2)$, $(m^2 > 0)$, we find

$$\langle \varphi(x; m^2)\, \varphi(x'; m'^2)\rangle_0 = i\varrho(m^2)\, \delta(m^2 - m'^2)\, \Delta^{(+)}(x - x'; m^2)\,, \tag{5}$$

from which we derive also,

$$\begin{cases} \langle [\varphi(x; m^2), \varphi(x'; m'^2)]\rangle_0 &= i\varrho(m^2)\, \delta(m^2 - m'^2)\, \Delta(x - x'; m^2)\,, \\ \langle \{\varphi(x; m^2), \varphi(x'; m'^2)\}\rangle_0 &= \varrho(m^2)\, \delta(m^2 - m'^2)\, \Delta^{(1)}(x - x'; m^2)\,, \\ \langle T\{\varphi(x; m^2), \varphi(x'; m'^2)\}\rangle_0 &= \tfrac{1}{2}\varrho(m^2)\, \delta(m^2 - m'^2)\, \Delta_F(x - x'; m^2)\,. \end{cases} \tag{5}$$

From (4) and (5) we see that, as far as vacuum expectation values of quantities quadratic in φ are concerned, $\varphi(x; m^2)$ behaves like a free field, its «strength» $[\varrho(m^2)]^{\frac{1}{2}}$ only, being determined by the coupling.

We can write down similar results for the Fermion field, though now we have to introduce two functions, $\varrho_1(m^2)$ and $\varrho_2(m^2)$ (using Lehmann's notation). For instance

$$\langle T\{\psi(x; m^2), \bar{\psi}(x'; m'^2)\}\rangle_0 = -\tfrac{1}{2}\, \delta(m^2 - m'^2)[\varrho_1(m^2)\, S_F(x - x'; m) + \varrho_2(m^2)\, \Delta_F\,(x - x'; m^2]\,.$$

Putting $\sigma_1(m^2) = \varrho_1(m^2) - \varrho_2(m^2)/2m$ and $\sigma_2(m^2) = \varrho_2(m^2)/2m$, we can write this in the form

$$\langle T\{\psi(x; m^2)\bar{\psi}(x'; m'^2)\}\rangle_0 = \tfrac{1}{2}\, \delta(m^2 - m'^2)[\sigma_1(m^2)\, S_F(x - x'; m) + \sigma_2(m^2)\, S_F(x - x'; -m)]\,;$$

where, (see reference [2]), eq. (22)), $\sigma_1 \geqslant 0$, $\sigma_2 \geqslant 0$.

IL NUOVO CIMENTO Vol. I, N. 3 1° Marzo 1955

On the ^{60}Ni Gamma-Gamma Directional Correlation Function.

S. Colombo

Istituto Nazionale di Fisica Nucleare - Sezione di Milano

A. Rossi and A. Scotti

Istituto di Fisica dell'Università - Milano
Istituto Nazionale di Fisica Nucleare - Sezione di Milano

(ricevuto il 15 Febbraio 1955)

An accurate remeasurement of the ^{60}Ni gamma-gamma directional correlation function has been made. Care was taken to minimize or, whenever possible, to eliminate systematic errors, for which precise methods of correction are not available.

A cylindrical piece of ^{60}Co, obtained from a metal wire, (0.8 mm in diametre, 1 mm in length), was used as a practically point source. Gamma rays were detected by means of cylindrical Anthracene phosphors (1″ in diametre, 1″ in length), viewed by Du Mont Type 6291 photomultipliers. The resolving time of the coincidence circuit was kept very stable about $4 \cdot 10^{-8}$ s.

By proper discrimination at high level, spurious coincidences due to Compton scattering of single quanta, and coincidences due to positron contamination were avoided. This leads to a rather low efficiency of the detectors: a good statistical accuracy was obtained, however, within a reasonably long measuring time.

The effect of the finite angular resolution of the counters has been taken into account by means of an experimental method proposed by Lawson and Frauenfelder [1], which has proved quite adequate.

The rate of genuine coincidences has been measured for seven values of the angle α between the counter axes, from 90° to 180°. The ratio $A(\alpha) = W(\alpha)/W(90°)$ of the rate at angle α to the rate at 90° was then formed.

In the following table the experimental results, and the theoretically calculated values for the undisturbed $4(E2)2(E2)0$ cascade are reported.

α	$A_s(\alpha)$	σ	$A_t(\alpha)$
90°	(1)	—	1.00000
105°	1.0082	$6 \cdot 10^{-4}$	1.00856
120°	1.0329	$5 \cdot 10^{-4}$	1.03385
135°	1.0717	$6 \cdot 10^{-4}$	1.07292
150°	1.1163	$8 \cdot 10^{-4}$	1.11719
165°	1.1526	$10 \cdot 10^{-4}$	1.15290
180°	1.1667	$12 \cdot 10^{-4}$	1.16667

[1] J. S. Lawson and H. Frauenfelder: *Phys. Rev.*, **91**, 649 (1953).

In this table:

$A_s(\alpha)$ is the experimental value, obtained from the measured data by means of a least square fit to the usual form of the function, corrected for finite angular resolution;

σ is the standard deviation of $A_s(\alpha)$, derived from total number of counts through least square method, including the uncertainty due to the correction factors, (the standard deviation of the values of $A(\alpha)$, as directly measured, is about $2 \cdot 10^{-3}$);

$A_t(\alpha)$ is the theoretical value.

The comparison confirms, within the statistical accuracy, the usual assignment of spins and multipole orders, and does not show significant attenuation of the correlation, in agreement with the last results obtained by the Illinois group [1,2] in similar experimental conditions, by LEMMER and GRACE [3] at very low temperature, and recently by STEFFEN [4].

Our results are at variance with previous measurements made by the Zürich group [5], which had suggested, as a possible explanation, the influence of external fields, and those made by DAS and SEN [6], which had led to a different spin and multipole order assignment. The first results are now considered as affected by unsufficiently corrected systematic errors [7]; the latter, by poor statistical accuracy.

A more detailed paper will be submitted for publication to *Il Nuovo Cimento*.

---

[2] J. S. LAWSON, H. FRAUENFELDER and W. K. JENTSCHKE: *Phys. Rev.*, **91**, 484 (1953).

[3] H. R. LEMMER and M. A. GRACE: *Proc. Phys. Soc.*, A **67**, 1051 (1954).

[4] R. M. STEFFEN: to be published in *Am. Journ. Phys.*

[5] H. AEPPLI, H. FRAUENFELDER, E. HEER and R. RÜETSCHI: *Phys. Rev.*, **87**, 379 (1952).

[6] S. DAS and S. K. SEN: *Ind. Journ. Phys.*, **25**, 451 (1951).

[7] H. FRAUENFELDER: *Angular Correlation*, a chapter from K. SIEGBAHN's book on *Nuclear Spectroscopy*, (Amsterdam, 1954).

LIBRI RICEVUTI E RECENSIONI

AAGE BOHR – *Rotational states of atomic nuclei*; København, Ejnar Munksgaard forlag, 1954, p. 1-55.

Questa monografia è sostanzialmente una discussione riassuntiva dei lavori di A. BOHR e di vari altri autori, in particolare B. R. MOTTELSON sul modello di nucleo proposto inizialmente da A. BOHR.

Viene mostrato come tale modello, fondato, com'è noto, sull'idea che alcuni aspetti della dinamica nucleare possano essere spiegati assumendo un moto collettivo del nucleo, sia in accordo con un gran numero di fatti sperimentali; in particolare con gli spettri di eccitazione dei primi livelli nucleari specialmente con $A > 140$; e con le forti transizioni di quadrupolo elettrico che anzi permettono l'identificazione dei livelli rotazionali.

Non è facile commentare una teoria che, sebbene abbia avuto considerevoli successi, è ancora in evoluzione. Ciò che si può dire è che l'esposizione di A. BOHR è estremamente chiara.

G. MORPURGO

Direttore responsabile: G. POLVANI Tipografia Compositori - Bologna

Questo fascicolo è stato licenziato dai torchi il 23-II-1955